

RELIABILITY OF MARINE STRUCTURAL COMPONENTS

A thesis submitted for the Degree of Master of Science in the Faculty of
Engineering of the University of Glasgow

by

Alexandre José Lopes Guedes da Silva

Department of Naval Architecture and Ocean Engineering

University of Glasgow

© Alexandre Guedes da Silva, 1995

ProQuest Number: 11007816

All rights reserved

INFORMATION TO ALL USERS

The quality of this reproduction is dependent upon the quality of the copy submitted.

In the unlikely event that the author did not send a complete manuscript and there are missing pages, these will be noted. Also, if material had to be removed, a note will indicate the deletion.



ProQuest 11007816

Published by ProQuest LLC (2018). Copyright of the Dissertation is held by the Author.

All rights reserved.

This work is protected against unauthorized copying under Title 17, United States Code
Microform Edition © ProQuest LLC.

ProQuest LLC.
789 East Eisenhower Parkway
P.O. Box 1346
Ann Arbor, MI 48106 – 1346

Thesis
10303
Copy 1



To

My Parents, my wife ANA
and my daughter LEONOR.

ABSTRACT

The use of strength formulations' characteristic of marine structural components in reliability assessment is investigated throughout a series of systematic studies.

The marine structural components used were the stiffened plate and the ring and stringer stiffened cylinder and the design scenario is their resistance to compressive loads (buckling) which is the most common failure modes in marine structures.

The systematic studies provided a good understanding of the behaviour of the several strength formulations when they are used in reliability calculations. Also, the importance of all uncertainties involved was analysed and commented.

The formulations considered for the stiffened plates buckling strength were the proposals of Faulkner, Guedes Soares, Ivanov and Rousev, Carlsen, Ueda and Yao, Soreide and Czujko, Valsgard, ABS, Dier and Dowling and Stonor et al. The formulations are fully described in the text along with the discussion of their reliability assessment results.

The formulations considered for the ring-stringer stiffened cylinders buckling strength were the proposals of several codes of practice API Bul 2U, RCC, DnV CN-30.1 and ECCS-29. They are fully described in the text along with the discussion of their uncertainties and reliability assessment.

The strength modelling parameters are the most important variables in the reliability assessment and they were investigated for the case of the ring-stringer stiffened cylinders. All formulations were compared with two large test results databases and the uncertainties were derived for all cases.

Finally the last chapter aggregates the conclusions of the systematic studies for the stiffened plates and cylinders with the demonstration of the importance of good strength modelling for the reliability based design of structures. The methodology for good strength modelling is described and used in improving the strength formulations for the ring-stringer stiffened cylinders.

LIST OF CONTENTS

ABSTRACT	(ii)
LIST OF CONTENTS	(iii)
LIST OF FIGURES	(ix)
LIST OF TABLES	(xi)
NOTATION	(xiii)
Stiffened Plates (Chapter 2)	(xiii)
Ring-stringer stiffened cylinders (Chapter 3).....	(xvi)
ACKNOWLEDGEMENTS	(xx)
DECLARATION	(xxi)
CHAPTER 1 - INTRODUCTION	1
1.1 - General.....	1
1.2 - Review of the reliability methods.	4
1.3 - Review of the design methods for plates and cylinders	8
1.3.1 - Stiffened plates.	9
1.3.2 - Ring and stringer stiffened cylinders.....	10
1.4 - Aims and scope of the thesis	10
CHAPTER 2 - RELIABILITY ANALYSIS OF STIFFENED PLATES	12
2.1 - Introduction.....	12
2.2 - Strength formulations for unstiffened plates.	13

2.2.1 - Formulations for longitudinal strength under compressive loads.....	15
2.2.1.1 - Faulkner formulation.	15
2.2.1.2 - Ivanov and Rousev formulation.	17
2.2.1.3 - Carlsen formulation.	17
2.2.1.4 - Guedes Soares formulation.	17
2.2.1.5 - Ueda and Yao formulation.	18
2.2.1.6 - Soreide and Czujko formulation.	19
2.2.2 - Formulations for transverse strength under compressive loads.	19
2.2.2.1 - Faulkner formulation.	19
2.2.2.2 - Valsgard formulation.	20
2.2.2.3 - ABS formulation.	20
2.2.3 - Formulations for biaxial strength under compressive loads.	20
2.2.3.1 - Faulkner formulation.	21
2.2.3.2 - ABS formulation.	21
2.2.3.3 - Other formulation.	21
2.2.4 - Model uncertainty for stiffened plates.	22
2.3 - Strength formulations for stiffened plates.	23
2.3.1 - Formulations for longitudinal strength under compressive loads.....	24
2.3.1.1 - Faulkner formulation.	24
2.3.1.2 - Carlsen formulation.	26

2.3.2 - Model uncertainty for longitudinal strength of stiffened plates.....	27
2.4 - Reliability assessment of plates.....	27
2.4.1 - Reliability of unstiffened plates under compressive loading.....	29
2.4.2 - Reliability of stiffened plates under compressive loading.....	39
2.5 - Conclusions.....	42

CHAPTER 3 - RELIABILITY ANALYSIS OF RING-STRINGER STIFFENED CYLINDERS44

3.1 - Introduction.....	44
3.2 - Strength Formulations for Ring-stringer Stiffened Cylinders.....	48
3.2.1 - Formulations for ultimate strength under axial compression loads.....	51
3.2.1.1 - API Bulletin 2U.....	51
3.2.1.1.1 - Local buckling.....	52
3.2.1.1.2 - Bay instability.....	54
3.2.1.2 - RCC Formulation.....	58
3.2.1.3 - DnV Classification Note 30.1.....	59
3.2.1.4 - European Convention for Constructional Steelwork Formulation.....	60
3.2.2 - Formulations for ultimate strength under radial pressure loads.....	62
3.2.2.1 - API Bul 2U.....	62
3.2.2.1.1 - Local shell buckling.....	62

3.2.2.1.2 - Bay instability.	63
3.2.2.2 - RCC Formulation	64
3.2.2.3 - DnV Classification Note 30.1	65
3.2.3 - Formulations for ultimate strength under combined loads.	66
3.2.3.1 - API Bul 2U	66
3.2.3.2 - RCC Formulation	67
3.2.3.3 - DnV Classification Notes (30.1)	67
3.3 - Evaluation of the model uncertainty for the strength formulations.	68
3.3.1 - Description of the available experimental data.	68
3.3.1.1 - Aerospace programmes	69
3.3.1.1.1 - Technion Tests.....	70
3.3.1.2 - Offshore programmes	70
3.3.1.2.1 - UCL Tests	71
3.3.1.2.2 - Imperial College Tests.....	72
3.3.1.2.3 - Glasgow University Tests.....	73
3.3.1.2.4 - CBI Tests.....	73
3.3.1.2.5 - DnV Tests.....	75
3.3.2 - Model uncertainty of the axial compression formulations.	76
3.3.3 - Model uncertainty of radial pressure formulations.	82
3.3.4 - Model uncertainty of combined loading formulations.	85
3.4 - Reliability analysis of ring-stringer stiffened cylinders.	90

3.4.1 - Reliability of ring-stringer stiffened cylinders under axial compression loads.....	93
3.4.2 - Reliability of ring-stringer stiffened cylinders under radial pressure loads.....	96
3.4.3 - Reliability of ring-stringer stiffened cylinders under combined loading.....	98
3.5 - Conclusions.....	100
3.5.1 - Uncertainty analysis.....	100
3.5.2 - Reliability analysis.....	102

CHAPTER 4 - MODELLING FOR STRENGTH AND RELIABILITY ASSESSMENT.....104

4.1 - Introduction.....	104
4.2 - Strength modelling criteria.....	105
4.2.1 - Statistical criteria.....	105
4.2.2 - Strength requirements.....	106
4.3 - Case Study - Improvement of the strength formulation for ring-stringer stiffened cylinders.....	108
4.3.1 - Introduction.....	108
4.3.2 - Modelling the axial strength.....	110
4.3.2.1 - Column type buckling.....	110
4.3.2.1.1 - Curved shell buckling.....	111
4.3.2.1.2 - Two term equation.....	113
4.3.2.2 - Stringer tripping.....	117
4.3.3 - Modelling the radial strength.....	117

4.3.3.1 - Local shell buckling	119
4.3.4 - Modelling the combined load strength.....	119
4.4 - Importance of the variables in the reliability assessment.....	122
4.4.1 - Model uncertainty variables.	122
4.4.2 - Strength variables.....	125
4.4.3 - Load variables.....	126
CHAPTER 5 - CONCLUSION AND FUTURE DEVELOPMENT.....	128
REFERENCES.....	131
APPENDIX 1 - PLATES RELIABILITY ANALYSIS - GRAPHICAL OUTPUT.....	153
APPENDIX 2 - CYLINDERS UNCERTAINTY MODELLING - TABLES.....	164
APPENDIX 3 - CYLINDERS UNCERTAINTY MODELLING - GRAPHICAL OUTPUT.....	173
APPENDIX 4 - CYLINDERS RELIABILITY ANALYSIS - GRAPHICAL OUTPUT.....	201

LIST OF FIGURES

Fig. 2.1 - Stiffened plates in compression.	12
Fig. 2.2 - Histogram of the ratio of the stiffener by the plate area($A_s/b*t$).....	14
Fig. 2.3 - Load-end shortening curves for plates in compression with initial deformations.....	15
Fig. 2.4 - Interframe collapse mode in stiffened plates.....	24
Fig. 2.5 - Reliability index (β_f) for longitudinally loaded plate element as predicted by MVRM and FORM methods, as a function of plate slenderness (β). Also indicated is the plate strength (ϕ_F) as predicted by equation (2.1).....	30
Fig. 2.6 - Effects of the strength model uncertainty in the reliability assessment. Faulkner formulation for longitudinally loaded simply supported plates with initial deflections and residual stresses (eqs. (2.1)-(2.7)).....	31
Fig. 2.7 - Reliability index (β_f) as function of plate slenderness (β) for longitudinally loaded simply supported plates with initial distortions and residual stresses with strength predicted by different methods.....	32
Fig. 2.8 - Sensitivity of (β_f) in relation to different variables as a function of plate slenderness (β) for the method of Guedes Soares (eq.(2.12)).	34
Fig. 2.9 - Sensitivity of (β_f) in relation to different variables as a function of plate slenderness (β) for the method of Faulkner (eqs. (2.1)-(2.7)).	34
Fig. 2.10 - Reliability index (β_f) as function of plate slenderness for simply supported plates subjected to transverse loading with strength predicted by Faulkner (eq.(2.17)), by Valsgard (eq.(2.18)) and ABS(eq.(2.19)). (Plate aspect ratio $\cong 3.3$).....	36
Fig. 2.11 - Reliability index (β_f) as function of plate slenderness for simply supported plates with initial distortions biaxially loaded with strength predicted by different methods.	38
Fig. 2.12 - Reliability index (β_f) as function of plate slenderness for stiffened plates with initial distortions longitudinally loaded with strength predicted by different methods.	40
Fig. 3.1-Ring-Stringer stiffened cylinder.....	44
Fig. 3.2-Loading types.....	45

Fig. 3.3(a-d)-Ring-Stringer cylinder buckling modes.	46
Fig. 3.4-Fabrication defects.....	49
Fig. 3.5-Idealised residual stress distribution.....	50
Fig. 3.6-External pressure failure mode (3-hinge mechanism).....	65
Fig. 3.7(a-i)-Uncertainty analysis - RCC - Axial compression (pop. 52 specimens).....	81
Fig. 3.8(a-i)-Uncertainty analysis - RCC - Radial pressure (pop. 11 specimens).....	84
Fig. 3.9(a-i)-Uncertainty analysis - RCC - Combined Loading (pop. 35 specimens).....	88
Fig. 3.10-Reliability index (β_f) for axially loaded ring-stringer cylinder as a function of the shell thickness for $N_s=35$ as predicted by the different formulations.....	94
Fig. 3.11-Sensitivity of (β_f) in relation to different variables as a function of the number of stringers with $N_s=35$ for the biased RCC formulations (eq.(3.33))-(eq.(3.34)).	94
Fig. 3.12-Comparison of the mean thickness required by ISO safety level for axially loaded ring-stringer cylinder as a function of the number of stringers as predicted by the different formulations.....	95
Fig. 3.13-Comparison of the mean thickness required by ISO safety level for radially loaded ring-stringer cylinder as a function of the number of stringers as predicted by the different formulations.....	97
Fig. 3.14- Comparison of the mean thickness required by ISO safety level for a combined axial compression and radial pressure loaded ring-stringer cylinder as a function of the number of stringers as predicted by the different formulations.....	99
Fig. 4.1 - Curved shell buckling knockdown factors	112
Fig. 4.2 - Test data and empirically-derived lower bound design curves (the solid line indicates the range for each R/t group).....	115
Fig. 4.3 - Comparison of test pressures with predicted failure pressures for stringer stiffened cylinders.....	118
Fig. 4.4(a-i) - Uncertainty analysis - RCC (New Proposal)- Combined Loading (pop. 35 specimens)	120

LIST OF TABLES

Table 2.1 - Model uncertainty for unstiffened plates.....	22
Table 2.2 - Model uncertainty for stiffened plates.....	27
Table 2.3 - Description of the basic variables used in the unstiffened plates reliability assessment.....	29
Table 2.4 - Comparison of the longitudinal strength formulations for different design conditions.....	33
Table 2.5 - Reliability index for a plate element under longitudinal load for different values of correlation between the variables (eq.(2.1))......	35
Table 2.6 - Comparison of the transverse strength formulations for different design conditions.....	37
Table 2.7 - Comparison of the biaxial strength formulations for different design conditions.(W_0 is the weight per unit length corresponding to a plate of 22 mm).....	38
Table 2.8 - Description of the stiffener dimensions and the resistance modelling parameter.....	40
Table 2.9 - Comparison of the longitudinal strength formulations for stiffened plates for different design conditions.....	41
Table 3.1-Sample of models of aerospace test programmes.....	69
Table 3.2-UCL Test specimens - Geometry, material properties and test result.....	71
Table 3.3-IC Test specimens - Geometry, material properties and test result.....	72
Table 3.4-GU Test specimens - Geometry, material properties and test result.....	73
Table 3.5-CBI Test specimens - Geometry, material properties and test result.....	74
Table 3.6-DnV Test specimens - Geometry, material properties and test result.....	76
Table 3.7- X_m for axial compression formulations.....	77
Table 3.8 - Bias & COV of model uncertainty factor for axial compression formulation.....	78

Table 3.9- X_m for radial pressure formulations.	82
Table 3.10 - Bias & COV of model uncertainty factor for radial pressure formulations.	83
Table 3.11- X_m for combined loading formulations.	86
Table 3.12 - Bias & COV of model uncertainty factor for combined axial compression and radial pressure formulations.	87
Table 3.13 - Description of the basic variables used in the stiffened cylinder reliability analysis.	91
Table 3.14 - Comparison of the axial compression strength formulations for ring and stringer stiffened cylinders.(ISO safety level).	96
Table 3.15 - Comparison of the radial pressure strength formulations for ring and stringer stiffened cylinders.(ISO safety level).	98
Table 3.16 - Comparison of the combined load interaction formulations for ring and stringer stiffened cylinders.(ISO safety level).	99
Table 4.1 - Comparison of the different curved shell knockdown factors.	115
Table 4.2 - Modelling parameters for different equations considered in axial compression strength.	116
Table 4.3 - Strength modelling parameters for the different strength formulation for stiffened and unstiffened plates.	123
Table 4.4 - Strength modelling parameters for the different strength formulation for ring and stringer stiffened cylinders.	124
Table 4.5 - Typical uncertainty level for physical properties and structural dimensions.	126

NOTATION

Stiffened Plates (Chapter 2)

a = Plate length.

A_e = Plate-stiffener effective cross sectional area.

A_s = Stiffener cross sectional area.

A_t = Plate-stiffener full cross sectional area.

b = Plate breadth (width).

b_e = Effective width of plate.

b'_e = Tangent or reduced width of plate.

E = Young modulus of Elasticity.

E_t = Tangent modulus of Elasto-Plasticity.

$f_X(\mathbf{x})$ = Joint probability density function of X .

$G(\mathbf{x})$ = Limit state function.

I'_e = Moment of inertia of stiffener and reduced width of plate.

k = Buckling coefficient.

M_s = Stillwater bending moment.

M_w = Wave induced bending moment.

P_f = Probability of failure.

$p_r = (\sigma_p/\sigma_0)$, Proportional limit.

PSF = Partial Safety Factor.

q_0 = Nominal lateral pressure.

$r = (\sqrt{I/A})$, Plate-stiffener radius of gyration.

R_r = Residual stress reduction factor.

R_t = Biaxial compression reduction factor.

- R_x = Longitudinal strength ratio of a plate in biaxial compression.
- R_y = Transverse strength ratio of a plate in biaxial compression.
- R_τ = Shear stress reduction factor.
- t = Plate thickness.
- w_0 = Maximum amplitude of initial distortions.
- W = Section modulus of plate-stiffener.
- \bar{X}_m = Test strength/ Predicted strength.
- z_p = Distance from mid-plane of plate to the neutral axis.
- Z_0 = Midship section modulus.
- α = (a/b), Plate aspect ratio.
- $\underline{\alpha}$ = Sensitivity vector.
- β = $(b/t \sqrt{\sigma_0/E})$, Plate slenderness.
- β_f = Generalised reliability index.
- δ_0 = Nondimensional initial distortions.
- $\Delta\phi_r$ = Reduction factor due to residual stresses.
- ϕ_{Ay} = Nondimensional plate transverse strength predicted ABS.
- ϕ_C = Nondimensional plate strength predicted Carlsen.
- ϕ_{Cs} = Nondimensional stiffened plate strength predicted Carlsen.
- ϕ_F = Nondimensional plate strength predicted Faulkner.
- ϕ_{Fs} = Nondimensional stiffened plate strength predicted Faulkner.
- ϕ_{Fy} = Nondimensional plate transverse strength predicted Faulkner.
- ϕ_{GS} = Nondimensional plate strength predicted by Guedes Soares.
- ϕ_I = Nondimensional plate strength predicted by Ivanov and Roussev.
- ϕ_S = Nondimensional plate strength predicted by Soreide and Czujko.
- ϕ_U = Nondimensional plate strength predicted by Ueda et al.
- ϕ_{Vy} = Nondimensional plate transverse strength predicted by Valsgard.

- ϕ_x = Nondimensional plate strength in x direction.
- ϕ_y = Nondimensional plate strength in y direction.
- Φ = Normal standardised distribution.
- γ = Magnification factor in Perry-Robertson formula.
- η = Width of the weld tension block normalised by plate thickness.
- $\lambda c = \left(a / \pi r \sqrt{\sigma_0 / E} \right)$, Column slenderness.
- σ_{cr} = Buckling stress.
- σ_e = Elastic buckling stress.
- σ_{ed} = Mean edge stress.
- $\sigma_E = \left(\pi^2 E r^2 / a \right)$, Euler stress.
- $\sigma_{JO} = \left(1 - \sigma_0 / 4 \sigma_E \right)$, Johnson-Ostenfeld stress.
- σ_p = Proportional limit stress.
- $\sigma_{ps} \cong \frac{\sigma_p - \sigma_r}{\sigma_0} \cong \frac{\sigma_0 - \sigma_r}{\sigma_0}$, Structural proportional limit.
- σ_r = Mean compression residual welding stress in the plate.
- σ_s = Mean applied stress in the plate.
- σ_u = Ultimate compression stress.
- σ_x = Mean axial compression stress in x direction.
- σ_y = Mean axial compression stress in y direction.
- σ_{yu} = Ultimate axial compression stress in y direction.
- σ_0 = Yield stress.
- τ = Mean shear stress.
- τ_u = Ultimate shear stress.
- ξ = Imperfection factor in Perry-Robertson formula.

Ring-stringer stiffened cylinders (Chapter 3)

A_C = Cross sectional area of one ring stiffener.

A_S = Area of stringer stiffener.

B = Bias for knockdown factor.

c = Interaction equation coefficient.

C = Reduced buckling coefficient.

C_X = Parameter affecting stiffener position.

d_f = Breadth of flange.

d_w = Height of web.

e_s = Distance from centre line of shell to centroid of stringer stiffener.

E = Modulus of elasticity.

$g = M_x M_\theta L t \frac{A_s}{I_s}$.

$G = \frac{E}{2} (1 + \nu)$, Shear modulus.

I = Moment of inertia of stringer and shell.

I_e = Moment of inertia of stringer including effective width of shell.

I'_e = Moment of inertia of stringer and reduced effective width of shell.

I_s = Moment of inertia of stringer about its centroidal axis.

J_s = Torsional stiffness constant of stringer stiffener.

k_p = Effective pressure correction factor.

$k_{\theta L}$ = Factor accounting for boundary conditions under radial pressure.

L = Ring frame spacing.

L_e = Effective width of shell in the longitudinal direction.

m = Number of half waves into which the shell will buckle in the longitudinal direction.

M_x = $L/\sqrt{R t}$ API shell length parameter.

M_θ = $s/\sqrt{R t}$ API shell width parameter.

n = Number of half waves into which the shell will buckle in the circumferential direction.

N_e = Elastic buckling load.

N_s = Number of stringers.

p = Applied radial pressure.

p_c = Inelastic failure pressure.

p_{eL} = Theoretical failure pressure.

p_s = Structural proportional limit.

p_{ss} = Shell and stiffener pressure.

p_u = Ultimate radial failure load.

R = Radius to centre line of shell.

R_a = Ratio of applied axial stress to ultimate axial compression stress.

R_c = Radius to centroid of ring stiffener.

R_h = Ratio of applied hoop stress to ultimate hoop stress.

R_r = Residual stress reduction factor.

s = Stringer spacing.

s_e = Shell effective width.

s'_e = Shell reduced effective width.

- t = Thickness of shell.
- t_f = Thickness of flange.
- t_w = Thickness of web.
- X_m = Model uncertainty factor or modelling parameter
- $Z_L = 0.954 L^2/R t$, Batdorf shell length parameter.
- Z_p = Plastic modulus.
- $Z_s = 0.954 s^2/R t$, Batdorf shell width parameter.
- α_0 = Factor to account for imperfections.
- α_{xB} = Reduction factor.
- α_{xL} = Reduction factor.
- $\alpha_{xL} C_x$ = Reduction factor.
- $\alpha_{\theta L}$ = Reduction factor.
- δ_p = Out of straightness of stringer shell.
- δ_s = Maximum deflection of shell from the true circular arc between stringers.
- Δ = Allowable stress when compact section requirements are not met.
- η = Plasticity reduction factor, welding residual stress tension block parameter.
- λ = Shell reduced slenderness parameter.
- ν = Poisson's ratio.
- ρ = Mean shell knockdown factor.
- ρ_s = Shell knockdown factor.
- σ_c = Inelastic buckling stress.
- σ_{cl} = Elastic buckling stress as a column.
- σ_{cr} = Theoretical elastic instability stress.

σ_e = Elastic buckling stress.

σ_{eq} = Equivalent applied stress.

σ_{icr} = Imperfect elastic shell buckling stress.

σ_{sh} = Elastic critical stress for unstiffened shell including imperfections.

σ_u = Bay average collapse stress.

σ_{ueq} = Equivalent ultimate stress.

σ_{ux} = Ultimate axial buckling stress.

$\sigma_{u\theta}$ = Ultimate radial buckling stress.

σ_x = Applied axial compression stress.

σ_{xc} = Allowable stress when compact section requirements are not met.

σ_y = Yield stress.

σ_θ = Applied radial pressure stress.

ACKNOWLEDGEMENTS

The author wishes to express his warmest gratitude:

To Professors Douglas Faulkner and Carlos Guedes Soares, his supervisors and Heads of the respective departments in Glasgow and Lisboa, for their expertise guidance, advice and encouragement throughout the duration of the author's study.

To Prof. Marian Kmiecik, visiting professor in Lisboa, for his continuous encouragement, suggestions and fruitful discussion.

To Dr. P.K.Das, his co-supervisor in Glasgow, for his continuous encouragement, support and suggestions during his stay in Glasgow.

To my colleagues in both departments for their continual encouragement and fruitful discussion about the subjects of each other.

To the Portuguese Government-Junta Nacional de Investigação Científica e Tecnológica, who has provided the financial support and to Instituto Superior Técnico-Universidade Técnica de Lisboa, who granted the author a six-month licence that allowed the course of study in Glasgow.

Finally, many thanks should go to my family, especially to my beloved wife, Ana, and to my beautiful daughter Leonor, for their love and constant support.

DECLARATION

The work described in this thesis was carried out in the Departments of Naval Architecture and Ocean Engineering at the University of Glasgow and at Instituto Superior Técnico-Universidade Técnica de Lisboa under the able supervision of Professors Douglas Faulkner and Carlos Guedes Soares.

The studies represent original work carried out by the author, and I also certify that no part of this thesis has been submitted previously in any form to any other University for the award of a degree. Where use has been made of material provided by others, due acknowledgement has been made in the text.

July, 1995.

Alexandre José Lopes Guedes da Silva

CHAPTER 1 - INTRODUCTION

1.1 - General

Safety is nowadays one of the major concerns of the maritime industries, since the loss of human lives and the ecological disasters put an enormous pressure on all marine activities, especially in shipping and offshore installations. These activities depend on highly complex structures that must resist external and internal actions.

Traditionally these structures were designed using the working stress concept that consists of a deterministic approach to the structural design in which calculations are carried out using fixed values of the variables. In this concept the loading is usually considered as the maximum probable load that occurs during the specified life of the structure. The resulting stresses arising from this load are then limited to a fraction of the yield stress, defined as the allowable stress or working stress. However, it is commonly recognised that this approach does not provide a balanced safety distribution within the structure.

A more sound design method has been gaining importance in recent years. This method, named probability based limit state design, enables the description of all uncertainties in resistance, loading and modelling in a more rational way¹. This probability approach is justified by the observation that many of the design variables exhibit statistical irregularity² and is aimed at providing a quantitative measure of safety or serviceability. This quantitative measure is the probability of failure³ and has an relative meaning according to Ditlevsen⁴. Reliability of a structure is then defined as the probability of its normal functioning (non-failure) under the expected environmental actions during its service life.

The first efforts to apply the reliability analysis concept to a structure was developed in the field of aircraft by Pugsley⁵ and in civil engineering by Freudenthal⁶, and is now widely applied in the marine, civil, electronic, electrical, mechanical, aeronautical and nuclear fields.

Structural reliability theory is concerned with the rational treatment of uncertainties in structural engineering and with the corresponding methods for assessing the safety or serviceability of structures. This theory has grown rapidly during the last two decades and has evolved from academic research to practical applications. It has become a design tool based in scientific methods rather than being a scientific theory⁴.

The main objective of its application to design is to achieve a uniform and consistent reliability within a structural system.

The structural reliability theory is nowadays being used as the framework to the new limit state oriented design codes in several engineering areas and particularly for marine structures⁷⁻¹⁰. These codes have also been developed under important considerations that arise from research to past experience¹¹:

- recognition that a more uniform reliability throughout a structure leads to an increase in overall safety.

- cost and weight benefits exist if lower notional safety levels can be adopted as a result from improved knowledge of the phenomena.

- recognition that the limit state approach to failure is more correct than the working stress approach in which a single admissible stress is use in the design of the different components leading to various levels of safety in different structures designed for the same working stress.

- recognition of the statistical nature (randomness) of design variables associated with the loading and strength.

The reliability approach for design proved to be successful for new types of structures or applications. One example, was the work by the Rule Case Committee⁷ (RCC) for the design of Tension Leg Platforms (TLP's). For the more common marine structures, ships and jacket platforms the existing proposals are based on several years of research and are only now starting to be used in current design⁹. The American Petroleum Institute⁸ (API) proposal for jacket structures undergoes many years of study and calibration in order to produce uniform reliability throughout the platform. The SHIPREL project¹⁰ aims at the development of the foundations for probabilistically based ship design rules.

Depending on the problem to be solved one can address component or system reliability. In the case of statically determinant structures, the failure of a single component leads to the failure of the whole structure and thus a component reliability analysis can easily tackle the problem. However, in the case of statically indeterminate structures the systems approach should be used because the structure is able to withstand a failure of one or several components by redistributing the load to the remaining operational components^{12,13}. This is particularly true in complex structures such as ships or offshore platforms that are considerably statically indeterminate thus redundant¹⁴⁻¹⁶.

For the marine structures the two fundamental structural components are the stiffened plates and the stiffened cylinders (see fig. 2.1 and 3.1). These components

present similar orthogonal framing systems with the spacing between small stiffeners much smaller than between the large stiffeners. However, they have a fundamental difference; the curvature of the shell element. The stiffened plate applies to a large variety of structures, such as, ships, semi-submersibles, TLP's and others. They are found in flat bottom structures, side shells, decks and other structures. The stiffened cylinders are normally divided in two categories, the ring stiffened cylinders and the ring-stringer stiffened cylinders. For this study the second type was considered due to its greater similarity to the stiffened plate. This type of cylinder is usually found as main structural elements in the legs of buoyant offshore platforms such as semi-submersibles and tension leg platforms.

From all applications of stiffened plates its application in ships is by far the most important. The ships in service are subjected to several load types. The most important are the stillwater and the wave induced bending moments. These bending moments are resisted by the longitudinal tension/compression of the plating system mainly of deck and bottom. Thus the individual stiffened plate element is usually designed to withstand buckling under longitudinal compression.

Transverse loading effects that can significantly reduce the plate strength is taken into account by models of biaxial compression^{17,18}. Lateral pressure effects are also being studied^{19,20} and considered to be utilised in design of side and bottom structures.

In spite of the recognised system behaviour of this kind of structure, it has been traditionally treated as a problem of component failure instead of a system. This is due to the highly complex redistribution mechanism that occurs after the strains for a single element passed the value corresponding to its maximum load which will, in many cases, lead to overload of other elements and to their successive collapse. Thus for practical purposes the maximum load carrying capacity for a plate element will in many situations also indicate the collapse of the whole panel.

A recent work²¹ presents the results of different approaches to this problem, comparing the case of a single plate with systems of several plates in parallel. From this study one can conclude that an high correlation between the plates implies the collapse of the whole panel. The high correlation exists because all plate elements are subjected to the same load and they all have the same geometry and material. Nevertheless, further work is necessary in order to properly model the redistribution mechanisms to prevent the use of a too conservative model in design. Also from this study was clear that the large differences between predictions from the different formulations indicate the need of studying their model uncertainties.

The design of the ring-stringer stiffened cylinder is a problem of a single component failure. Its large dimension and role played in the structure justified this kind of assumption. However offshore structures are in general treated as highly complex structural systems composed of many interconnected single components. Jacket platforms are handle in such a way that only a finite number of failures are prone to occur²² and a system reliability analysis is carried out assuming these failure modes associated in a certain way (series, parallel, etc.). However in practical cases the combination of all possible failure modes leads to unsolvable problems. Thus some simplifications and assumptions are necessary and only the most important failure modes are considered in the analysis.

The identification of these most important failure modes is a very time consuming task and the available algorithms in use are far from optimum^{12,23,24}. During the past decade extensive research has been performed in order to optimise these algorithms and several approximate methods were developed²⁵. But in spite of this development the full application of structural system reliability theory to practical design is still in his infancy, it is already understood and used as an important qualitative design tool in offshore engineering²⁶.

1.2 - Review of the reliability methods.

Structural reliability has justification in the random nature of the variables involved in structural analyses. In a report²⁷ produced for the ASCE Task Committee on Structural Safety a general idea of the probability-based design is presented. The first measure of structural safety was proposed by Cornell¹ in 1969 under the name of Mean Value First-Order Second Moment Reliability Method (MVFOSM) and consists of an index (reliability index) obtained as the ratio of mean safety margin to its standard deviation.

In a paper presented by Mansour²⁸ at the Annual Meeting of SNAME in 72, he gives the first serious contribution to the probabilistic analysis of ships. In the paper a probabilistic model for ship structural design is developed.

In this same year the ASCE Task Committee on Structural Safety (ASCE-TCSS) produced a review paper²⁹ presenting the state-of-art up to the early 70's. In 74 the ASCE-TCSS presented a group of six very important papers^{3,30-34} addressing several topics ranging from structural safety and design to reliability of structural systems.

The Cornell index soon proved to be limited because it is not invariant to different equivalent formulations of a same problem and is not robust with non-linear safety margins and requires normal distributed variables. To avoid the invariance and robust problems Hasofer and Lind³⁵ proposed another reliability index (geometric reliability index) which is defined as the shortest distance of the failure surface from its origin in standardised normal space. The last constraint has been removed by Rackwitz and Fiessler³⁶ who proposed an equivalent normal tail approximation for non-normal distributions and an iterative algorithm (Rackwitz-Fiessler Algorithm) which is known as the Advanced First-Order Second Moment Reliability Method (AFOSM).

To calculate the Hasofer and Lind geometric reliability index (β_f), Rackwitz and Fiessler in their iterative algorithm use a limit state function defined as follows:

$$G(\underline{x}) = \sigma_0 \phi_x - \sigma_s \quad (1.1)$$

in which the terms σ_s represents the load and $\sigma_0 \phi_x$ the resistance where σ_0 is the yield stress of the material. Both terms can depend on several random variables as appropriate for the case studied and $G(\underline{x}) < 0$ denotes the failure condition.

The probability of failure defined as the n-fold integral in the failure domain:

$$P_f = \int_{G(\underline{x}) \leq 0} f_x(\underline{x}) \, d\underline{x} \quad (1.2)$$

is simply obtained by:

$$P_f = \Phi(-\beta_f) \quad (1.3)$$

where $f_x(\underline{x})$ is the joint probability density function of the design variables in the vector $\underline{x}=(x_1, x_2, \dots, x_n)$ and Φ is the normal standardised distribution.

The partial safety factors (PSFs) and the sensitivities are other two values provided by the reliability analysis and are associated with the importance of the different random variables in the reliability problem. The partial safety factors are given by the ratio of the specified values of the design variables and their values at the design point $\underline{x}^*=(x_1^*, x_2^*, \dots, x_n^*)$.

$$PSF_i = \frac{x_i}{x_i^*} \quad (1.4)$$

The sensitivities are given by the unit vector $\underline{\alpha}=(\alpha_1, \alpha_2, \dots, \alpha_n)$:

$$\alpha_i = -\frac{\partial}{\partial x_i} G(x_i) / \left[\sum_{x_k} \left(\frac{\partial}{\partial x_k} G(x_k) \right)^2 \right]^{1/2} \quad (1.5)$$

Alternative reliability indices were proposed by Veneziano³⁷ and Ditlevsen³⁸. They are both more general and more difficult to apply. Ditlevsen³⁸ also discusses several versions of reliability indices and refers the problem of invariance.

In the beginning of the 80's another work³⁹ from ASCE integrates all elements relevant to the reliability analyses and its application to fixed jacket platforms.

Based on the Rosenblatt transformation Gollwitzer and Rackwitz⁴⁰ developed a general procedure that allows the treatment of problems involving non-normal and correlated random variables and in a later work⁴¹ they proposed a procedure of searching for the reliability index by using first order reliability concepts with quadratic optimisation with multiple non linear constraints.

From all algorithms available for reliability analysis the Rackwitz-Fiessler one is the most popular mainly due to its efficiency and simplicity. However other proposals⁴²⁻⁴⁴ claim to be more accurate and efficient.

The methods mentioned above prove to behave correctly in the presence of linear limit state surfaces however significant error occurs in the presence of curved surfaces. To handle this problem correctly several approaches^{41,45-47} were developed. Madsen⁴⁵ proposed to extend the first order reliability method to a second order approach to obtain a better approximation of the failure probability. Gollwitzer and Rackwitz⁴¹ proposed a joint procedure with first order concepts and quadratic optimisation with multiple non-linear constraints.

Recently more enhanced and robust methods for evaluating reliability are being developed. They are based in Monte Carlo (MC) simulation methods and can be divided in two different classes: i) the zero-one indicator-based methods which use the random variable's space (x-space) and ii) the semi-analytical, conditional expectation methods based in the transformed variable's space (u-space). Because MC methods are very time consuming variance reduction techniques (VRT) are usually applied to increase their efficiency. Stratified sampling and, in particular Latin hypercube sampling are one type of VRT. Another type is the importance sampling technique⁴⁸. A general VRT are the conditional expectation methods, namely the i) directional simulation methods and the ii) axis-orthogonal simulation methods. A good description of these methods can be find in a recent review⁴⁹.

The development of system reliability methods has progressed in parallel with the work for single components. The development of practical methods for structural system reliability analysis was initiated by Moses⁵⁰ who proposed the incremental load method in the formulation of the system safety margin equation. The basic idea behind this method is that a structure is progressively "unzipped" as successive members or components reach their strength capacity until overall failure occurs^{50,51}. Later Moses extended the incremental load method to identify the most important or significant failure modes using the deterministic truncating criteria²³. This method is attractive in that it can allow for the post-ultimate behaviour of a failed component.

After Moses presented the incremental load method several other useful methods have been proposed⁵²⁻⁶¹. The most relevant are briefly described here:

-Murotsu et al.⁵³ proposed a heuristic procedure of automatically identifying the stochastically dominant failure modes with probabilistic truncating criteria. Their proposal are used to system reliability analysis of two dimensional framework structures under combined axial force, bending moment and shear force based on plastic failure criteria.

-Thoft-Christensen and Sorensen⁵⁹ presented two formulations of the so called " β -unzipping" method for frame structures in which yielding failure was consider. Later Thoft-Christensen²⁶ extended the method to take into account the various failure elements, such as failure due to yielding, buckling, fatigue, punching, shear etc, by which the system safety index at different failure levels was evaluated.

-Melchers and Tang⁶⁰, extended the incremental load method to truss structures with a more general member behaviour to derive the limit state expression and proposed an iterative approach, the so called "Truncated Enumeration Method (TEM)", to systematically determine the probabilistic most dominant failure modes through an exhaustive searching procedure.

-Lee and Faulkner⁶¹ have presented the "extended incremental load method". This extends the conventional incremental load method by Moses⁵⁰ to include structures under multiple loading conditions which has been a major limitation of the incremental load method. Moreover it can more realistically allow for the post-ultimate behaviour of a failed component that can now be characterised by the post-ultimate slope and the residual strength. Also, strength formulae can be used in the limit state equation based on the utilised strengths of components failed at each incremental

stage. This method has been successfully used in the reliability analysis of TLP's ⁶².

All of the above mentioned methods look at the problem in terms of failure events. The complementary approach, or so called the "stable configuration or survival set approach", was suggest by Bennett⁶³. This was proposed as an alternative for system reliability analysis and it was claimed that it could predict upper bounds of system failure probabilities. However, computational work is much more expensive than the methods mentioned earlier.

The application of reliability methods to marine structures is reviewed in several works^{25,26,64-67}. The study of the application of reliability to the design of stiffened plates and cylinders has been done over the years and several significant contributions exists^{21,68-73}.

Due to the growing importance of structural reliability several text books had been published ^{12,13,74-78} and a series of software packages had been developed⁷⁹⁻⁸². They constitute the fundamental contribution to the establishment and dissemination of this theory.

1.3 - Review of the design methods for plates and cylinders

The prediction of the structural behaviour of these components is essential for the correct design of marine structures, particularly their behaviour under compressive loads⁸³. The emphasis with the compressive strength of the components is due to the fact that the primary modes of collapse of the main structures are closely linked to their compressive failure. In general most structures are designed for this type of collapse and thus this will be the failure mode considered in the study.

These components generally fail in an elasto-plastic manner which requires good modelling of inelastic collapse. In Ref. [84] the authors present the two basic methods used for practical design: the plasticity η -method and the interaction ϕ -method.

$$\begin{aligned}\sigma_c &= \eta_s \sigma_e \\ \sigma_c &= \phi \sigma_0\end{aligned}\tag{1.6}$$

where σ_c represents the collapse stress, σ_e is the elastic buckling stress and σ_0 is the material yield stress. The η_s in this case represents the plasticity reduction factor but it

should be noted that it is also used in this thesis as the welding residual stress tension block parameter.

The η -method has most frequently been used for slender structures that are slightly affected by plasticity, that is, air and space-craft structures⁸⁵⁻⁸⁶. However, this method has been successfully used in incorporating the effects of residual stresses by the structural plasticity reduction factor (η_s).

The ϕ -method has most frequently been used for more stocky structures and is widely used in civil engineering and in marine structures. The ϕ function is an empirical function related to the structural slenderness. Several slenderness parameters may be used, but the most general one is the reduced slenderness ($\lambda = \sqrt{\sigma_0/\sigma_e}$). In this study all formulations used for the strength of the reinforced plates and cylinders are based in the ϕ -method.

1.3.1 - Stiffened plates.

The approach generally adopted to study the compressive strength of the reinforced plates is to isolate the behaviour of the unstiffened plate element and afterwards to predict the interactive collapse of the combination of the stiffener with the associated plate.

Several closed form expressions exist for predicting the behaviour of the unstiffened plate component. For their longitudinal strength under compressive loads the most relevant expressions are the proposals of Faulkner⁸⁷, of Ivanov and Rousev⁸⁸, of Carlsen⁸⁹, of Guedes Soares^{90,91}, of Ueda and Yao⁹² and of Soreide and Czujko⁹³. For the transverse strength under compressive loads the two relevant expressions result from the proposals of Faulkner¹⁹, of Valsgard⁹⁴ and ABS⁹⁵.

The biaxial strength under compressive loads is assessed by considering an interaction equation that accounts for the simultaneous action of longitudinal and transverse stresses. The most relevant interaction equations are the following: the interaction equation proposed by Faulkner et al.¹⁹, the ones proposed by Valsgard¹⁷, by Dier and Dowling⁹⁶, by Stonor et al⁹⁷ and the interaction equation adopted by the BS5400⁹⁸ and the Rules of both the American Bureau of Shipping (ABS)⁹⁵ and Det norske Veritas (DnV)⁹⁹.

For the longitudinal strength of stiffened plates under compressive loads several closed form expressions have been proposed. These closed form expressions are based

on the beam-column concept (stiffener plus associated width of plating). The most relevant formulations for marine structures are the ones of Faulkner¹⁰⁰ and Carlsen⁸⁹. The proposal of Faulkner is based on a Johnson-Ostenfeld type of column formulation together with the effective width approach for the plate behaviour while Carlsen uses the Perry-Robertson “first-yield” concept in his formulation.

1.3.2 - Ring and stringer stiffened cylinders.

The buckling strength of these components depends upon the loading conditions to which they are subject. There are models for describing the behaviour of the ring-stringer cylinders under axial compression, radial pressure and for the combination of these two loads. The stiffening system composed by the rings and stringers create the possibility of several types of failure modes under the applied loads. However, the normal design situation makes the combined stringer and shell buckling (bay instability) as the weakest failure mode. For bay instability, the stress is mainly a function of the moment of inertia of both the stringers and the attached shell. The reason behind the preference given to the bay instability as the design failure mode, is related to the fact that it produces less dramatic effects. This failure mode can be obtained by designing the stringers in such a way that the collapse can only be precipitated by the shell between stringers.

For the ultimate strength of ring-stringer cylinders several closed form expressions exist. In the study, the expressions presented in four different codes of practice^{6,98-100} were compared and discussed. For the axial compression load case the RCC⁶ formulation and the two proposals of API¹⁰¹ (orthotropic and discrete formulations) were used. Also the Det norske Veritas and the ECCS formulations¹⁰²⁻¹⁰³ were considered. For the radial pressure load case the RCC formulation, the two proposals of API (orthotropic and discrete formulations) along with DnV were used. For the combined load case three different interaction formulations were use (RCC, API and DnV).

1.4 - Aims and scope of the thesis

The major aim of the thesis is to demonstrate the use of reliability based methods for the development of design rules for marine structural components. The emphasis is put in demonstrating the importance of good strength modelling for the reliability assessment and the design of structures. Through sensitivity analysis it is evaluated

how the importance and uncertainty of the different variables is reflected in the partial safety factors and in the reliability analysis.

The study is based on the buckling strength formulations for the reinforced plates and cylinders. However many of the conclusions are general and can be easily applied to other components. The study also provides a useful insight into the problems facing the designer when using probabilistic based methods in the design of such components.

Very useful information about the behaviour of the formulations to the different design parameters is provided by systematic studies. This information constitutes an important aid to decision making in reliability design.

In this work only the component reliability is addressed. However, the results in terms of the adequacy of the strength formulations can be extended to system reliability because the component formulations are also used in system reliability analysis.

In Chapter 2 the relevant stiffened and unstiffened plate strength formulations are described and used in the systematic studies. For each load case the reliability index and the importance measures are evaluated for the different formulations and slendernesses. Also an economical comparison based in the structural weight is done for several safety levels in all load cases.

In Chapter 3 the ring-stringer stiffened cylinder's strength formulations are described and their model uncertainty evaluated using a new updated test specimens database. For each load case the reliability index and the variables importance are evaluated for the different formulations. Using these results an optimisation study was performed for fixed safety levels using the mean thickness concept.

In Chapter 4 the importance of good strength modelling for reliability based design is discussed. A strength modelling criteria is presented and used in the improvement of the strength formulations for ring and stringer stiffened cylinders. At closure some considerations are made about the importance of the random variables in the reliability assessment.

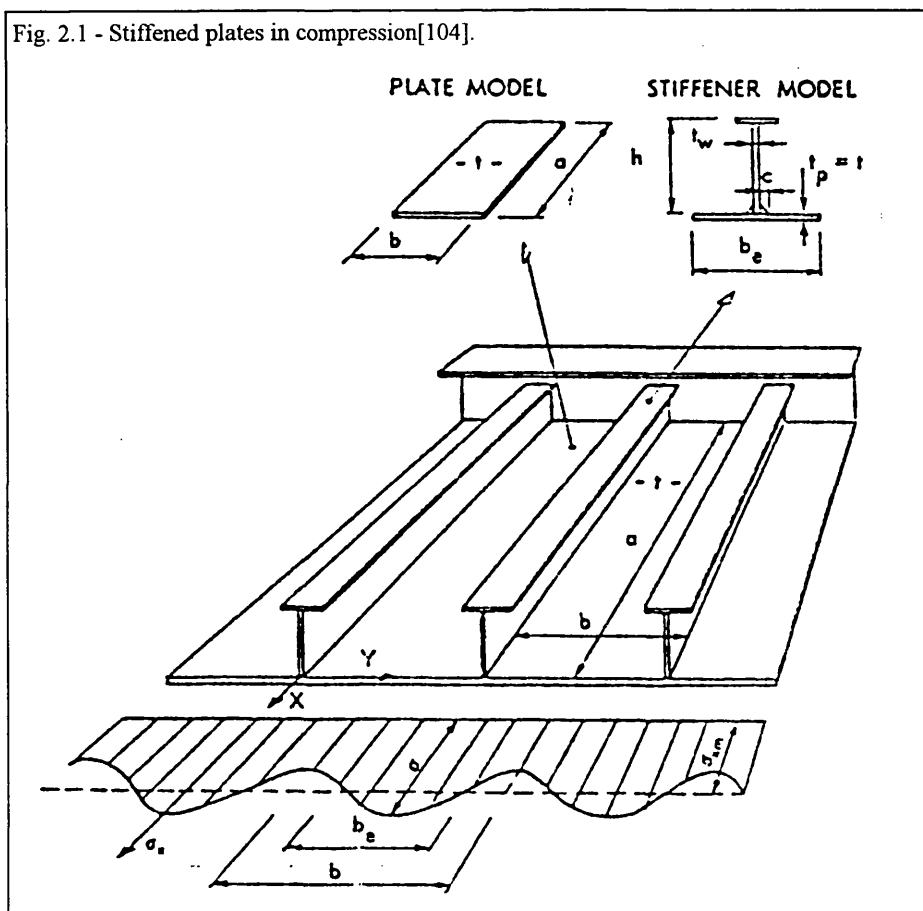
The full presentation of the results of the study is included in the four appendices. In Appendix 1 the graphical output of the plates reliability analysis is presented. Appendix 2 presents the tables of the cylinders uncertainty modelling results. Appendix 3 presents the graphical output of the cylinders uncertainty modelling and Appendix 4 presents the graphical output of the cylinder's reliability analysis.

CHAPTER 2 - RELIABILITY ANALYSIS OF STIFFENED PLATES

2.1 - Introduction.

Stiffened plates are the main structural component in marine structures. They are composed of plates reinforced by stiffeners closely spaced in the longitudinal direction and by transverse girders sparsely spaced (Figure 2.1). These components can be found in ships, semi-submersibles, TLP's and other marine structures. They exist in flat bottom structures, side shells, decks and other structures.

The prediction of their behaviour is essential for the correct design of marine structures, particularly their behaviour under compressive loads. The emphasis with the compressive strength of the stiffened plates, is due to the fact that the primary mode of collapse of the main structures is closely linked with the compressive failure of the stiffened plate. Overall collapse results from the simultaneous buckling of both longitudinal and transverse stiffeners. In practice, most structures are designed to avoid such type of collapse by using heavy transverse stiffeners. This leads to inter-frame



buckling of stiffened plate as the design mode.

The approach generally adopted to study this problem is to isolate the behaviour of the unstiffened plate element and afterwards to predict the interactive collapse of the combination of the stiffener with the associated plate. The study of these two sub-problems is, from a reliability point of view, fundamental to the correct understanding of the effect of the various parameters on the stiffened plate behaviour.

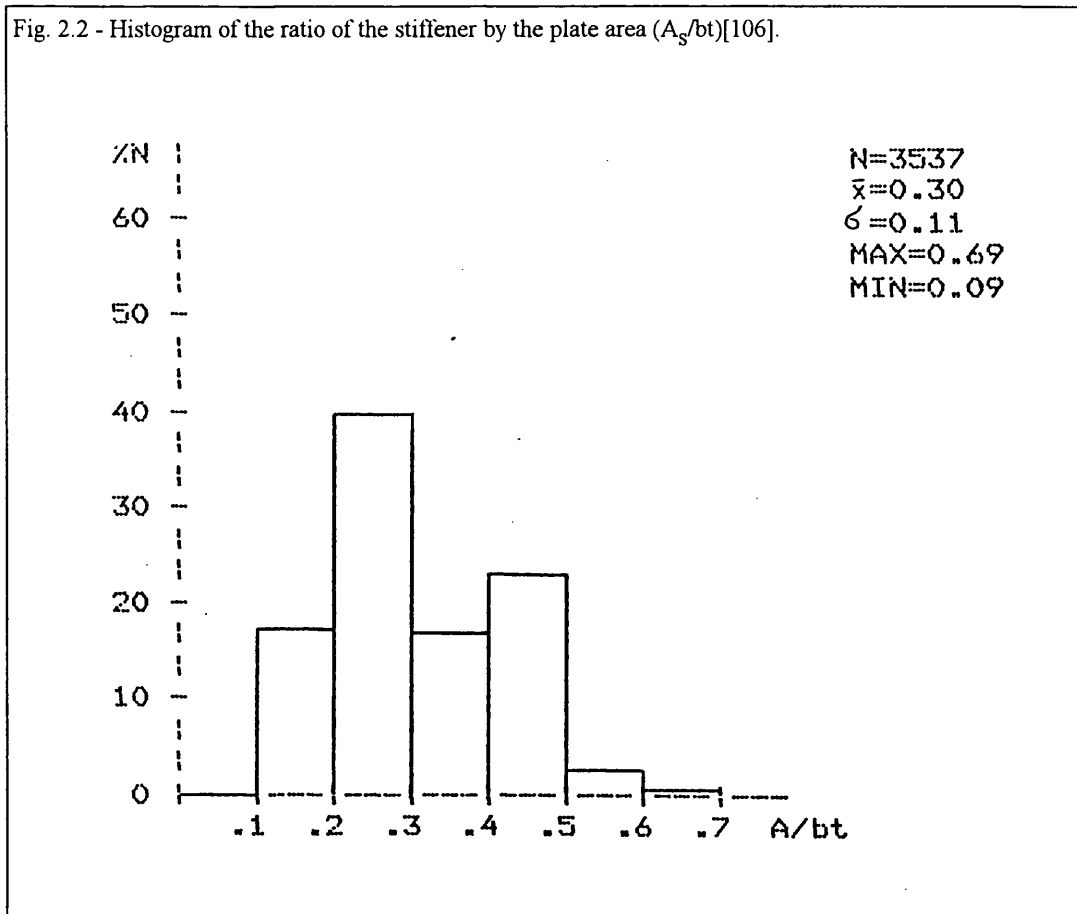
In this chapter the behaviour of the stiffened plate is studied under uniaxial and biaxial loading. The relative importance of each of the load types will change with the type of structure and for each one from location to location. In the present case a structural component (stiffened plate) located amidships and in the deck will be considered and a first order reliability method (FORM) will be used⁷⁹ to calculate the generalised reliability index (β_f). For describing of the plate strength various formulations are considered and comparison of their results is done. The study is divided in two parts. In the first, the reliability assessment of the unstiffened plate is conducted for all compressive load cases (longitudinal, transverse and biaxial) and in the second the reliability of stiffened plates is assessed for longitudinal compression.

Previous works^{21,73} have already focused on this problem. In Ref. [73] Guedes Soares considered a plate element under uniaxial loading and has conducted an uncertainty analysis based on second moment methods. In that study he predicted the uncertainty in the strength assessments and identified the most important variables. The study considered only strength variables and was further developed in²¹ by the extensive reliability assessment of unstiffened plates.

2.2 - Strength formulations for unstiffened plates.

In the case of a ship, the strength and stiffness of its primary deck structure depends critically on the behaviour of individual rectangular plate elements contained between stiffeners¹⁰⁵, which comprise typically 65% to 85% of the hull cross-sectional area (range equivalent to A_s/bt between [0.2, 0.5] in fig. 2.2)¹⁰⁶. This relatively large proportion of plating justified the extensive analytical, numerical and experimental studies undertaken for unstiffened plates over the past decades. This research led to a solid understanding of the behaviour of this component. In Ref. [104] an interesting insight is given to the influence of several parameters in the strength of unstiffened plates, such as the aspect ratio, residual stresses, initial distortions, boundary conditions and loading types.

Fig. 2.2 - Histogram of the ratio of the stiffener by the plate area (A_s/bt)[106].

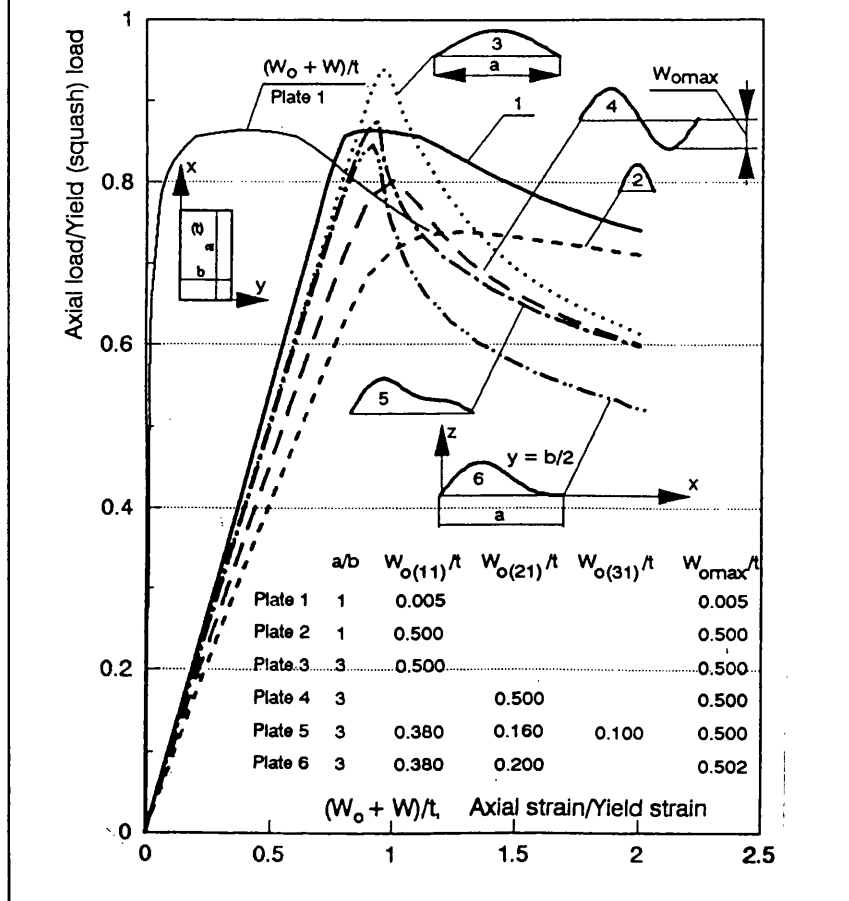


Strength is defined here as the maximum load carrying capacity that, for a given configuration, will be reached at different strains depending on the level of initial distortions and residual stresses.

In elasto-plastic collapse and particularly when the plates have initial defects, their load carrying capacity may still be significant after the maximum load is achieved, as shown for example in figure (2.3). However, the load shedding that occurs after the strains have passed the value corresponding to the maximum load will in many cases lead to overload of other elements and to their successive collapse.

Although for analysis purposes one can use any of the numerical codes available¹⁰⁷, it is more convenient for design to use closed form expressions. They are more appropriate to study the influence of various relevant parameters and are fundamental to the use of available reliability codes.

Fig. 2.3 - Load-end shortening curves for plates in compression with initial deformations[108].



2.2.1 - Formulations for longitudinal strength under compressive loads.

Different closed form expressions for longitudinal strength under compressive loads have been proposed in the past. Due to their importance in design some of them were considered in this work and their predictions compared from a reliability point of view. The methods of Faulkner⁸⁷, of Ivanov and Rousev⁸⁸, of Carlsen⁸⁹, of Guedes Soares^{90,91}, of Ueda and Yao⁹² and of Soreide and Czujko⁹³ were chosen and are briefly described in this section.

2.2.1.1 - Faulkner's formulation.

It is probably fair to say that Faulkner's formulation is the most widely used formulation for predicting the compressive strength of plate elements. The basis of the method was proposed in 1965¹⁰⁹ and their full description with its incorporation in stiffened plate design can be found in Ref. [87]. The general form of the expression is:

$$\left. \begin{aligned} \phi_F &= \frac{\sigma_u}{\sigma_0} = \frac{a_1}{\beta} - \frac{a_2}{\beta^2}, & \text{for } \beta \geq 1.0 \\ &= 1.0 & \text{for } 0 \leq \beta < 1.0 \end{aligned} \right\} \quad (2.1)$$

where β is the plate slenderness:

$$\beta = \frac{b}{t} \sqrt{\frac{\sigma_0}{E}} \quad (2.2)$$

with b and t being the plate width and thickness, σ_0 is the yield stress and E is the material's modulus of elasticity (Young's modulus). The constants a_1 and a_2 account for boundary conditions:

$$a_1=2.0 \text{ and } a_2=1.0 \text{ for simple support.} \quad (2.3a)$$

$$a_1=2.5 \text{ and } a_2=1.56 \text{ for clamped support.} \quad (2.3b)$$

Residual stresses, σ_r , are accounted explicitly by decreasing the plate strength by:

$$\Delta\phi_{Fr} = \frac{\sigma_r}{\sigma_0} \left(\frac{E_t}{E} \right) \quad (2.4)$$

where the magnitude of the compressive stresses is given by:

$$\frac{\sigma_r}{\sigma_0} = \frac{2\eta}{(b/t) - 2\eta} \quad (2.5)$$

and the width η of the weld tension block zone is suggest to be typically between 3 to 4.5.

The tangent modulus of elasticity E_t is given by:

$$\left. \begin{aligned} \frac{E_t}{E} &= \left(\frac{a_3 \beta^2}{a_4 + p_r (1 - p_r) \beta^4} \right)^2, & \text{for } 0 \leq \beta \leq 1.9/\sqrt{p_r} \\ &= 1.0, & \text{for } \beta > 1.9/\sqrt{p_r} \end{aligned} \right\} \quad (2.6)$$

The ratio of the structural proportional limit to yield stress is given by $p_r = (\sigma_p - \sigma_r)/\sigma_0$. The values for p_r normally lie between 0.5 and 0.75 and for design Faulkner⁸⁷ advises the use of 0.5. The constants a_3 and a_4 depend on the boundary conditions and are:

$$a_3=3.62 \text{ and } a_4=13.1 \text{ for simple support.} \quad (2.7a)$$

$$\alpha_3=6.31 \text{ and } \alpha_4=39.8 \text{ for clamped support.} \quad (2.7b)$$

An alternative formulation to equation (2.6) consists in approximating them with segments of straight lines, as proposed by Guedes Soares and Faulkner¹¹⁰ :

$$\left. \begin{aligned} \frac{E_t}{E} &= \frac{(\beta-1)}{1.5}, & \text{for } 1 \leq \beta \leq 2.5 \\ &= 1.0, & \text{for } \beta \geq 2.5 \end{aligned} \right\} \quad (2.8)$$

2.2.1.2 - Ivanov and Rousev formulation.

The method proposed by Ivanov and Rousev⁸⁸ uses another philosophy in that no account is given to residual stresses but initial deflections are considered explicitly. This method is of little use for perfect plates but proved reasonable for average levels of imperfection⁷³:

$$\phi_I = \frac{1}{1 + (0.3\beta + 0.08) w_0} \quad (2.9)$$

where $w_0 = \delta_0/t$ and w_0 is the non-dimensional amplitude of maximum distortions. The average values of w_0 can be predicted by the expression due to Faulkner $\delta_0/t = 0.11\beta^2$ where the coefficient 0.11 adopted in Ref. [73] is the average between the results of Faulkner⁸⁷ (0.12) and Antoniou¹¹¹ (0.10).

2.2.1.3 - Carlsen formulation.

The method proposed by Carlsen⁸⁹ accounts explicitly for both types of initial defects (initial deflections and residual stresses):

$$\phi_C = \phi_F \left(\frac{1}{1 + \sigma_r/\sigma_0} \right) \left(1 - \frac{0.75 w_0}{\beta} \right) \quad (2.10)$$

The coefficients for ϕ_F in this case are $\alpha_1 = 2.1$ and $\alpha_2 = 0.9$ for simple supports.

2.2.1.4 - Guedes Soares formulation.

The method proposed by Faulkner has been extended by Guedes Soares⁹⁰ so as to take into account explicitly both initial deflections and residual stresses:

$$\phi_{GS} = (1.08 \phi_F) \left\{ \left(1 - \frac{\Delta\phi_{Fr}}{1.08 \phi_F} \right) (1 - 0.0078 \eta) \right\} \left\{ 1 - (0.626 - 0.121 \beta) \frac{\delta_0}{t} \right\} \left(0.665 + 0.006 \eta + 0.36 \frac{\delta_0}{t} + 0.14 \beta \right) \quad (2.11)$$

where this expression is valid for $\beta > 1.0$.

In this expression the first term indicates the strength of a perfect plate. The first and second term will give the strength of a plate with residual stresses while the first and third term predict the effect of initial deflections. Whenever there are both effects the four terms must be used since the last one models the interaction between initial deflections and residual stresses.

This expression, which was derived for simply supported plates, can also be used for clamped plates if the adequate expression for ϕ_F is use, i.e. choosing the appropriate values for the coefficient α_i in equations (2.3b, 2.7b).

Another equation was proposed by Guedes Soares⁹¹ which depends only on plate slenderness and has inbuilt the influence of the average levels of initial deflections and residual stresses existing in merchant ships:

$$\left. \begin{aligned} \phi_{GS_m} &= \frac{1.6}{\beta} - \frac{0.8}{\beta^2}, & \text{for simple supports.} \\ &= \frac{2.0}{\beta} - \frac{1.25}{\beta^2}, & \text{for clamped supports.} \end{aligned} \right\} \quad (2.12)$$

or in warships:

$$\left. \begin{aligned} \phi_{GS_w} &= \frac{1.5}{\beta} - \frac{0.75}{\beta^2}, & \text{for simple supports.} \\ &= \frac{1.85}{\beta} - \frac{1.15}{\beta^2}, & \text{for clamped supports} \end{aligned} \right\} \quad (2.13)$$

2.2.1.5 - Ueda and Yao formulation.

Ueda and Yao⁹² have made a least square fit to results of finite element calculations and proposed for simply supported plates with initial deflections the following expression:

$$\phi_U = \frac{1.338 w_0^2 + 4.380 w_0 + 2.647}{\beta + 6.130 w_0 + 0.720} - 0.271 w_0 - 0.088 \quad (2.14)$$

2.2.1.6 - Soreide and Czujko formulation.

Soreide and Czujko⁹³ studied plates under biaxial loading but proposed also an equation for almost perfect plates uniaxially loaded:

$$\phi_{s0} = \frac{2.74}{\beta} - \frac{2.56}{\beta^2} + \frac{0.921}{\beta^3} \quad (2.15)$$

To account for initial deflections and residual stresses, the previous equation ϕ_{s0} should be modified to become:

$$\phi_s = 1.52 \phi_{s0} \left\{ 1 - 2.528 \left(\frac{w_0}{b/t} \right)^{0.113} \left(\frac{1.207}{\beta} - \frac{1.467}{\beta^2} + \frac{0.59}{\beta^3} \right) \right\} \quad (2.16)$$

However, this formulation is inconsistent for very small imperfections and thus should be restricted to the range of $\delta_0 t/b$ between 0.01 and 0.10.

2.2.2 - Formulations for transverse strength under compressive loads.

When the plates are loaded on the edge of their larger dimension, it is considered that they have a transverse loading. Their mode of failure is significantly different from that under longitudinal load. While in the later case they fail with multiple waves, depending on their length, in the first one they always collapse in a half wave mode.

The expressions for transverse plate strength are less common than the previous ones for longitudinal strength and the three most relevant were considered for the study.

2.2.2.1 - Faulkner formulation.

The ultimate strength of plates under transverse load can be calculated by the following equation proposed by Faulkner et al.¹⁹:

$$\phi_{Fy} = \frac{0.9}{\beta^2} + \frac{1.9}{\beta\alpha} \left(1 - \frac{0.9}{\beta^2} \right) \quad \text{for } \beta \geq 1 \text{ and } \beta\alpha \geq 1.9 \quad (2.17)$$

where $\alpha = a/b$ is the plate aspect ratio, a is the plate length and b its width. This formulation is based in Blanc's method¹¹² and according to Valsgard⁹⁴ their results

present a significant skewness with slenderness, overestimating the plate strength for stocky plates and underestimating for slender ones.

2.2.2.2 - Valsgard formulation.

In the same report⁹⁴ Valsgard proposed a different formulation fitted to his numerical calculations:

$$\phi_{vy} = \frac{\phi_F}{\alpha} + 0.08 \left(1 - \frac{1}{\alpha}\right) \left(1 + \frac{1}{\beta^2}\right)^2 \quad (2.18)$$

2.2.2.3 - ABS formulation.

ABS formulation⁹⁵ is based on the Bryan elastic buckling stress combined with Johnson approach to account for the effects of plastic deformation. Thus, the buckling stress σ_{cr} of a plate transversely loaded is given by:

$$\phi_{Ay} = \frac{\sigma_{cr}}{\sigma_0} = \begin{cases} \sigma_e & \sigma_e \leq 0.5 \sigma_0 \\ 1 - \frac{1}{4} \frac{\sigma_0}{\sigma_e} & \sigma_e > 0.5 \sigma_0 \end{cases} \quad (2.19)$$

where σ_e is the elastic buckling stress given by:

$$\sigma_e = \sigma_0 \left(\frac{\pi^2}{12(1-\nu^2)} \frac{k}{\beta^2} \right) \quad (2.20)$$

and the buckling coefficient k accounts for the type of loading and of boundary conditions. For a wide plate with linearly varying transverse load k is given by¹¹³:

$$k = \left(1 + \frac{1}{\alpha^2}\right)^2 \frac{2.1}{\psi + 1.1} \quad \text{for } 0 \leq \psi \leq 1 \quad (2.21)$$

where the ψ factor is such that when the stresses on one transverse edge of the plate are σ on the other they are $\psi\sigma$ (thus, for uniform compressive stress $\psi=1$).

2.2.3 - Formulations for biaxial strength under compressive loads.

The strength of plates under biaxial load is assessed by considering an interaction equation that accounts for the simultaneous action of longitudinal and transverse

stresses. In this interaction equation the longitudinal and transverse strength is predicted by the different expressions given in the previous sections. Several interaction equations have been proposed^{17,19,95-99} and from them five were considered in the study.

2.2.3.1 - Faulkner formulation.

Faulkner et al.¹⁹ proposed in an early work the following parabolic interaction:

$$R_x + R_y^2 = 1 \quad (2.22)$$

where $R_x = \sigma_x / \sigma_0 \phi_x$ and $R_y = \sigma_y / \sigma_0 \phi_y$ are the ratios of the applied stresses by the respective plate strength in that direction, which are given by $\phi_x = \phi_F$ and $\phi_y = \phi_{Fy}$ respectively.

2.2.3.2 - ABS formulation.

The quadratic interaction seems to have gained acceptance in design codes:

$$R_x^2 + R_y^2 = 1 \quad (2.23)$$

It has been adopted in the rules of the American Bureau of Shipping (ABS)⁹⁵, in the BS 5400⁹⁸ and in the Det norske Veritas (DnV)⁹⁹. This quadratic interaction is referred in the text as the ABS formulation. This interaction requires normalising strengths based on a combination of Bryan and Johnson models. For longitudinal and transverse strength eqs.((2.19)-(2.21)) must be used with $k=4$ for the longitudinal case.

2.2.3.3 - Other formulations.

Valsgard¹⁷ generalised Faulkner proposal by including cross terms and by making the exponent of R_x a variable γ :

$$R_x^\gamma - \zeta R_x R_y + R_y^2 = 1 \quad (2.24)$$

On the basis of his numerical results for a plate with aspect ratio of 3, he proposed the following values for $\gamma=1$ and $\zeta=0.25$. The normalising equations are (2.1) and (2.18), respectively for the longitudinal and transverse directions.

Dier and Dowling⁹⁶ have considered the interaction curve not only in the first quadrant (biaxial compression) but also in the others (compression combined with tension and biaxial tension):

$$R_x^2 + 0.45 R_x R_y + R_y^2 = 1 \quad (2.25)$$

In view of all the uncertainty of the results Stonor et al⁹⁷ proposed the following lower bound interaction:

$$R_x^{1.5} + R_y^{1.5} = 1 \quad (2.26)$$

For Dier and Dowling (eq.(2.25)) and Stonor (eq.(2.26)) interactions Faulkner's expressions were used.

2.2.4 - Model uncertainty for unstiffened plates.

In this section the results of several uncertainty analysis^{90,114,115} are presented along with a short comments extracted from original references. The results are summarised in Table 2.1.

	Formulation	Sample	\bar{X}_m	$V_{Xm}\%$
Longitudinal compression	Faulkner	100	0.98	11%
	G. Soares	233	1.00	7%
Transverse compression	Faulkner	20	0.70	33%
	Valsgard	20	0.89	30%
	ABS	20	1.17	44%
Biaxial compression	Faulkner	385	0.94	24%
	ABS	385	1.21	31%

Table 2.1 - Model uncertainty for unstiffened plates.

For the longitudinal strength Guedes Soares⁹⁰ based his proposal (eq.(2.11)) on the analysis of 233 results. In that work Guedes Soares refers the uncertainty associated

with Faulkner's formulation ($\bar{X}_m=0.98$ and $V_{Xm}=11\%$) and quantifies the uncertainty of his proposal ($\bar{X}_m=1.0$ and $V_{Xm}=7\%$).

In two recent studies^{114,115} conducted at IST the model uncertainty for the transverse and biaxial strength is evaluated for several formulations. For the transverse case it was used the experimental work of Becker^{116,117} and Bradfield¹¹⁸. However, the results from Becker experiments on small tubes of square section has some drawbacks, especially for not allowing a good definition of the boundary conditions at the plate edges. The presence of weld induced stresses and initial deflections not accounted by the formulations can explain the characteristic overprediction of strength in Faulkner and Valsgard formulations ($\bar{X}_m=0.7$ and $\bar{X}_m=0.89$). ABS is clearly a conservative formulation ($\bar{X}_m=1.17$).

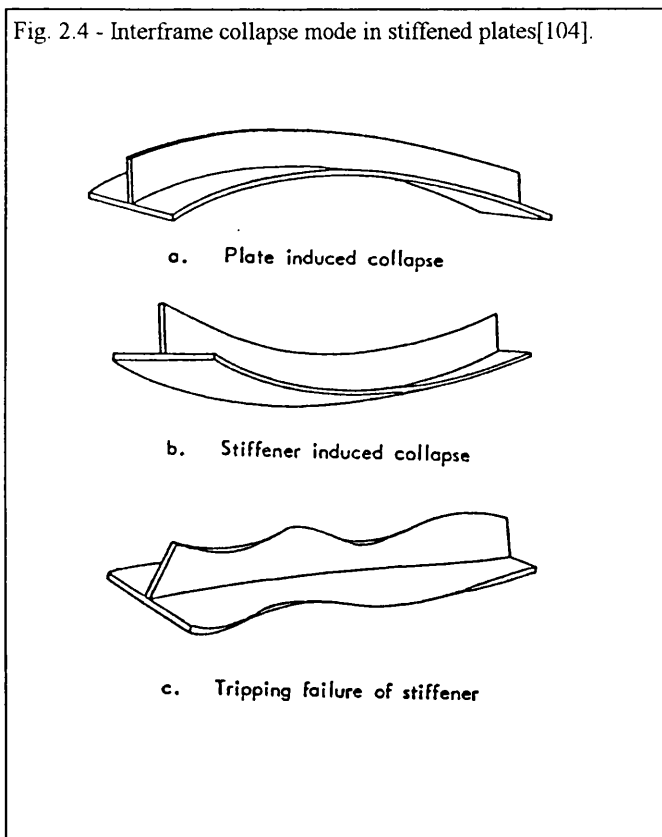
For the biaxial strength case published results of experimental work^{97,116,117} and of numerical calculations^{96,119} were used to assess the model uncertainty. The database used has 385 results from which 343 are numerical predictions by Dowling et al.^{96,119} and the remaining 42 are from the two experimental series of Becker et al.^{116,117} with 18 and 8 test models respectively, and from the 16 test models of Stonor et al.⁹⁷. The results indicate that Faulkner formulation is clear a mean value formulation but has significant scatter in the results.

2.3 - Strength formulations for stiffened plates.

The behaviour of stiffened plates under compression is relatively complicated due to the large number of possible combinations of plate and stiffener geometry, boundary conditions and loading. However, Smith et al.¹²⁰ systematised all this complexity in three main types of collapse, namely plate collapse, interframe flexural buckling and overall grillage collapse.

Plate collapse is the typical response of short stiffened panel, with a length equivalent to the width of the plate between stiffeners. In orthogonally stiffened panels the corresponding failure mode is the overall grillage collapse, which involves the failure of both longitudinal and transverse stiffeners. Optimum resistance can be attained by designing a stiffened panel in which the overall grillage and plate collapse modes occur for the same level of loading. However, such panels are very sensitive to imperfections and collapses violently¹²¹. From a safety point of view these characteristics are undesirable and therefore stiffened plates are generally designed with interframe flexural buckling as the weakest failure mode.

Fig. 2.4 - Interframe collapse mode in stiffened plates[104].



Interframe flexural buckling is a typical case of interactive collapse, triggered by the local buckling of either the plate or the stiffener. It is possible to have a failure towards the stiffener outstands (plate induced - PIF) or towards the plate (stiffener induced - SIF)¹²². The local failure of the stiffener (Fig. 2.4) may be due to flexural buckling¹²³ or to torsional buckling¹²⁴.

2.3.1 - Formulations for longitudinal strength under compressive loads.

The closed form expressions used in design are based on a beam-column concept, mainly due to Ostapenko¹²⁵. In this concept one isolated stiffener with an associated width of plating is considered as representative of the whole panel behaviour.

Several closed form expressions for longitudinal strength under compressive loads have been proposed^{89,100,126-129}. The methods of Faulkner¹⁰⁰ and Carlsen⁸⁹ were chosen and their predictions compared from a reliability point of view. These two methods are orientated to marine structures and are briefly described in this section.

2.3.1.1 - Faulkner's formulation.

In Ref. [100] Faulkner proposed a method based on a Johnson-Ostenfeld type of column formulation together with the effective width approach for plate behaviour. When a plate or a strut has a very high elastic buckling stress it happens that the unstable failure does not occur before the development of a certain degree of plastic deformation. This phenomenon obviously changes the collapse stress and, an empirical way of accounting for that effect is due to Johnson and Ostenfeld. According to them,

whenever the Euler buckling stress σ_E is higher than half the yield stress σ_0 , the critical buckling stress is given by:

$$\sigma_{JO} = \sigma_0 \left(1 - \frac{\sigma_0}{4\sigma_E} \right) \quad (2.27)$$

The effective width formulation is a way of expressing the diminishing of strength that a plate exhibits in the post-buckling regime. This weakening effect is expressed by a reduction of the width that effectively resists the compressive loads⁸⁷. According to Faulkner's method¹⁰⁰, the ultimate strength of a stiffened plate, modelled as a stiffener with an associated width of plate, is given by:

$$\phi_{Fs} = \frac{\sigma_u}{\sigma_0} = \frac{\sigma_{ed}}{\sigma_0} \left[\frac{A_s + b_e t}{A_s + bt} \right] \quad (2.28)$$

$$\frac{\sigma_{ed}}{\sigma_0} = 1 - \frac{1}{4} \left(\frac{a}{\pi r_{ce}} \right)^2 \frac{\sigma_0}{E}, \quad \text{for } \sigma_E \geq 0.5\sigma_0 \quad (2.29)$$

with $r_{ce}^2 = \frac{I_e'}{A_s + b_e t}$ and EI_e' is the buckling flexural rigidity of the stiffener with the reduced effective width of the plate b_e' given by :

$$\left. \begin{aligned} \frac{b_e'}{b} &= \frac{1}{\beta} \sqrt{\frac{\sigma_0}{\sigma_{ed}}} R_r & \beta \geq 1 \\ &= R_r & 0 \leq \beta < 1 \end{aligned} \right\} \quad (2.30)$$

The effective width of the plate b_e , is related to the slenderness as follows:

$$\frac{b_e}{b} = \left[\frac{2}{\beta} \sqrt{\frac{\sigma_0}{\sigma_{ed}}} - \frac{1}{\beta^2} \left(\frac{\sigma_0}{\sigma_{ed}} \right) \right] R_r, \quad \text{for } \beta \geq 1 \text{ and } \frac{\sigma_{ed}}{\sigma_0} \geq 0.7 \quad (2.31)$$

which implicitly account for initial deflection. The effects of residual stresses, biaxial loading and shear stresses can be reflected in the effective widths which should be reduced by the factors R_r , R_y and R_τ , respectively:

$$\left. \begin{aligned} R_r &= 1.0 - \left(\frac{2\eta}{b/t - 2\eta} \right) \left(\frac{\beta^2}{2\beta - 1} \right) \frac{E_t}{E}, & \text{for } \beta \geq 1.0 \\ &= 1.0, & \text{for } \beta < 1.0 \end{aligned} \right\} \quad (2.32a)$$

$$R_y = 1 - \left(\frac{\sigma_y}{\sigma_{yu}} \right)^2, \quad \sigma_y \leq 0.25 \sigma_0 \quad (2.32b)$$

$$R_{\tau} = \left[1 - \left(\frac{\tau}{\tau_0} \right)^2 \right]^{\frac{1}{2}} \quad (2.32c)$$

The tangent modulus of elasticity E_t is given by equations (2.6)-(2.8) and η the width of the weld tension zone. The method requires an iterative procedure to calculate the correct value of σ_{ed}/σ_0 but usually two to four iterations are sufficient.

2.3.1.2 - Carlsen formulation.

The method proposed by Carlsen⁸⁹ is based on a Perry-Robertson "first yield" formulation together with an effective width approach for the plate strength. The average stress in a plate-stiffener combination is given by:

$$\phi_{Cs} = \frac{\sigma_u}{\sigma_0} = \frac{A_e}{A_t} \left[\frac{(1 + \gamma^2 + \xi) - \sqrt{(1 + \gamma^2 + \xi)^2 - 4\gamma^2}}{2\gamma^2} \right] \quad (2.33)$$

where $\gamma^2 = \frac{\sigma_0}{\sigma_E}$ and $\xi = \frac{A_t \delta_0}{W}$ are respectively the Perry-Robertson magnification and imperfection factors.

Due to its small influence on strength of the assembly, the plate is considered to be fully effective when calculating σ_E and the section plate-stiffener modulus W . The stiffener deflection amplitude is always assumed to be $\delta_0 = 0.0015 a$. For plate induced failure, account is take for the shift of neutral axis due to loss of effectiveness of plate by $\delta_0 = 0.0015 a + z_p \left(\frac{A_t}{A_e} - 1 \right)$ where z_p is the distance from the neutral axis to the midplane of the plate.

The effective width of plate used to calculate the effective cross sectional area $A_e = A_s + b_e t$ is given by:

$$\frac{b_e}{b} = \frac{1.8}{\beta} - \frac{0.8}{\beta^2}, \quad \max = 1.0 \quad (2.34a)$$

$$\frac{b_e}{b} = 1.1 - 0.1\beta, \quad \max = 1.0 \quad (2.34b)$$

for the cases of plate induced and stiffener induced failures, respectively. These formulations are based on initial deflections equal to $0.01b$ and residual stresses of

0.2 σ_0 . To account for residual stresses in the stiffener the predicted strength is reduced by 5%.

2.3.2 - Model uncertainty for longitudinal strength of stiffened plates.

In Ref. [104] it can be found the results of a uncertainty analysis carried by Guedes Soares and Soreide for several strength formulations for longitudinally loaded stiffened plates. This study has been updated in a recent report¹⁸ where 119 test models used for the analysis are compiled in a database and were collected from the experimental work done by Faulkner¹³⁰, Horne and Narayan^{131,132}, Mathewson and Vinner¹³³, Smith¹³⁴ and Dowling¹³⁵. The results of the uncertainty analysis are summarised in Table 2.2.

	Sample	\bar{X}_m	$V_{X_m}\%$
Faulkner	119	0.951	12.6%
Carlsen PIF	119	1.192	16.9%
Carlsen SIF	119	1.022	16.3%

Table 2.2 - Model uncertainty for stiffened plates.

In Ref. [18] the results are organised by source of experiments in order to detect possible error sources and thus a compilation of results by type of welding procedure and boundary conditions is available. Two important conclusions were drawn in that work, first Faulkner formulation is the most reliable method for all cases studied, i.e. type of welding and boundary conditions, with the best bias and lowest COVs. Second the results for the plate induced failure are always more conservative than the ones for the stiffener induced failure and this is due to the fact that the effective width of plate recommended to calculate the effective area is always greater in SIF than in PIF.

2.4 - Reliability assessment of ship plates.

In this study two types of load effects in the ship hull were considered: global bending moments and local hydrostatic pressures. The still-water and the wave induced loads, which are the two main load¹³⁶⁻¹³⁸ components, will induce vertical bending

moments in the hull girder, leading to in-plane loads in deck and bottom plates. The wave induced load will be alternating between tension and compression as a function of the wave position along the ship. The strength of the plates under the different loading will be assessed from the existing formulations, as described in the previous sections.

Reference was made to past experience to choose for this study the most serious situation of the plate in compression. The values for the still-water bending moment were derived from the work of Guedes Soares and Moan¹³⁶ and the ones for the wave-induced moments were taken from the Rules of Classification Societies⁹⁹. Furthermore, the bottom plates will be subject to lateral pressure, which does not occur with deck plates, and which is taken with the nominal values prescribed by the Rules.

The hydrostatic pressure on the ship sides is resisted by the transverse frames and the associated plating, leading therefore to transverse stresses on deck and bottom plates. The relative magnitude of these stresses were estimated on the basis of calculations on a sample ship. In the study the transverse stresses will be given as a percentage of the stresses induced by the vertical bending moment in the hull (the transverse loading considered is 1/3 of the longitudinal load).

The transformation from load to load effect, i.e. from the bending moments to the stresses applied to the plates is made through the section modulus of the ship. It was assumed that typical ships has a section modulus given by the Rules of Classification Societies, in which case the normal in-plane stresses in the deck or bottom will be a function of the nominal stillwater and wave induced bending moments and of the ship section modulus Z_0 :

$$\sigma_s = g(M_s, M_w, Z_0) = \frac{M_s + M_w}{Z_0} \quad (2.35)$$

where Z_0 is referred to the deck or bottom depending on the case considered. The ultimate capacity of a plate element will depend on the material as given by the yield stress σ_0 and of the collapse mode as given by ϕ_x as described before.

Finally the limit state function is given by eq.(1.1) subtracting the load σ_s from the resistance $\phi_x \sigma_0$.

2.4.1 - Reliability of unstiffened plates under compressive loading.

In Ref. [73] the uncertainty of the predictions has been compared on the basis of a Mean Value second moment Reliability Method (MVRM), accounting only for the strength variables. Thus, the first step of the work was to compare the results of this previous approach with the ones obtained with the methodology now used (FORM).

The reliability method (FORM) requires the definition of the set of random variables to be used along with the failure surface (eq. (1.1)). Table 2.3 summarises the set of variables used in this study, namely the dimensions of a typical ship deck plate, its material properties and the ship section modulus with the corresponding loads.

Variables		Distribution	Mean	COV
Yield stress	σ_0 (MPa)	Log - normal	306.3	0.1
Young modulus	E (MPa)	Log - normal	2.0 E5	0.04
Length	a (m)	Normal	2.0	0.01
Width	b (m)	Normal	0.75	0.01
Thickness	t (m)	Normal	Variable	0.04
Width of weld	η (adim.)	Normal	5.25	0.07
Still-water bending moment.	M_s (MN)	Normal	2174.0	0.55
Wave bending moment.	M_w (MN)	Gumbel	8631.3	0.07
Section modulus	Z_0 (m ³)	Deterministic	78.14	-----

Table 2.3 - Description of the basic variables used in the unstifened plates reliability assessment.

The reliability index (β_f) plot (fig.(2.5)) compares the values obtained by the two different methodologies using the strength equation of Faulkner (eq.(2.1)) for different values of plate thickness (plate slenderness $\beta = b/t \sqrt{\sigma_0/E}$). It is apparent that both methodologies give almost the same results. The figure also shows the prediction of the strength equation, being apparent that the reliability indexes decrease quicker than the prediction method itself, as the plate slenderness (β) increases.

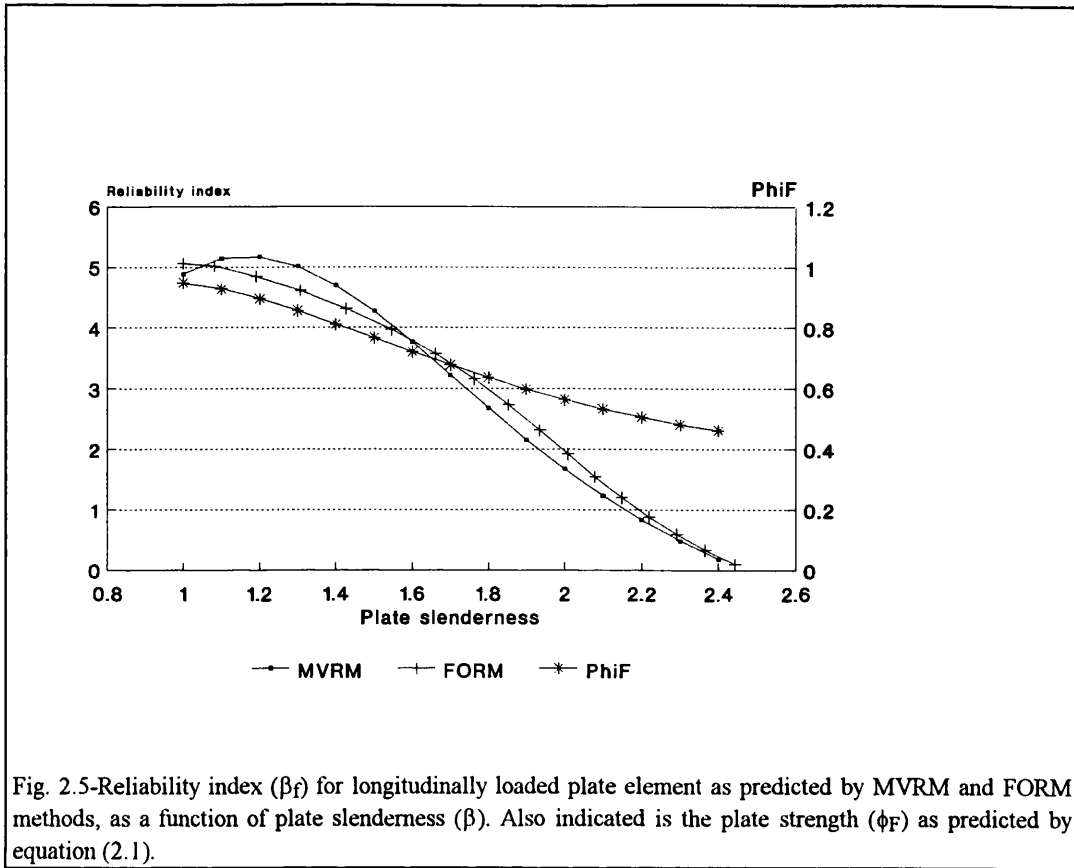


Fig. 2.5-Reliability index (β_f) for longitudinally loaded plate element as predicted by MVRM and FORM methods, as a function of plate slenderness (β). Also indicated is the plate strength (ϕ_F) as predicted by equation (2.1).

The sensitivity plots (fig. (A1.1)-(A1.2)) shows the relative importance of the different variables. It must be noticed that for both formulations the sensitivities for the load variables (M_s , M_w) have negative signs but are shown with positive values. The corresponding variables show for both methods similar behaviour except for the sensitivity with respect to the wave induced load. This is the result of using different types of probability density functions to describe this variable. In the MVRM one implicitly assumes that all variables are normally distributed while in the FORM analysis M_w has been model as a Gumbel distribution. The behaviour of the variables associated with plate slenderness (σ_0 , E , t , b) reflects the behaviour of Faulkner formulation for intermediate plates ($d\phi_F/d\beta = \text{maximum}$ for this range).

In this preliminary study the model uncertainty was not considered to allow comparison with the previous results⁷³. However, the importance of incorporating the model uncertainty related with the strength formulation is fundamental to the reliability assessment. In Fig.(2.6) the results for Faulkner formulation (eqs.(2.1)-(2.7)) are presented for three different model uncertainties (No bias), ($X_m=0.98$, $COV_{X_m}=11\%$) and ($X_m=0.98$, $COV_{X_m}=22\%$).

The results are compared for the three levels of safety in current use¹³⁹. The first refers to the Actual Design Safety (ADS) level for the Gulf of Mexico platforms, the second is the one proposed by ISO and the last is the recommendation of UK-National Petroleum Directorate (NPD). Comparing the results for the (ADS), one obtains differences in the weight of the structure of 45% between the extreme cases (FLK-unbiased and FLK-2bias). Also it can be seen that for the same difference in COV's (Δ COV=11%) corresponds two different gains in weight, i.e. for FLK-unbiased to FLK-biased the difference in weight is 13% and for FLK-biased to FLK-2bias is 29%. Other important aspect is again related to the growing differences in weight that occurs for higher safety levels (the differences between FLK-unbiased to FLK-biased are 13% for ADS, 21% for ISO and 36% for NPD).

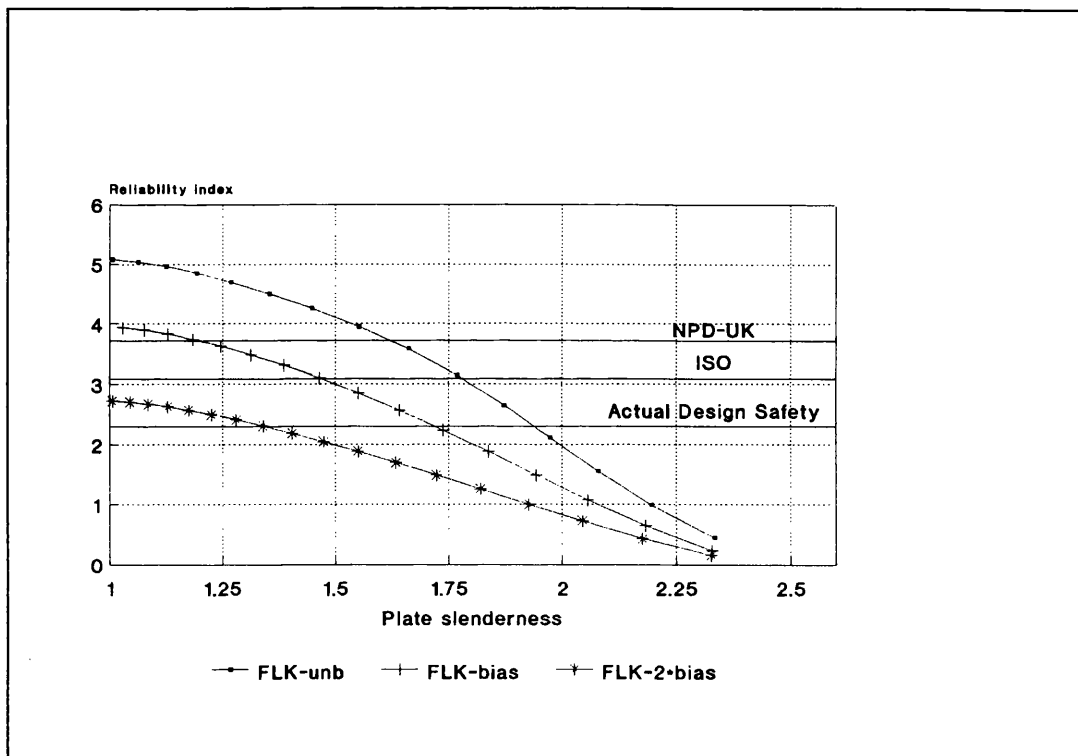


Fig. 2.6- Effects of the strength model uncertainty in the reliability assessment. Faulkner formulation for longitudinally loaded simply supported plates with initial deflections and residual stresses (eqs. (2.1)-(2.7)).

From the corresponding sensitivity plots (figs. (2.9), (A1.3)-(A1.4)) the importance of the strength modelling parameter is clear which increases in importance for high model uncertainties. From the other random variables the two reasonably important ones are the material yield strength (particularly for stocky plates) and the plate thickness. The width of weld tension zone grows in importance for slender plates but the two bending moments are the most important load variables.

Reliability results for different strength formulations used for the design of unstiffened plates are shown in figure (2.7). These formulations account for an average level of initial distortions and residual stresses. The plot presents the variation of the

reliability index (β_f) with the plate slenderness parameter (β) and allows for direct comparison of the formulations with the three standard levels of reliability considered ADS, ISO and NPD. The variation of reliability was again achieved by varying the plate thickness (t) and consequently the plate slenderness (β). This type of approach allows the comparison of the economy of the different formulations and the evaluation of their efficiency for design (see Table 2.4).

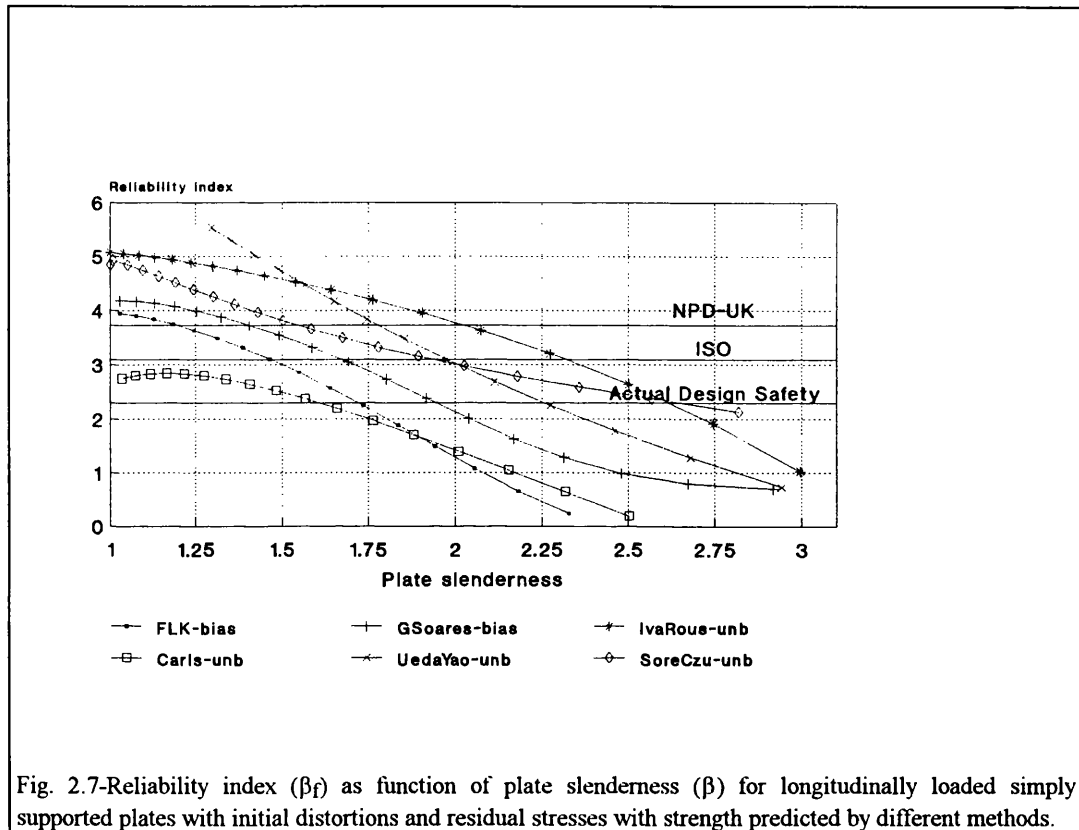


Fig. 2.7-Reliability index (β_f) as function of plate slenderness (β) for longitudinally loaded simply supported plates with initial distortions and residual stresses with strength predicted by different methods.

In this study all formulations were used, but only two can reasonably be compared (Faulkner(FLK) and Guedes Soares(GS)) because these two are the ones for which uncertainty values were derived⁹⁰. The other formulations are just used to exemplify the large differences that can arise in reliability analysis if the designer does not carefully choose the proper strength formulation and shops around. The reliability index (β_f) plot shows large spread in the results as one could expect from the differences in the formulations. Ivanov/Roussev and Ueda/Yao proposals only incorporate the plate deflections while the others also consider the residual stresses. This fact explains why these two formulations predict the highest values of reliability. The maximum difference in weight occurs for the actual safety level between the formulations of Soreide and Carlsen and is about 61%.

		Actual Design	ISO	UK-NPD
Safety levels	β_f	2.3	3.09	3.72-
GUEDES SOARES	β	1.94	1.67	1.4
	W/W ₀	85.8%	100%	119.1%
FAULKNER	β	1.72	1.47	1.19
	W/W ₀	96.9%	113.5%	140.1%

Table 2.4 - Comparison of the longitudinal strength formulations for different design conditions.

To adimensionalise the results it was selected the design point (W_0) which corresponds to the weight of single component (unstiffened plate) calculated with the formulation that with the minimum use of material satisfies the ISO safety requirement. That value, $W_0=0.103$ (ton/m) corresponds to the weight per unit length of one plate with a mean thickness of 17.6 mm designed with Guedes Soares formulation.

From Table 2.4 and figure (2.7) is clear that the methods of Guedes Soares (eq.(2.12)) and of Faulkner (eq.(2.10)) show the same type of dependence on plate slenderness (β) with GS formulation producing more economical design. The difference in weight for the structure is around 14% and is almost constant for the different safety levels $\Delta W/W_0 \in (12.9\%, 17.6\%)$. Also, it can be seen that for both formulations the difference in weight for the two limit safety levels (ADS and NPD) is about 43% (with 39% for GS and 46% for FLK), which indicates that much caution should be put by the designer/ruling body in the selection/establishing of the proper safety level for design.

The sensitivity plots (fig. (2.8)-(2.9)) show the importance of the variables in the formulations of GS and FLK. They show the same general trend for the variables but in the case of GS the importance of the modelling parameter is almost equivalent to the yield stress. This last aspect is a direct consequence of the low uncertainty of this formulation (COV=7%). The sensitivities obtained for the other methods (fig. (A1.5)-(A1.8)) have similar behaviour to these ones and are presented in Appendix 1. Inspection of the figures shows that the variables that contribute most to the reliability are the modelling parameter, the material yield stress⁷³, the plate thickness and the two loading variables, the still-water and the wave induced moments.

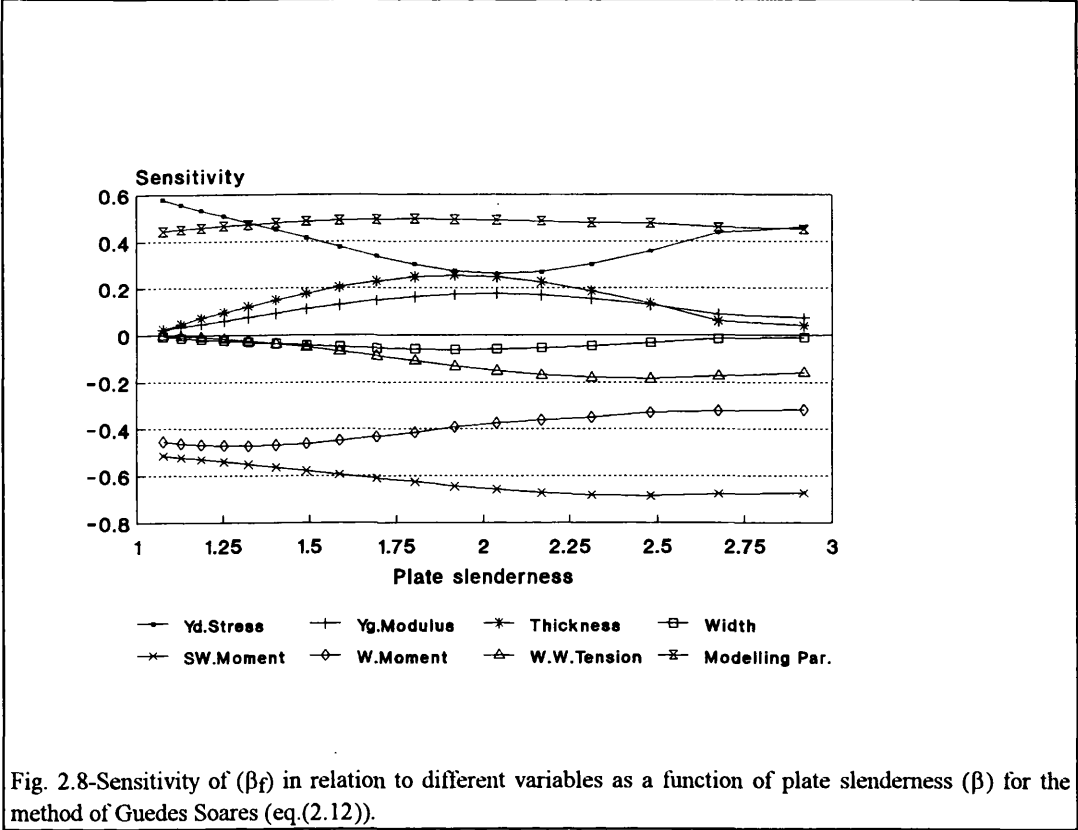


Fig. 2.8-Sensitivity of (β_f) in relation to different variables as a function of plate slenderness (β) for the method of Guedes Soares (eq.(2.12)).

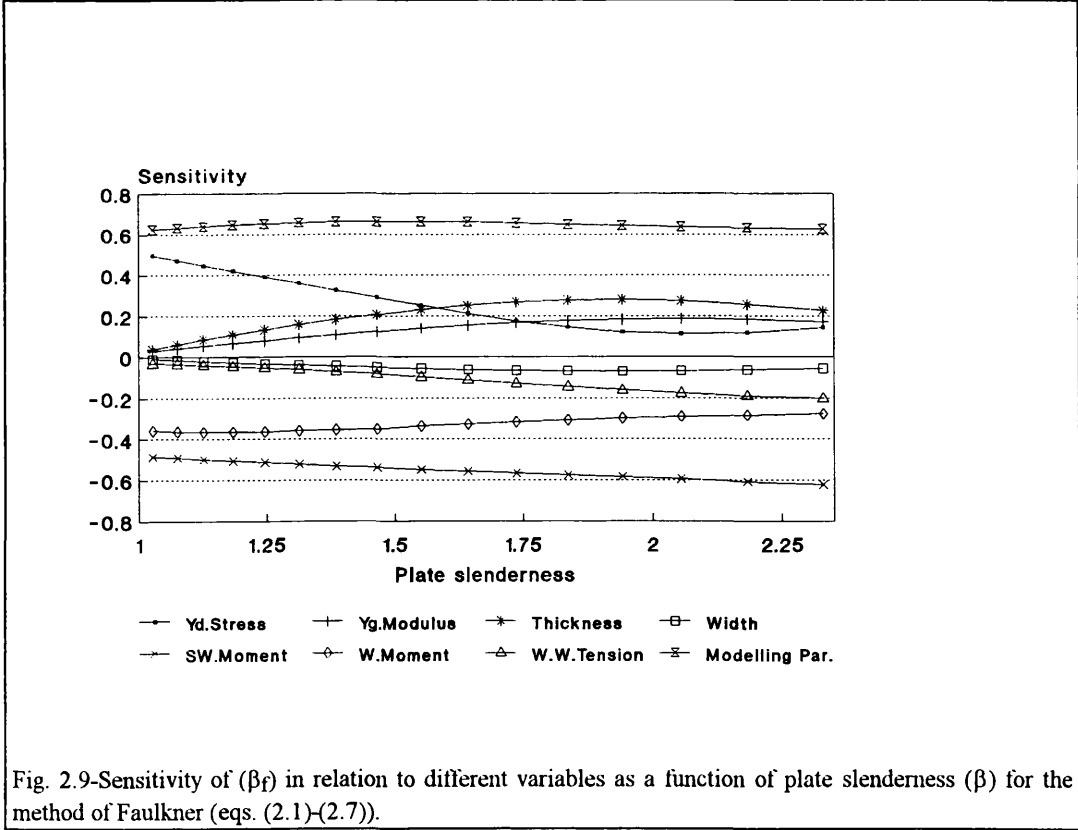


Fig. 2.9-Sensitivity of (β_f) in relation to different variables as a function of plate slenderness (β) for the method of Faulkner (eqs. (2.1)-(2.7)).

One additional conclusion of the present work is the importance that the correlation between variables has on the reliability of the plate elements. This importance was

studied through a series of calculations that have been conducted for a plate element considering different levels of correlation between the material properties (σ_0 , E), the geometrical characteristics (b , t) and the loading variables (M_s , M_w).

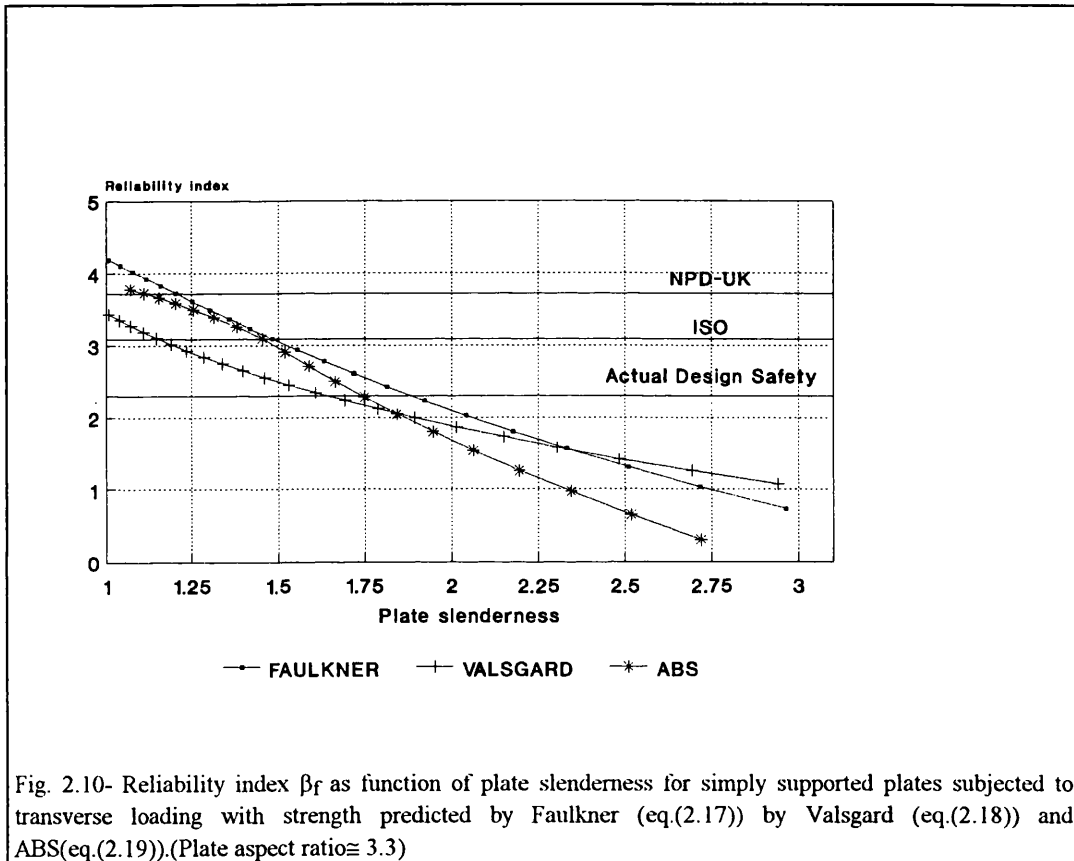
$\rho(\sigma_0, E)$	$\rho(b, t)$	$\rho(M_s, M_w)$	β
0.0	0.0	0.0	4.71
0.5	0.0	0.0	4.62
1.0	0.0	0.0	4.54
0.0	0.5	0.0	4.72
0.0	-0.5	0.0	4.70
0.0	0.0	-1.0	6.01
0.0	0.0	-0.5	4.85
0.0	0.0	0.5	4.08
0.0	0.0	1.0	3.66
0.5	-0.5	-1.0	5.82
1.0	0.5	1.0	3.57

Table 2.5 - Reliability index for a plate element under longitudinal load for different values of correlation between the variables.(eq.(2.1))

The results are show in Table 2.5 and apparently the correlation between the material properties or between the geometrical characteristics leads to very small changes in the value of the reliability index. However, the correlation between the loading variables induces significant changes, which range from 3.66 to 6.01, while the value of β_f for no correlation was 4.71. Furthermore, when there is additional correlation between material and geometrical variables the previous result maintains its scatter [3.57-5.82].

The reliability of unstiffened plates under transverse compression was also assessed in order to consolidate the results obtained for the longitudinal compression case. Thus, a similar procedure was used to assess the reliability of plates subjected to transverse compression. However, the intensity of the transverse load considered was only one third of the value used for the longitudinal load, which is a realistic loading situation for the deck of a ship.

For this load case the three formulations presented in section 2.2.2 were assessed. The variation of β_f with the two relevant parameters, plate slenderness (fig. (2.10)) and aspect ratio (fig. (A1.12)), was achieved by varying respectively the plate thickness (t) and the plate length (a). The model uncertainty for these formulations is presented in Table 2.1 and is quite high. The sensitivity plots (figs.(A1.9)-(A1.11)) shows the reliability results controlled mainly by the modelling parameter with all the other variables playing a discrete role.



In figure (2.10) the results for β_f are presented for a mean aspect ratio of 3.3. From the plot is clear that both Valsgard (VG) and ABS formulations are more conservative than Faulkner's (FLK). Only for very slender plates VG predicts higher values of reliability which is a reflect of his conclusions about FLK formulation, which according to him underpredicts the strength of the slender plates⁹⁴.

From Table 2.6 and figures (2.10) and (A1.12) is clear that Faulkner formulation produces more economical designs. To adimensionalise the results it was used the weight per unit length of one plate with a mean thickness of 19.7 mm designed with Faulkner formulation. The difference in weight between Faulkner formulation and ABS is in average 6% with a minimum of 1.5% for $\beta \cong 1.4$. For Valsgard the difference is higher and varies between $\Delta W/W_0 \in (15\%, 30\%)$. Again it is important to refer the

differences in weight for the two limit safety levels (ADS and NPD) with Δ ABS= 54%, Δ FLK= 56% and Δ VG= 78%.

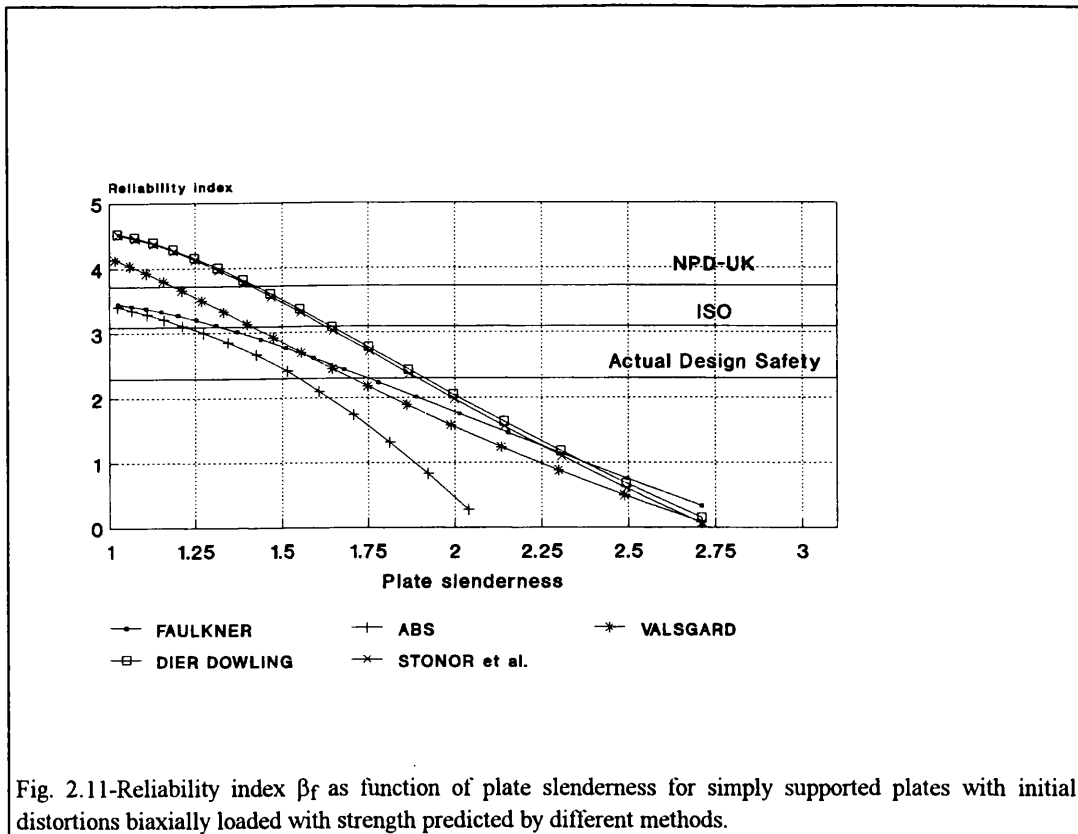
In Fig. (A1.12) given in Appendix 1 is presented the variation of β_f with the aspect ratio (α). The results confirms Faulkner formulation as the most economic one for the design of unstiffened plates subjected to transverse loading. The sensitivity plots for the three formulations are presented in (figs.(A1.9)-(A1.11)). The relative importance of the variables is more or less the same of the longitudinal case, with the strength modelling parameter, the yield stress and the thickness being the relevant strength variables and the two bending moments confirming their importance as dominant load variables.

		Actual Design	ISO	UK-NPD
Safety levels	β_f	2.3	3.09	3.72-
FAULKNER	β	1.887	1.493	1.211
	W/W ₀	79.1%	100%	123.3%
VALSGARD	β	1.644	1.161	0.923
	W/W ₀	90.8%	128.6%	161.7%
ABS	β	1.74	1.46	1.124
	W/W ₀	85.8%	102.3%	132.8%

Table 2.6 - Comparison of the transverse strength formulations for different design conditions.

The reliability of unstiffened plates under biaxial compressive loads was formulated considering that the interaction equations were the limit state functions with the incorporation of the modelling parameters presented in Table 2.1. Calculations have been performed for the formulations of Faulkner (FLK), American Bureau of Shipping (ABS), Valsgard (VG), Dier and Dowling (DD) and Stonor et al. (ST).

The effects of plate slenderness and load combination in the reliability were studied and the results are given in figures (2.11) and (A1.13). The comparison of the different designs is given in Table 2.7 and is only possible for Faulkner (eqs. (2.1), (2.17) and (2.22)) and ABS (eqs. (2.19)-(2.21) and (2.22)) because they are the only ones which incorporate the modelling uncertainty.



The reliability index (β_f) plot (fig. (2.11)) shows the variation of the reliability with plate slenderness for an aspect ratio of $\alpha=3.3$ and a load ratio of $\sigma_y/\sigma_x = 0.333$. From the plot is clear that the biased formulations give more conservative predictions. That fact indicates the danger of underestimating the structural safety if the unbiased formulations are used for the design. The comparison of Faulkner's and ABS approaches shows significant differences for intermediate and slender plates with identical predictions for the stocky range.

		Actual Design	ISO	UK-NPD
Safety levels	β_f	2.3	3.09	3.72
FAULKNER	β	1.75	1.327	-
	W/W_0	75.8%	100%	-
ABS	β	1.554	1.224	-
	W/W_0	85.4%	108.4%	-

Table 2.7 - Comparison of the biaxial strength formulations for different design conditions. (W_0 is the weight per unit length corresponding to a plate of 22 mm)

In Fig. (A1.13) the results for the reliability index for several load ratios are presented. When this ratio is zero the curves indicate the results for the longitudinal load case with $\beta \cong 1.5$. Again, it can be seen that FLK formulation gives better results than ABS confirming in this way the results of the previous study. In Table 2.7 the results for FLK and ABS are summarised and for this load case the average difference between the formulations is 10% with $\Delta W/W_0 \in (8\%, 13\%)$ which is similar to the transverse load case. Again, the differences in weight for the two limit safety levels (ADS and ISO) is high, 28% in average with $\Delta ABS = 27\%$ and $\Delta FLK = 32\%$.

From Faulkner's sensitivity plot (fig. (A1.14)) it is clear that the variables shows the same behaviour as for the uniaxial load cases i.e., the important variables are the modelling parameter, the yield strength, the thickness and the bending moments, both still-water and wave induced.

2.4.2 - Reliability of stiffened plates under compressive loading.

For the reliability analysis of stiffened plates it was considered the same ship plate dimensions and location as for the unstiffened plate case. Also, the loading considered was identical to the previous case and was based in the still-water and wave-induced bending moments. The stiffener considered was a T-bar with dimensions presented in Table 2.8. The stiffener dimensions were considered constant after a previous study that indicates their very low importance as random variables.

In the same table is also presented the three resistance modelling parameters for the plate and stiffener induced collapse of stiffened plates. These values were extracted from Ref. [18] and were derived with the use of 119 test models. The remaining random variables used in the study were the σ_0 , E , t , b , a , η , M_s and M_w and are presented in Table 2.3.

The reliability problem was formulated considering the strength models for the collapse of stiffened plates proposed by Faulkner and Carlsen to build the limit state functions. Calculations have been performed for Faulkner's formulation as given by equations (2.25)-(2.28) and for the formulation by Carlsen, given by equations (2.30)-(2.31a) and (2.30)-(2.31b), for PIF and SIF respectively.

Variables		Distribution	Mean	COV
Depth of the stringer web	d_w (mm)	Deterministic	180	-
Thickness of the stringer web	t_w (mm)	Deterministic	18	-
Width of the stringer flange	d_f (mm)	Deterministic	60	-
Thickness of the stringer flange	t_f (mm)	Deterministic	18	-
Resistance modelling parameter - Faulkner formulation	$X_{mF}(ad.)$	Lognormal	0.951	0.126
Resistance modelling parameter - Carlsen - PIF formulation	$X_{mCp}(ad.)$	Lognormal	1.192	0.169
Resistance modelling parameter - Carlsen - SIF formulation	$X_{mCs}(ad.)$	Lognormal	1.022	0.163

Table 2.8 - Description of the stiffener dimensions and the resistance modelling parameter.

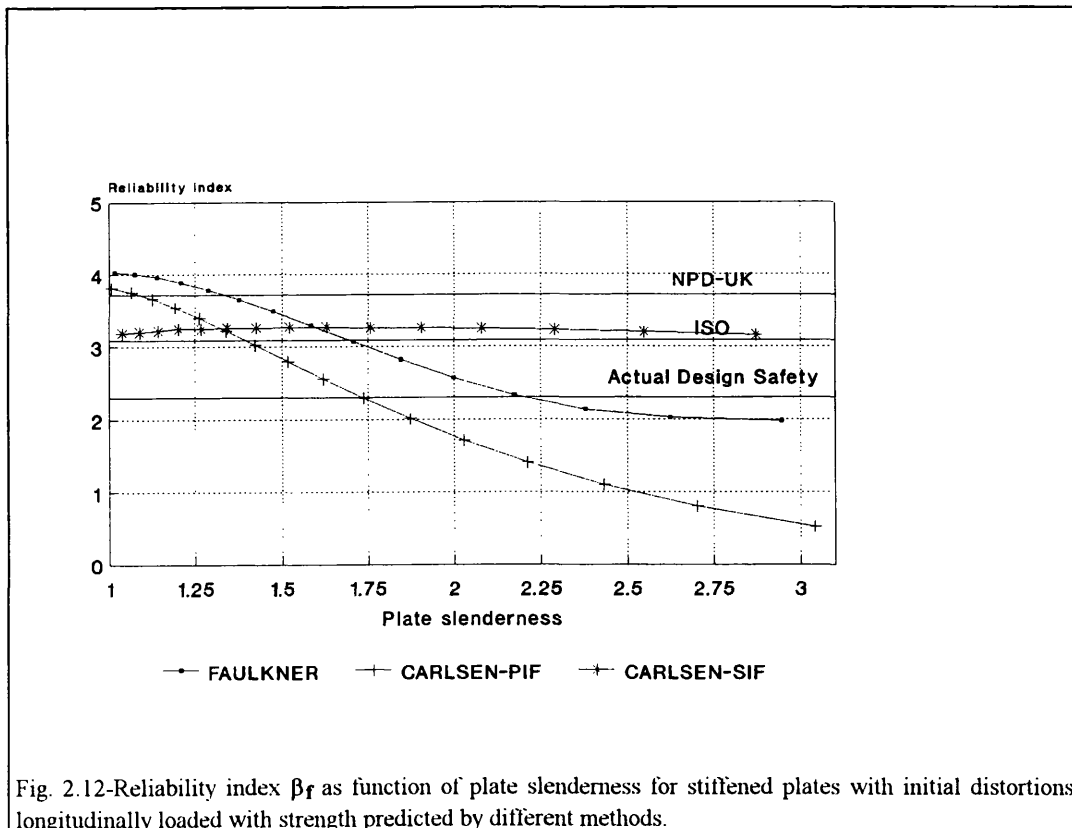


Fig. 2.12-Reliability index β_f as function of plate slenderness for stiffened plates with initial distortions longitudinally loaded with strength predicted by different methods.

The resulting reliability index plot is shown in figure (2.12). The plot presents the variation of the reliability index (β_f) with the plate slenderness parameter (β) and allows for direct comparison of the economic efficiency for design of both formulations. The results are summarised in Table 2.9.

From Fig. (2.12) it is clear that Faulkner and Carlsen-PIF have a similar behaviour with an almost constant difference between them, Carlsen-PIF gives structures 16% heavier than Faulkner's (18.6% for actual design level, 16.2% for ISO level and 17.6% for NPD level). Also from the plot is clear that Carlsen-SIF is not sensitive to the variation of plate thickness and can produce unsafe design for slender and very slender plates.

The sensitivity plot (fig.(A1.15)) for Faulkner formulation shows similar results as the ones for the unstiffened plate case, pointing out the important role that the resistance modelling parameters, the yield stress and the thickness play in these formulations. The sensitivities obtained for the other method shown in Appendix 1 (fig. (A1.16)-(A1.17)) present similar behaviour but different importance for the variables.

The design point chosen for comparison (W_0) corresponds to the weight of single component (plate plus stiffener) designed with the formulation that with the minimum use of material satisfies the ISO safety requirement. That value, $W_0=0.336$ (ton) corresponds to the weight of one stiffened plate with a mean thickness of 17.2 mm designed with Faulkner formulation.

		Actual Design	ISO	UK-NPD
Safety levels	β_f	2.3	3.09	3.72-
FAULKNER	β	2.205	1.702	1.334
	W/W_0	82.9%	100%	120.7%
CARLSEN - PIF	β	1.741	1.4	1.091
	W/W_0	98.3%	116.2%	142%

Table 2.9 - Comparison of the longitudinal strength formulations for stiffened plates for different safety conditions.

From Table 2.9 is clear that Faulkner formulation produces more economical design. Also in Table 2.9 it can be seen that for both formulations the difference in

weight for the two limit safety levels is about 45%, which indicates that much caution should be put by the designer and ruling body in the selection or the establishing of the proper safety level for design.

Finally, it is also important to stress that a relatively small difference in the levels of uncertainty of the formulations ($\Delta\text{COV}=4.3\%$) results in a significant difference in the final designs when a reliability based design method is used ($\Delta W/W_0=16\%$).

2.5 - Conclusions.

The conclusions for this study can be subdivided in two groups. The first group summarises the particular conclusions for each load case and the second group contains the general considerations about the reliability assessment of plates.

The conclusion that among all resistance variables, the yield stress is one of the most important is in agreement with the findings in⁷³, where it was also showed that the relative importance of the yield stress decreased with increasing plate slenderness.

For the unstiffened plates under longitudinal compression it is shown that MVRM and FORM give almost the same results for the strength equation of Faulkner (eq.(2.1)). It is also shown that for this particular formulation the reliability results are quite sensitive with respect to slenderness for intermediate plates. This happens because $d\phi_f/d\beta$ is maximum for this range (this fact can also explain the relative dependency of the variables with the plate slenderness). The study for this load case show that Guedes Soares, in his proposal had considerably improved the model of Faulkner, with gains in structural weight of about 14%. It is also important to refer that Ivanov/Rousev, Ueda/Yao and Soreide/Czujko formulations can only be used if an appropriated bias is derived, otherwise they can lead to unsafe designs. Carlsen formulation is quite conservative and also requires the evaluation of its uncertainty.

For the transverse compression case it is clear that the high model uncertainties (COV's over 30%) dominate the reliability results. Thus, it seems important to make an effort to improve these formulations. For design, Faulkner formulation is recommended for stocky and intermediate plates and Valsgard proposal should be used for slender and very slender plates.

Also, for the combined loading case Faulkner interaction is recommended for design, especially for intermediate and slender plates. Again, is important to refer the

dangers that may arise from the incorrect use of uncalibrated formulations (Valsgard, Dier and Dowling and Stonor).

Finally, for the stiffened plates under longitudinal compression the method of Faulkner is also recommended with structures 16% lighter than Carlsen-plate induced formulation. The other proposal of Carlsen, stiffener induced failure, shows no dependency upon plate slenderness (variation of plate thickness) and thus may produce unsafe design for intermediate and slender plates.

The first general conclusion is of course, the need to incorporate in the reliability assessment the uncertainty related with the strength model^{65,139,140}. This is particularly important when the level of uncertainty is high because in that case the modelling parameter clearly dominates the reliability results. From the other resistance variables it can be said that the yield stress is the most important one. The loading variables are in general as important as the most relevant resistance variables. It is also necessary to recall the importance of the correct definition of the random variables, especially if they are correlated. An incorrect definition of the variables can lead to large differences in the final reliability results.

Other important conclusion deals with the economic efficiency for design of the different formulations. This study confirms previous work¹⁴⁰ regarding this aspect of design and it can be said that the less uncertain a formulation is, the better it is from an economic point of view. In fact, in all cases studied were the less uncertain formulations who predicts the most economic structural design (GS for longitudinal strength and FLK for the others).

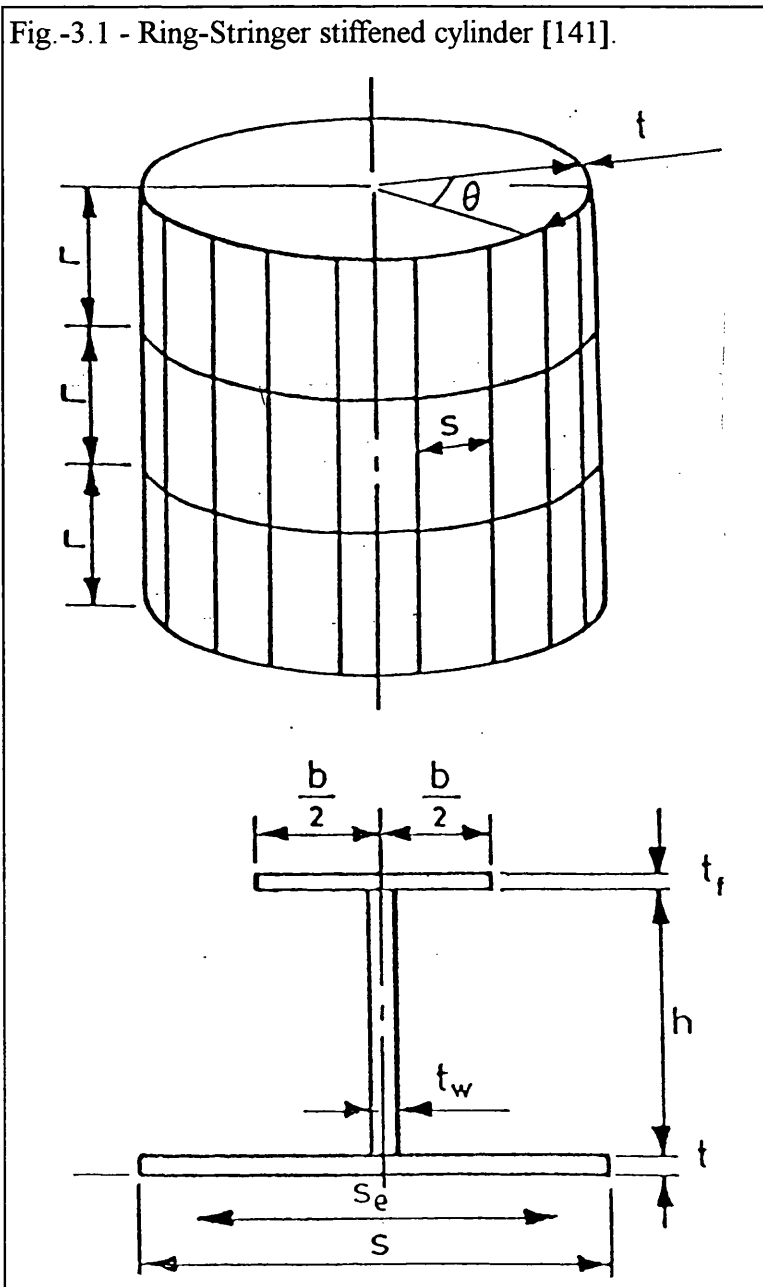
Finally, one important aspect that should be taken in consideration are the safety levels used for design with advanced level 2 reliability methods. These methods provide the direct derivation of the partial safety factor and contribute for the reduction of human errors⁶⁵. But from the results is clear that large differences in weight arises from the adoption of one safety level or the other. Thus, in this particular aspect of design specific guidance should be established by the ruling authorities.

CHAPTER 3 - RELIABILITY ANALYSIS OF RING-STRINGER STIFFENED CYLINDERS

3.1 - Introduction.

The ring-stringer stiffened cylinder also known as orthogonally stiffened cylinder is a typical component of marine structures. It is widely used in offshore platforms as main structural elements especially in the legs of buoyant offshore platforms such as semi-submersibles and tension leg platforms.

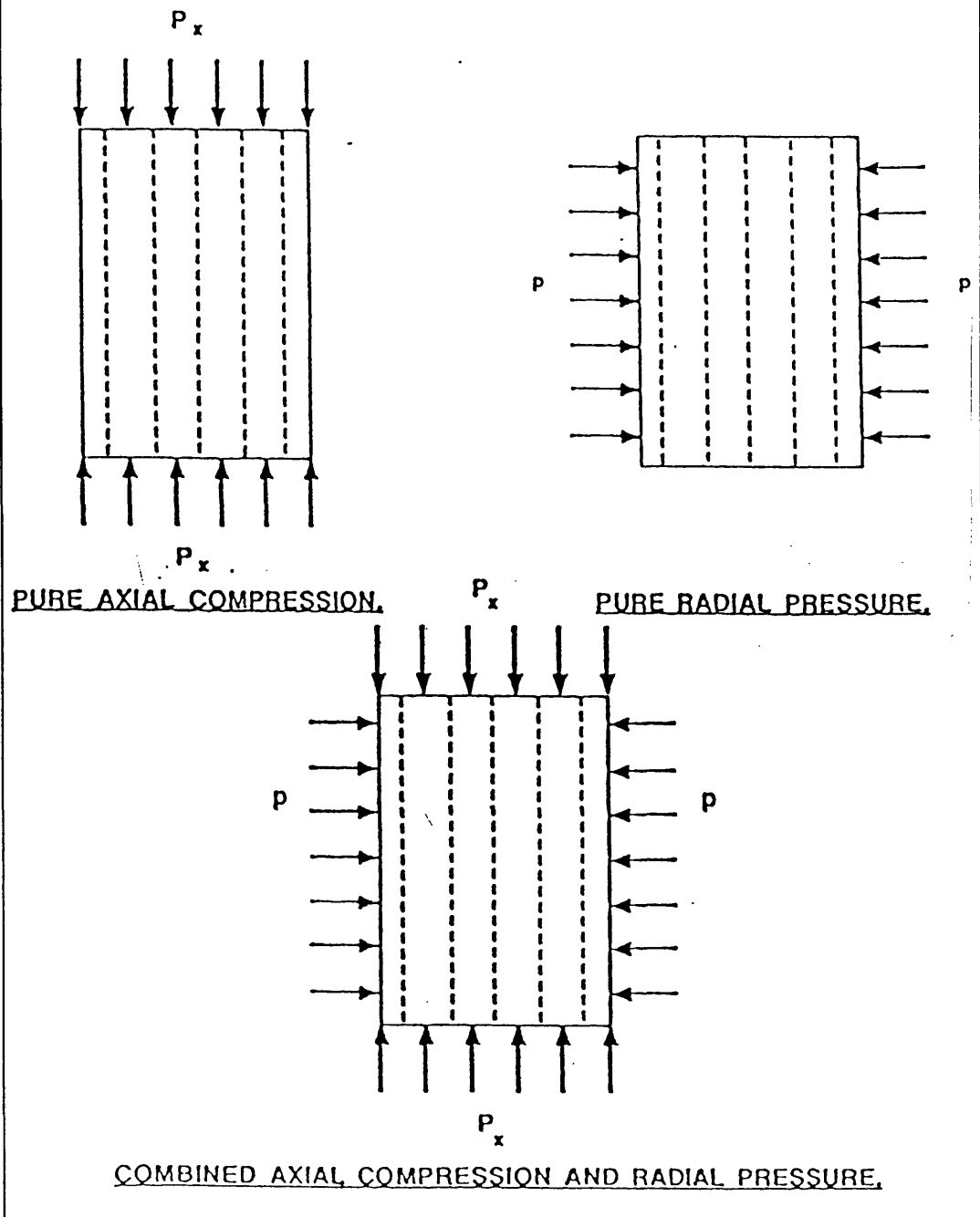
This component consists of a fabricated cylinder with a stiffening system composed



of longitudinal stringer stiffeners supported laterally by more widely spaced ring frames (fig. 3.1). This type of component is particularly suited to resist high axial loads and bending moments in combination with external pressure.

These components have large dimensions (over 10 meters of diameter) due to their application in the legs of the semi-submersible and TLP's. Because of that they are produced by butt welding cold or hot formed plates. The stiffeners are also welded to the cylinder in such a way that the structural continuity of the stringers is guaranteed. This type of fabrication introduces geometrical imperfections as well as residual

Fig-3.2 - Loading types [141].



stresses.

The geometrical parameters used to describe the ring-stringer stiffened cylinders and their typical range of variation are:

The radius upon thickness ratio - R/t [100 - 500].

The stringer spacing upon thickness ratio - s/t [25 - 130].

The Batdorf width parameter - Z_s [4 - 60].

The Batdorf length parameter - Z_l [10 - 700].

The ring spacing upon radius ratio - L/R [0.2 - 1.6].

The ratio between the stiffeners and shell areas [0.1 - 0.6].

These components are subjected to axial compression, external pressure and combined loads as shown in fig. 3.2 and they may fail by buckling in several modes¹⁰¹:

- local shell buckling, i.e., buckling of the shell between stiffeners. The stringers remain straight and the rings remain round (Fig. 3.3 a).
- bay instability, i.e., buckling of the stringers together with the attached shell plate between rings. The rings and the ends of the cylinders remain round (Fig 3.3 b).

Fig.-3.3a - Local shell buckling[141].

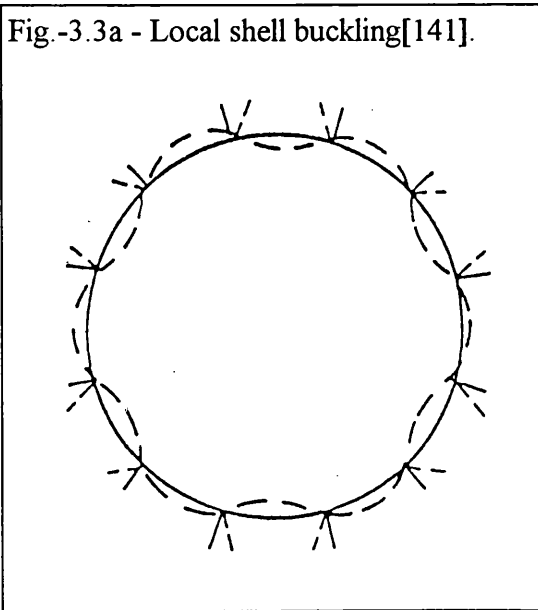
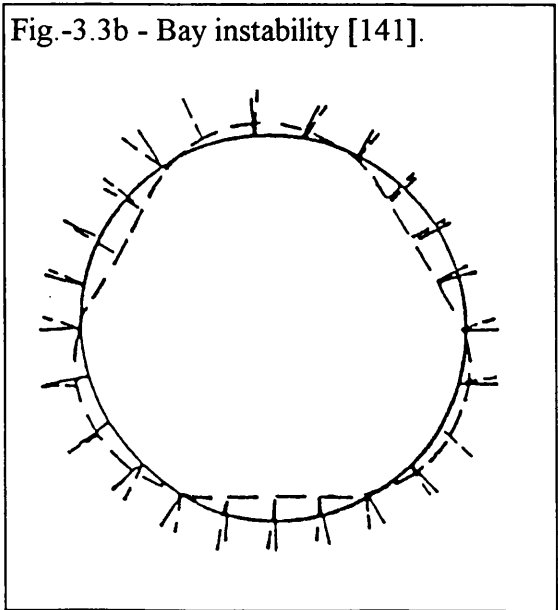


Fig.-3.3b - Bay instability [141].



- general instability, i.e., buckling of one or more rings together with the attached shell plus stringers (Fig. 3.3 c).

- local stiffener buckling, i.e., torsional buckling of stiffeners or local buckling of web and flange. The shell remains undeformed (Fig. 3.3 d).

Fig.-3.3c - General instability[141].

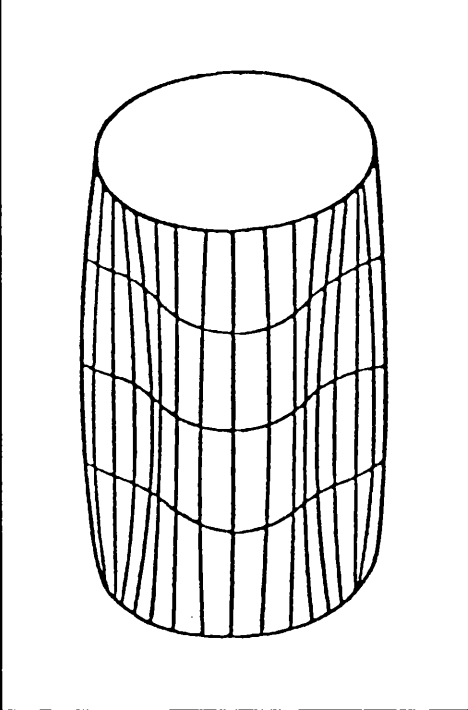
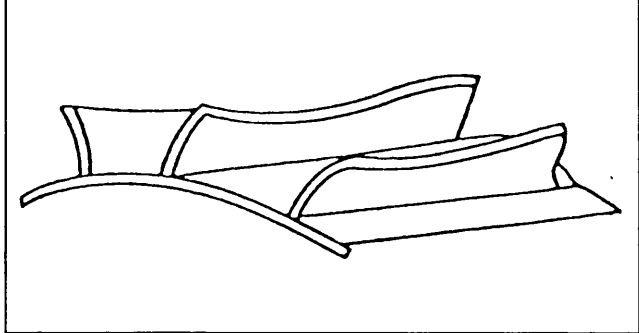


Fig.-3.3d - Local stiffener buckling [141].



At present several strength formulations are available which allow the prediction of the buckling loads for these different failure modes.

In this chapter they are presented and compared with the available experimental results in order to analyse their relative advantages and disadvantages^{141,142}. A systematic study quantified the modelling uncertainty³ of all these formulations. Finally, a reliability study allows the analysis of the behaviour of the formulas when the relevant variables are considered to be random. The effect of including the modelling uncertainty in the formulation is also considered.

Two types of formulations are considered - lower bound and mean value. The first category can be characterised by the underprediction of the strength for a specific percentile over all the test specimens representative of the modelled phenomena. The DnV formulations¹⁰², the ECCS formulations¹⁰³ and the API orthotropic formulations^{101,143} fall in this category. The mean value formulation is characterised by an average prediction of the strength for all test specimens, in this category we can find the Rule Case Committee formulations⁷ and the API-discrete formulations¹⁰¹. The mean value formulations are used to predict the strength while the lower bound formulations are intended for the design of the cylinders. Behind these formulation several series of experiments were conducted all over, especially in UK under the Department of Energy sponsorship^{83,144,145} and in USA sponsored mainly by Conoco Inc. and ABS.

Due to the uncertainties involved in the evaluation of the loads and in the strength of this type of structure it is now commonly accepted that its design should be reliability based. As pointed out by Frieze¹⁴⁶ the uncertainty in the resistance of the structure plays a dominant role in its safety and cost. The model uncertainty represented by the modelling uncertainty or parameter is normally the larger share of the overall resistance uncertainty. However, it can always, within certain limits, be reduced or be assessed in order to choose the best formulation among others. This is in fact the *leit motiv* of the work presented in this chapter.

3.2 - Strength Formulations for Ring-stringer Stiffened Cylinders.

The buckling of these components is a function of the loading conditions to which they are subjected. There are models for describing the behaviour under axial compression, others for radial pressure and some for the combination of these two loads. Bending, torsion and other loads are normally decomposed into these two basic types¹⁰¹. The component (see Fig. 3.1) is composed of three types of elements, the cylindrical shell, the longitudinal stiffeners (stringers) and the radial stiffeners (rings). The role played in the strength of the structure by the stringers is to stabilise the shell and provide better resistance to the axial compression loads by carrying part of the load as well as increasing the resistance of the associated shell. The stiffeners can also be effective to resist radial pressure if they are spaced less than one half buckling wave length as for the shell without stringers. The ring frames stabilise the stringers and ensure that the external pressure is resisted and that shell circularity is maintained.

Due to axial compression several waves can be formed in both the longitudinal and circumferential directions. For external pressure a single longitudinal half wave is formed while several waves are formed in the circumferential direction. The use of this stiffening system of the shell creates the possibility of several types of failure modes under the applied loads.

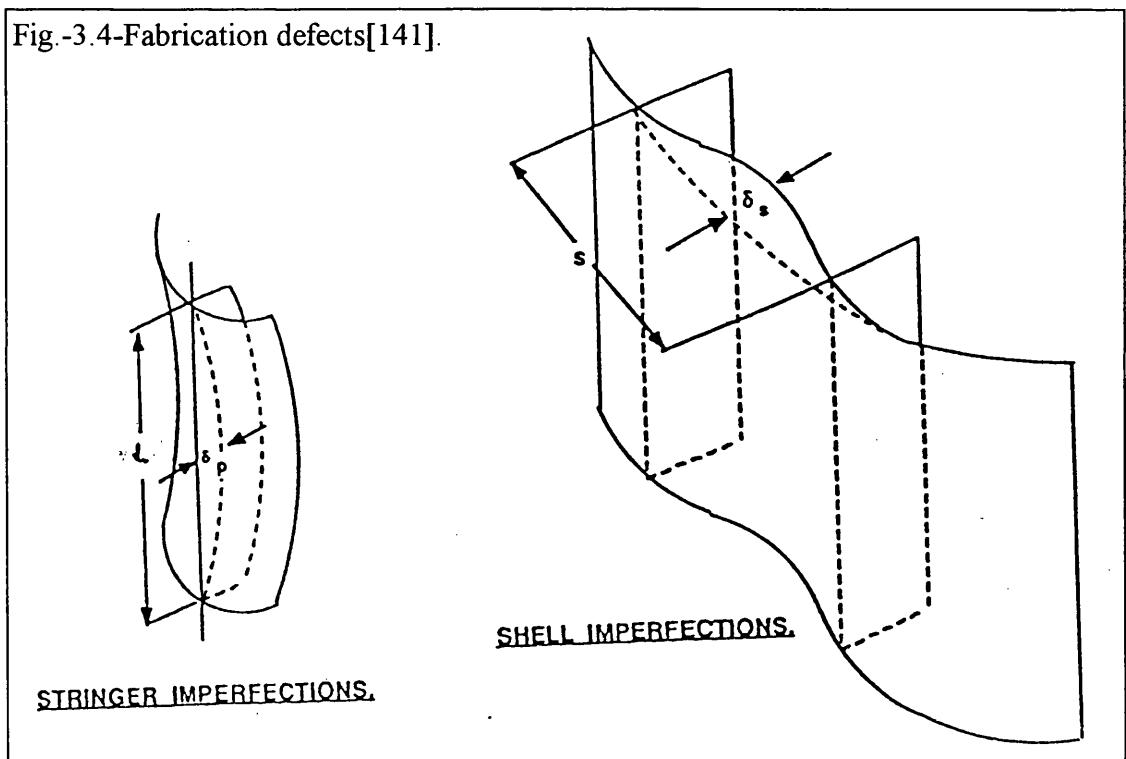
The stringers introduce two possible types of failure - local buckling of the stringers and combined stringer and shell buckling (bay instability). In practice they are designed to avoid local buckling and to ensure that bay instability is the most probable failure mode. In bay instability, the collapse stress is mainly a function of the moment of inertia of both the stringers and the attached shell and the effective width of the shell. The reason behind the preference given to the bay instability as failure mode, is due to the fact that the local instability of the stringers may precipitate collapse.

The rings also introduce two types of failure - local buckling of the rings and combined buckling of ring and stiffened shell (general instability). The general instability induces very large distortions and is the most serious type of failure in these structures. In this mode, the failure stress is mainly a function of the moment of inertia of both the ring and the effective width of shell. The stringers and the rings are normally designed to avoid local buckling.

The spacing between stringers influence the type of buckling that may occur. For broad panelled cylinders, local shell buckling may arise and precipitate failure. For narrow panelled cylinders the bay buckling is dominant.

Initial imperfections and residual stresses introduced during the fabrication process,

Fig.-3.4-Fabrication defects[141].



considerably affects the buckling strength of these components. The type of imperfections shown in figure (3.4) are the overall out of straightness, the out of circularity of ring frames and the local deviation from the straight generator.

Some example of code recommendations for the imperfection levels are as follows:

DnV - 1984

$$\begin{cases} \frac{\delta_p}{L} \leq \frac{0.0015}{1 + 0.5 L/R} \\ \frac{\delta_s}{s} \leq \frac{0.01}{1 + s/R} \end{cases}$$

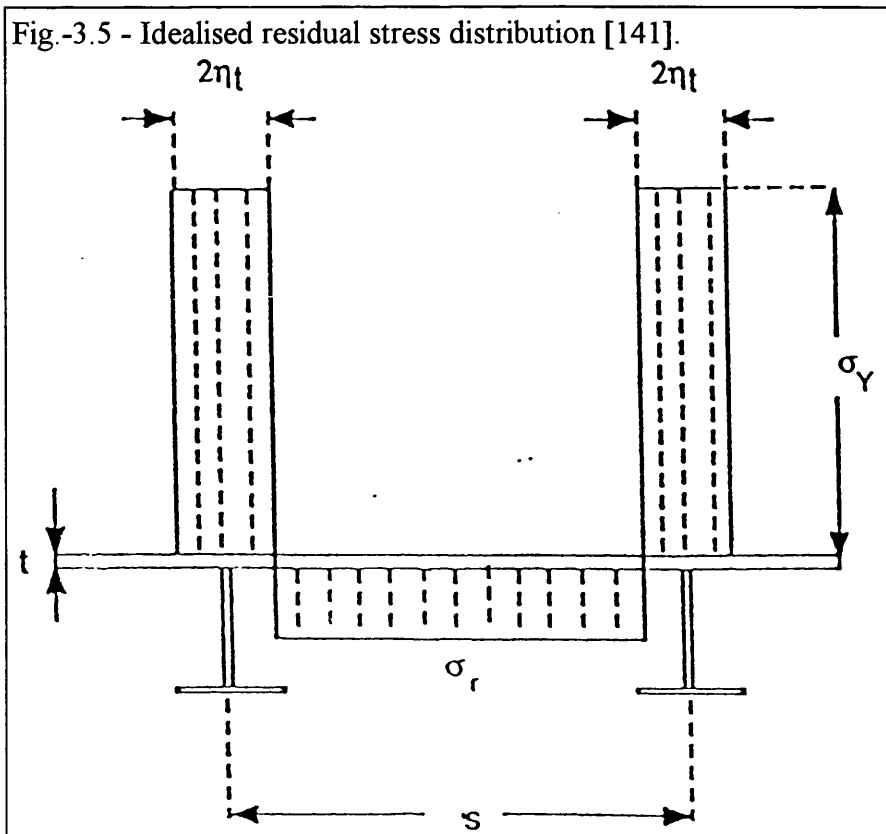
ECCS

$$\begin{cases} \frac{\delta_P}{L} \leq 0.0015 \\ \frac{\delta_S}{s} \leq 0.008 \end{cases}$$

in which δ_p is the out-of-straightness of stringer-shell combination and δ_s is the maximum deflection of shell from the true circular arc between stringers.

The reduction of buckling strength due to weld induced residual stress may be quite large. An idealised residual stress distribution is shown in figure (3.5) and it can be seen later that it has been taken into account while formulating the ultimate strength model for axial compression both by the RCC and API formulations.

The formulations are presented and discussed by type of phenomena that they intend to model. In the following sub-chapters all the formulations used in the work will be described. For axial compression 5 different type of formulations were studied, the RCC, the API orthotropic and discrete, the DnV and ECCS expressions. For the radial pressure 4 formulations were studied, the RCC, the API orthotropic and discrete and the DnV expressions. Three different interaction formulations were used for load combination, the RCC, the API and the DnV.



3.2.1 - Formulations for ultimate strength under axial compression loads.

Three different codes of practice¹⁰¹⁻¹⁰³ actually in use for offshore design present four different formulations for the design of ring and stringer stiffened cylinders. The API Bul 2U includes two different formulations; the orthotropic plate method which was derived from the ASME Code Case N-284, and the discrete stiffener approach which was derived from the RCC work. The main concern is the analysis of the failure modes considered by the rules, i.e., local shell buckling and bay instability. Those are the failure modes observed in the test specimens, thus the ones suited for direct comparison with the predictions.

3.2.1.1 - API Bulletin 2U

This code¹⁰¹ covers for the following failure modes of stringer and ring stringer stiffened cylinder:

- Local shell buckling.
- Bay instability.
- General instability.

In addition, failure modes due to buckling of stiffening elements and buckling of the cylinder as a column are also covered.

The bulletin recommends that the stiffeners be sized so that the first mode of failure will be local buckling of the shell between stiffeners. In order to avoid mode interaction between local buckling with bay instability and general instability, the code recommends that the elastic bay instability or general instability stress should be 1.2 times the elastic local shell buckling stress.

The buckling design procedure is based on classical linear theory. The elastic critical buckling stress σ_{cr} is modified by the so-called capacity reduction factor α_{ij} (Knockdown factor) to take into account the effect of imperfections.

$$\sigma_{icr} = \alpha_{ij} \sigma_{cr} \quad (3.1)$$

Further, the imperfect elastic stress is modified by a plasticity reduction factor η to cater for the inelastic effects.

$$\sigma_e = \eta \sigma_{icr} \quad (3.2)$$

The plasticity reduction factor is given by:

$$\left. \begin{aligned}
 \eta &= 1, & \text{for } \Delta \leq 0.55 \\
 &= \frac{0.45}{\Delta} + 0.18, & \text{for } 0.55 < \Delta \leq 1.6 \\
 &= \frac{1.31}{1 + 1.15\Delta}, & \text{for } 1.6 < \Delta < 6.25 \\
 &= \frac{1}{\Delta}, & \text{for } \Delta \geq 6.25
 \end{aligned} \right\} \quad (3.3)$$

where $\Delta = \frac{\sigma_{icr}}{\sigma_y}$

3.2.1.1.1 - Local buckling.

The compact section requirement which precludes stiffener buckling prior to shell buckling are identical to those specified by AISI¹⁴⁷ for fully effective sections.

The flat bar stiffeners, the flanges of a tee stiffeners and the outstanding legs of angle stiffener must comply with:

$$\frac{h_s}{t_s} \leq 0.375 \sqrt{E/\sigma_y} \quad (3.4)$$

where h_s is the full width of a flat bar stiffener or outstanding leg of angle stiffener and one half of the full width of the flange of a tee stiffener and t_s is the thickness of the bar, leg of angle or flange of tee.

For the web of tee stiffeners or the leg of angle stiffener attached to shell the following relation must hold:

$$\frac{h_s}{t_s} \leq 1.0 \sqrt{E/\sigma_y} \quad (3.5)$$

where h_s is the full depth of a tee section or full width of an angle leg and t_s is the thickness of the web or angle leg.

If the compact section requirement is not met, then the allowable stress should be used as a substitute for the yield stress in determining the local shell buckling stress for axial compression or bending. It should also substitute the yield stress when calculating bay instability and general instability stresses for all load conditions.

$$\sigma_{xc} = (1.28 - 0.75\lambda_s)\sigma_y, \quad \text{for } 0.375 < \lambda_s < 0.846 \quad (3.6a)$$

where σ_{XC} is the allowable stress and the slenderness λ_s is given by

$$\lambda_s = \frac{h_s}{t_s} \sqrt{\sigma_y / E} \quad (3.6b)$$

The shell elastic buckling stress is given by:

$$\sigma_{cr} = \alpha_{XL} C_X \frac{Et}{R} \quad (3.7)$$

where

$$\left. \begin{aligned} \alpha_{XL} C_X &= \frac{3.254}{M_\theta^2} + 0.0253 \alpha_0 M_\theta^2, & \text{for } 1.5 < M_\theta < 3.46 \\ &= 0.605 \alpha_0, & \text{for } M_\theta > 15 \end{aligned} \right\} \quad (3.8)$$

and

$$\left. \begin{aligned} \alpha_0 &= 0.207, & \text{for } R/t \geq 610 \\ &= \frac{169 \bar{c}}{195 + R/t} < 0.9, & \text{for } R/t < 610 \end{aligned} \right\} \quad (3.9)$$

$$\left. \begin{aligned} \bar{c} &= 2.64, & \text{for } M_x \leq 1.5 \\ &= 3.13 / M_x^{0.42}, & \text{for } 1.5 < M_x < 15 \\ &= 1.0, & \text{for } M_x > 15 \end{aligned} \right\} \quad (3.10)$$

with the API shell length and width parameters given by:

$$\left. \begin{aligned} M_x &= L / \sqrt{Rt} \\ M_\theta &= s / \sqrt{Rt} \end{aligned} \right\} \quad (3.11)$$

For values of M_θ less than 1.5 use $M_\theta=1.5$. For M_θ values between 3.46 and 15 the value of $\alpha_{XL} C_X$ is obtained by linear interpolation. The equation (3.8) for the reduction factor $\alpha_{XL} C_X$ with $M_\theta < 15$ is based in Timoshenko's equation¹⁴⁸ while for $M_\theta > 15$ is based in Koiter's equation¹⁴⁹. The inelastic buckling stress is then calculated using equation (3.2) and (3.3) replacing σ_{icr} by σ_{cr} .

3.2.1.1.2 - Bay instability.

Orthotropic theory.

The theoretical buckling load for bay instability is determined using orthotropic shell theory. The theory is based on the modified equation given in reference [143] and it takes into account effective membrane thickness in the longitudinal direction and bending rigidity. It was modified to include the geometry of stiffened shells in which the stringers are not necessarily closely spaced. This has been taken into account by taking the effective width of shell in the circumferential direction.

The limitations of the equations are as follows:

- i) The number of stringers must be greater than 3 times the number of circumferential waves.
- ii) The bay instability stress shall not exceed 1.5 times the local buckling stress.

The evaluation of the elastic buckling load is carried out by minimising (3.12) where $m \geq 1$ and $n \geq 2$.

$$N_e = \frac{A_{33} + \left(\frac{A_{12}A_{23} - A_{13}A_{22}}{A_{11}A_{22} - A_{12}^2} \right) A_{13} + \left(\frac{A_{12}A_{13} - A_{11}A_{23}}{A_{11}A_{22} - A_{12}^2} \right) A_{23}}{Y} \quad (3.12)$$

where:

$$\left. \begin{aligned} A_{11} &= E_x \left(\frac{m\pi}{L} \right)^2 + G_{x\theta} \left(\frac{n}{R} \right)^2 \\ A_{22} &= E_\theta \left(\frac{n}{R} \right)^2 + G_{x\theta} \left(\frac{m\pi}{L} \right)^2 \\ A_{33} &= D_x \left(\frac{m\pi}{L} \right)^4 + D_{x\theta} \left(\frac{m\pi}{L} \right)^2 \left(\frac{n}{R} \right)^2 + D_\theta \left(\frac{n}{R} \right)^4 + \frac{E_\theta}{R^2} \\ A_{12} &= (E_{x\theta} + G_{x\theta}) \left(\frac{m\pi}{L} \right) \left(\frac{n}{R} \right) \\ A_{13} &= \frac{E_{x\theta}}{R} \left(\frac{m\pi}{L} \right) + C_x \left(\frac{m\pi}{L} \right)^3 \\ A_{23} &= \frac{E_\theta}{R} \left(\frac{n}{R} \right) \end{aligned} \right\} \quad (3.13)$$

$$Y = \left(\frac{m\pi}{L} \right)^2 \quad (3.14)$$

The rigidity parameters are given by:

$$\left. \begin{aligned}
 C_x &= \frac{E A_s z_s}{L} \\
 E_x &= \frac{E t}{1-\nu^2} \left(\frac{s_e}{s} \right) + \frac{E A_s}{s} \\
 E_{x\theta} &= \frac{\nu E t}{1-\nu^2} \\
 E_\theta &= \frac{E t}{1-\nu^2} \\
 D_x &= \frac{E t^3}{12(1-\nu^2)} \left(\frac{s_e}{s} \right) + \frac{E I_s}{s} + \frac{E A_s^2}{s} \\
 D_{x\theta} &= \frac{\nu E t^3}{6(1-\nu^2)} + \frac{G t^3}{6} \left(1 + \frac{s_e}{s} \right) + \frac{G J_s}{s} \\
 D_\theta &= \frac{E t^3}{12(1-\nu^2)} \\
 G_{x\theta} &= \frac{G t}{2} \left(1 + \frac{s_e}{s} \right)
 \end{aligned} \right\} \quad (3.15)$$

The imperfection factors are:

$$\left. \begin{aligned}
 \alpha_{XB} &= 0.65, & \text{for } \bar{A}_s \geq 0.06 \\
 &= \alpha_{XL}, & \text{for } \bar{A}_s < 0.06
 \end{aligned} \right\} \quad (3.16)$$

where $\bar{A}_s = \frac{A_s}{st}$ and α_{XB} is given by equation (3.9) with $\bar{c} = 1.0$.

The elastic buckling stress is given by

$$\sigma_e = \alpha_{XB} \frac{N_e}{t_x} \quad (3.17)$$

where $t_x = \frac{A_s + s_e t}{s}$ and $s_e = 1.9 t \sqrt{E/\sigma_e} \leq s$. If the shell is not fully effective an iterative procedure must be carried out. When convergence is achieved it is possible to calculate the bay average collapse stress by using the plasticity reduction factor given by equation (3.3).

$$\sigma_u = \eta \sigma_e \quad (3.18)$$

Discrete stiffener method.

An alternative method is also recommended by API Bul 2U for determining the bay instability buckling load for stringer stiffened cylinder without the limitations imposed by the orthotropic shell theory. This method is based on a procedure proposed by Faulkner⁶⁸ for the RCC formulation⁷. In this method, the elastic buckling stress is given by a two term equation accounting for the contributions of the unstiffened curved shell element plus the effective column.

$$\sigma_e = \sigma_{sh} + \sigma_{cl} \quad (3.19)$$

where the unstiffened curved shell contribution (σ_{sh}) is given by:

$$\sigma_{sh} = \frac{\alpha_{XL} C_X E t/R}{1 + A_S/st} \quad (3.20)$$

and $\alpha_{XL} C_X$ coefficient is calculated using equation(3.8) to (3.11).

The effective column contribution (σ_{cl}) is given by the following procedure:

(i) Evaluation of the shell elastic buckling stress using a Koiter's¹⁴⁹ type formulation:

$$\left. \begin{aligned} \sigma_{cr} &= \left(\frac{3.62}{M_\theta^2} + 0.0253 M_\theta^2 \right) Et/R, & \text{for } M_\theta < 3.46 \\ &= 0.605 Et/R, & \text{for } M_\theta \geq 3.46 \end{aligned} \right\} \quad (3.21)$$

(ii) Introduction of a knockdown factor to account for the shell initial imperfections:

$$\left. \begin{aligned} \rho_s &= 0.27 + \frac{1.57}{M_\theta^2} + \frac{29.6}{M_\theta^4} + 0.008 \left(1 - \frac{R}{300t} \right) M_\theta, \\ &\quad \text{for } 3.46 < M_\theta < 8.57 \\ &= 1 - 0.018 M_\theta^{2.5} + 0.023 M_\theta^2 \left(1 - \frac{R}{300t} \right), \\ &\quad \text{for } M_\theta \leq 3.46 \end{aligned} \right\} \quad (3.22)$$

(iii) Calculation of the bias correction for the lower bound knockdown factor:

$$\left. \begin{aligned} B &= 1.15, & \text{for } \lambda_n = \sqrt{\sigma_y/\rho_s \sigma_{cr}} \geq 1.0 \\ &= 1 + 0.15\lambda_n, & \text{for } \lambda_n < 0.06 \end{aligned} \right\} \quad (3.23)$$

(iv) Mean knockdown factor:

$$\rho = B \rho_s \quad (3.24)$$

(v) Evaluation of the elastic buckling stress for the imperfect shell:

$$\sigma_{icr} = \rho \sigma_{cr} \quad (3.25)$$

(vi) Consider the welding residual stress tension block parameter $\eta = 4.5$ for continuous structural fillet welds.

(vii) Evaluation of the residual stress reduction factor:

$$R_r = 1.0 - \left(\frac{2\eta}{s/t - 2\eta} \right) \left(\frac{\lambda_n^4}{(1 + 0.25\lambda_n^4)^2} \right) \left(\frac{\lambda_n^2}{1.05\lambda_n - 0.28} \right), \text{ for } \lambda_n > 0.53 \quad (3.26)$$

$$= 1.0, \quad \text{for } \lambda_n \leq 0.53$$

(viii) Shell reduced slenderness parameter:

$$\lambda = \sqrt{\sigma_y / \sigma_{icr}} \quad (3.27)$$

(ix) Shell reduced effective width:

$$\frac{s'_e}{s} = (0.53/\lambda) R_r, \quad \text{for } \lambda \geq 0.53 \quad (3.28)$$

$$= 1.0, \quad \text{for } \lambda < 0.53$$

(x) Evaluation of the second moment of area of stringer plus reduced effective width of shell (e_s is the distance from the centreline of the shell to the centroid of the stringer stiffener):

$$I'_e = I_s + \left(A_s e_s^2 \frac{s'_e t}{A_s + s'_e t} \right) + \frac{s'_e t^3}{12} \quad (3.29)$$

(xi) Shell effective width:

$$\frac{s_e}{s} = (1.05/\lambda - 0.28/\lambda^2) R_r, \quad \text{for } \lambda \geq 0.53 \quad (3.30)$$

$$= 1.0, \quad \text{for } \lambda < 0.53$$

(xi) Evaluation of the effective column term:

$$\sigma_{cl} = \frac{\pi^2 E I'_e}{L^2 (A_s + s_e t)} \quad (3.31)$$

The inelastic buckling stress is then evaluated using the Ostenfeld-Bleich equation¹⁵⁰.

$$\left. \begin{aligned} \sigma_c &= \sigma_e, & \text{for } \sigma_e &\leq \sigma_y p_s \\ &= \sigma_y (1 - p_s (1 - p_s) \sigma_y / \sigma_e), & \text{for } \sigma_e &> \sigma_y p_s \end{aligned} \right\} \quad (3.32)$$

In⁶⁸ the value of 0.5 is proposed for the structural proportional limit p_s for the case of nonstress relieved shells.

Then the value of σ_c is used to correct the shell effective width by introducing a new value of $\lambda = \sqrt{\sigma_c / \sigma_{icr}}$ in (3.30). Finally the bay average collapse stress using the corrected s_e is given by

$$\sigma_u = \sigma_c \left[\frac{A_s + s_e t}{A_s + s t} \right] \quad (3.33)$$

3.2.1.2 - RCC Formulation

The Rule Case Format has been proposed⁷ by a committee established by Conoco Inc. and ABS to develop design rules for tension leg platforms. One of the tasks of the Committee was to formulate design guidance for the ultimate strength of stiffened cylindrical components subjected to various kind of loading.

The formulation is based on an approach similar to that developed for flat stiffened panels¹⁵¹ in which two modes of failure are considered for axial compression, one due to stiffened shell column buckling and the other is the stiffener tripping. In this formulation, the critical buckling stress is determined assuming a single half-wave forms between rings. The critical stress is then given as the summation of the buckling stress for an unstiffened shell between rings and that for the stinger acting as a column between rings. A reduced effective width is used based on curved shell element buckling. The bias factors for the elastic knock-down factors are taken from test results of aerospace industry. The welding residual stress effect is taken into account by the structural tangent modulus. Inelastic buckling is considered through the Ostenfeld-Bleich formulae.

This formulation is similar to the one presented previously by API in the alternative method. The elastic buckling stress is given in the same way by the two term equation (3.19). However the unstiffened curved shell contribution is simply given by:

$$\sigma_{sh} = \frac{0.605 \rho_s E (t/R)}{1 + A_s / s t} \quad (3.34)$$

in which the shell knockdown factor is assumed to be 0.75.

The effective column term is given by a similar procedure to the one used in the API rules. The evaluation of the elastic buckling stress for the imperfect shell is done using equations (3.21) to (3.25) in which the term M_θ is replaced by $Z_s = 0.954 M_\theta^2$, known as the Batdorf width parameter. Then for the calculation of the residual stress reduction factor equation (3.26) is to be used with λ_n replaced by λ and several choices for η :

$$\eta \begin{cases} = 4.5 & \text{for continuous structural fillet welds} \\ = 3.0 & \text{for light fillets or where shakeout is significant} \\ = 0.0 & \text{for stress relieved structure} \end{cases}$$

Finally the elastic critical stress for the column is evaluated using eqs. (3.28)-(3.31).

The inelastic buckling stress of the effective cross-section is obtained from the Ostenfeld-Bleich equation (3.32) using for the structural proportional limit the values of:

$$P_s \begin{cases} = 0.5 & \text{for non stress relieved shells} \\ = 0.75 & \text{for stress relieved shells} \end{cases}$$

At the last step the bay average collapse stress is given by the procedure used in equation (3.33) using the corrected shell effective width.

3.2.1.3 - DnV Classification Note 30.1

This code¹⁰² recognises three categories of longitudinally stiffened cylindrical shells, denominated as Categories A, B and C.

In category A are classified the sparsely stiffened shells $(s/t > 3\sqrt{R/t})$ which behave basically like unstiffened shells. The stiffeners are only accounted for the cylinder total cross sectional area and moment of inertia.

Category B includes shells with closely spaced heavy stiffeners $(s/t < 3\sqrt{R/t})$. By neglecting the effect of curvature the code recommends that the strength of such structure can be taken equal to the strength of an equivalent stiffened flat plate.

Finally category C is reserved to the shells with closely spaced light stiffeners $s/t < 3\sqrt{R/t}$ and $R/t > 1/4 E/\sigma_y$. The behaviour is assumed to be like an orthotropic shell.

This last category of shells is the one considered in this study and the evaluation of the bay instability stresses for them is as follows:

$$\sigma_u = \frac{\sigma_y}{\sqrt{1+\lambda^4}} \quad (3.35)$$

in which $\lambda = \sqrt{\frac{\sigma_y}{\sigma_e}}$ is the reduced slenderness.

The elastic buckling resistance is given by:

$$\sigma_e = C \frac{\pi^2 E}{12(1-\nu^2)} \left(\frac{t}{L}\right)^2 \quad (3.36)$$

in which the reduced buckling coefficient C accounts for the type of loading, shell proportions, boundary conditions, degree of stiffening and geometrical imperfections:

$$C = K \sqrt{1 + 0.13 \left(\frac{Z_t}{K}\right)^2} \quad (3.37)$$

in which $K = \frac{1+\gamma}{1+a}$, $a = \frac{A_s}{st}$, $\gamma = \frac{12(1-\nu^2)I}{st^3}$ and $I = I_s + \frac{e_s^2 A_s}{1+a}$.

3.2.1.4 - European Convention for Constructional Steelwork Formulation

In this formulation¹⁰³ the elastic buckling is determined by a two term equation, accounting for unstiffened shell buckling and column buckling. The shell is assumed to be simply supported and to buckle with one half wave in the axial direction and the stiffener eccentricity is neglected.

$$\sigma_{cr} = \frac{\pi^2 E I_e}{(A_s + st) L^2} + \frac{C_x}{\left(1 + \frac{A_s}{st}\right)} \frac{E}{\sqrt{3(1-\nu^2)}} \left(\frac{t}{R}\right) \quad (3.38)$$

in which

3.2.2 - Formulations for ultimate strength under radial pressure loads.

Four different formulations were studied for the case of radial pressure, three of them are presented in the codes of practice^{101,102} and the fourth is that one proposed by Oliveira¹⁵² in the RCC work.

3.2.2.1 - API Bulletin 2U

As for the case of axial compression this code covers the same types of failure (local buckling, bay buckling and general buckling). It also makes the same type of recommendation to the relative magnitudes of the critical stresses and for the design of the stiffeners to resist local buckling.

To resist radial pressure ring stiffeners are much more effective than stringers and the buckling stress is increased for values of $L/R < 2.85 \sqrt{R/t}$. For greater spacing between rings the buckling pressure is the same as that of an unstiffened cylinder (local shell buckling).

3.2.2.1.1 - Local shell buckling.

Due to the assumption that one-half wave is formed between the stringers, they are supposed to be ineffective when $N_s/2$ is less than the number of circumferential buckle waves for a similar unstiffened cylinder.

The shell elastic buckling stress is given by:

$$\sigma_{cr} = \frac{P_{eL} R}{t} k_{\theta L} \quad (3.43)$$

$$\text{where } \left. \begin{aligned} k_{\theta L} &= 1, & \text{for } M_x \geq 3.42 \\ &= 1 - \varepsilon \psi, & \text{for } M_x < 3.42 \end{aligned} \right\} \quad (3.44)$$

$$\text{with } \varepsilon = \frac{1}{1 + L_e t/A}, \quad A = A_c \left(R/R_c \right)^2, \quad L_e = 1.56 \sqrt{R t} + t_w \leq L.$$

$$\text{and } \left. \begin{aligned} \psi &= 1, & \text{for } M_x \leq 1.26 \\ &= 1.58 - 0.46 M_x, & \text{for } 1.26 < M_x < 3.42 \\ &= 0.0, & \text{for } M_x \geq 3.42 \end{aligned} \right\} \quad (3.44A)$$

The theoretical failure pressure p_{eL} is given by minimising the following equation

$$P_{eL} = \frac{Et/R}{n^2 - 1} \left[\frac{(n^2 + \lambda^2 - 1)^2}{12(1 - \nu^2)} \left(\frac{t}{R} \right)^2 + \frac{\lambda^4}{(n^2 + \lambda^2)^2} \right], \quad \text{for } n \geq 0.5 N_s \quad (3.45)$$

with $\lambda = \pi R/L$. The inelastic buckling stress is then calculated using equation (3.2) and (3.3) replacing σ_{icr} by σ_{cr} .

3.2.2.1.2 - Bay instability.

Orthotropic shell theory.

The procedure for evaluation of the bay instability due to radial pressure is identical to the one used for axial compression (eq.(3.18)). The differences are in the evaluation of the elastic buckling load (eq.(3.12)) in which the term Y , given in equation (3.14), is replaced by $Y = \left(\frac{n}{R}\right)^2$ and the shell is considered all effective, i.e., $s_e=s$. Also the evaluation of the elastic buckling stress is different:

$$\sigma_e = \alpha_{\theta L} \frac{N_e}{t} k_{\theta L} \quad (3.46)$$

in which no imperfections are considered $\alpha_{\theta L} = 1.0$ and $k_{\theta L}$ is given by equations (3.44) and (3.44A).

Alternative method.

The use of this method is recommended when limitations of the orthotropic shell theory are not met. This formulation is based in Miller's work¹⁵³ and consists of a two term equation, accounting for both the contribution of the unstiffened cylinder and the shell plus stiffener combination. Thus the inelastic failure pressure is given by the following equation:

$$p_c = (p_{eL} + p_s) k_p \quad (3.47)$$

in which the effective pressure correction factor k_p is given by:

$$\left. \begin{aligned} K_p &= 0.25 + \frac{0.85}{500} g, & \text{for } g \leq 500 \\ &= 1.10, & \text{for } g > 500 \end{aligned} \right\} \quad (3.48)$$

where $g = M_x M_\theta L t \frac{A_s}{I_s}$.

The local buckling pressure for the unstiffened shell is given by the following equations:

$$\left. \begin{aligned}
p_{eL} &= \frac{1.27}{A^{1.18} + 0.5} E (t/R)^2, & \text{for } M_x > 1.5 \text{ and } A < 2.5 \\
&= \frac{0.92}{A} E (t/R)^2, & \text{for } 2.5 < A < 0.208 R/t \\
&= 0.836 C_p^{-1.061} E (t/R)^3, & \text{for } 0.208 < C_p < 2.85 \\
&= 0.275 E (t/R)^3, & \text{for } C_p > 2.85
\end{aligned} \right\} \quad (3.49)$$

where $A = M_x - 1.17$ and $C_p = A/R/t$.

The shell plus stiffener contribution is calculated using

$$p_s = \frac{16}{s L^2} |e_s| A_s \sigma_y \quad (3.50)$$

The bay instability stress is given by :

$$\sigma_u = \frac{p_c (R+t)}{t} k_{\theta L} \leq \sigma_y \quad (3.51)$$

where $k_{\theta L}$ is given by equations (3.44) and (3.44A).

3.2.2.2 - RCC Formulation

A theoretical approach to this failure model is made difficult by the complex interactions between stringer bending and shell instability and so the model is necessarily semi-empirical¹⁴².

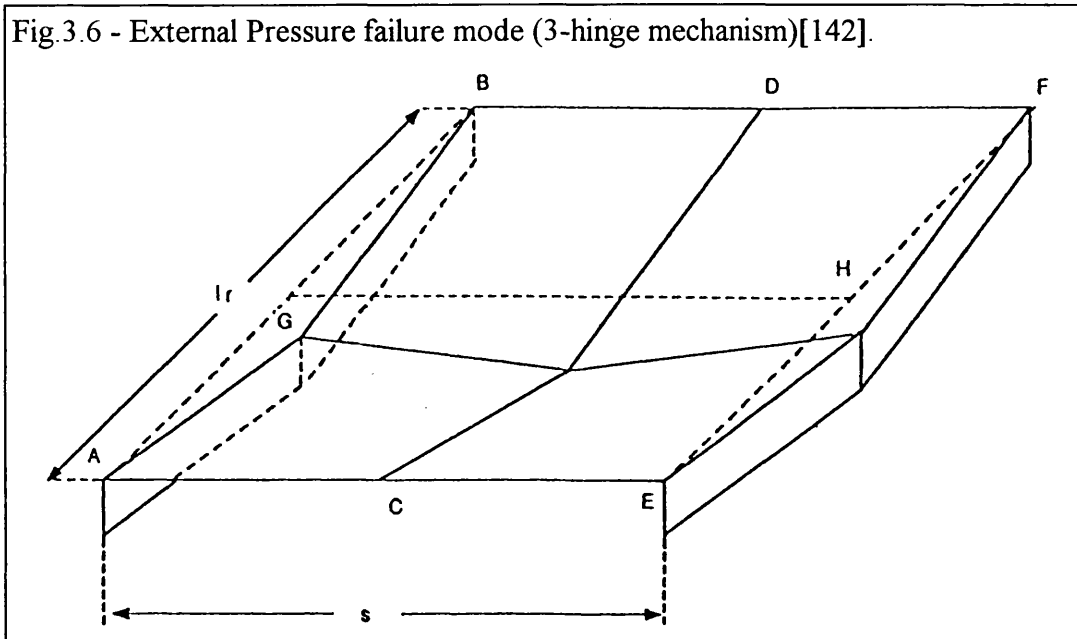
In this model an energy approach is used with the material assumed to behave in a rigid/perfectly plastic manner so that elastic and strain hardening effects are neglected. Furthermore the rings are assumed to be sufficiently strong to preclude their failure before bay instability occurs. The assumed collapse mechanism is illustrated in fig.(3.6) and is based on the following assumptions:

- the stiffeners fail by a 3-hinge mechanism
- the shell between stiffeners fail by a combination of 3 circumferential and 3 longitudinal hinges

Equating the rates of external work and internal energy dissipation, de Oliveira arrives to the following expression:

$$\frac{P_u}{\sigma_y} = \left(9.728 f_1 Z_p / s L^2 + 1.368 t^2 (2/L^2 + 1/s^2) f_2 f_3 \right) \leq t/R \quad (3.52)$$

Fig 3.6 - External Pressure failure mode (3-hinge mechanism)[142].



with the plastic modulus of the stringer given by:

$$Z_p = t_w \left\{ (d_w + t)^2 - (d_f t_f / t_w)^2 + 2(d_w + t) d_f t_f / t_w \right\} / 4 \quad (3.53)$$

and the functions f_1 , f_2 and f_3

$$\left. \begin{aligned} f_1 &= 1 + \left(\left(s^2 / R t \right) / 35.06 \right)^{1.75} \\ f_2 &= 1 + \left(\left(s^2 / R t \right) / 30.55 \right)^{3.50} \\ f_3 &= 1 + 2.65 \left(t / L \right) \left(E / \sigma_y \right) \left(t / 2 R \right)^{1/2} \end{aligned} \right\} \quad (3.54)$$

The bay instability stress is given simply by:

$$\sigma_u = \frac{P_u R}{t} \quad (3.55)$$

3.2.2.3 - DnV Classification Note 30.1

In this Note the same procedure is used for axial compression and for radial pressure. In this way the bay instability stress due to radial pressure is given by

equation (3.35). The elastic buckling stress used in the above mentioned equation is given by (eq. (3.36)) using the following reduced buckling coefficient:

$$C = K \sqrt{1 + \frac{0.4}{K^2} Z} \quad (3.56)$$

where $K = 2(1 + \sqrt{1 + \gamma})$, γ and I are calculated in the same way as in the axial compression case.

3.2.3 - Formulations for ultimate strength under combined loads.

Several interaction equations exist for all the different possible load combinations. In¹⁵⁴ seven of them are discussed and analysed. In the present case only interaction equations involving axial and hoop compression will be considered, mainly due to the frequent occurrence of these loads and their greater magnitude. Bending can be transformed into an equivalent axial compression load. This is supported by several tests¹⁵⁵, with R/t ratio greater than 150. However for $R/t < 48$ the buckling stress for bending are higher¹⁵⁶ which limits the validity of this assumption to cylinders with $R/t > 48$.

3.2.3.1 - API Bulletin 2U

The interaction equation for combination of axial and hoop compression recommended by the code is based on a modification of the Huber-Hencky-Von Mises failure theory.

$$R_a^2 - c R_a R_h + R_h^2 = 1.0 \quad (3.57)$$

$$\left. \begin{aligned} \text{where } R_a &= \frac{\sigma_x}{\sigma_{ux}} \\ R_h &= \frac{\sigma_\theta}{\sigma_{u\theta}} \\ c &= \frac{1.5(\sigma_{ux} + \sigma_{u\theta})}{\sigma_y} - 2.0 \end{aligned} \right\} \quad (3.58)$$

The buckling stresses for any combination of longitudinal and hoop compression are determined by the following procedure:

1. Calculate σ_{ux} and $\sigma_{u\theta}$, ultimate collapse stresses for an individual buckling mode from any of the previous sets of equations.

2. Solve for $\sigma_{u\theta}$ in (eq.(3.57)) by letting $\sigma_x = \sigma_\theta \left(\frac{N_x}{N_\theta} \right) \left(\frac{k_x}{k_\theta} \right)$ where $k_x = t/t_x$ and $k_\theta = k_{\theta L}$ (see equations (3.17) and (3.44)).

3.2.3.2 - RCC Formulation

This formulation is based on Odlands method¹⁵⁷ for unstiffened and ring stiffened shell under combined loads, which was extended for use with stringer-stiffened shells by Faulkner¹⁵⁸.

$$\frac{p}{p_u} + 1.5 \frac{\sigma_x}{\sigma_{ux}} - 0.5 \left(\frac{\sigma_x}{\sigma_{ux}} \right)^2 - \frac{p}{p_u} \frac{\sigma_x}{\sigma_{ux}} = 1.0 \quad (3.59)$$

An alternative formulation exists and it is similar to API Bulletin 2U interaction model. It is given by (eq.(3.60)) with the coefficient c presented in equation (3.61):

$$R_a^2 + c \left(\frac{\sigma_x}{\sigma_y} \right) \left(\frac{\sigma_\theta}{\sigma_y} \right) + R_h^2 = 1.0 \quad (3.60)$$

$$c = 2 \frac{\sqrt{\left(1 - \left(\frac{\sigma_{ux}}{\sigma_y} \right)^2 \right) \left(1 - \left(\frac{\sigma_{u\theta}}{\sigma_y} \right)^2 \right)}}{\left(\frac{\sigma_{ux}}{\sigma_y} \right) \left(\frac{\sigma_{u\theta}}{\sigma_y} \right)} - 1.0 \quad (3.61)$$

3.2.3.3 - DnV Classification Notes (30.1)

The DnV proposal is based in an equivalent stress approach according to Huber-Von Mises, which is expressed by the following set of equations. The equivalent applied stress is given by:

$$\sigma_{eq} = \sqrt{\sigma_x^2 - \sigma_x \sigma_\theta + \sigma_\theta^2} \quad (3.62)$$

and it is used in the evaluation of the ultimate equivalent buckling stress via the λ parameter

$$\lambda^2 = \frac{\sigma_y}{\sigma_{eq}} \left(\frac{\sigma_x}{\sigma_{ux}} + \frac{\sigma_\theta}{\sigma_{u\theta}} \right) \quad (3.63)$$

and
$$\sigma_{ueq} = \frac{\sigma_y}{\sqrt{1 + \lambda^4}} \quad (3.64).$$

3.3 - Evaluation of the model uncertainty for the strength formulations.

Experiments are generally aimed to validate both theoretical models or engineering solutions. In this study they are of utmost importance because it is the only way to assess the level of uncertainty existing in the different strength formulations for ring and stringer stiffened cylinders. Thus, a systematic study was performed to provide the model uncertainty^{3,65} (eq.(3.65)) of all these formulations.

$$X_m = \frac{\sigma_t}{\sigma_u} = \frac{\text{Experimental strength}}{\text{Predicted strength}} \quad (3.65)$$

Test data must be reliable and relevant in order to produce the correct assessment. This was assured by following a systematic procedure in which all important parameters were checked. These parameters can be divided in the following groups:

- Geometrical properties, i.e. the length, radius, thickness, ring and stringer dimensions and spacing, number of bays.
- Material properties, i.e. yield stress (tensile or compressive), the rate of loading, modulus of elasticity.
- Geometric imperfections, shape and maximum of initial distortions.
- Method of production, welding, machining, residual or relieved stresses.
- Test conditions, i.e. boundary conditions, experimental collapse loads starting from local failure, if any.

3.3.1 - Description of the available experimental data.

The collected experimental data can be subdivided into two major groups; Aerospace and Offshore. The first group is the outcome of an extensive aerospace research programme carried out in the mid 1960's. These tests were mainly conducted in the elastic range and the majority of them used high strength steel and aluminium alloys test specimens. In these specimens a large number of stringers were used which implies a close space between them. Also they were machine finished which means minimal imperfections and residual stresses.

The second group is a result of an emerging interest from the offshore industry. Steel is the dominant material used and the fabrication methods have inherent initial imperfections and induce important residual stresses. This type of structures normally fail in the elastoplastic range. To understand correctly this type of failure more tests

were conducted in the 1970's mainly in UK universities and in the 1980's by Conoco/ABS.

From the aerospace data 193 axial compression test specimens have been considered; 84 steel and 109 aluminium. The offshore data is composed of 99 test specimens from which 52 (48 steel and 4 aluminium) were tested under axial compression, 12 steel specimens were tested under radial pressure and 35 steel specimens tested under combined axial and radial loading. The details of these test specimens are shown in Tables (3.1-3.6) and a brief description of the test programmes is given hereafter.

3.3.1.1 - Aerospace programmes

The test programmes in the aerospace field begun in the mid 1960's basically in USA the results of which have been reported in Refs. [159,160] as early as 1965. In the 1970's the most important tests were conducted in the Technical Institute of Israel - Department of Aeronautical Engineering¹⁶¹⁻¹⁶⁹. From these two programmes up to 193 test data have been collected.

These results are useful for providing information on elastic buckling strength because the tests were mainly conducted in the elastic range and the majority of them used high strength materials.

A sample of the geometries and material properties of these specimens and the test results is given in Table 3.1. The complete database is presented in Tables A2.1-A2.2 in Appendix 2.

Model	Mat.	Tk	Ns	Rad	L	dw	tw	E	SigY	Sigu
AB1	alu.	0.257	85	120.	110.4	1779	0.9	73.6	594.0	139.32
AB2	alu.	0.253	85	120.1	110.5	1757	0.9	73.6	594.0	147.42
AB3	alu.	0.253	85	120.1	153.8	1747	0.9	73.6	594.0	102.60
AB4	alu.	0.253	85	120.1	153.8	1742	0.9	73.6	594.0	109.08
AB5	alu.	0.252	85	120.2	129.8	1700	0.8	73.6	594.0	114.48
AB6	alu.	0.254	85	120.1	129.7	1484	0.9	73.6	594.0	129.06
4-L	stl.	0.247	132	127.6	90.66	0.267	1059	196.0	462.0	158.76
4-M	stl.	0.238	132	127.5	59.95	0.269	1.06	196.0	462.0	162.54
4-S	stl.	0.227	132	127.5	30.6	0.274	1.06	196.0	462.0	139.02
5-L	stl.	0.229	132	127.5	90.56	0.241	1.06	196.0	462.0	150.78
5-M	stl.	0.236	132	126.4	59.45	0.236	1.05	196.0	462.0	127.26
5-S	stl.	0.242	132	127.5	30.6	0.254	1.06	196.0	462.0	148.68
6-L	stl.	0.3	132	127.8	145.6	0.296	1.06	196.0	462.0	148.68
6-S	stl.	0.307	132	127.7	39.6	0.32	1.06	196.0	462.0	164.64
7-L	stl.	0.286	132	127.8	145.7	0.323	1.06	196.0	462.0	178.08

Table 3.1-Sample of models of aerospace test programmes

3.3.1.1.1 - Technion Tests

The first series of tests¹⁶¹ were aimed at studying the influence of stiffener and shell geometry on the applicability of a linear theory for predicting collapse. A practical parameter turned out to be the ratio between the stiffener area and the cylinder area (A_s/st) and good correlation with linear theory was found for A_s/st . Investigation results¹⁶² also indicate good agreement with the linear theory. In the investigation Z_s also proved to be a suitable parameter, and good agreement was achieved with increasing values of Z_s and A_s/st . In these tests the sensitivity of the test specimens to boundary conditions was highlighted.

The last groups of experiments¹⁶³⁻¹⁶⁹ were aimed at developing a non-destructive technique of assessing the strength of stringer-stiffened cylinders by means of vibration correlation techniques.

3.3.1.2 - Offshore programmes

In the context of offshore design, the material used was steel and, due to the method of fabrication, the structures had considerable inherent initial imperfections (deflections and residual stresses). These structures generally failed in the elasto-plastic range. In the 1970's there was a large test programme in UK Universities and elsewhere in Europe and by Conoco/ABS in the early 1980's. As far as possible, the details of the specimens tested have been taken from the original sources and have been incorporated in the present study after a careful review.

The various number of test data that have been considered in this study are shown in Tables (3.2-3.6) with their details, including their experimental collapse loads and mode of failure. The experiments are broadly divided into three groups and summarised as follows; *Axial Compression* - 48 steel and 4 aluminium specimens; *Radial Pressure* - 12 steel specimens; *Combined Axial and Radial Loading* - 38 steel specimens.

The number and variety of test data, particularly the dimensions and construction methods used in their fabrication allows to say that the test database is not biased by scale and fabrication effects. On the other hand, the formulations use average values for residual stresses and initial deformations allowing the use of all the experimental data for their calibration.

3.3.1.2.1 - UCL Tests

The UCL test programme^{170,171} consisted of 18 specimens tested under axial compression. The specimens were approximately 1/20th scale. The specimens were manufactured from thin sheet steel having properties fairly representative of those in full scale structures. The cylinders were built up segmentally by rolling and machining the steel sheets into curved panels and then welded together with stiffeners. The stiffeners were of flat bar and welded at right angles to the shell. The initial deformations were measured and in general two types of them were noted. One was of "overall" type, i.e. in the form of one half-wave in the longitudinal direction producing ovalities in the circumferential direction. The second one was of localised character and occurred in the form of 'blips' at each stiffener. The magnitude of these imperfections were reported to have been within DnV's tolerance limits.

Model	Styp	Tk	Ns	Rad	L	dw	tw	E	SigY	Sigu
UC1	BE	0.81	20	160.7	64.3	6.48	0.81	210.0	324.0	265.68
UC2	BE	0.81	40	160.0	177.6	6.48	0.81	210.0	320.0	329.6
UC3	BE	0.81	20	161.4	179.1	12.96	0.81	210.0	322.0	244.72
UC4	BE	0.81	30	159.8	177.4	12.96	0.81	213.0	320.0	307.2
UC5	BE	0.81	40	159.6	177.1	12.96	0.81	203.0	338.0	351.52
UC6	BE	0.81	40	226.6	251.6	6.48	0.81	211.0	311.0	202.15
UC7	BE	0.81	40	226.5	251.4	12.96	0.81	211.0	311.0	267.46
UC8	BE	0.81	20	289.5	321.0	12.96	0.81	201.0	309.0	157.59
UC9	BE	0.81	40	288.2	319.8	12.96	0.81	211.0	340.0	224.40
A1	BE	0.81	8	76.2	101.6	12.7	0.81	205.0	298.65	282.36
A2	BE	0.81	8	76.2	101.6	12.7	0.81	205.0	298.65	284.80
A3	BE	0.81	8	76.2	101.6	12.7	0.81	205.0	298.65	292.95
A4	BE	0.81	8	76.2	101.6	12.7	0.81	205.0	298.65	252.50
B1	BE	0.81	40	226.8	353.8	12.96	0.81	210.0	313.0	256.66
B2	BE	0.81	20	226.8	353.8	12.96	0.81	210.0	324.0	174.96
B3	BE	0.81	20	226.8	251.7	12.96	0.81	210.0	284.0	170.40
B4	BE	0.81	20	226.8	176.9	12.96	0.81	210.0	281.0	171.41
B5	BE	0.81	40	226.8	353.8	13.00	1215	210.0	318.0	260.76

Table 3.2-UCL Test specimens - Geometry, material properties and test result.

These test specimens were categorised into broad panelled and narrow panelled ones. The collapse of the narrow panelled cylinders was characterised by overall buckling while for the broad panelled ones it was due to local buckling. The average residual stresses ranged from $0.25\sigma_y$ for the narrowest panel to $0.08\sigma_y$ for the broadest panel.

The specimens had clamped boundary conditions and were tested under conditions of controlled end shortening. The geometry and material properties of these specimens and test results are given in Table 3.2.

3.3.1.2.2 - Imperial College Tests

In the research programme¹⁷²⁻¹⁷⁴ sponsored by the Department of Energy, UK. six small scale stringer stiffened cylinder tests were carried out at Imperial College and one of the main objectives of these tests were to test specimens fabricated in different way as those adopted by University College. The specimens were fabricated by welding first the longitudinal stiffeners to a flat plate of the length corresponding to the cylinder diameter. The stiffened plate was then wrapped round a mandrel and the cylinder was formed by T-butt weld. The cylinders were relieved from residual stresses after their fabrication. No residual stress measurements were taken. In order to ensure a rigid end condition, steel annuli were attached to the ends of the specimen, both inside and outside the cylindrical shell by use of a resin compound. Geometric deformation measurements were taken and subsequently evaluated in terms of 'best fit' cylinder. The boundary of each cylinder was rigidly clamped against rotation.

Specimens IC1 to IC3 were tested under axial compression. IC1 failed by a ridge type panel mechanism between stiffeners at mid height. In IC2 the mechanism was formed at the end of the cylinder. In IC3 panel buckling was noted at mid height including sideways tripping of the stiffeners. Specimens IC4 to IC6 were nominally identical to specimens IC1 to IC3 respectively. The load was applied eccentrically to these specimens. Failure load of these specimens are less than those of IC1-IC3 series

Model	Styp	Tk	Ns	Rad	L	dw	tw	E	SigY	Sigu	
IC1	BE	0.84	40	160	65.0	6.72	0.84	201.0	348.0	334.0	
IC2	BE	0.84	20	160	65.0	6.72	0.84	201.0	348.0	336.0	
IC3	BE	0.84	40	160	180.0	13.4	0.84	201.0	348.0	332.0	
IC4	BE	0.84	40	160	65.0	6.72	0.84	201.0	348.0	372.0	
IC5	BE	0.84	20	160	65.0	6.72	0.84	201.0	348.0	327.0	
IC6	BE	0.84	40	160	180.0	13.4	0.84	201.0	348.0	356.0	
SLDA	BE	0.63	20	160	160.0	13.6	0.63	210.0	365.0	281.1	
SLDE	BE	0.63	40	160	160.0	6.72	0.84	202.0	365.0	401.5	
DnV1	BE	0.84	40	160	64.0	6.72	0.84	202.0	344.0	325.4	
DnV7	BE	0.84	40	160	128.0	6.72	0.84	202.0	344.0	345.4	
DnV10	BE	0.84	40	160	192.0	6.72	0.84	202.0	344.0	350.9	
Model	Styp	Tk	Ns	Rad	L	dw	tw	E	SigY	Pu	
DnV3	BE	0.84	40	160.0	64.0	6.72	0.84	202.0	344.0	1.890	
DnV6	BE	0.84	40	159.8	128.0	6.72	0.84	202.0	344.0	0.960	
DnV11	BE	0.84	40	159.9	192.0	6.72	0.84	202.0	344.0	0.631	
Model	Styp	Tk	Ns	Rad	L	dw	tw	E	SigY	Sigu	Pu
DnV4	BE	0.84	40	160.0	64.0	6.72	0.84	202.0	344.0	335.7	1.236
DnV8	BE	0.84	40	159.9	128.0	6.72	0.84	202.0	344.0	289.6	0.775
DnV12	BE	0.84	40	160.0	192.0	6.72	0.84	202.0	344.0	183.7	0.479
SLDB	BE	0.63	20	160.0	160.0	3.60	0.63	205.0	365.0	26.0	0.22
SLDC	BE	0.63	20	160.0	160.0	3.60	0.63	205.0	365.0	246.0	0.145
SLDF	BE	0.63	40	160.0	160.0	3.60	0.63	205.0	365.0	26.0	0.236
SLDG	BE	0.63	40	160.0	160.0	3.60	0.63	205.0	365.0	240.0	0.153

Table 3.3-IC Test specimens - Geometry, material properties and test result.

due to eccentric loading and they showed similar behaviour.

Further research was done with similar test specimens but under different load conditions (radial pressure and combined loading). The geometry and material properties of these specimens and test results are given in Table 3.3.

3.3.1.2.4 - Glasgow University Tests

These tests were carried out by Glasgow University from the middle of 1978 to the middle 1979 and this research was sponsored by the Department of Energy as part of the marine technology programme¹⁷⁵.

Three test specimens 1/8th in scale of stringer stiffened cylinders were fabricated from thin steel plates. In all these specimens extensive strain gauge measurements were taken. Axial shortening and out-of-surface displacements in the shells were recorded at each increment of loading. All of these specimens failed due to bay instability. The geometry and material properties of these specimens and test results are given in Table 3.4.

Model	Styp	Tk	Ns	Rad	L	dw	tw	E	SigY	Sigu
GU1	BE	2.00	20	570.0	890.0	32.00	2.00	191.0	234.0	147.42
GU2	BE	6.00	8	570.0	760.0	95.00	6.00	197.0	300.0	291.00
GU3	BE	3.00	30	590.0	650.0	45.0	3.00	204.0	420.0	289.80

Table 3.4-GU Test specimens - Geometry, material properties and test result.

3.3.1.2.4 - CBI Tests

This test programme^{154,176} forms one of the largest test programmes aimed at establishing the behaviour of orthogonally stiffened cylinders used in the offshore industry and was sponsored mainly by Conoco Inc, Houston and the American Bureau of Shipping. It was initiated in 1982 and under Phase I programme were tested 14 multi-bay test specimens under axial compression, 8 under radial pressure and 22 under combined axial and radial loading.

In Phase II programme (1985/86) six more orthogonally stiffened cylinders were tested: 1 multi-bay specimen under axial compression, 1 under radial pressure and 4 under combined loading. These cylinders had large radius-to-thickness ratios R/t equal to 300 and 500. The geometry and material properties of the test specimens and results are given in Table 3.5.

Model	Styp	Tk	Ns	Rad	L	dw	tw	df	ff	E	SigY	Sigu	Srl	
2-1A	BE	1.958	36	571.5	228.6	30.48	1.94	0.0	0.0	218.3	386.5	255.99		
2-1AE	EL	2.047	36	569.2	228.6	30.48	2.07	10.2	2.1	209	409	295.49		
2-2A	BE	1.963	18	570.5	228.6	30.48	1.94	0.0	0.0	221	387.6	240.75		
2-3A	BE	1.877	36	570.8	571.5	30.48	1.88	0.0	0.0	198.1	412.8	301.7		
2-3AE	BE	2.192	36	569.3	571.5	30.48	2.16	0.0	0.0	212.2	512.5	336.52		
2-3AR	BE	1.9	36	571	571.5	30.48	1.86	0.0	0.0	215.3	442	255.23	No	
2-3ATR	TE	1.958	36	571.5	571.5	22.86	1.94	15.2	1.9	189.5	408.2	331.4	No	
2-4A	BE	1.963	18	568.5	571.5	30.48	1.95	0.0	0.0	210.5	419	240.68		
2-5A	BE	1.956	48	952.4	381	30.48	1.92	0.0	0.0	199.4	416	226.55		
2-6A	BE	1.994	24	949.2	381	30.48	1.95	0.0	0.0	201.5	408.4	176.57		
2-7A	BE	1.908	48	951.7	762	30.48	1.94	0.0	0.0	210.5	412	252.13		
2-7AR	BE	1.956	48	953.3	762	30.48	1.96	0.0	0.0	196	418	229.65	No	
2-8A	BE	1.88	24	950.8	762	30.48	1.95	0.0	0.0	204.5	423	181.6		
2-9A	BE	1.946	40	361.2	289.5	30.48	1.95	0.0	0.0	199.7	342.9	323.69		
2-9ATC	BE	2.085	40	362.8	289.5	30.48	2.01	0.0	0.0	195.9	342.9	269.78	No	
Model	Styp	Tk	Ns	Rad	L	dw	tw	df	ff	E	SigY	Pu	Srl	
2-1C	BE	1.956	36	571.4	228.6	30.48	1.91	0.0	0.0	215.7	393.2	0.787		
2-2C	BE	1.948	18	569.2	228.6	30.48	1.91	0.0	0.0	203.1	385.9	0.759		
2-3C	BE	1.920	36	570.2	571.5	30.48	1.92	0.0	0.0	209.2	396.7	0.354		
2-5C	BE	1.961	48	949.7	381.0	30.48	1.97	0.0	0.0	200.5	408.4	0.341		
2-6C	BE	1.974	24	953.6	381.0	30.48	1.95	0.0	0.0	198.2	409.0	0.313		
2-7C	BE	1.938	48	949.8	762.0	30.48	1.91	0.0	0.0	210.2	403.4	0.170		
2-8C	BE	1.895	24	950.9	762.0	30.48	1.91	0.0	0.0	202.4	421.9	0.150		
2-9C	BE	1.928	40	360.7	289.6	30.48	1.93	0.0	0.0	192.2	325.7	1.03		
Model	Styp	Tk	Ns	Rad	L	dw	tw	df	ff	E	SigY	Sigu	Pu	Srl
2-1B	BE	1.966	36	571.1	228.6	30.48	1.96	0.0	0.0	217.7	395.7	82.11	0.736	
2-1D	BE	1.958	36	569.4	228.6	30.48	1.92	0.0	0.0	216.2	396.9	209.80	0.52	
2-2B	BE	1.961	18	571.8	228.6	30.48	1.94	0.0	0.0	209.5	390.5	79.84	0.629	
2-2D	BE	1.956	18	570.5	228.6	30.48	1.93	0.0	0.0	201.7	384.7	157.68	0.345	
2-3B	BE	1.854	36	570.8	571.5	30.48	1.86	0.0	0.0	210.5	425.0	40.26	0.335	
2-3BTR														No
2-3D	BE	1.908	36	571.5	571.5	30.48	1.87	0.0	0.0	208.3	391.8	117.14	0.283	
2-3G														No
2-3GTR														No
2-4B	BE	1.976	18	570.1	571.5	30.48	1.97	0.0	0.0	217.2	425.3	37.16	0.290	
2-4C	BE	1.971	18	569.6	571.5	30.48	1.92	0.0	0.0	200.5	432.7	29.92	0.285	
2-4D	BE	1.946	18	570.3	571.5	30.48	1.88	0.0	0.0	207.4	417.5	102.45	0.223	
2-5B	BE	1.971	48	953.2	381.0	30.48	1.98	0.0	0.0	207.7	398.4	63.64	0.324	
2-5D	BE	1.969	48	953.2	381.0	30.48	1.98	0.0	0.0	207.7	398.4	173.33	0.248	
2-6B	BE	1.963	24	951.7	381.0	30.48	1.80	0.0	0.0	200.1	404.6	62.46	0.282	
2-6D	BE	1.958	24	952.1	381.0	30.48	1.96	0.0	0.0	202.5	415.7	115.96	0.170	
2-7B	BE	1.961	48	954.9	762.0	30.48	1.96	0.0	0.0	209.4	406.2	28.82	0.139	
2-7D	BE	1.925	48	956.6	762.0	30.48	1.90	0.0	0.0	206.9	422.3	95.90	0.134	
2-7BE	BE	1.803	48	954.2	762.0	30.48	1.82	0.0	0.0	203.2	406.3	33.16	0.148	
2-7DF	BE	1.829	48	950.5	762.0	30.48	1.81	0.0	0.0	199.1	417.9	93.63	0.124	
2-7G														No
2-8B	BE	1.895	24	953.2	762.0	30.48	1.91	0.0	0.0	205.5	422.6	29.92	0.125	
2-8D	BE	1.880	24	953.4	762.0	30.48	1.88	0.0	0.0	204.9	422.6	77.01	0.095	
2-9B	BE	1.943	40	361.0	289.6	30.48	1.94	0.0	0.0	193.0	341.5	75.84	1.03	
2-9D	BE	1.963	40	360.4	289.6	30.48	1.96	0.0	0.0	197.8	341.8	205.59	0.787	
2-9D1D	BE	2.078	40	359.7	360.7	30.48	2.00	0.0	0.0	197.8	330.8	314.18	0.870	

Table 3.5-CBI Test specimens - Geometry, material properties and test result.

This test programme was structured to investigate the effects of several parameters on the buckling of stiffened shells subjected to combinations of axial compression and radial pressure loads. These included the effects of shell and stiffener geometry, residual stresses, initial deformations and material yield strength. Radial displacement, axial shortening and strain gage measurements were made on all models during test. All specimens were found to be fabricated within prescribed tolerances and the maximum measured deformations were close to the prescribed tolerances. The test specimens were designed to study the interaction of various geometrical parameters with the local shell buckling and bay instability buckling modes.

Groups 2-1 and 2-5 had narrow panels and short bay lengths, with 2-1 having an $R/t = 300$ and 2-5 having an $R/t = 500$. Groups 2-3 and 2-7 had narrow panels and long bay lengths for the same R/t ratios as groups 2-1 and 2-5, respectively. Similarly, groups 2-2 and 2-6 had wide panels and short bay lengths and groups 2-4 and 2-8 had wide panels and long bay lengths. Groups 2-9, however, had $R/t = 190$ with very narrow panels but moderately long bay length.

Each group of models exhibited consistent responses, acting similarly to other models of the same group and similarly to other groups. The responses can be categorised for the two generalised loading categories as follows: axial loading cases (type A specimens) and pressure loading cases (type B, C and D specimens). For the first category, at collapse most of the specimens failed in the end bays.

For the second, the general trend was, form a local shell buckle pattern in the middle bay. This pattern was typically an alternating in-out wave in adjacent panels with the inward wave being dominant. With increasing pressure a bay instability wave mode would then develop and cause final specimen collapse.

The non-stress relieved specimens exhibited lower critical buckling stresses and significantly different buckling wave action than the comparable stress relieved specimens.

3.3.1.2.5 - DnV Tests

Tests of four aluminium specimens¹⁷⁷ were carried out by DnV in order to validate their formulations. High strength aluminium was chosen in order to make use of the lower capacity requirement of the test rigs.

Specimens NV1 to NV3 failed in panel buckling mode, while in NV4 both panel and local buckling were observed. The geometry and material properties of these specimens and test results are given in Table 3.6.¹⁷⁸

Model	Styp	Tk	Ns	Rad	L	dw	tw	E	SigY	Sigu	
NV1	BE	3.50	80	1250.0	634.0	21.81	3.50	70.0	462.0	120.00	
NV2	BE	3.00	85	1250.0	570.0	18.81	3.00	70.0	462.0	112.00	
NV3	BE	3.00	85	1250.0	570.0	18.81	3.00	70.0	462.0	117.00	
NV4	BE	3.00	60	1250.0	570.0	21.81	3.00	70.0	462.0	113.00	
KINRA	BE	2.85	24	725.5	152.4	35.6	2.95	210.0	283.83	192.37	
NV3	BE	3.00	85	1250.0	570.0	18.81	3.00	70.0	462.0	117.00	
NV4	BE	3.00	60	1250.0	570.0	21.81	3.00	70.0	462.0	113.00	
KINRA	BE	2.85	24	725.5	152.4	35.6	2.95	210.0	283.83	192.37	Pu
KINRA1	BE	6.57	24	913.9	228.6	51.60	4.72	210.0	290.7	112.2	1.862
KINRA2	BE	2.85	24	728.3	152.4	35.70	2.95	210.0	258.1	83.3	0.776

Table 3.6-DnV Test specimens - Geometry, material properties and test result.

3.3.2 - Model uncertainty of the axial compression formulations.

The different strength formulations given in sub-chapter 3.2.1 were compared with the various test data available and described above. The resulting model uncertainty factor i.e. the model parameter X_m (eq.(3.64)) for the axial formulations are shown in Table 3.7. for the 52 steel and aluminium specimens .

API Bul 2U (discrete analysis) and RCC formulations exhibit moderate uncertainty (Coefficient Of Variation =13.7%) and consistent values for the offshore steel specimens, with X_m in the range of [0.82, 1.4] for API and [0.82, 1.35] for RCC. However, the inclusion of the aluminium specimens with very low experimental strength ($X_m \leq 0.5$) for API formulation, causes a noticeable degradation in API results, leading to a high uncertainty (COV=18.5%).

Both formulations are similar except that the knockdown factor associated with the shell term is different. This apparently small conceptual difference leads to large differences in the results for the specimens failing in the elastic range. This is particularly true for 3 of the 4 the aluminium specimens (NV1, NV2 and NV3) which exhibit for API-2U predictions a theoretical strength much higher than the test value. With RCC formulation these two values are quite consistent and only a small deviation occurs. In order to track down the difference between these two formulations a detailed study was done, and the result points out that API overpredicts the elastic critical stress in the shell by a factor of 2.5 over RCC, due to its higher knockdown factor. The ranges of DnV and ECCS results are respectively X_m [0.56 - 1.66] and X_m [0.79 - 2.16]. A large scatter can be observed for both formulations with COV's over 5% and with surprising results for lower bound formulations with many specimens (more than the allowable 5%) failing large below the predictions.

X _m - Axial Compression					
	API ortho	API disc	RCC	DnV	ECCS
UC1	0,820	1,063	1,064	0,864	1,086
UC2	1,310	1,134	1,169	1,342	1,627
UC3	0,760	0,971	0,972	0,825	1,029
UC4	0,960	1,077	1,077	1,012	1,258
UC5	1,049	1,112	1,118	1,094	1,374
UC6	0,955	0,824	0,839	1,046	1,236
UC7	0,943	1,019	1,023	1,018	1,294
UC8	0,528	0,929	0,920	0,877	1,112
UC9	0,820	0,921	0,919	1,004	1,215
A1	0,946	1,053	1,055	0,957	1,109
A2	0,954	1,062	1,064	0,965	1,119
A3	0,981	1,093	1,094	0,993	1,151
A4	0,846	0,942	0,943	0,856	0,992
B1	1,010	1,005	1,015	1,151	1,424
B2	0,598	0,860	0,857	0,841	0,989
B3	0,600	0,886	0,884	0,764	0,940
B4	0,610	0,876	0,875	0,673	0,856
B5	0,977	0,998	1,007	1,105	1,443
2-1A	0,662	0,816	0,816	0,669	0,788
2-1AE	0,723	0,873	0,873	0,725	0,823
2-2A	0,621	0,992	0,991	0,637	0,809
2-3A	0,854	1,031	1,029	1,000	1,271
2-3AE	0,802	0,903	0,906	0,946	1,178
2-3AR	0,674	1,019	0,984	0,788	0,996
2-3ATR	0,929	1,401	1,355	1,061	1,384
2-4A	0,586	1,025	1,021	0,904	1,142
2-5A	0,573	0,832	0,832	0,618	0,829
2-6A	0,432	0,920	0,917	0,565	0,920
2-7A	0,864	1,032	1,028	1,198	1,471
2-7AR	0,803	1,255	1,238	1,147	1,416
2-8A	0,502	1,070	0,981	1,118	1,781
2-9A	0,944	0,986	0,988	0,957	1,137
2-9ATC	0,787	0,858	0,856	0,798	0,949
IC1	0,960	1,015	1,019	0,983	1,189
IC2	0,966	1,269	1,270	1,021	1,289
IC3	0,963	1,017	1,024	1,003	1,260
IC4	1,069	1,131	1,135	1,095	1,324
IC5	0,940	1,235	1,236	0,994	1,254
IC6	1,032	1,091	1,098	1,075	1,351
SLDA	0,885	1,308	1,306	1,332	2,048
SLDE	1,361	1,345	1,364	1,531	1,898
DnV1	0,946	0,998	1,002	0,967	1,165
DnV7	1,180	1,095	1,118	1,207	1,486
DnV10	1,358	1,133	1,175	1,387	1,681
GU1	0,670	0,931	0,928	0,879	1,054
GU2	0,970	1,092	1,093	0,983	1,144
GU3	0,721	0,831	0,831	0,775	0,987
NV1	0,945	0,475	0,917	1,470	1,860
NV2	1,031	0,518	0,973	1,585	1,990
NV3	1,077	0,541	1,017	1,656	2,079
NV4	0,960	0,812	0,990	1,511	2,157
KINRA	0,678	0,860	0,859	0,679	0,741

Table 3.7-X_m for axial compression formulations, showing with shadow the accepted test specimens for API orthotropic formulation.

The API orthotropic formulation by contrast to the discrete one produces very good results for the aluminium specimens X_m [0.95 - 1.08] and very poor ones for the steel specimens with X_m ranging from [0.43 - 1.36] and a COV=25%. It is also important to stress that for a lower bound formulation the API orthotropic formulation produces results highly unconservative.

Other interesting results arises from IC specimens, which in general are more resistant than the prediction of all the formulations. This can be related to their small size and different fabrication process.

The statistical analyses are carried out using Offshore and Aerospace data for all the formulations. The Offshore data is divided into two sets of populations: 48 steel specimens and 52 (48 steel plus 4 aluminium) specimens. The Aerospace data is divided into 3 sets of population, namely, (i) 84 steel specimens, (ii) 109 aluminium specimens, (iii) 193 specimens, i.e. a combination of (i) and (ii) steel and aluminium specimens.

MODEL CODE	OFFSHORE		AEROSPACE		
	STEEL	STEEL + ALU.	STEEL	ALUMINIUM	STEEL + ALU.
	Population=48	Population=52	Population=84	Populat.=109	Populat.= 193
API Bul 2U	0.857	0.868	0.813	1.178	1.019
Orthotropic	24.78%	23.98%	19.19%	26.92%	31.02%
Discrete	1.025	0.991	0.652	1.025	0.863
	13.68%	18.44%	36.06%	53.77%	55.51%
RCC	1.024	1.020	1.332	1.893	1.649
	13.68%	13.29%	27.51%	27.96%	32.87%
DnV CN 30.1	0.967	1.012	1.633	2.051	1.869
	21.26%	25.07%	19.09%	23.29%	24.72%
ECCS	1.209	1.271	2.875	4.409	3.741
	23.57%	27.66%	34.08%	35.37%	41.10%

Table 3.8 - Bias & COV of model uncertainty factor for axial compression formulation.

From the results shown in Table 3.8 it can be seen that both API Bul 2U discrete and RCC predict almost similar results for the 48 offshore steel specimens, while for 52 offshore steel and aluminium specimens RCC gives better results than the API Bul 2U. This confirms the robustness of the RCC formulation for axial compression ($COV_{RCC}=13.3\%$ vs $COV_{API}=18.4\%$).

Figure (3.7(b)) and (A2.3(b)) show the scatter of the modelling parameter for the two formulations. The deviation of the aluminium specimens with respect to API results is clearly visible. To check the formulation skewness - tendency of the formulation uncertainty to vary with some property of the cylinder - X_m was plotted against the test and predicted strength and some relevant adimensional geometrical parameters. The results are presented in figures (3.7(b)-3.7(i)) and (A2.3(b)-A2.3(i)) with RCC clearly independent of the parameters and API showing some dependency upon the slenderness, with tendency to over predict the strength of high slender cylinders.

For the aerospace data there is a wide difference in the results between RCC and API Bul 2U discrete formulations and it may be again due to the different knockdown factor used in both formulations. The RCC results produce high bias $X_m=1.65$ and reasonable $COV_{RCC}=33\%$ (conservative design) while API 2U discrete formulation produce low bias $X_m=0.86$ (clearly over predicts the strength of the steel specimens $X_m=0.65$) and gives high $COV_{API}=56\%$. It can be seen in figures (A2.4(a)-A2.4(i)) and (A2.5(a)-A2.5(i)) the large scatter in the results for these two formulations as well as the strong skewness which both exhibit. However, it may be noted that these two formulations are not suitable for Aerospace data because in these specimens the stiffeners had greater width, low height and were closely spaced.

For the offshore data set the mean and COV as calculated by DnV Tech. CN30.1 and ECCS are as follows:

<u>DnV</u> :	Mean	=	1.012	<u>ECCS</u> :	Mean	=	1.271
	COV	=	25.07%		COV	=	27.66%

while, for the DnV formulation, the bias is good but the spread of the model uncertainty factor is wide and this reflects in the high COV values. The assumption of orthotropic behaviour for the narrow panelled cylinders ($Z_s < 9$) produces the large scatter observed in Table 3.7 while the unstiffened shell behaviour for the broad panels ($Z_s > 9$) produces much better results. From this, it is clear that the first assumption is the responsible for the large uncertainty in DnV results ($COV_{DnV} > 20\%$).

Both the DnV and the ECCS formulations (figs. (A2.6(c)) and (A2.8(c))) exhibit significant skewness and a decreasing level of conservatism with decreasing slenderness (failure became dominated by yielding).

The aerospace test specimens (figs. (A2.7(a)) and (A2.9(a))) show high conservatism for both formulations with ECCS producing an enormous scatter which clearly indicates that this formulation is not suited for application to very closely

spaced stringer stiffened cylinders. Both formulations are highly skewed with respect to slenderness, overpredicting the strength of less slender cylinders.

The API orthotropic formulation indicates a clear difference in the results obtained with specimens fabricated with different materials ($X_m < 1.0$ for steel and $X_m > 1.0$ for aluminium) which may lead to unsafe design of steel structures. Another interesting result indicates that the limitation imposed by the formulation for the bay instability stress, that it must be less than 1.5 times the local buckling stress, exclude more than 70% of the steel specimens, both offshore and aerospace and 90% of the aerospace aluminium. This is a clear example of poor modelling because the remaining models do not exhibit different behaviour of the excluded ones (see accepted models in table 3.7).

From the results of Table 3.8 one can say that the statistical results produced by API Bul 2U orthotropic theory are comparable with API 2U discrete analysis for the offshore test specimens with the bias and COV of the order of 0.87 and 24.% and 0.99 and 18.44% respectively. However from figures (A2.1(a) and A2.3(a)) can be clearly seen that the results for both formulations have distinct patterns, being the orthotropic formulation more skewed to the relevant geometrical parameters. For the aerospace data the bias and COV are 1.019 and 31.% respectively which indicates a fairly mean value formulation for this data set.

Table A2.3 shows the X_m and the associated buckling modes ($m*n$) for some specimens out of 84 aerospace steel specimens using orthotropic theory. These specimens were chosen in which the buckling modes were obvious from the test results. In some specimens it is observed that, although X_m is near unity, the correlation between the theoretical values of buckling modes and the experimental results is not good.

The results of the statistical analysis are plotted in graphs using different parameters for 5 sets of population and are presented in figures (3.7) and (A2.1-A2.9) and commented in the Appendix 2. The results obtained for RCC with the 52 (48 steel plus 4 aluminium) specimens are presented in figures 3.7(a)-3.7(i):

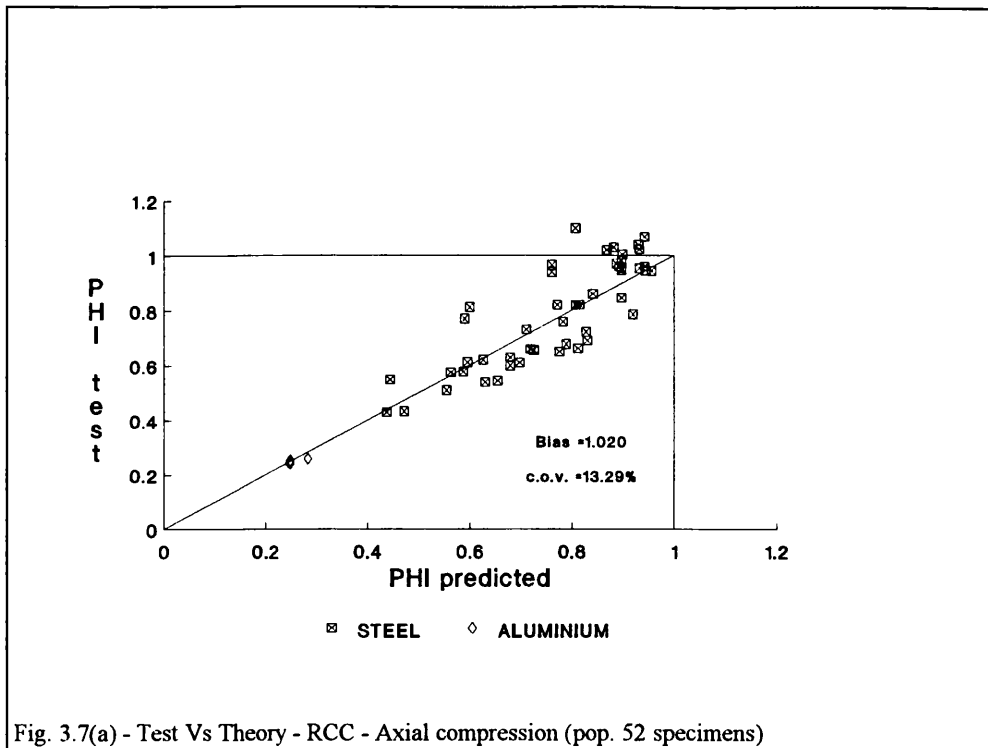


Fig. 3.7(a) - Test Vs Theory - RCC - Axial compression (pop. 52 specimens)

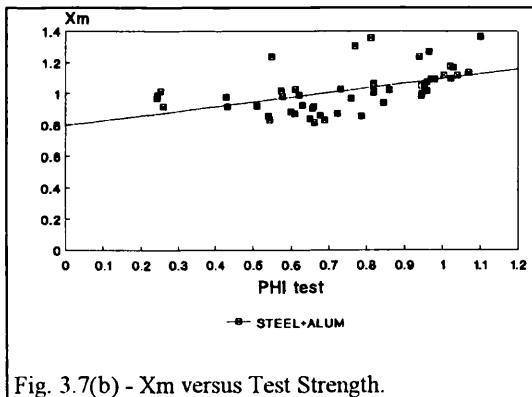


Fig. 3.7(b) - X_m versus Test Strength.

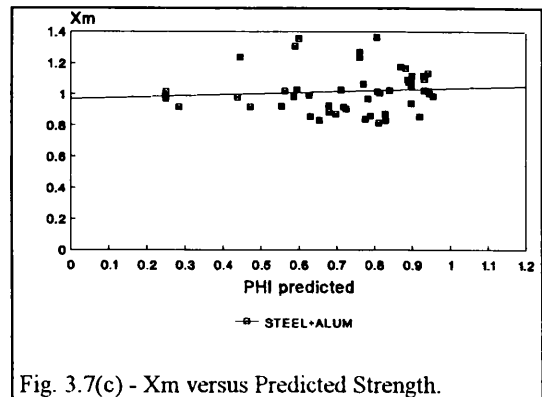


Fig. 3.7(c) - X_m versus Predicted Strength.

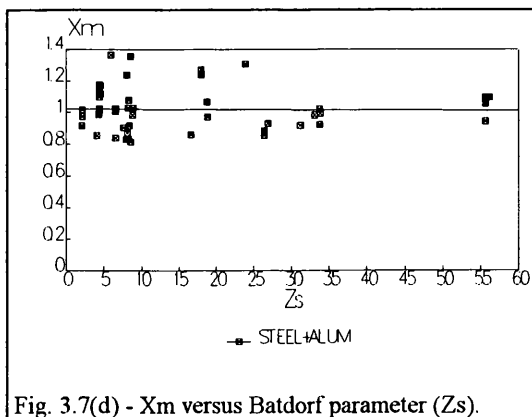


Fig. 3.7(d) - X_m versus Batdorf parameter (Z_s).

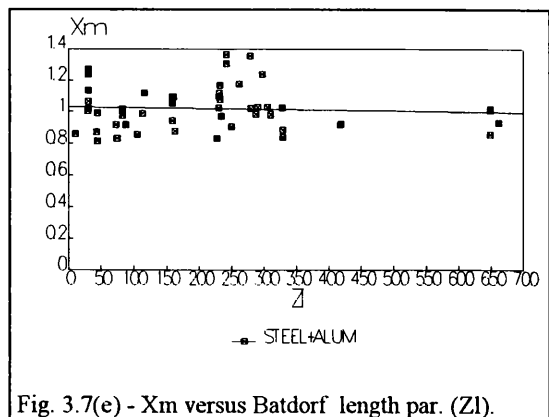
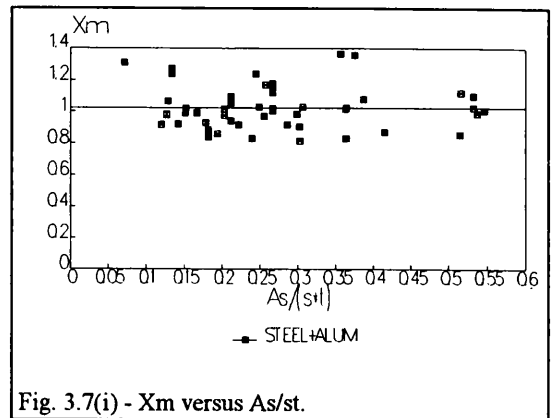
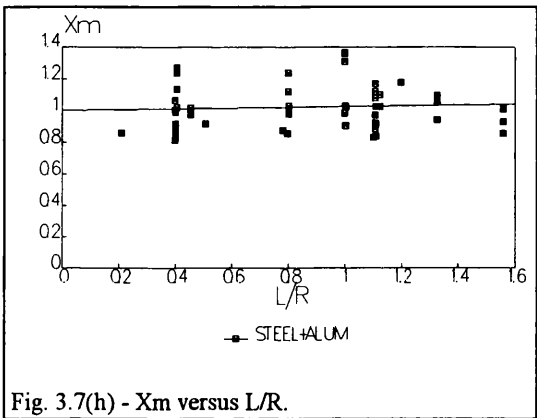
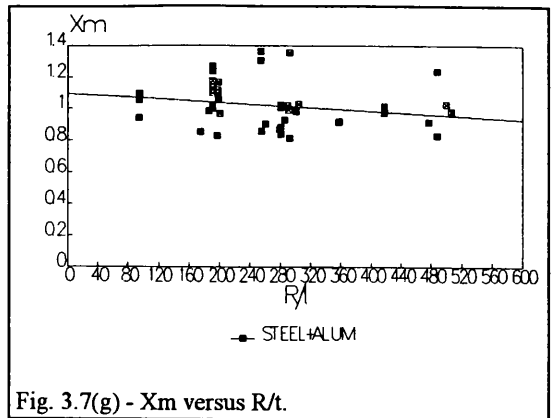
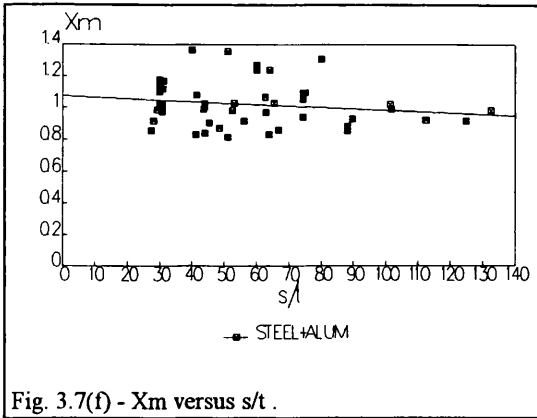


Fig. 3.7(e) - X_m versus Batdorf length par. (Z_l).



3.3.3 - Model uncertainty of radial pressure formulations.

The model uncertainty values X_m under radial pressure for 11 test specimens are given in Table 3.9 for different strength formulations and their statistic in Table 3.10. One specimen was discarded because its geometry was not consistent with other specimens used in the sample.

Xm-Radial pressure				
	API ortho	API disc	RCC	DnV
2-1C	0,601	1,130	0,938	0,762
2-2C	0,576	1,236	0,859	0,872
2-3C	1,041	1,006	1,094	1,417
2-5C	0,659	1,124	1,034	1,183
2-6C	0,407	1,044	1,075	1,399
2-7C	1,702	1,164	0,904	2,099
2-8C	0,385	1,550	1,070	2,549
2-9C	0,810	1,237	0,867	0,849
DnV3	1,155	1,513	1,048	1,225
DnV6	0,999	1,087	0,998	1,325
DnV11	1,245	1,252	0,813	1,706

Table 3.9- X_m for radial pressure formulations.

From the results one can easily understand that RCC is by far the best of all the formulations, with little scatter X_m [0.81,1.09] and consistent values for the bias $X_m=0.973$ and for the COV=10.3 %. Its a mean value formulation particularly well suited for the geometric range of the offshore structures (Offshore data set).

	OFFSHORE
MODEL CODE	STEEL Population=11
API Bul 2U Orthotropic	0.871 46.16%
Discrete	1.213 14.53%
RCC	0.973 10.29%
DnV CN 30.1	1.399 39.0%

Table 3.10 - Bias & COV of model uncertainty factor for radial pressure formulations.

The test/ RCC theory plot (fig. 3.8(a)) shows a very good correlation, with all points lying in the vicinity of the oblique line. The formulation shows an almost perfect agreement with test results for all slenderness (fig. 3.8(b)), (fig. 3.8(c)) and little or no skweness with the geometrical parameters (fig. 3.8(d)) - (fig. 3.8(i)).

The API discrete formulation is also a reasonable fit (moderate COV and no skweness) for offshore structural design and can be considered a good lower bound formulation $X_m=1.213$ and COV=14.5% with all specimens failing above prediction (fig.(A2.11(a))). This formulation shows a good correlation between predictions and test results with a moderate scatter for X_m [1.0,1.55] for the very slender cylinders (fig. A2.11(b)) and doesn't show significant dependency on slenderness or on the geometrical parameters (fig. A2.11(b)) - (fig. A2.11(i)). By contrast the orthotropic formulation is not suited and can be dangerous to offshore structural design (see Appendix 2 - Sec. 2.1)

The DnV formulation is highly conservative for slender cylinders and can produce unsafe designs for medium and stocky ones (fig. A2.12(c)). It has a bias of $X_m=1.4$ and a COV=39.0%. The formulation can be considered as a poor lower bound formulation (bias high above one and more than 25% of the specimens fails under the predictions). It also exhibits a high scatter of X_m [1.2,2.5] for slender and very slender cylinders and

a great dependency on the slenderness and geometric parameters (fig. A2.10(b)) - (fig. A2.10(i)).

Nevertheless, it should be noted the small sample size and the likely increase of the COV's with the future addition of more test specimens.

The variation of X_m for the RCC formulation with predicted strength, test strength, and with other parameters for RCC formulation are shown in figures 3.8(a) - 3.8(i).

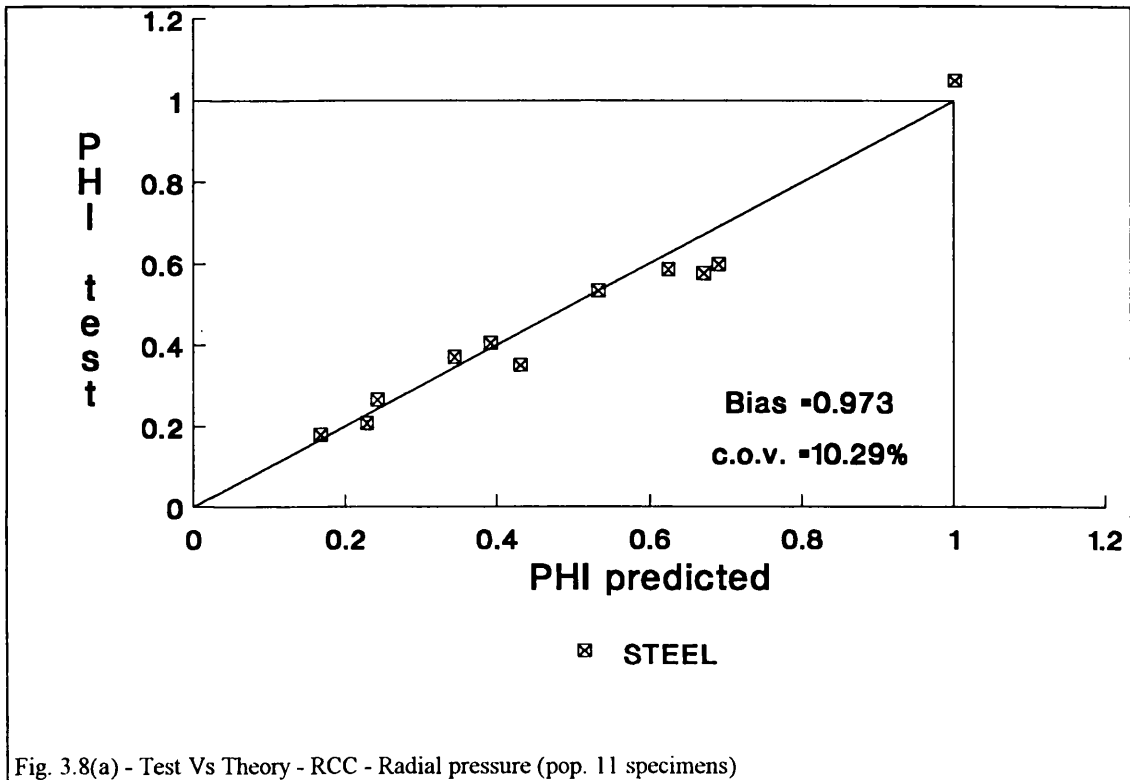


Fig. 3.8(a) - Test Vs Theory - RCC - Radial pressure (pop. 11 specimens)

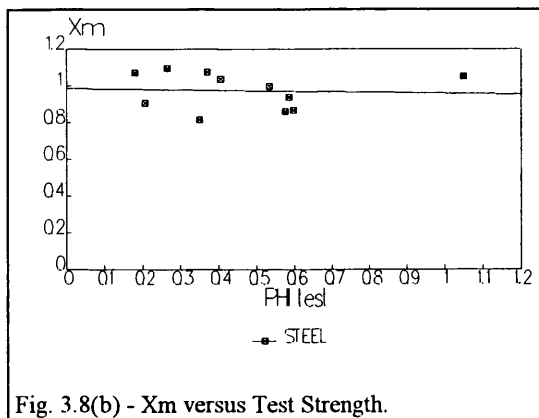


Fig. 3.8(b) - X_m versus Test Strength.

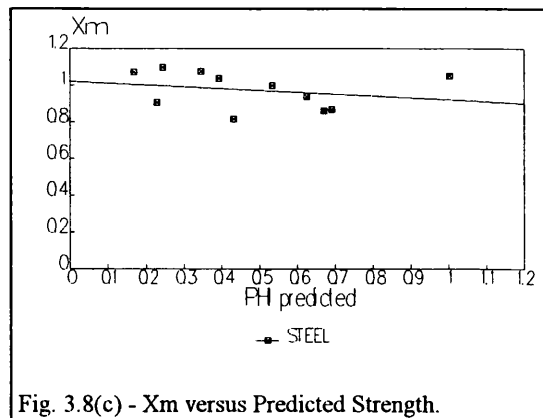


Fig. 3.8(c) - X_m versus Predicted Strength.

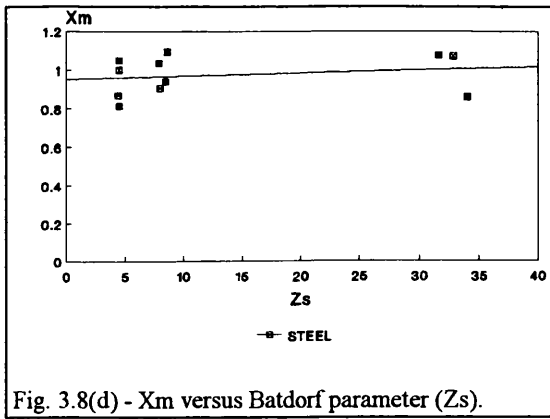


Fig. 3.8(d) - X_m versus Batdorf parameter (Z_s).

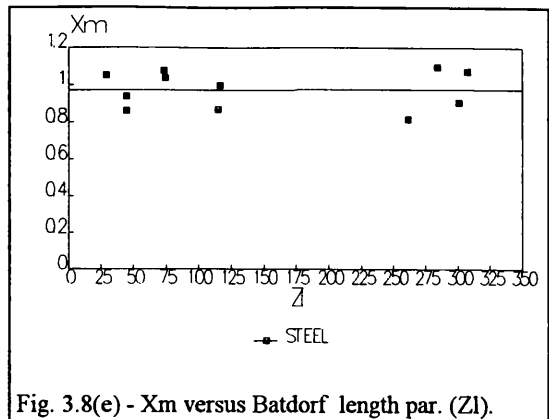


Fig. 3.8(e) - X_m versus Batdorf length par. (Z_l).

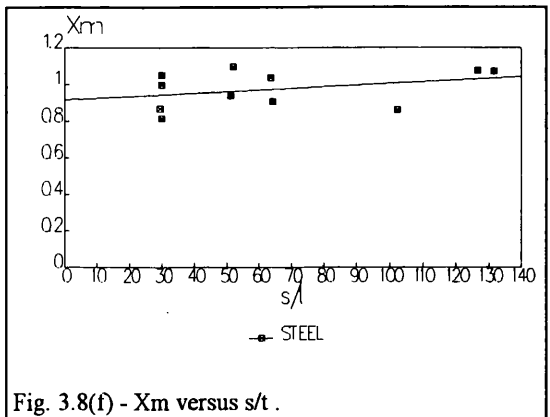


Fig. 3.8(f) - X_m versus s/t .

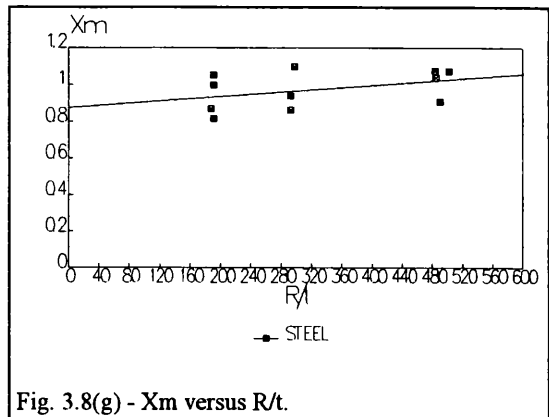


Fig. 3.8(g) - X_m versus R/t .

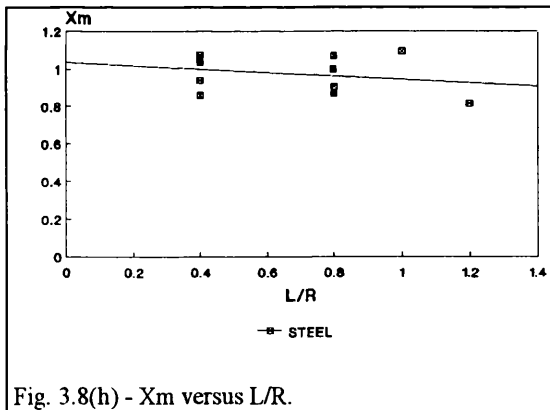


Fig. 3.8(h) - X_m versus L/R .

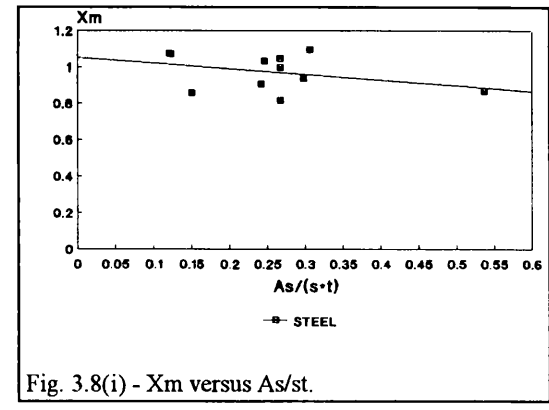


Fig. 3.8(i) - X_m versus As/st .

3.3.4 - Model uncertainty of combined loading formulations.

The model uncertainty values X_m are shown in Table 3.11 for all the test specimens and their statistics are shown in Table 3.12. In assessing the statistics of the modelling parameter two sets of population were used: CBI-Phase I results (population = 22 specimens) and Offshore data set (population = 35 specimens) which includes all specimens available for both hydrostatic and general combined loading. Axial compression and radial pressure results were not used, as they would produce results identical to single load action models.

The predictions use the experimental values of the load components at failure and calculates the proportions in which the load approaches the failure surface. Thus X_m represents the ratio of test to predicted axial strengths in the presence of external radial pressure. The same results were obtained for radial strength in the presence of axial load. The parameters ϕ_x and ϕ_θ are calculated using the single load action of the appropriate strength model.

From Table 3.11 one can see a moderate scatter for these formulations with X_{mRCC} [0.60,1.95], X_{mAPI} [0.73,1.63] and X_{mDnV} [0.89,2.25] with the highest values of X_m in RCC and API occurring for the specimen 2-3GTR (which was a test specimen tested at CBI under Phase II with T-bar stiffeners and residual stresses).

Xm-Combined Loading			
	API	RCC	DnV
2-1B	1,056	0,940	1,025
2-1D	0,988	0,986	1,135
2-2B	1,105	0,876	1,000
2-2D	0,955	0,898	0,894
2-3B	1,010	1,127	1,574
2-3BTR	0,977	1,377	1,633
2-3D	1,013	1,180	1,580
2-3G	1,225	1,410	1,897
2-3GTR	1,626	1,952	2,081
2-4B	1,119	1,118	1,480
2-4C	1,145	1,081	1,559
2-4D	1,138	1,162	1,531
2-5B	1,151	1,142	1,311
2-5D	1,152	1,238	1,373
2-6B	1,169	1,277	1,530
2-6D	0,965	1,097	1,143
2-7B	0,983	0,811	1,828
2-7BE	1,203	1,015	2,373
2-7D	1,138	1,020	2,194
2-7DF	1,134	1,026	2,250
2-7G	1,051	1,033	1,916
2-8B	1,399	1,029	2,288
2-8D	1,327	1,058	2,120
2-9B	1,184	0,827	1,150
2-9D	1,034	0,816	1,325
2-9DTD	1,388	1,203	1,955
SLDB	0,972	1,257	1,605
SLDC	1,520	1,811	2,247
SLDF	0,920	0,602	1,541
SLDG	1,148	1,099	2,149
DnV4	1,251	0,933	1,998
DnV8	1,235	1,315	2,207
DnV12	1,177	0,980	2,075
KINRA1	0,793	0,785	1,508
KINRA2	0,732	0,710	1,293

Table 3.11- X_m for combined loading formulations.

From the statistics one can see a clear change in the uncertainty of the formulations if one considers the CBI Phase I specimens alone or the full population. Thus, with almost no change in the bias, API shows a moderate raise in its COV value 13.9% to 19.7%, RCC shows a high raise in its COV almost doubling its initial value of 13.2% to 24.8% . DnV shows an interesting decrease in its COV value from 28.9% to 25.3%.

The test/theory plot (fig. 3.9(a)) shows for RCC formulation a fair correlation between predictions and test results with a moderate scatter for X_m to all slenderness with the exception of the very slender cylinders in which the maximum scatter occurs (fig. 3.9(b)). The formulation also shows some tendency to over predict the strength of stocky cylinders (fig. 3.9(c)) and doesn't show significant dependency of the geometrical parameters (fig. 3.9(d)) - (fig. 3.9(i)).

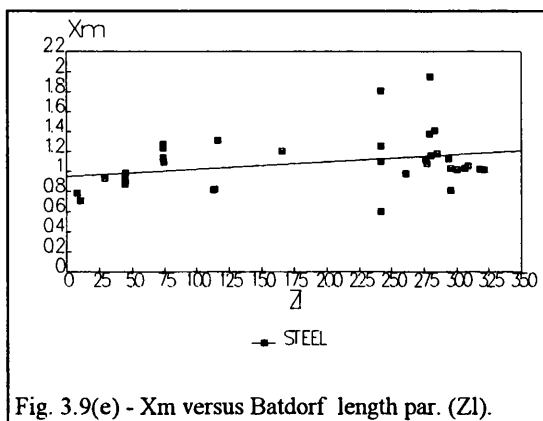
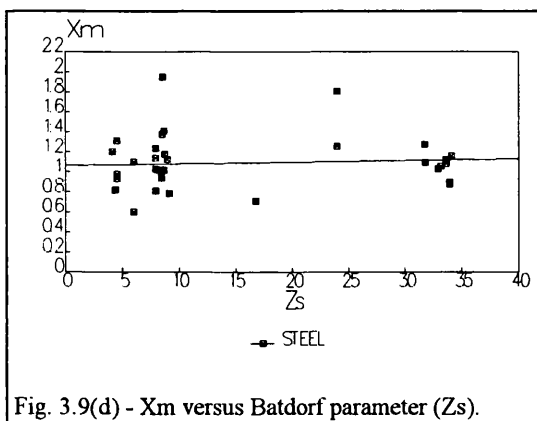
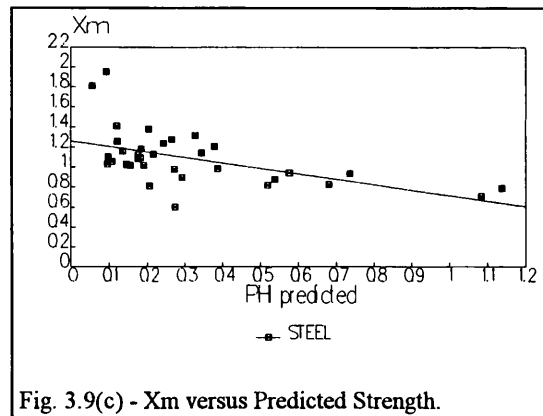
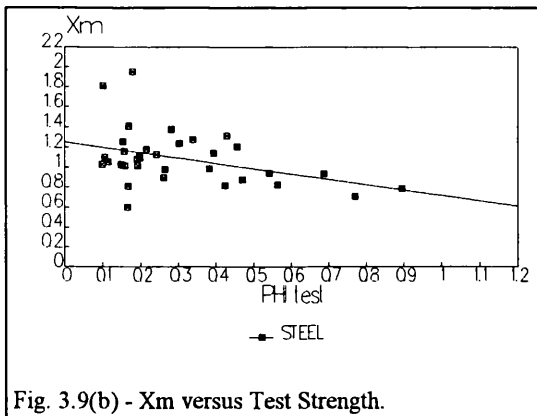
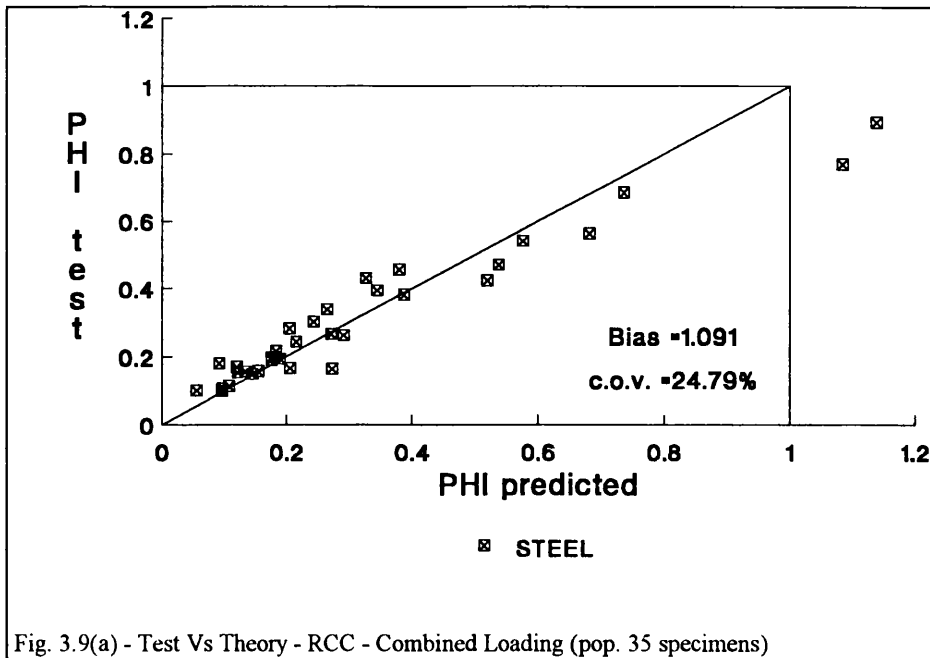
The API formulation shows almost the same results as RCC (fig. A2.13(a)) - (fig. A2.13(i)) with tendency to overpredict the strength of stocky cylinders (fig. A2.13(c)). The DnV formulation shows a poor correlation between predictions and test results (fig. A2.14(a)) and also exhibits a great dependency of the slenderness and the geometrical parameters (fig. A2.14(c)) - (fig. A2.14(i)).

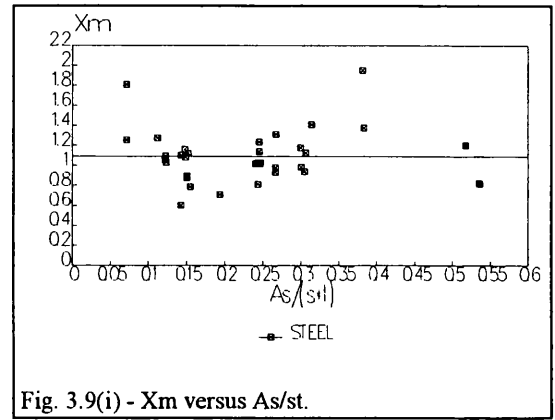
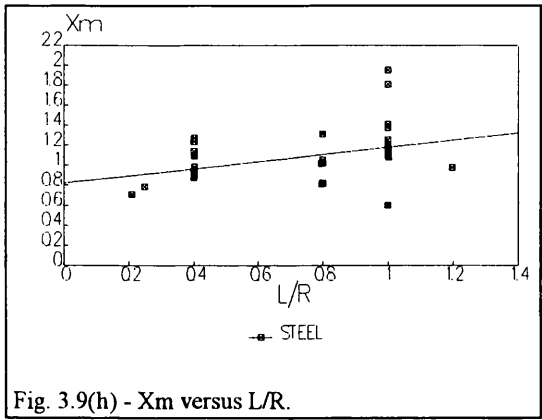
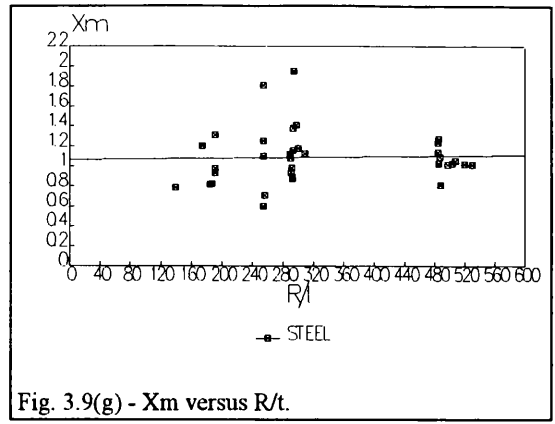
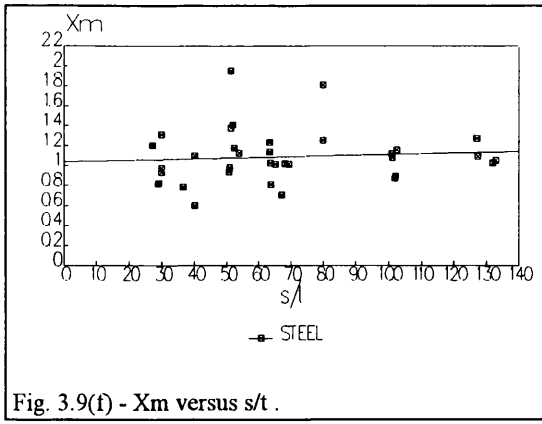
As conclusion one can point out that both RCC and API proved acceptable mean value formulations and are suited for the design of offshore structures but further improvement is needed to reduce the uncertainty of these formulations. The DnV formulation is a poor lower bound formulation highly skewed with slenderness and the geometrical parameters considered.

MODEL CODE	OFFSHORE	
	STEEL	STEEL
	Population=22	Population=35
API Bul 2U	1.180	1.163
Discrete	13.86%	19.72%
RCC	1.042	1.091
	13.16%	24.79%
DnV CN 30.1	1.573	1.679
	28.89%	25.29%

Table 3.12 - Bias & COV of model uncertainty factor for combined axial compression and radial pressure formulations.

The variation of X_m with predicted strength, test strength and with other parameters for RCC the all population is shown in the following figures 3.9(a) - 3.9(i).





3.4 - Reliability analysis of ring-stringer stiffened cylinders.

The previous section gives a good understanding of the model uncertainty associated with the different strength formulations used in the design of ring and stringer stiffened cylinders. However, this is not sufficient to quantify the real consequences in cost and weight of the different levels of uncertainty. Thus, in this chapter an attempt is made to quantify the differences. The approach chosen is identical to the one used by Faulkner and Warwick in reference [140] and consists in comparing from a reliability point of view, the several formulations under the various load cases considered - axial compression, radial external pressure and their combination.

The approach has some similarities to the one used in the stiffened plates case with the reliability being carried out using an advanced level 2 algorithm (first and second order reliability methods) which not only determines the failure probability with an accuracy approaching that of the level 3 procedure, but also provides partial safety factors (eq(1.4)) which can be used in design.

However the methodology used for the comparison of the formulations is different. While for the stiffened plates the reliability index was obtained by varying only the thickness (and consequently the plate slenderness) in the case of the cylinders a surface of reliability results (β_f) was obtained, for each formulation, by varying both the shell thickness and the number of stringers. From this surface lines of iso-safety lines were extracted and transformed in plots showing the variation of mean thickness (t_m) defined by equation (3.66) with the number of stringers.

$$t_m = t + \frac{A_s}{s} \quad (3.66)$$

The ring-stringer stiffened cylinder considered for the study has similar dimensions to the corner columns of the Hutton and Joillet TLPs. Its geometrical and material data was extracted from Ref. [140] and are listed in Table 3.13.

Static and dynamic random loads will be considered for both axial compression and radial pressure along with its corresponding model uncertainty. The static loading includes the static and the quasi-static loads, resulting the first from the weight of the structure, weight of permanent ballast and permanently installed equipment, machinery with the liquids at operating levels and external hydrostatic pressure in calm sea, calculated on the basis of a datum reference level such as the mean sea level.

Variables		Distribution	Mean	COV
Yield stress	σ_y (MPa)	Lognormal	391.0	0.07
Young modulus	E (MPa)	Lognormal	2.0 E5	0.04
Thickness	t (mm)	Normal	Variable	0.04
Radius	R (mm)	Normal	6250.0	0.04
Length	L (mm)	Normal	5500.0	0.04
Dynamic axial compression	N_d (MN)	Gumbel	64.0	0.20
Static axial compression	N_s (MN)	Lognormal	112.5	0.10
Dynamic axial compr. modelling parameter	XN_s (ad.)	Lognormal	1.0	0.15
Static axial compress. modelling parameter	XN_d (ad.)	Lognormal	1.2	0.2
Dynamic radial pressure	p_d (MPa)	Gumbel	0.252	0.20
Static radial pressure	p_s (MPa)	Lognormal	0.482	0.10
Dynamic radial press. modelling parameter	Xp_s (ad.)	Lognormal	1.0	0.05
Static radial pressure modelling parameter	Xp_d (ad.)	Lognormal	0.9	0.2
Resistance modelling parameter	X_m (ad.)	Lognormal	variable	variable
Number of stringers	N_{string}	Deterministic	variable	-
Depth of the stringer web	d_w (mm)	Deterministic	300.0	-
Thickness of the stringer web	t_w (mm)	Deterministic	15.0	-
Width of the stringer flange	d_f (mm)	Deterministic	189.0	-
Thickness of the stringer flange	t_f (mm)	Deterministic	19.0	-
Width of weld	η (adim.)	Deterministic	4.5	-
Proportional limit	p_r (adim.)	Deterministic	0.5	-

Table 3.13 - Description of the basic variables used in the stiffened cylinder reliability analysis.

The quasi-static loading (load that is non-oscillatory in nature yet is not static) includes the load due to wind, current, wave drift and quasi-static motion (offset and set down from initial position). The dynamic load effects results from the hydrodynamic loading¹⁷⁹ due to waves and motion of the structure. The values for the loading variables were extracted from Ref. [140] and are listed in Table 3.13.

Both random and deterministic variables are used in the study, the first group being subdivided in two categories: resistance and loading variables. The set of resistance variables is formed by the:

- Yield Stress - It is a Normal random variable, well defined by a large number of data and possesses a moderate uncertainty (COV=7%). However for reliability purposes a LOGNORMAL type is usually used in order to avoid convergence problems with formulations much dependent of this variable, i.e. negative values for the yield stress.
- Young Modulus - It is a Normal random variable well defined with low uncertainty (COV=4%). A LOGNORMAL type is usually used for the same reasons as for the yield stress.
- Thickness - It is the cylindrical shell thickness that is a NORMAL random variable with low uncertainty (COV=4%). This uncertainty depends on the quality control procedures existing in the steel mill.
- Radius - It is the cylinder internal radius that is a NORMAL random variable with low uncertainty (COV=4%). This uncertainty is much dependent of the quality control procedures existing in the construction site. This variable shows different behaviour under the different loading conditions, being a resistance variable for axial compression and acting as a loading variable for radial pressure.
- Resistance modelling parameter - It is a LOGNORMAL random variable with its definition dependent of the test data available and its uncertainty dependent of the resistance model used in the different formulations.

The loading set of variables is formed by:

- Length - It is the length between the two consecutive rings measured at its flange mid thickness that is a NORMAL random variable with low uncertainty (COV=4%). This uncertainty is much dependent of the quality control procedures existing in the construction site.

- Static loading - Axial compression and/or radial pressure that are described by LOGNORMAL random variables with the same moderate uncertainty (COV=10%).
- Dynamic loading - Axial compression and/or radial pressure that are described by TYPE I Extreme random variables with the same high uncertainty (COV=20%). However, it is important to note that usual values of COV of [7%, 10%] are recommended for the extreme type distributions, in this case the high COVs were used for the comparison with previous results¹⁴⁰.
- Static load modelling parameter - It is a LOGNORMAL random variable with its definition dependent of the test data available. It has high uncertainty (COV=20%) for both load models.
- Dynamic load modelling parameter - It is a LOGNORMAL random variable with its definition dependent of the test data available. It has high uncertainty (COV=15%) for the axial model and low uncertainty (COV=5%) for the radial.

The deterministic set is composed of some variables with random nature, geometry of the stiffeners and residual stresses parameter, but due to their small influence in the problem were disregarded as random and considered deterministic. This helped to reduce the complexity of the problem by reducing several dimensions in the failure surface.

3.4.1 - Reliability of ring-stringer stiffened cylinders under axial compression loads.

The first step in the study was determining the validity domain for the reliability surface in terms of shell thickness and number of stringers. For the axial compression case using the mean values of the variables and considering the uncertainty validity domain, it is possible to say that the mean value for thickness is in the range $t_k \in [12.5-47.5]$ (mm) and the number of stringers varies with thickness with the maximum range $N_s \in [15-60]$ for $t_k = 20$ (mm) and two minimum, $N_s \in [15-60]$ and $N_s \in [15-60]$ for $t_k = 12.5$ (mm) and $t_k = 47.5$ (mm), respectively.

The next step is to calculate for each formulation the reliability indices for each pair of (N_s, t_k) in order to build the respective reliability surface. The methodology used was similar to the one used for the stiffened plate and a series of plots like the one presented in figure (3.10) were calculated for the different number of stringers (the curves for the different formulations come together in order to show their differences).

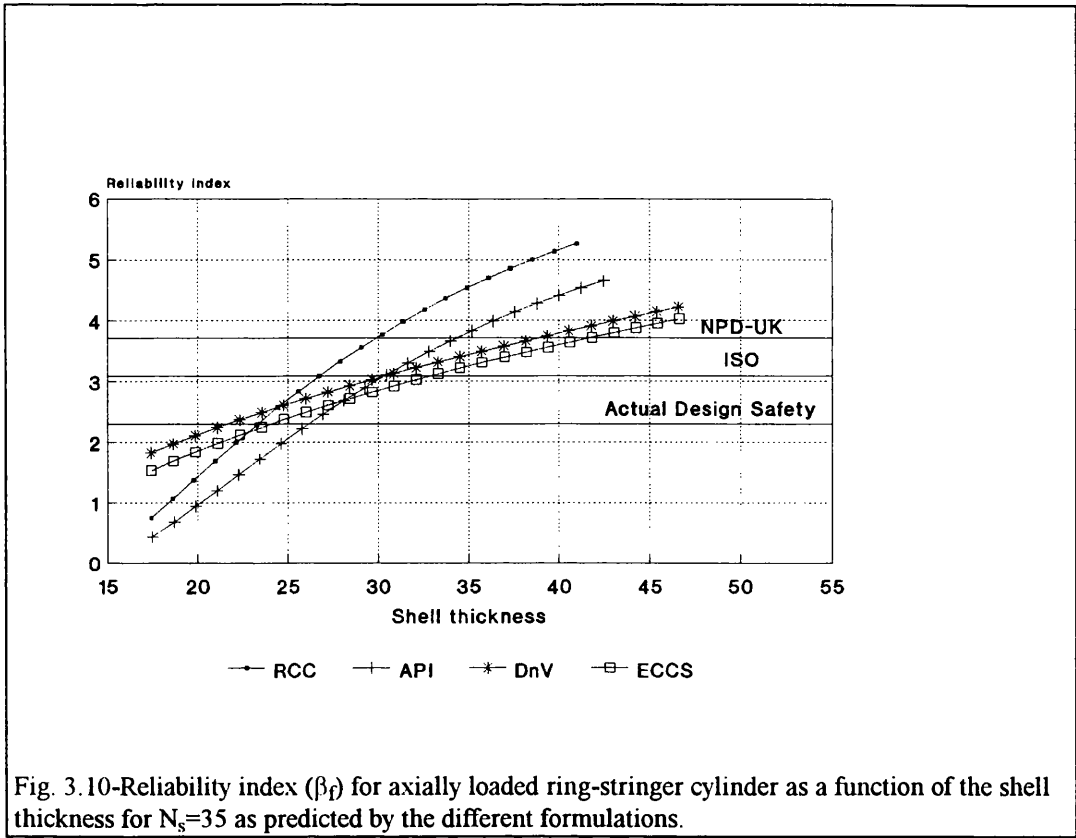


Fig. 3.10-Reliability index (β_f) for axially loaded ring-stringer cylinder as a function of the shell thickness for $N_s=35$ as predicted by the different formulations.

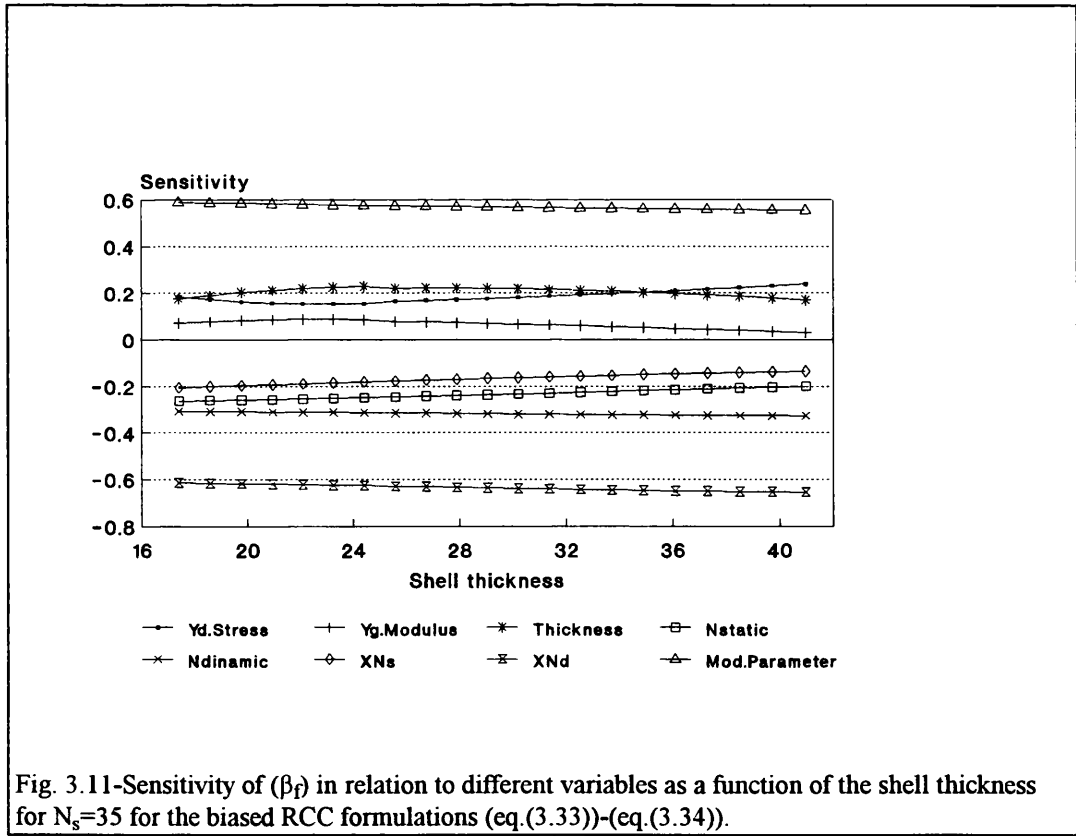


Fig. 3.11-Sensitivity of (β_f) in relation to different variables as a function of the shell thickness for $N_s=35$ for the biased RCC formulations (eq.(3.33))-(eq.(3.34)).

The intersection of the different curves with the safety levels defines the coordinates (N_S , t_k) of the points of equal safety on each reliability surface and allows the determination of the iso-safety lines for the different formulations.

It is also possible to obtain for each formulation the sensitivity plots which show the relative importance of the random variables. In figure (3.11) the sensitivity plot for RCC is shown and it's possible to see the strength modelling parameter as the most important variable. In Appendix 4 the plots for the other formulation are given for $N_S=35$.

The mean thickness versus the number of stringer stiffeners plot (Fig. (3.12)) indicates the weight variation of the structure as a function of the number of stringers used. This results will allow weight and cost optimisation of the structure. From the plot it is possible to say that the RCC formulation is the one which gives the best results. This formulation behaves in the same manner for the three safety levels considered and diminishes its variation with N_S as this variable increases. API formulation shows a similar behaviour as RCC but clearly overpredicts the structural design. DnV and ECCS formulations have both similar behaviour and shows small weight savings with the increased number of stringers.

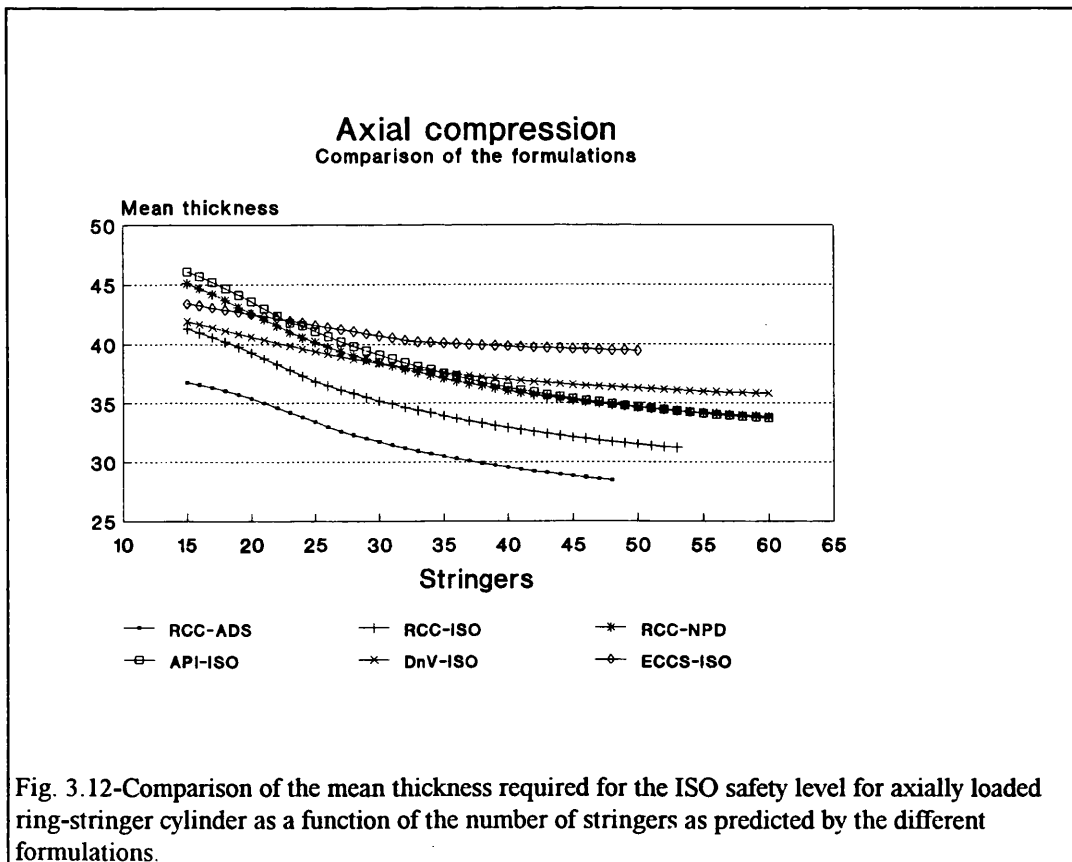


Table 3.14 summarises the differences in the prediction for the ISO safety level. The formulation results are compared for the minimum weight point and for two fixed numbers of stringers ($N_s=20$ and $N_s=50$).

As conclusion it is obvious that the RCC is the best formulation and it allows the design of much lighter and cheaper structures. API and DnV produces in average 10% heavier and costly structures. ECCS is the formulation with the worse results producing structures 17% heavier than RCC. The difference in weight resulting from the different safety levels is in average 10% and for the two limit levels (ADS and NPD) a 22% increase in weight is necessary.

	Model Uncertainty		Minimum weight point			$N_s=20$		$N_s=50$	
	\bar{X}_m	$V_{Xm}\%$	N_s	t_m	Δ	t_m	Δ	t_m	Δ
RCC	1.01	13.2	53	31.25	100%	39.3	100%	31.6	100%
API	0.99	18.4	60	33.74	108%	43.57	111%	34.7	110%
DnV	1.01	25.1	60	35.82	115%	40.6	103%	36.3	115%
ECCS	1.27	27.7	50	39.43	126%	42.5	108%	39.4	125%

Table 3.14 - Comparison of the axial compression strength formulations for ring and stringer stiffened cylinders.(ISO safety level)

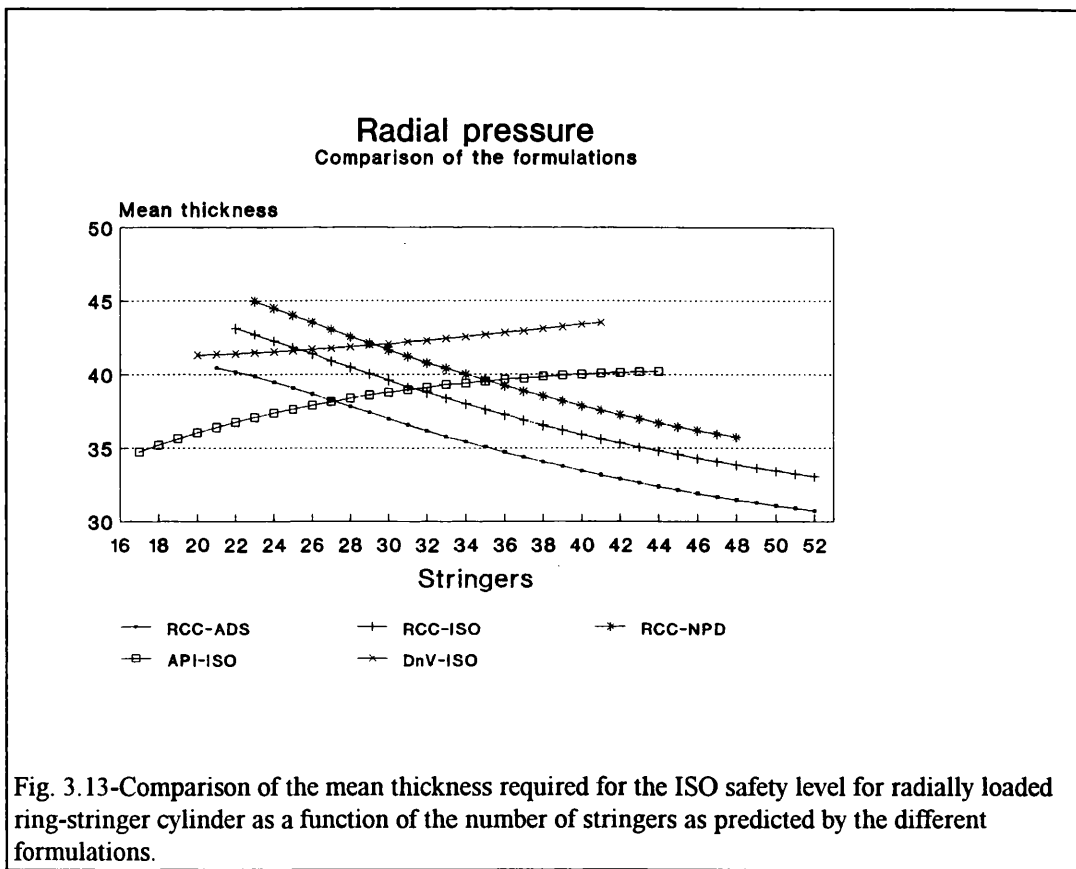
Finally, with respect to the minimum weight design point it is important to refer that it lies for all formulations in the limits of their applicability range. The minimum cost design point is not evident from the results due to the small variation of the mean thickness with the number of stringers in the vicinity of the minimum weight design point. Because there are different costs involved, a proper merit function should be applied in the optimisation process.

3.4.2 - Reliability of ring-stringer stiffened cylinders under radial pressure loads.

Again, the first step is determining the validity domain for the reliability surface in terms of shell thickness and number of stringers. The cylinder used in this example has

half of the length of the one used in the axial compression case. For this load case the mean value for thickness is in the range $t_k \in [12.5-40.]$ (mm) and the number of stringers varies with thickness with the maximum range $N_s \in [18-51]$ for $t_k = 22.5$ (mm) and two minimum, $N_s \in [24-33]$ and $N_s \in [23-35]$ for $t_k = 12.5$ (mm) and $t_k = 40$ (mm), respectively.

In Appendix 4 an illustrative example ($N_s=35$) for this load case of the variation of the reliability with the shell thickness is given. In the sensitivity plots presented there the strength modelling parameter is again the most important variable.



The mean thickness versus the number of stringer stiffeners plot (Fig. (3.13)) indicates RCC formulation as the one which gives the best results. This formulation behaves in the same manner for the three safety levels considered and it almost maintains its rate of variation with N_s for the whole range considered. The behaviour of API and DnV formulations is similar and is the opposite to the one of RCC. These two formulations produces heavier structures with the increased number of stringers.

Table 3.15 summarises the differences in the prediction for the ISO safety level. The formulation results are compared for the minimum weight point and for two fixed numbers of stringers ($N_s=24$ and $N_s=40$).

The conclusions for these cases are similar to the axial compression cases with the RCC formulation allowing the design of much lighter structures. The minimum weight design point again lies for all formulations in the limits of their applicability ranges. API formulation produces in average structures similar to RCC but 5% heavier when comparing for the minimum weight design point. DnV formulation produces in average 10% heavier structures and its minimum weight design is 25% higher than RCC.

	Model Uncertainty		Minimum weight point			N _S =24		N _S =40	
	\bar{X}_m	V _{Xm} %	N _S	t _m	Δ	t _m	Δ	t _m	Δ
RCC	0.97	10.3	52	33.1	100%	42.3	100%	35.9	100%
API	1.21	14.5	17	34.8	105%	37.4	88%	40.0	111%
DnV	1.40	39.0	22	41.4	125%	41.5	98%	43.4	121%

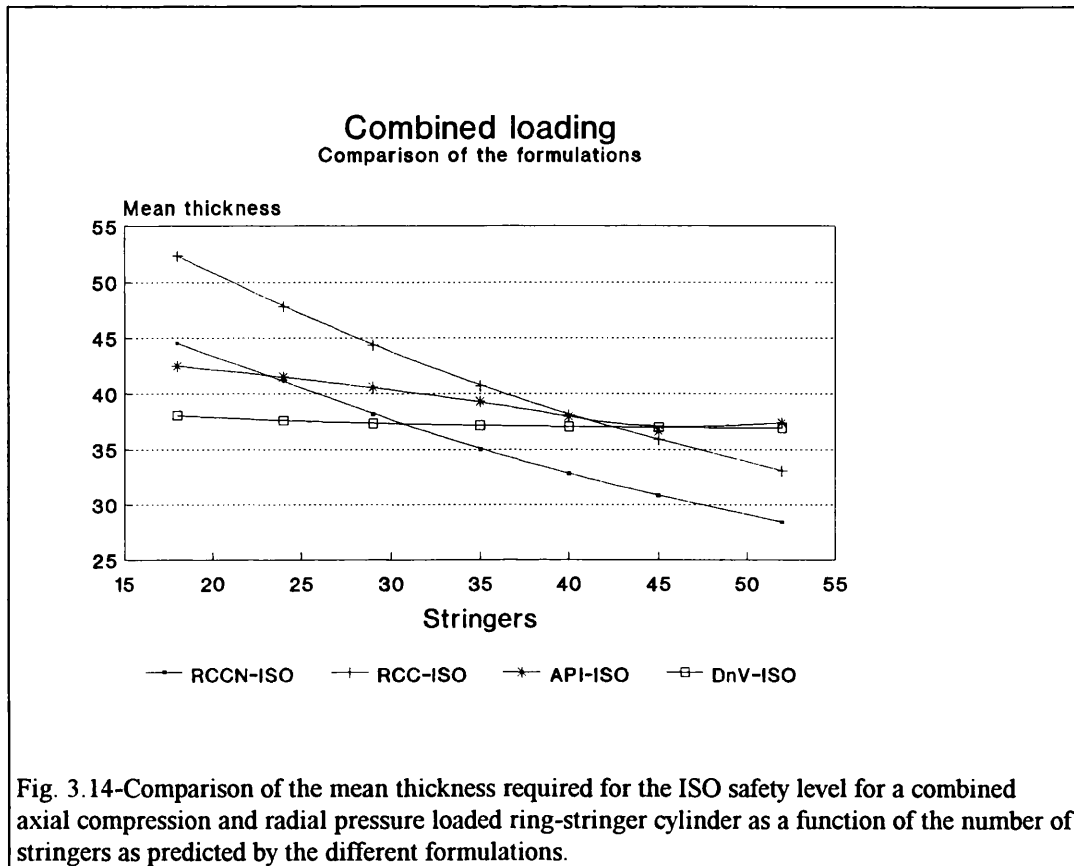
Table 3.15 - Comparison of the radial pressure strength formulations for ring and stringer stiffened cylinders.(ISO safety level)

Again, the minimum cost design point is not evident from the results and a merit function should be applied. Also the difference in weight resulting from the different safety levels is in average 6% and for the two limit levels (ADS and NPD) it is around 13%.

3.4.3 - Reliability of ring-stringer stiffened cylinders under combined loading.

The cylinder used in this example has half of the length of the one used in the axial compression case and it is identical to the one used for radial pressure. For this load case the mean value for thickness is in the range $t_k \in [15.-45.]$ (mm) and the number of stringers varies with thickness with the maximum range $N_S \in [17-51]$ for $t_k = 22.5$ (mm) and two minimum, $N_S \in [21-39]$ and $N_S \in [15-32]$ for $t_k = 15.$ (mm) and $t_k = 45$ (mm), respectively.

In Appendix 4 an illustrative example ($N_S=35$) for this load case of the variation of the reliability with the shell thickness is given. In the sensitivity plots presented there the strength modelling parameter is again the most important variable.



The mean thickness versus the number of stringer stiffeners plot (Fig. (3.14)) indicates both RCC formulations as the ones which give the best results. The two RCC proposals behave in the same manner and they almost maintain their rate of variation with N_S for the whole range considered. The behaviour of API and DnV formulations is similar but DnV shows almost no variation with the increased number of stringers.

	Model Uncertainty		Minimum weight point			$N_S=24$		$N_S=45$	
	\bar{X}_m	$V_{Xm}\%$	N_S	t_m	Δ	t_m	Δ	t_m	Δ
RCC new	1.13	16.3	50	29.08	100%	41.2	100%	30.8	100%
RCC	1.09	24.8	50	33.83	116%	47.8	116%	35.9	117%
API	1.16	19.7	44	36.57	126%	41.5	101%	36.7	119%
DnV	1.68	25.3	46	36.99	127%	37.6	91%	37.0	120%

Table 3.16 - Comparison of the combined load interaction formulations for ring and stringer stiffened cylinders.(ISO safety level)

Table 3.16 summarises the differences in the predictions for the ISO safety level. The formulation results are compared for the minimum weight point and for two fixed numbers of stringers ($N_S=24$ and $N_S=45$).

The conclusions for this case are similar to the axial compression case with both RCC proposals allowing the design of much lighter and cheaper structures. The minimum weight design point for DnV lay in the mid range while for all the other formulations is in the limits of their applicability ranges. The difference between the two RCC proposals is 16%. API formulation produces in average 10% heavier structures than RCC new and for the minimum weight design point the difference is about 26%. DnV formulation produces in average 6% heavier structures and its minimum weight design is 27% higher than RCC new.

3.5 - Conclusions.

The conclusions for this study can be subdivided in two parts. In the first part the conclusions related with the uncertainty analysis performed in section 3.3 will be presented and the second part will present and discuss the conclusions drawn from the reliability analysis of the ring-stringer stiffened cylinders (section 3.4).

3.5.1 - Uncertainty analysis.

The collected data can be subdivided into two groups; experimental and computational. The first group is the outcome of extensive experimental research programmes carried out in several countries and are compiled in Tables (3.1-3.6 and A2.1-A2.3). These tests were conducted for two distinct fields of application (Aerospace and Offshore) and the materials used were steel and aluminium alloys. The specimens tested covers a wide range of dimensions, loading types and other parameters.

The second group (Tables A2.5-A2.6.) is a result of a research programme carried out at Imperial College and focuses only on Offshore applications. It consists of a large database with specimens failing in elastic and elastoplastic ranges. Steel is the material specified and initial deflections were considered. However, this database in a preliminary phase of the study proved to be inadequate because it provokes strong skewness in the results. Due to that fact this database had to be discarded, which led to the use of just the experimental results in this study. Thus, two different databases were considered:

-the aerospace database with 193 axial compression test specimens; 84 steel and 109 aluminium.

-the offshore database with 99 test specimens from which 52 (48 steel and 4 aluminium) were tested under axial compression, 12 steel specimens were tested under radial pressure and 35 steel specimens tested under combined axial and radial loading.

The aerospace database was found to be useful for providing information on elastic buckling strength. It is a balanced database in terms of the material used (50% of the specimens were in steel and 50% in aluminium). However, the stiffeners and the very small scale were important penalties to their use to calibrate the formulations considered here.

The offshore database proves to be more efficient one for the calibration procedure because the formulations were more appropriate for the welded stiffened cylinders used in offshore construction. The material used in these test specimens was mainly welded steel and most of them had initial imperfections. Their number and variety were sufficiently broad to cover practical geometries and fabrication effects. Also a large number of multi-bay specimens existed which reduces the uncertainty related with the test boundary conditions. They failed mostly in the elasto-plastic range. The weakness of this database is the relatively small number of radial pressure test specimens, reducing the level of confidence in the final results. The strength is the fact that a significant number of test specimens exist for the other loading types.

It is also important to mention that after the study was completed several more aerospace test specimens were gathered. The geometry and material properties of these specimens and test results are given in Table A2.3.

The uncertainty analysis performed for the axial compression case clearly shows that the aerospace database does not provide a good fit to any of the formulations considered (COV's over 20% to all cases). For the offshore specimens, RCC gives the best results of all. For the other formulations, the API discrete stiffener analysis gives acceptable results, the API orthotropic shell approach is very poor and both the DnV and the ECCS formulations exhibit large uncertainty and skewness that significantly reduces their value.

For the radial pressure case one can easily understand that RCC is by far the best formulation. It is a mean value formulation particularly well suited for the geometric range of the offshore structures. The API discrete formulation is also a good fit (moderate COV and no skewness) for offshore structural design and can be considered

a good lower bound formulation. By contrast the API orthotropic formulation is not suitable and can be dangerous for offshore structural design.

For the combined load case the statistics show a clear change in the uncertainty of the formulations, considering the CBI Phase I specimens alone or the full population. This clearly indicates one danger of this type of calibration procedure. RCC and API formulations were calibrated with CBI test specimens and gave very good results. But when compared with an updated database they became medium to poor formulations. The DnV formulation is highly conservative for slender cylinders and can produce unsafe design for medium and stocky ones.

A further improvement to RCC was obtained by using RCC proposals for the ultimate strength under axial compression and radial pressure in the API interaction formulation (eq.(3.57)) The results obtained are presented and discussed in the next Chapter (see section 4.3.4). As final conclusion for the combined load case one can point out that both RCC (the new proposal) and API proved acceptable mean value formulations and are suitable for the design of offshore structures.

3.5.2 - Reliability analysis.

For the reliability analysis of ring-stringer stiffened cylinders it is quite clear that the more correct a formulation is the better results it gives. This is a direct consequence of the principles of good strength modelling referred in the next chapter and has as visible face in the modelling parameter. This variable proved again to be the most important strength variable dominating entirely the final design points for the formulations with COV_{X_m} values over 20%.

For the axial compression case it is clear that the RCC is the best formulation and it allows the design of much lighter (around 10%) and cheaper structures. The other formulations (API, DnV and ECCS) produce heavier and costly structures, thus with reduced interest for design.

For the radial pressure case the conclusions indicate RCC as the formulation allowing the design of lighter structures. API produces in average structures similar to RCC but heavier when comparing for the minimum weight design point and DnV produces in all cases heavier structures. In this case seems correct to state that probably API design is cheaper than RCC due to the reduced number of stiffeners required. In this case both RCC and API could be used for design with only DnV having a reduced interest for design.

For the combined load case the conclusions are similar to the axial compression case with both RCC proposals allowing the design of much lighter and cheaper structures. The other two formulations (API and DnV) produce heavier and costly structures, thus with reduced interest for design.

As general conclusion the use of RCC formulations is recommended for the design of the ring and stringer stiffened cylinders in all load cases considered in the study (axial compression, radial pressure and combined axial compression and radial pressure).

Other conclusion already drawn for the plate case is related with the large differences in weight and cost arising from the adoption of one safety level or other.

As a final remark, the optimisation process regarding costs requires proper merit functions because there are different costs apart than the material ones involved in the production of this particular structure.

CHAPTER 4 - MODELLING FOR STRENGTH AND RELIABILITY ASSESSMENT.

4.1 - Introduction.

In this chapter, the principles that allows good strength modelling for reliability based design will be discussed, with emphasis on the similarities and the differences between strength and reliability assessments. In fact, if a designer uses a poor strength formulation for the design of a structure or a component it can easily happen that this same structure according to the formula is considered strong enough but, when is looked from a reliability point of view it can be found to be an unsafe structure.

In the previous chapters several formulations were compared from both strength and reliability, point of view. These formulations account, under different loading conditions, for the ultimate buckling strength of the two most important marine components (the stiffened plates and the stiffened cylinders). The accuracy and consistency of these formulations along with their economic efficiency was checked and discussed. From the reliability study it was clearly shown that small differences in the strength formulation are normally amplified when reliability is used. This fact and the evidence that the strength modelling parameters are the most important variables in the formulations confirms previous recommendations^{65,140} that great effort should be put in the correct modelling of strength.

However, a series of difficult questions arises: What are the correct formulations for design? What are their limitations? Are they reliable? How can they be improved? To contribute to answer these questions in the next paragraphs a methodology for good strength modelling will be described^{65,139} and applied for the improvement of the strength formulations for stringer stiffened cylinders¹⁴¹.

4.2 - Strength modelling criteria.

The strength formulations aim to reproduce in a simplified manner the behaviour of certain components or structures to the different existing surrounding conditions. They relate the components' most important variable and/or parameters in such a way, that the final result reflects the strength of the component. To achieve this goal strength modelling can be based on various criteria. On one hand, it may be based purely on the

results of test data and an empirical fit for the best equation. On the other hand, it may be based purely on structural mechanics of failure or a combination of both. Whatever approach one might follow, it is desirable that the method should be robust and produce consistent results

There are various statistical criteria and strength requirements which should be borne in mind when formulating or updating any strength model. These are thoroughly discussed by Faulkner in Ref. [139] and summarised hereafter.

4.2.1 - Statistical Criteria.

- (a) mean value formulations are preferred and are essential for meaningful in-service assessments;
- (b) the modelling parameter X_m should be close to unity over the geometry and material range of interest; its mean bias should be within $0.95 < X_m < 1.05$;
- (c) the modelling uncertainty V_{X_m} should be kept as low as possible and overall values < 0.15 should be achievable for the ultimate strength of most components;
- (d) X_m should show low correlation with any basic variables or their non-dimensional ratios, that is, no skewness should be inherent in the model;
- (e) where the modelling uncertainty V_{X_m} varies noticeably with some of the basic variables or slenderness parameters then it should be evaluated in ranges;
- (f) sample sizes are to be quoted for samples sizes less than 15, goodness of fit tests should be applied and confidence limits determined.

4.2.2 - Strength Requirements.

- (a1) formulations should be *strength of materials* type whose parameters reflect the mechanics of failure; curve fitting should be restricted to secondary terms (such as shell knockdown factors) and not for failure predictions, inelasticity effects, etc.;
- (b1) models should be relatively simple to apply; but over simplification may neglect important factors and may restrict the range of applicability and often leads to lack of robustness;
- (c1) avoid different levels of sophistication and cater for average imperfections;
- (d1) the ranges of relevant geometrical parameters and material properties should be clearly stated - normally identical to test data ranges;

- (e1) restrictions based on ultimate stress for metals are to be avoided ($\sigma_u/2.35$ in lieu of σ_y is still used in some codes to this day);
- (f1) all important modes of component collapse failure should be catered for and all assumptions clearly stated;
- (g1) for multiple loads acting simultaneously empirical or analytical interaction failure equations are generally suitable; these should be consistent and give rise to no anomalies when checking safety;
- (h1) cross-section slenderness proportions of stiffeners should be properly restricted where buckling collapse can occur;
- (i1) test data should be checked as being reputable and relevant, and any limitations are to be carefully noted;

The strength models which have been adopted in various codes generally take into account fabrication and imperfection effects. For example, the RCC strength formulations for compressed stringer stiffened cylinders⁶⁸ allow implicitly for imperfections by the use of empirical elastic knockdown factors for shell buckling terms. However, the use of these formulas based on average imperfections does not correctly account for their effect when the imperfections have large amplitudes. It would therefore seem possible in principle to incorporate different levels of knockdown to cater for slight, average and severe levels of deformation using, for example, a Koiter type approach^{149,180} as has been done for unstiffened tubes¹⁸¹ and for ring framed cylinders¹⁸². For a good strength model, allowance should be made to take this into consideration.

Residual shrinkage forces arising from the welding of stiffeners provide the main cause of stiffener and shell or plate deformations. At the same time, the residual compressive stresses themselves have an adverse effect on buckling loads and compression strength. That is the reason because most of the offshore structural components failed due to inelastic collapse. There are various formulations which can be used for inelastic buckling but most of these are overly conservative for slender structures. The one which Faulkner recommends in Ref. [139] is the Ostenfeld-Bleich formulation¹⁵⁰ because it accounts for the effect of residual stresses explicitly, has a good agreement with test data and is relatively simple. The inelastic collapse stress for the column is given by eq.(3.32) and has been extended to local buckling^{139,183}.

An important type of interaction equation often found in design codes is used to define failure when more than one load system acts. These equations can sometimes be derived theoretically but, whenever possible, they should be validated by comparison with appropriate experimental results. Faulkner¹⁵⁸ extended the semi-empirical interaction equation of Odland¹⁵⁷ and used it in the RCC work (eq.(3.59)). The

advantages of the Odland type interaction equations are that for stocky shell geometry's the model tends towards the von Mises yield criterion, whereas for slender structures the failure criterion approaches linear interaction.

One important aspect of strength modelling is the one related with when to use the different strength models (criteria b1). While strength assessment equations are normally general equations, indicating explicitly and in detail the effects of each of the relevant parameters, design equations must be simple and account for the specificity of the structure that they intend to model because normally they are used in the absence of knowledge of some of the parameters (i.e., in the early stage of the project).

In Refs.[91,184] Guedes Soares proposed a methodology to simplify complex models into more simple expressions to be used in the design of specific structures, but with the quality and robustness of the original formulations. This methodology is divided into two different parts. The first, is based in a probabilistic technique in which a simple strength assessment expressions is obtained by weighting the general model by the probability distributions of its less significant variables for a particular type of structures (in Ref.[91] this was done for the design of merchant and naval ships plates and in Ref.[184] the merchant ships were subdivided into two classes with tankers in one side and Ro-Ro, containers, and bulk carriers). The result of this weighting is a bias B given by a mean value and a coefficient of variation.

The second part of the methodology consists in transforming the simple strength assessment expression in a design equation. This is done by incorporating the level of safety^{185,186} selected for design through the use of partial safety factors. From the case studied by Guedes Soares a partial safety factor for the strength equation was given by $\gamma_B = 1 - \beta_T \alpha V_B$ where V_B is the bias variability, β_T is the desired level of safety and α is a factor proposed by Lind¹⁸⁵ and varies between 0.7 and 1.0. Thus, design equation is obtained by multiplying the simple strength assessment expression by a characteristic bias B_c given by $B_c = \bar{B} \gamma_B$. Other way to derive the partial safety factors is by using directly the PSFs for the different random variables as given by the First Order Reliability Methods (eq.(1.4)). One example of the use of Guedes Soares methodology is presented in section 2.2.1.4 for the case of unstiffened plate subjected to longitudinal compression. In the example equations (2.12) and (2.13) were obtained from equation (2.11) using this methodology and incorporating a level of safety for the characteristic value of the bias of 2.5 standard deviations below the mean. ($\beta_T \alpha = 2.5$)

For determining the importance of the variables Guedes Soares uses the following philosophy⁹⁰: "The number of variables included in the design equation must be such

that the strength predictions are always within a narrow scatter band independently of the value of the variables not represented explicitly in the equation”.

Finally, in addition to the statistical criteria and the strength requirements four guiding principles should be adopted when considering strength models for design:

- they must be able to describe all likely buckling modes with adequate accuracy (X_m bounded by 0.95 to 1.05 and $V_{Xm} < 0.15$ for single applied loads);
- initial imperfections, load eccentricities and other defects should be discussed even if they are not explicitly allowed for; the strength assessment models should aim to replicate average achievable standards of construction while the design models should be derived using the existing data for the specific type of structures;
- boundary conditions, including symmetry and anti-symmetry conditions, must reflect the actual behaviour of the structural component;
- choice of solution must be based on anticipated buckling behaviour of the shell and stiffeners.

4.3 - Case Study - Improvement of the strength formulations for ring-stringer stiffened cylinders

4.3.1 - Introduction.

After the uncertainty analysis done in Section 3.3 was felt that some room exists for the improvement of RCC formulations. In this section will be presented with detailed discussion the results obtained for this improvement study. In the initial stage of the study some assumptions were made and a strategy was adopted.

One important assumption was ignoring shell buckling (buckling of curved shell plating between stringers and ring frames) as being an ultimate strength limit state. However, it may be used as a serviceability limit state by some designers for the case of external pressure loads, and this will be considered.

Thus, the study considers only the following modes of ultimate collapse for orthogonally stiffened cylinders under single or combined loads:

- (a) Bay instability - buckling of stringers and associated shell between rings and bulkheads which maintain form. For axial compression the two most likely forms of collapse are:

- (i) column type buckling of stringers and associated plating (fig.(3.3b));

(ii) sideways tripping of the stringers (this is not regarded as local buckling)(fig.(3.3d)).

In both case interaction effects from shell buckling are likely.

(b) General instability - buckling of the cylinder between bulkheads including rings (fig.(3.3c));

(c) Overall buckling - buckling of the complete cylinder as a column under axial compression.

Where significant shear actions exist, then tension field type actions could be set up to modify interframe collapse (a). However, very little review was undertaken on shearing effects arising from torsion or transverse loads because in offshore structures the shear stresses arising from such actions are small. It was therefore given low priority to this matter but it is nevertheless adequately covered and simplified approximate solutions are given.

Also, the simplified procedures resulting from this study are aimed at:

- avoiding local buckling of stiffener cross-sections, that is, webs and flanges are proportioned conservatively;
- proportioning ring frames conservatively to ensure that general instability is preceded by interframe collapse.

The weight penalty arising from these procedures is small.

At last, the overall collapse mode (c) was ignored on the grounds that in practical offshore stiffened structures it is unlikely to occur, and any beam-column interaction effects are, in any case, adequately covered by axial stressing arising from such actions being allowed for in the procedures for combined axial loads and bending.

In respect to the essential strategy used in the study, it can be summarised in five steps:

1. identify the best starting points from Section 3.3 review for the various load types;
2. from the modelling criteria (Section 4.2) greatest priority was placed on good physical modelling of the failure mechanisms;
3. where sample size is less than 15 one must not be unduly influenced by low modelling (V_{xm}) achieved, for example, from good regression curve fits;
4. greater emphasis was placed on axial compression as being the most important load type and for which more data exists;

5. the explicit effects of initial shape imperfections were ignored in strength modelling for design; they are implicitly covered by knockdown factors which are functions of R/t and Z_s .

With regard to this last step, it was generally found that where imperfection data exists for the test models, the average values were in general within defined construction tolerances. However, the effects of initial weld induced stresses were modelled (with no shakeout) for axial compression strength.

4.3.2 - Modelling the axial strength.

It will be seen from the data of Section 3.3 that the RCC strength formulations consistently provide the best models in terms of mean bias and COV. These were therefore used as the best starting point.

When examining interframe collapse data, it was noticed that sideways tripping of flat bar stiffeners appeared at final collapse of a surprising number of models. As this sideways tilting was never adequately monitored during the tests, it has not been possible to confidently identify those models whose failure were definitely induced by sideways tripping of the stringers.

The final appearance of tripping may be a late stage consequence of failure. Nevertheless, past research has shown¹⁸⁷ that this mode of failure may, for sparsely stiffened panels, be precipitated by plate element or shell buckling or destabilising actions and evidence for this can be seen in some of the tests. It was therefore felt that this mode of failure should be modelled separately from column induced failure, especially as when it does occur it affects the whole stiffener and is not a local failure.

4.3.2.1 - Column-type buckling.

The RCC strength formulations are given in Section 3.2. For axial compression the most influential terms are:

- (a) the curved shell imperfect inelastic buckling stress $\rho\sigma_{cr}$, which provides the basis for the effective width (EW) and reduced effective width (REW) equations through the slenderness parameter:

$$\lambda = \sqrt{\sigma_y / \rho\sigma_{cr}} \quad (4.1)$$

(b) the two term elastic panel buckling stress:

$$\sigma_e = \sigma_{cl} + \rho_s \sigma_{sh} \quad (4.2)$$

where the first term is for the column buckling of the stringers and associated shell and the second is for the unstiffened shell;

(c) the weld-induced residual stress reduction factor $R_r \leq 1$ which is applied to the EW and REW equations;

(d) the structural tangent modulus approach to convert σ_e into inelastic collapse σ_{ic} for different levels of weld tension block parameters η .

For reasoning presented in Section 4.2.2 and developed in Ref. [139] no attempt was made to improve (c) and it was also felt it would be hard to improve the treatment of inelastic effects (d). The modelling of inelastic effects has been established by the Structural Stability Research Council as being the most rational way of incorporating the degrading effects of both cold-forming and weld induced residual stresses¹⁵¹ and has previously been well validated from flat panel test data. The first two factors will now be examined more fully against a target of $\bar{X}_m = 1.02$ and $V_{X_m} = 13.3\%$ as seen from the 52 test models using RCC formulation.

4.3.2.1.1 - Curved Shell Buckling.

The RCC perfect buckling stress σ_{cr} uses the Koiter parabola for $Z_s \leq 11.4$ and the unstiffened cylinder expression for higher values of the width parameter. The lower bound knockdown factor ρ_n expressions in the ranges $Z_s \leq 11.4$ and $11.4 < Z_s \leq 70$ were based on a good curve fit to Fig.C3.2 of Appendix C to the 1977 DnV Rules¹⁸⁸. These were thought to be mainly based on aerospace data with 5% lower bound. To achieve a mean knockdown factor, a rather arbitrary bias factor B was applied to reflect that shape effects build up to their maximum effect at the critical slenderness $\lambda = 1$:

$$\left. \begin{aligned} B &= 1.15, & \text{for } \lambda_h &= \sqrt{\sigma_y / \rho_s \sigma_{cr}} \geq 1.0 \\ &= 1 + 0.15\lambda_h, & \text{for } \lambda_h &< 1 \end{aligned} \right\} \quad (4.3)$$

The mean knockdown factor was then taken to be:

$$\rho = B \rho_s \quad (4.4)$$

This preference for the DnV based data was for two reasons. It was thought to be the best curved panel buckling data available and the knockdown expressions derived

increased as functions of Z_s and R/t , which were thought to be of greatest importance for shape imperfection effects.

Two improvements were tried. The first and simplest was to adjust the arbitrary bias factor B . It was argued that most of the test models and likely practical structures have $\lambda \geq 1$ in which case the RCC formulation gives $B=1.15$ for mean correction. Allowing $V_{X_m}=15\%$, as noted from various curved shell buckling test data, a 5% lower bound would require a correction of 1.25. As an alternative approximation the effect of this increase in B on the mean value of the modelling parameter can be estimated from the approximate derivatives:

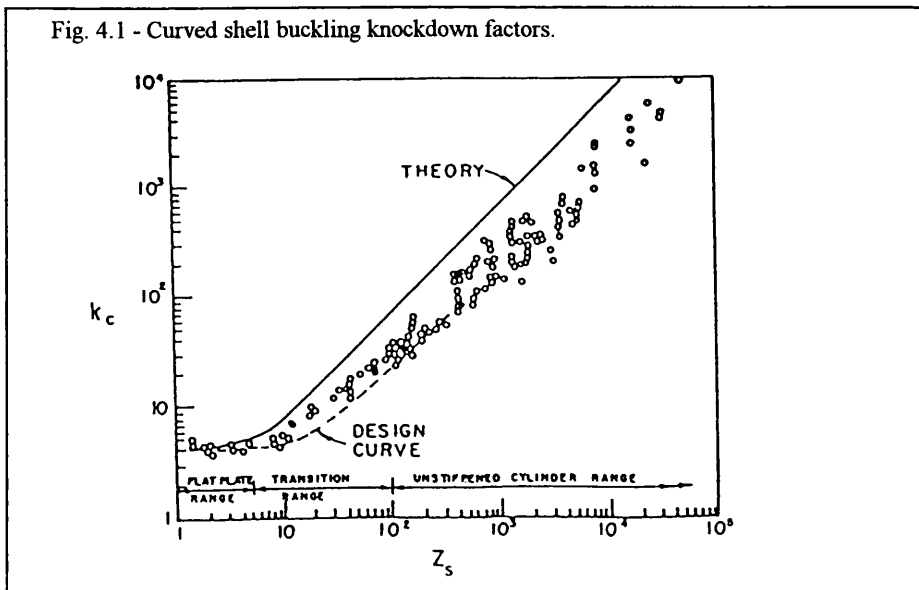
$$\frac{dB}{B} = \frac{2(\gamma + b_e/b)}{\gamma b_e/b} = \frac{d\sigma_u}{\sigma_u} \quad (4.5)$$

Values of $b_e/b \in [0.70, 0.95]$ at failure are typical for test models with $\lambda \in [0.80, 1.20]$ and $\gamma = A_s/st \in [0.20, 0.40]$. For a required increase in $d\sigma_u/\sigma_u = 0.02$ (to give 0.02 reduction in X_m) this suggests $dB/B \in [0.043, 0.072]$. This leads to a new average value of $B=1.22$ for $\lambda \geq 1$ which is close to 1.25 derived above. Changing the upper limit of B from 1.15 to 1.25 lead to $\bar{X}_m = 1.006$ and $V_{X_m} = 13.2\%$ which is an improvement.

The second improvement was tried by using test data referred by Kinra¹⁷⁸ and shown in Fig. 4.1. Best fit knockdown factors for curved shell buckling were derived from this data and are:

$$\begin{aligned} \rho_m &= Z_s^{-0.2} && \text{mean} \\ \rho_k &= 1.17 Z_s^{-0.33} && \text{lower bound} \end{aligned} \quad (4.6)$$

However, this makes no reference to R/t , which is thought to be nearly as influential as Z_s in accounting for the effects of shape imperfections. The first equation was



therefore modified to include R/t effects along the lines of the DnV data and assuming that R/t=300 was an average for the data (unfortunately, this was unable to be checked). This gave:

$$\rho = \left[1 + 0.1 \left(1 - \frac{R}{300 t} \right) \right] Z_s^{-0.2} \quad \text{for } Z_s \leq 100, \quad R/t \leq 600 \quad (4.7)$$

However, when this curved shell knockdown model was used this gave $\bar{X}_m=1.03$ and $V_{Xm}=14.7\%$ which worsens the match with the 52 test data.

4.3.2.1.2 - Two term equation.

The elastic perfect buckling stress in the RCC formulations is based on the sum of a column buckling load for the stringers and associated shell and an unstiffened shell buckling load. In stress terms this is:

$$\sigma_e = \frac{\pi^2 E I_e'}{L^2 + (A_s + s_e t)} + \rho_s \frac{0.605 E (t/R)}{1 + A_s/s t} \quad (4.8)$$

Initially, this was an intuitive approach put forward at Glasgow and inspired by the Bryan equation for pressure collapse of perfect ring frame cylinders. By the time RCC work was underway, theoretical confirmation for this model has been provided¹⁸⁹ although the denominator in the first term should strictly be $A_s + s t$ and for the second term $\rho_s=1.0$, but RCC studies found a good fit with test data using eq.(4.8) and $\rho_s=0.75$ - lower values such as $\rho_s=0.5$ were found to be worse. These findings were confirmed in the present study. However, putting $\rho_s=1$ did improve the mean bias $\bar{X}_m=1.00$, with only a slight worsening in $V_{Xm}=13.8\%$ (compared with 13.3%).

It has been argued that stringers in compression should be treated as beam-columns on an elastic foundation, the foundation being the hoop radial stiffness provided by the circular cylinder $\beta=Est/R^2$. This would then lead to an increase in the column buckling load to:

$$\rho_{cr} = \frac{\pi^2 EI}{L^2} \left(m^2 - \frac{BL^4}{m^2 \pi^4 EI} \right) \quad (4.9)$$

where m is the number of half waves to be found in the lowest buckling load. However, when the cylinder itself is also under compression, as of course it is in real structures, the radial stiffness is much less in the radially outward direction than in the

radially inward direction. This arises from the Poisson hoop expansion. Moreover, the two foundation stiffnesses are then load dependent, that is, they vary with the applied compression load.

These effects were examined theoretically in this study. For the range of practical structures, it was found that the Poisson induced radial stiffness term arising from the load as it approaches typical buckling stress levels, more or less cancels the natural radial stiffness β (above) for the unstiffened cylinder. This suggests that foundation stiffness effects should not be modelled for column collapse. It also follows that column collapse for single bay tests will tend to occur outwards, as indeed is observed. For multi-bay practical structures continuity would usually require that adjacent bays buckle alternately in and out, in which case the inward failures may be expected to follow after the first outward bay collapses. However, practical man-made structures may not behave this way because initial shape imperfections generally occur inwards; also some degree of external pressure would of course encourage inward collapse. The subject is clearly complex and the best advice is to assume simple supports at the ring frames and ignore foundation effects.

The possible attraction of providing a less arbitrary choice for ρ_s for the unstiffened shell buckling term was explored. The ESDU data sheets¹⁸¹ for unstiffened cylinders are useful because they allow for imperfect shape as measured from a wide range of experimental data. From Fig.2 of Ref. [181] the mean imperfection is defined as:

$$\frac{\delta_m}{t} = 0.04 \left(\frac{RL}{t^2} \right)^{0.18} \quad (4.10)$$

The coefficient can be increased for different cumulative probability levels and chosen confidence levels from Fig.3 of Ref. [181]. For example, the 95% probability value (5% upper probability of being exceeded) with a 95% confidence value requires a 3.45 multiplying factor (or 3.9 with 99% confidence). In order to relate imperfect elastic buckling strength to any required level of imperfection, the knockdown factor can be determined from an analysis by Koiter^{149,180}:

$$\rho_s = 1 - \frac{c}{2} \left(\frac{\delta}{t} \right) \left[\sqrt{1 + \frac{4}{c} \left(\frac{t}{\delta} \right)} - 1 \right] \quad (4.11)$$

where $c = (3/2)\sqrt{3(1-\nu^2)} = 2.48$ for $\nu=0.3$ and δ is the peak to trough value in the axial direction. Substituting eqs.(4.10) in (4.11) gives the mean knockdown for the unstiffened shell term:

$$\rho_s = 1 - \frac{1}{20} \left(\frac{RL}{t^2} \right)^{0.18} \left\{ \left[1 + 40 \left(\frac{t^2}{RL} \right)^{0.18} \right]^{\frac{1}{2}} - 1 \right\} \quad (4.12)$$

Alternatively, using $\lambda=L/R$ this leads to:

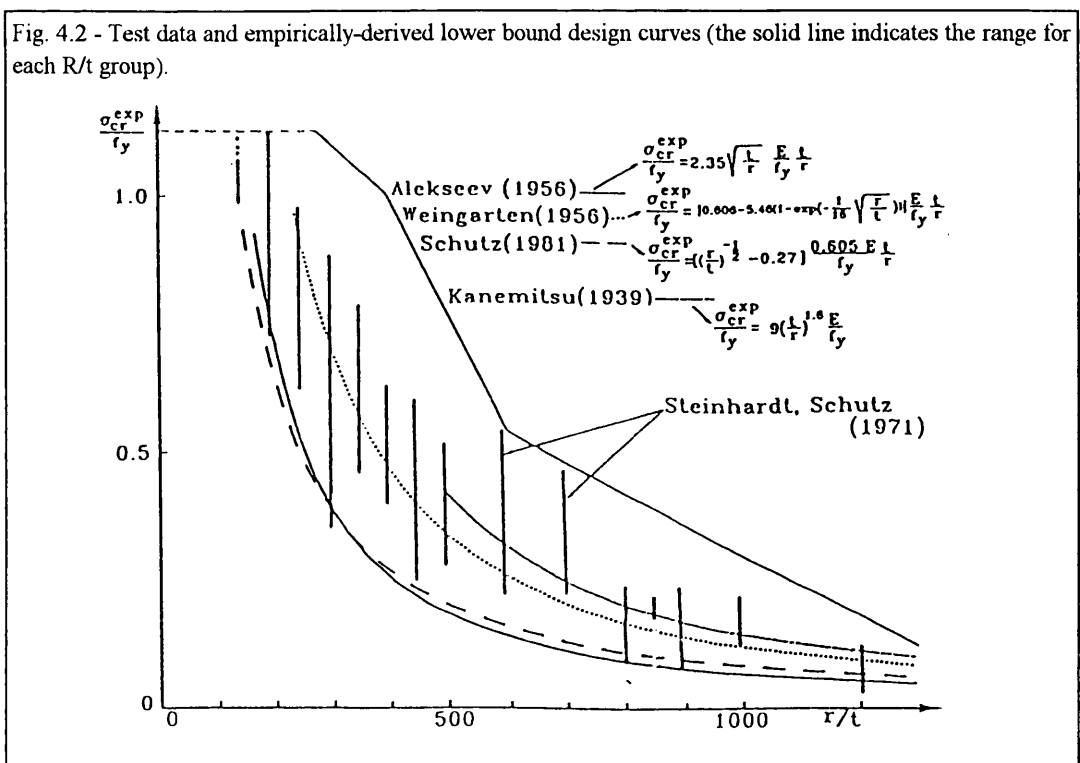
$$\rho_s = 1 - \frac{1}{20} \lambda^{0.18} \left(\frac{R}{t} \right)^{0.36} \left\{ \left[1 + \frac{40}{\lambda^{0.18}} \left(\frac{t}{R} \right)^{0.36} \right]^{\frac{1}{2}} - 1 \right\} \quad (4.13)$$

Taking $\lambda=5$ and 1 leads to the following knockdown factors which are compared with DnV results¹⁸⁸:

R/t	100	200	300	400	500	600
Eq.(4.13) $\lambda=5$.44	.41	.38	.36	.34	.33
DnV	.45	.43	.41	.39	.37	.35
Eq.(4.13) $\lambda=1$.49	.45	.42	.41	.39	.38

Table 4.1 - Comparison of the different ρ_s curved shell knockdown factors.

Although these values agree quite well they considerably underestimate knockdown as measured from test¹⁹⁰ and shown in figure 4.2.



These equations when applied to eq.(4.8) also appreciably worsen the fit with stringer stiffened test data, and so this investigation was terminated. Referring to Fig.(4.2) a very good fit to the dotted mean curve is given by:

$$\rho_s = 2900 \left(\frac{R}{t} \right)^{-1.46} \quad (4.13)$$

For example, with R/t=300, a typical value for many of the stringer stiffened tests, this leads to $\rho=0.70$, which is close to 0.75 assumed by the RCC. It seems reasonable, therefore, to stick with this value. Other study was leaving out $1+A_s/st$ in the second term denominator of eq.(4.8) and this gave $\bar{X}_m = 1.008$ and $V_{Xm} = 13.5\%$.

Case N ^o	Description	\bar{X}_m	$V_{Xm}\%$
0	RCC formulations	1.02	13.3
1	Curved Panel: $B = 1 + 0.25\lambda_h, \lambda_h \leq 1$ $= 1.25 \text{ for } \lambda_h > 1$	1.01	13.2
2	$\rho = \left[1 + 0.1 \left(1 - \frac{R}{300t} \right) \right] Z_s^{-0.2}$	1.03	14.7
3	Two term eq. for σ_c: $\rho_s = 1 - \frac{\alpha}{40} \left(\sqrt{1 + \frac{40}{\alpha}} - 1 \right), \alpha = \left(\frac{RL}{t^2} \right)^{0.18}$	1.06	14.8
4	$\rho_s = 1.0$ in the second term	1.00	13.8
5	First term = $\frac{\pi^2 E I'_e}{A_s + st}$... not $s_{em}t$	1.05	13.9
6	Cases 4 and 5 together	1.02	13.5
7	Second term = $\rho_s 0.605E(t/R)$ with no denominator and $\rho_s = 0.75$	1.01	13.5
8	Combined result: Cases 1 and 7 together	0.99	13.5

Table 4.2 - Modelling parameters for different equations considered in axial compression strength.

The final study was to look at separate inelastic modelling of the column term and the unstiffened shell term as suggested by Odland⁸⁴. In principle this might, for example, take the form:

$$\sigma_{ic} = \frac{E_t}{E} \sigma_c + \frac{\sqrt{E_s E_t}}{E} \rho_s \sigma_s \quad (4.13)$$

but in practice it is the loads that are added (otherwise collapse stress approaching twice the yield could result). This was examined but no improvement was found.

A summary of the various studies is given in Table 4.2. and the final recommended choice of axial compression strength model is to keep with the RCC strength formulation but incorporate change n° 1 as described above.

4.3.2.2 - Stringer Tripping.

Tripping has been mentioned earlier and is regarded as a primary mode of interframe collapse. Although a theory for this was advanced nearly 10 years ago for RCC consideration¹⁸⁷, it was never widely discussed nor does it appear in API 2U as a limit state.

The present formulations in land-based and in marine structure codes simply ignore rotational constraints to the stiffener toes provided by the plating or shell. In this, they are making the usually justified engineering assumption that this will be conservative. However, further work has shown theoretically¹⁹¹, backed up by experiments, that this assumption can be non-conservative due to destabilising actions for plate or shell buckling. This, and earlier remarks, would seem to confirm the importance of the subject. Stiffener tripping has also emerged as a topic of some interest and concern in reliability studies for ring frame strength in submarine pressure hulls^{192,193}. Further work on this subject should be aimed at deriving sensible tripping ultimate limit state (ULS) strength equations for design.

4.3.3 - Modelling the radial strength.

Although the RCC formulation achieves a mean bias of $\bar{X}_m=0.97$ and a $V_{Xm}=10.3\%$ for the 11 steel test models, one can not be happy with it. With three adjust factors (f1, f2 and f3), it follows naturally that it will fit the data because it is made to do so. One can not be overly influenced by the low COV because of the small sample size. The

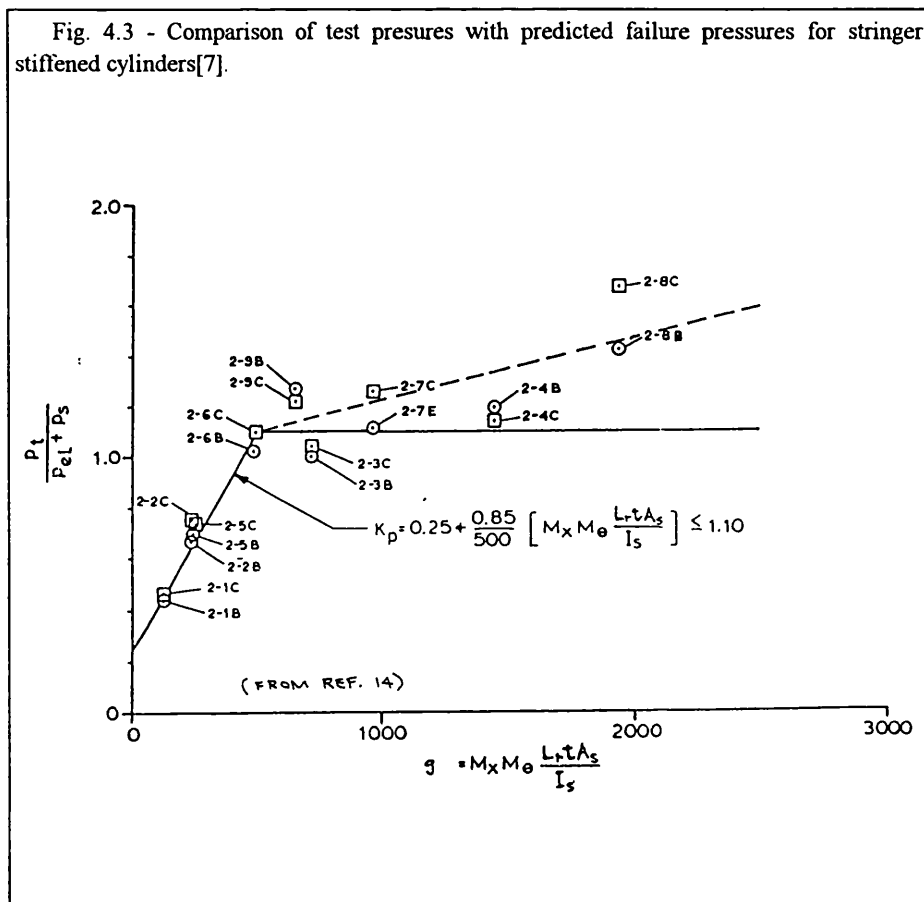
sample size. The main objection to this formulation, according to Faulkner¹⁴¹, is that it was never debated by the whole Rule Case Committee to benefit from the technical evaluation of other formulations.

Although the RCC had early on suggested a three-hinge collapse as a dominant mechanism for the stringers, Faulkner¹⁴¹ does not agree that the plastic section modulus Z_p used in the formula totally ignores the effect of its attachment to the plating, except for a small extension of area (t_w) to the web. For flat bar stiffeners this makes a difference of 2:1. Throughout the increased loading, the stringers are bending integrally with their associated plating and it is unreal to assume they detach themselves at the point of collapse. The concept of shell boundary hinges in the RCC model is welcome, but greater emphasis on in-plane membrane actions is required.

The API formulation leads to a mean bias for the 11 steel models of $\bar{X}_m = 1.21$ and $V_{x_m} = 14.5\%$, which have been improved to $\bar{X}_m = 1.14$ and $V_{x_m} = 13.4\%$, simply by changing the adjustment coefficient K_p when $g > 500$ to:

$$K_p = 0.98 + \frac{0.12g}{500} \quad (4.14)$$

This was done to improve the fit with test data in that range, to be closer to a mean



fit than a lower bound as shown by the dotted line in Fig.(4.3). However, API formulation is poor on the grounds that the two terms in the collapse pressure mix purely elastic shell behaviour with totally plastic stringer behaviour. The coarseness of K_p is other point against this formulation.

The recommendation is to keep with RCC formulation but be aware that further work should be carried. As final note it should also point out that the behaviour of T-bar stringers have not been tested under external pressure.

4.3.3.1 - Local shell buckling.

It should also be mentioned that shell buckling may be regarded as a limit state which some designer would wish to specify, perhaps as a serviceability limit state with a lower reliability index. This is on the basis that although the final ultimate failure pressure may be a lot higher, the shell deflections on buckling may be more than they would wish to tolerate. RCC test model for example, with $N=36$ stringers, experienced initial buckling at 77 psi, at which point the deformation of the shell was about $2t$. Final ULS was at 114 psi pressure (48% higher) when the permanent deformation of the shell, and the stringers in some cases, were well beyond $3t$. In such cases, the designer should use either the API 2U local shell buckling pressure (eq.(3.49)) which ignores the presence of the stringers, or the following equation:

$$P_{cr} = \frac{\left(\frac{N}{2}\right)^2 - 1}{12(1 - \nu^2)} E \left(\frac{t}{R}\right)^2 \quad (4.15)$$

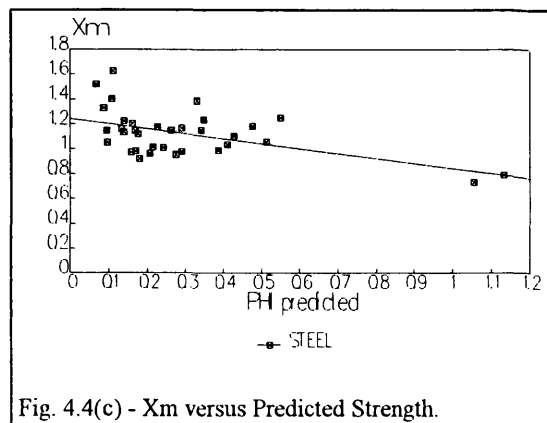
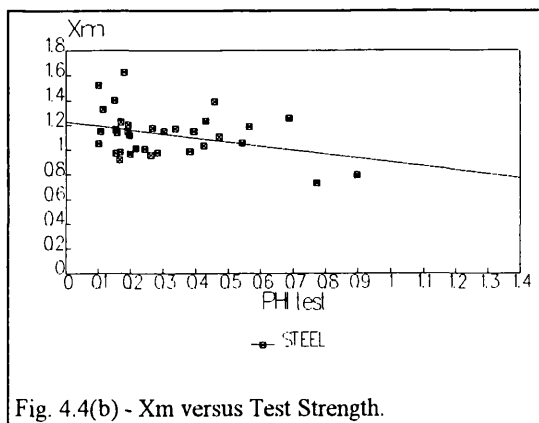
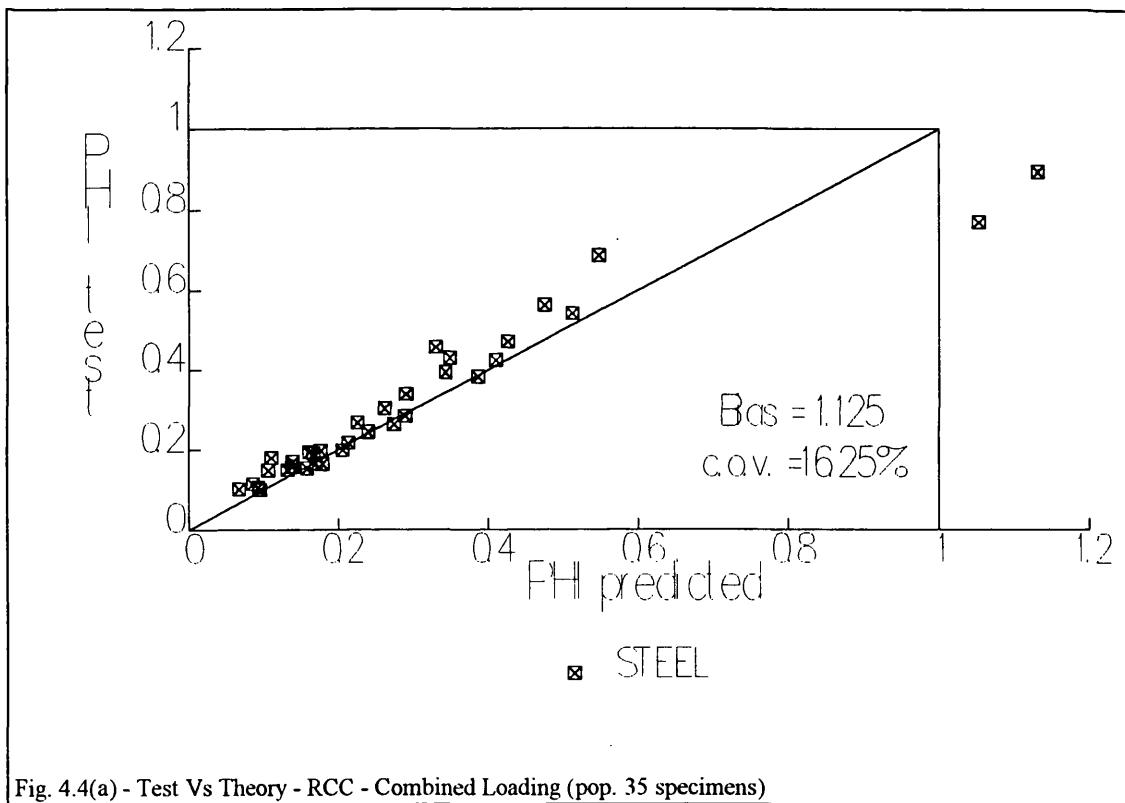
This equation is based on the Foppl unstiffened shell expression with the number of complete waves around the circumference taken $n=N/2$, where N is the number of stringers and these are assumed to provide sufficient supports at buckling antinodes.

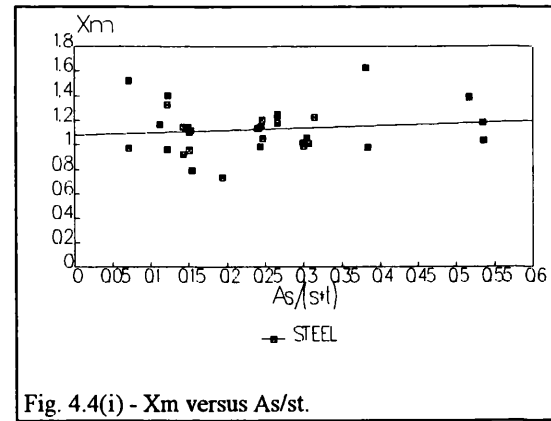
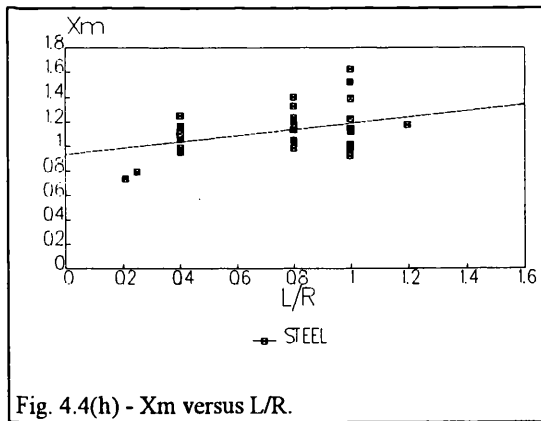
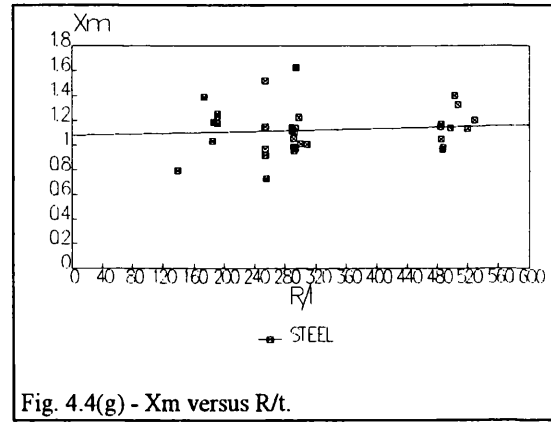
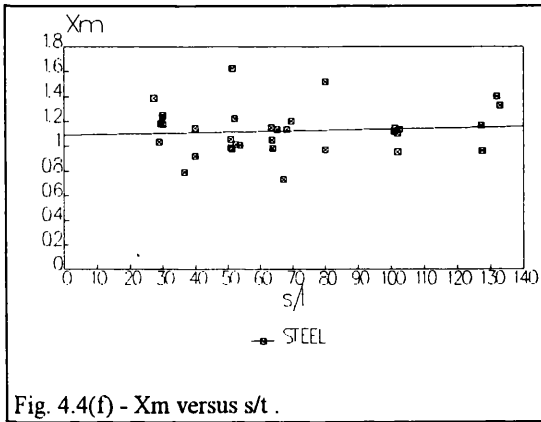
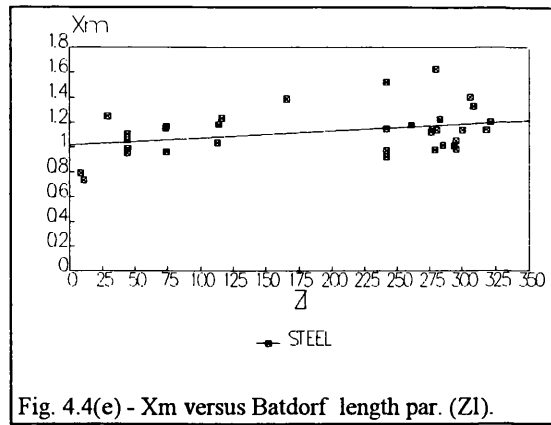
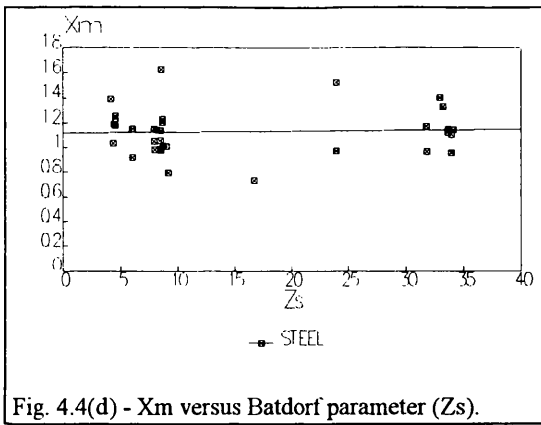
4.3.4 - Modelling the combined load strength.

Table 3.12 shows the model uncertainties for the API, RCC and DnV codes. RCC has by far the best mean bias ranging from 1.04 to 1.09 whilst the API has the best COV ranging from 13.9% to 19.7%. Because both RCC and API have similar interaction formulations, with only the C parameter defined differently, one further improvement was tried. Using RCC interaction with API C parameter and both RCC axial compression and radial pressure formulations one obtains for the 35 test models a

mean bias and the COV of $\bar{X}_m = 1.125$ and $V_{xm} = 16.25\%$. The result indicates an worsening for the mean bias (the formulation becomes more conservative) but an important reduction for the COV is achieved ($V_{xm} = 16.25\%$ against $V_{xm} = 24.8\%$). The results of the uncertainty analysis are presented in figure 4.4 and does not indicate major skewness with any of the relevant parameters. Thus, the recommendation is to keep with RCC interaction formulation incorporating the C parameter used in API (eq.(3.57)) (this is of course identical to API proposal for interaction formulation).

The variation of X_m with predicted strength, test strength and with other parameters for RCC the all population is shown in the following figures 4.4(a) - 4.4(i).





Global bending loads and its resulting maximum field stress must be added algebraically to the simultaneous axial compression and then the recommended compression strength limit states should be used, as discussed in Section 4.3.2.

Regarding global shear stresses arising from torsion or transverse loads, this has not so far been reviewed. If required, the ULS equations (including interaction) given in the 1977 DnV rules Appendix C are recommended at present. The general level of field stresses arising in shear were found to be very low in most practical structures in relation to ULS levels in shear. Values were every where less than 0.2 ULS and were

generally no more than 0.1 ULS. By the time they have gone through a quadratic type interaction equation, their influence is lost. Moreover, maximum shear stress seldom, if ever, occurs at the same time and position in the structure as maximum bending and/or axial compression. Therefore, neglecting shear effects is not unreasonable, except in way of openings or node connections.

4.4 - Importance of the variables in the reliability assessment.

The adequacy of a formulation is incorporated in the reliability assessment through a random variable - the modelling parameter. The importance of this variable along with all the other random variables used in reliability assessment depends upon two important factors:

- their level of uncertainty and;
- their role in the limit state function.

Their level of importance is given by both the sensitivities and the partial safety factors. These measures are the ones to be considered to decide if a certain variable should be used as random or as deterministic in a particular problem. The proper selection of the random variables allows the reduction of the complexity of the problem (limit state function) by reducing the dimension of the failure surface (normally consisting in an hyper-surface with its dimension equal to the number of random variables used).

It is also necessary to stress the importance of the correct definition of the variables, especially if they are correlated. The omission of correlation among the variables, if it exists, can lead to large differences in the final results.

4.4.1 - Model uncertainty variables.

Two different types of modelling parameter exists, the resistance and the load modelling parameters. They prove to be the most important variables in reliability assessment. Especially, the resistance modelling parameter that in all cases studied was the most important variable, which reinforces the idea that the emphasis should be put in the correct modelling of strength^{65,140}. These variables clearly dominate the final results, especially when their COVs were above 15%.

Modelling uncertainties are best assessed from test data as has been done in this study. However, we should always be aware of two limitations:

- (a) COVs obtained with small samples sizes are uncertain and must be regarded with caution especially if they are too low or too high;
- (b) the uncertainties may lie as much in the test conditions and results as with the analytical model;

There are two reasons for (a), one is purely statistical, and the other has to do with better curve fits by regression with small sample sizes. When the samples are small the value for the COV should be carefully analysed. When the COV is too low an increase above the test data levels is recommended. When it is too large a reduction is recommended.

Load Type	Formulation	Sample	\bar{X}_m	$V_{X_m}\%$
Unstiff. plate Longitudinal compression	Faulkner	100	0.98	11%
	G. Soares	233	1.00	7%
Stiff. plate Longitudinal compression	Faulkner	119	0.95	12.6%
	Carlsen-PIF	119	1.19	16.9%
	Carlsen-SIF	119	1.02	16.3%
Transverse compression	Faulkner	20	0.70	33%
	Valsgard	20	0.89	30%
	ABS	20	1.17	44%
Biaxial loading	Faulkner	385	0.94	24%
	ABS	385	1.21	31%

Table 4.3 - Strength modelling parameters for the different strength formulation for stiffened and unstiffened plates^{18,90,114,115}.

Regarding (b), the test arrangements and general standards of construction of the test models have been scrutinised in order to identify and reject suspect ones. Ideally, cross checks should also be made with appropriate numerical models¹³⁹. This has not been undertaken because of the limited timescale of the study. Against this background, it is therefore provisionally recommended the use of the subjective uncertainties presented in Tables 4.3 and 4.4 for the plates and cylinders respectively. The modelling parameters should be assumed to be lognormally distributed and are associated with the strength formulations used in the study.

Load Type	Formulation	Sample	\bar{X}_m	$V_{X_m}\%$
Axial compression	RCC new	52	1.01	13.2
	API discrete	52	0.99	18.4
	API ortho	52	0.87	24.0
	DnV	52	1.01	25.1
	ECCS	52	1.27	27.7
Radial pressure	RCC	11	0.97	10.3
	API discrete	11	1.21	14.5
	API ortho	11	0.87	46.2
	DnV	11	1.40	39.0
Combined loading	RCC new	35	1.13	16.3
	API	35	1.16	19.7
	DnV	35	1.68	25.3

Table 4.4 - Strength modelling parameters for the different strength formulation for ring and stringer stiffened cylinders¹⁴¹.

Finally, the load modelling parameters are lognormal random variables with their uncertainty dependent of the resistance models considered (chosen COV's varies in the study from 5% to 20%)(see Table 3.13).

4.4.2 - Strength variables.

This type of variables can broadly be divided in two groups. The first one is related with the material used in the components and the second one accounts for their dimensions. The material group of variables is formed by the:

- Yield Stress - It is the most important of all strength variables present in the different formulations used and when the modelling parameter has low COV it equals its importance. It is usually considered as a lognormal random variable. In the study moderate values of uncertainty were used (COV [7%-10%]).
- Young Modulus - In the study it has a small importance for both the plates and the cylinders. It is a well defined variable with low uncertainty (COV=4%) and is usually considered as a lognormal random variable.

The geometrical group of variables is formed by the:

- Thickness - The thickness has a moderate importance for both plates and cylinders but for some formulations its importance grows to the level of the yield stress. It is usually considered as a normal random variable with low uncertainty (COV=4%).
- Width, Length and Radius - These variables shown different behaviour under the different loading conditions, but has normally small or no importance. They are normal random variables with low uncertainties (COV[1%-4%]).

Other random variables related with the strength formulations exists. This is the case of the width of welded zone, the plate or shell deflections, the proportional limit, etc.. However, due to their low importance detected in a preliminary study they were considered deterministic variables. The same reasoning applies to the stiffener dimensions in the case of the stiffened cylinders.

In Table 4.5 the objective uncertainty levels for physical properties and structural dimensions are suggested¹⁴¹. The bias is the ratio of the mean expected value to the nominal design value and lognormal distributions are recommended for material properties. All other distributions can be taken as being normal, with the exception of

fabrication imperfections (η and δ) which have larger COV's and which are linked to the yield stress, so lognormal distributions are more appropriate.

Variable	Bias	COV %
Yield stress	1.1	6
Young's modulus	1.0	5
Welding stresses (η)	1.0	12
Initial deformations (δ)	1.0	25
Plate or shell thickness	1.0	3
Cross-section properties	1.0	4
Shell radius	1.0	5
Stiffener spacing	1.0	2

Table 4.5 - Typical uncertainty level for physical properties and structural dimensions¹⁴¹.

4.4.3 - Load variables.

These variables can be divided in two types. The first one is related to the static and quasi-static loads and the second is related to the dynamic loads. However in the study an important difference occurs between the plate and cylinder cases. For the plates it was considered that the model used to transform the load into the load action was an exact model (with no uncertainty involved). On the other hand, for the cylinders the load model uncertainty was accounted for in the two models used.

For the first and second types of load variables we find the:

- Static loading - Axial compression, transverse compression and radial pressure that are described by normal or lognormal random variables with the uncertainty COV[10%-55%] much dependent on the type of structure considered.

- and the Dynamic loading - Axial compression, transverse compression and radial pressure that are described by TYPE I Extreme random variables with the uncertainty COV[7%-20%] also dependent on the structure considered.

For this study the load variables were taken from several references^{21,70,140,162} and are presented in Tables 2.1 and 3.13. Nevertheless it worthwhile to say that these variables proved to be quite important, at the level of the most important resistant variables and were, for all cases, treated as random variables. This implies that, for load variables, care should be put in the selection of suitable distributions and in the development of methodologies to reduce their uncertainty.

CHAPTER 5 - CONCLUSION AND FUTURE DEVELOPMENT

The conclusions of the systematic studies for the stiffened plates and ring-stringer stiffened cylinders, which represent the bulk of conclusions of this thesis, are presented in the end of the respective chapters (see sections 2.5 and 3.5). Here, in this chapter, only some general conclusions will be presented along with a summary of the most important recommendations for the modelling of plates and cylinders. The chapter ends with the presentation of the perspectives for the future work.

The main conclusion of the thesis is the reinforcement of the idea that good strength modelling is crucial for a correct design. Reliability based formulations can make the design more consistent but they require in addition to the strength modelling an adequate probabilistic modelling. Its importance is determined by a series of factors from which the most relevant ones are the greater safety in the designs and the savings in material and construction costs that arises by the use of sound and robust formulations, i.e., good strength formulations.

Other general conclusion deals with the economic efficiency of the different design formulations. This study confirms previous work¹⁴⁰ regarding this aspect of design and it can be said that the less uncertain a formulation is, the better it is from an economic point of view. In fact, in all cases studied (plates and cylinders) the less uncertain formulations are the most economic structural design's. This is because the existence of uncertainty must always be compensated by increasing safety factors.

As a direct consequence of the above the strength modelling parameter can be considered the most important variable, this is particularly true when the formulations are fairly uncertain. From the other resistance variables it can be said that the yield stress is the most important one. The loading variables are in general as important as the most relevant resistance variables. It is also necessary to recall the importance of the correct definition of the random variables, especially if they are correlated.

Finally, one important aspect that should be taken in consideration is the choice of the safety levels used for design. From the results it is clear that large differences in weight arise from the adoption of one safety level or the other. Thus, in this particular aspect of design specific guidance should be established by the ruling authorities.

For the stiffened plates the most important conclusions are:

- Guedes Soares proposal for the strength of unstiffened plates under longitudinal compression improved the model of Faulkner including explicitly the effect of the initial deflections and by that it is recommended for design;
- Faulkner formulation is recommended for the design of stocky to intermediate unstiffened plates subjected to transverse compression; Valsgard proposal should be used for slender and very slender plates;
- Faulkner interaction formulation is recommended for the design of unstiffened plates subjected to biaxial compression;
- for the stiffened plates under longitudinal compression the method of Faulkner is also recommended with significantly lighter designs than Carlsen-plate induced formulation;
- unbiased formulations cannot be used for design. Appropriated bias should be derived to avoid unsafe designs;

For the ring stringer stiffened cylinders the most important conclusions are:

- the uncertainty study performed for the axial compression case clearly shows that the aerospace database does not provide a good fit to any of the formulations considered (COV's over 20% to all cases) and only the offshore database proved efficient for the calibration procedure;
- for the axial compression case it is clear that RCC is the best formulation. Its results in both the uncertainty study and in the reliability analysis shows a sound and robust formulation which allows the design of much lighter and cheaper structures.;
- for the radial pressure case RCC formulation is by far the best formulation. It is a mean value formulation particularly well suited for the geometric range of the offshore structures allowing the design of lighter structures;

- for the combined load case the conclusions are similar to the axial compression case with both RCC proposals allowing the design of much lighter and cheaper structures.;

Future developments of this work should be aimed at reducing the modelling uncertainties in the various formulations. This can be achieved in two different but complementary ways: first, conducting more experimental tests specially in the regions where exists large scatter in the actual data or in the areas with very few results. Second, by improving the formulations using the criteria and procedure presented in Chapter 4. In particular, a similar study to the one presented in section 4.3 should be carried out to the stiffened plates.

REFERENCES

- ¹**C.A. Cornell**, "Probability-Based Structural Code", J. of ACI, Dec. 1969.
- ²**B. Ellingwood and T.V. Galambos**, "Probability Based Criteria for Structural Design", Structural Safety, Vol. 1, 1982, pp.15-26.
- ³**A.H-S. Ang and C.A. Cornell**, "Reliability Basis of Structural Safety and Design", J. Struct. Div., ASCE, Vol. 100, N^o ST9, Sept. 1974, pp. 1755-1769.
- ⁴**O. Ditlevsen**, "Fundamental Postulate in Structural Safety", J. Engrg. Mech., ASCE, Vol 109, 1983, pp. 1096-1102.
- ⁵**A.G. Pugsley**, "A Philosophy of Aeroplane Strength Factors", British Aeronautical Research Committee, Report and Memo N^o1906, 1942.
- ⁶**A.M. Freudenthal**, "Safety and the Probability of Structural Failure", Trans. ASCE, N^o 121, 1956, pp. 1337-1397.
- ⁷**ABS-Conoco**, "Model Code for Structural Design of Tension Leg Platforms", Conoco-ABS TLP Rule Case Committee, Final Report, ABS, N.Y., Feb. 1984.
- ⁸**API-RP2A**, "Draft Recommended Practice for Planning, Designing and Constructing Fixed Offshore Platforms - Load and Resistance Factor Design", 1st Edition, American Petroleum Institute, Washington DC, December 1989.
- ⁹**Det norske Veritas (DnV-CN)**, "Structural Reliability Analysis of Marine Structures", Classification Notes 30.6, Norway, July 1992.
- ¹⁰**SHIPREL - Reliability Methods for Ship Structural Design**, BRITE/EURAM Project, Contract CT91-501.

¹¹**D. Faulkner**, "Development of a Code for the Structural Design of Compliant Deep Water Platforms", Department of Naval Architecture and Ocean Engineering, University of Glasgow, Rep. NAOE-84-65, Dec.1984.

¹²**P. Thoft-Christensen and Y. Murotsu**, "Application of Structural Systems Reliability Theory", Springer-Verlag, 1986.

¹³**H.O. Madsen, S. Krenk and N.C. Lind**, "Methods of Structural Safety", Prentice-Hall, Inc., 1986.

¹⁴**D. Faulkner**, "Reliability of Offshore Structures", SERC Marine Technology Seminar, London, 9-10 April 1984.

¹⁵**P.W. Marshall**, "The Design-Inspection-Redundancy Triangle", in 'The Role of Design, Inspection and Redundancy in Marine Structural Reliability', D. Faulkner et al. Ed., National Academic Press, 1984, pp.1-10.

¹⁶**J.G. de Oliveira and R.A. Zimmer**, "Redundancy Consideration in the Structural Design of Floating Offshore Platforms", in 'The Role of Design, Inspection and Redundancy in Marine Structural Reliability', D. Faulkner et al. Ed., National Academic Press, 1984, pp.293-327.

¹⁷**S. Valsgard**, "Numerical Design Prediction of the Capacity of Plates in Biaxial In-Plane Compression", Computers and Structures, Nº12 , 1980, pp. 729-739.

¹⁸**C. Guedes Soares, J.M. Gordo and J.M.Cruz**, "Design Rules for Stiffened Plates Under Compression", Dep. Naval Architecture and Ocean Engineering Report, Instituto Superior Técnico, Lisboa, December 1992.

¹⁹**D. Faulkner, J.C. Adamchak, J.G. Snyder and M.F. Vetter**, "Synthesis of Welded Grillages to Withstand Compression and Normal Loads", Computers and Structures, Nº3, 1973, pp. 221-246.

²⁰**P.C. Davidson, J.C. Chapman, C.S. Smith and J.P. Dowling**, "The Design of Plate Panels Subjected to Biaxial Compression and Lateral Pressure", Trans. RINA, Nº131, 1991, pp. 1-11.

²¹**C. Guedes Soares and A.G. Silva** , "Reliability of Unstiffened Plate Elements Under In-plane Combined Loading", Proc. 1991 OMAE - Vol.2, Safety and Reliability, 1991, pp. 265-276.

²²**M.J. Baker**, "The Reliability Concept as an Aid to Decision Making in Offshore Engineering", Proc. 4th Intl. Conference of Behaviour of Offshore Structures, Delft, The Netherland, July 1-5, 1985, pp. 75-94.

²³**F. Moses**, "System Reliability Developments in Structural Engineering", Structural Safety, Vol. 1, 1982, pp 3-13.

²⁴**Y.S. Feng and F. Moses**, "Optimum Design, Redundancy and Reliability of Structural Systems", Computers and Structures, Vol. 24, Nº 2, 1986, pp. 239-251.

²⁵**A. Karamchandani**, "Structural System Reliability Analysis Method", John A. Blume Earthquake Engineering Centre, Stanford Univ., USA, Report Nº 83, July 1987.

²⁶**P. Thoft-Christensen**, "Application of Structural Systems Reliability Theory in Offshore Engineering, State-of-Art", Proc. 3rd Intl. Conf. on Integrity of Offshore Structures, Univ. of Glasgow, Sept. 28-29, 1987, Paper Nº1, pp 1-24.

²⁷**A.M. Freudenthal, J.M. Garrelts and M. Shinozuka**, "The Analysis of Structural Safety", Journal of Structural Division, ASCE, Vol.92, NºST1, Feb. 1966, pp. 267-325.

²⁸**A.E. Mansour**, "Probabilistic Design Concepts in Ship Structural Safety and Reliability", Trans. SNAME, 1972, pp. 64-97.

²⁹**Task Committee on Structural Safety**, "Structural Safety - A Literature Review", J. Struct. Div., ASCE, Vol. 98, N^oST4, 1972, pp 845-884.

³⁰**B. Ellingwood and A.H-S. Ang**, "Risk-Based Evaluation of Design Criteria", J. Struct. Div., ASCE, Vol. 100, N^o ST9, Sept. 1974, pp. 1771-1788.

³¹**M.K. Ravindra, N.C. Lind and W. Siu**, "Illustrations of Reliability-Based Design", J. Struct. Div., ASCE, Vol. 100, N^o ST9, Sept. 1974, pp. 1789-1811.

³²**F. Moses**, "Reliability of Structural Systems", J. Struct. Div., ASCE, Vol. 100, N^o ST9, Sept. 1974, pp. 1813-1820.

³³**M. Shinozuka**, "Safety Against Dynamic Forces", J. Struct. Div., ASCE, Vol. 100, N^o ST9, Sept. 1974, pp. 1821-1826.

³⁴**J.T. Yao**, "Fatigue Reliability and Design", J. Struct. Div., ASCE, Vol. 100, N^o ST9, Sept. 1974, pp. 1827-1836.

³⁵**A.H. Hasofer and N.C. Lind**, "Exact and Invariant Second-Moment Code Format", J. of Eng. Mech. Div., ASCE, Vol.100, N^oEM1, Feb. 1974, pp. 111-121.

³⁶**R. Rackwitz and B. Fiessler**, "Structural Reliability Under Combined Random Load Sequences", Computers and Structures, Vol.9, 1978, pp 489-494.

³⁷**D. Veneziano**, "New Index of Reliability", J. of Eng. Mech. Div., ASCE, Vol.105, N^oEM2, 1979, pp. 277-296.

³⁸**O. Ditlevsen**, "Generalised Second Moment Reliability Index ", J. of Struct. Mech., Vol.7, N^o 4, 1979, pp. 435-451.

³⁹**The Committee on Reliability of Offshore Structures on the Committee on Structural Safety and Reliability of Structural Division**, "Application of Reliability

Methods in Design and Analysis of Offshore Platforms", J. of Struct. Eng., ASCE, Vol 109, N^o 10, Oct. 1983, pp 2265-2291.

⁴⁰**S. Gollwitzer and R. Rackwitz**, "Equivalent Components in First-Order System Reliability", Reliability Engineering, Vol.5, 1983, pp. 99-115.

⁴¹**S. Gollwitzer and R. Rackwitz**, "First-Order System Reliability of Structural Systems", Proc. 4th Intl. Conf. on Structural Safety and Reliability, Vol.1, Kobe, Japan, May 1985, pp. 171-218.

⁴²**X. Chen and N.C. Lind**, "Fast Probability Integration by Three-Parameter Normal Tail Approximation", Structural Safety, Vol.1, N^o4, 1983, pp.269-276.

⁴³**Y-T. Wu and P.H. Wirsching**, "New Algorithm for Structural Reliability Estimation", J. of Eng. Mech., Vol.113, N^o9, Sept. 1987, pp. 1319-1336.

⁴⁴**D.B. Parkinson**, "Solution for Second Moment Reliability Index", J. of Eng. Mech., Vol.104, N^oEM5, Oct. 1978, pp. 1267-1275.

⁴⁵**H.O. Madsen**, "First Order vs Second Order Reliability Analysis of Series Structures", Structural Safety, Vol.2, 1984, pp.207-214.

⁴⁶**A.D. Kiureghian, H-Z. Lin and S-J. Hwang**, "Second Order Reliability Approximations", J. of Eng. Mech., ASCE, Vol. 113, N^o8, Aug. 1987, pp.1208-1225.

⁴⁷**L. Tvedt**, "Second Order Probability by an Exact Integral", Proc. 2nd Working Conf. on Reliability and Optimisation of Structural Systems, London, U.K., 1988.(paper presented)

⁴⁸**G.I. Schueller and R. Stix**, "A Critical Appraisal of Methods to Determine Failure Probabilities", Structural Safety, Vol. 4, 1987, pp. 293-309.

⁴⁹**P. Bjerager**, "Methods for Structural Reliability Computations", Course in Reliability Problems: General Principles and Applications in Mechanics of Solids and Structures", CISM, Udine, Italy, July 1990.

⁵⁰**F. Moses**, "Structural System Reliability and Optimisation", Computers and Structures, Vol.7, 1977, pp.283-290.

⁵¹**F. Moses and B. Stahl**, "Reliability Analysis Format for Offshore Structures", Proc. 10th Offshore Technology Conf., OTC 3046, Houston, Texas, 1978, pp. 29-38.

⁵²**M. Gorman**, "Automatic Generation of Collapse Mode Equation", J. of Structural Div., ASCE, Vol.107, N^o.ST7, July 1981, pp. 1350-1354.

⁵³**Y. Murotsu, H. Okada, M. Yonezawa and K. Taguchi**, "Reliability Assessment of Redundant Structure", 3rd Intl. Conf. on Structural Safety and Reliability, 1981, pp.315-329.

⁵⁴**F. Moses and M.R. Rashedi**, "The Application of System Reliability to Structural Safety", Proc. 4th Intl. Conf. on Applications of Statistics and Probability in Soil and Structural Engineering, Vol.1, Univ. of Firenze, Italy, June 13-17, 1983, pp. 573-584.

⁵⁵**Y-T. Kam, R.B. Corotis and E.C. Rossow**, "Reliability of Non-linear Framed Structures", J. of Struct. Engg., ASCE, Vol.109, N^o 7, July 1983, pp. 1585-1601.

⁵⁶**O. Ditlevsen and P. Bjerager**, "Reliability of Highly Redundant Plastic Structures", J. of Engg. Mech., ASCE, Vol.110, N^o 5, May 1984, pp. 671-693.

⁵⁷**O. Ditlevsen and P. Bjerager**, "Methods of Structural System Reliability", Structural Safety, Vol. 3, 1986, pp.195-229.

⁵⁸**G.E. Edwards, A. Heidweiller, J. Kerstens and A. Vrouwenvelder**, "Methodologies for Limit State Reliability Analysis of Offshore Jacket Platforms", Proc. 4th Intl. Conference of Behaviour of Offshore Structures, Delft, The Netherlands, July 1-5, 1985, pp. 315-324.

⁵⁹**P. Thoft-Christiansen and J.D. Sorensen**, "Reliability Analysis of Elasto-Plastic Structures", Proc. 11th IFIP Conf. System Modelling and Optimisation, Copenhagen, Denmark, July 25-29, 1983, pp.555-565.

⁶⁰**R.E. Melchers and L.K. Tang**, "Dominant Failure Modes in Stochastic Structural Systems", Structural Safety, Vol.2, 1984, pp.127-143.

⁶¹**J-S. Lee and D. Faulkner**, "System Reliability Analysis of Structural System", Dept. of Naval Arch. and Ocean Engineering, Univ. of Glasgow, Report NAOE-88-33, May 1988.

⁶²**J-S. Lee and D. Faulkner**, "Reliability Analysis of TLP Structural Systems", 8th Intl. Symp. OMAE, The Hague, Netherlands, 1989.

⁶³**R.M. Bennett**, "Reliability Analysis of Frame Structures with Brittle Components", Structural Safety, Vol.2, 1985, pp.281-290.

⁶⁴**S.G. Stiansen and A.K. Thayamballi**, "Lessons Learnt from Structural Reliability Research and Applications in Maritime Structures", Proc. Marine Structural Reliability Symposium, The Ship Structure Committee and SNAME, Arlington, VA, Oct. 5-6, 1987, pp. 1-13.

⁶⁵**D. Faulkner, C. Guedes Soares and D.M. Warwick**, "Modelling Requirements for Structural Design and Assessment", Integrity of Offshore Structures-3, Elsevier Applied Science, 1988, 28 pp. 25-54.

⁶⁶**Y. Morutsu et al.**, "Reliability Assessment Techniques Applied to the Design of Marine Structures", Proc. 1991 OMAE - Vol.2, Safety and Reliability, 1991, pp. .

⁶⁷**J.C.P. Kam, M Birkinshaw and J.V. Sharp**, "Review of the Applications of Structural Reliability Technologies in Offshore Structural Safety", Proc. 1993 OMAE - Vol.2, Safety and Reliability, 1993, pp. 289-296.

⁶⁸**D. Faulkner, Y-N. Chen and J.G. Oliveira**, "Limit State Design Criteria for Stiffened Cylinders of Offshore Structures", ASME 4th Congress of Pressure Vessels and Piping Technology, Portland, Paper 83-OVP, June 1983.

⁶⁹**P.K. Das, P.A. Frieze and D. Faulkner**, "Structural Reliability Modelling of Stiffened Components of Floating Structures", Structural Safety, Vol. 12, Nº 1, May 1984, pp. 3-16.

⁷⁰**P.K. Das**, "The Reliability Analysis of Stiffened Cylinders using Deterministic and Stochastic Methods", Transactions of the Royal Institution of Naval Architects, Vol. 129, 1987, pp.171-187.

⁷¹**H.O. Madsen and M. Moghtaderi-Zadeh**, "Reliability of Plates under Combined Loading", Proc. Marine Structural Reliability Symposium, The Ship Structure Committee and SNAME, Arlington, VA, Oct. 5-6, 1987.

⁷²**M.A. Bonello, M.K. Chryssanthopoulos and P.J. Dowling**, "Probabilistic Strength Modelling of Unstiffened Plates Under Axial Compression", Proc. 1991 OMAE - Vol.2, Safety and Reliability, 1991.

⁷³**C. Guedes Soares**, "Uncertainty Modelling in Plate Buckling", Structural Safety, Vol.5, 1988, pp. 17-34.

⁷⁴**P. Thoft-Christiansen and M.J. Baker**, "Structural Reliability Theory and its Applications", Springer-Verlag, 1982.

⁷⁵**A.H-S. Ang and H.T. Tang**, "Probability Concepts in Engineering Planning and Design", Vol.II; Decision, Risk and Reliability, John Wiley and Sons, Inc, 1984.

⁷⁶**G. Augusti, A. Baratta and F. Casciati**, "Probabilistic Methods in Structural Engineering", Chapman & Hill, London, 1984.

⁷⁷**R.E. Melchers**, "Structural Reliability, Analysis and Prediction", Ellis Horwood Lim., Chichester, 1987.

⁷⁸**O. Ditlevsen**, "Uncertainty Modelling", Mc Graw-Hill Book Co., New York, 1982.

⁷⁹**Shasys-User's Manual**, John A. Blume Earthquake Engineering Centre, Stanford Univ., USA, 1988.

⁸⁰**Strurel-Structural Reliability Analysis, Users Manual**, RCP, Munchen, Germany, 1992.

⁸¹**Proban2- Theory Manual, Rep. N°89-2023**, A.S. Veritas Research, Norway, 1989.

⁸²**Ispud-Importance Sampling Procedure Using Design Points, Users Manual**, IFM, Innsbruck University, Austria, 1986.(Revised version 3, October 1989)

⁸³**J.P. Kenny and Partners Ltd.**, "Buckling of Offshore Structures", London, Granada, 1984.

⁸⁴**J. Odland and D. Faulkner**, "Buckling of Curved Steel Structures-Design Formulations", Integrity of Offshore Structures, ed. by D. Faulkner et al., Applied Science, 1981.

⁸⁵**G. Gerard and H. Becker**, "Handbook of Structural Stability, Part III - Buckling of Curved Plates and Shells", NACA TN 3783, 1957.

⁸⁶**E.H. Baker, L. Kovalevski and F.L. Rish**, "Structural Analysis of Shells", Mc Graw-Hill, 1972.

⁸⁷**D. Faulkner**, "A Review of Effective Plating for Use in the Analysis of Stiffened Plating in Bending and Compression", Journal of Ship Research, N^o 19, 1975, pp. 1-17.

⁸⁸**L.D. Ivanov and S.H. Rousev**, "Statistical Estimation of Reduction Coefficient of Ship's Hull Plates With Initial Deflections", The Naval Architect, N^o 4, 1979, pp.158-160.

⁸⁹**C.A. Carlsen**, "Simplified Collapse Analysis of Stiffened Plates", Norwegian Maritime Research, Vol.7, N^o 4, 1977, pp.20-36.

⁹⁰**C. Guedes Soares**, "Design Equation for the Compressive Strength of Unstiffened Plate Elements with Initial Imperfections", J. Constructional Steel Research, Vol.9, 1988, pp. 287-310.

⁹¹**C. Guedes Soares**, "A Code Requirement for the Strength of Plate Elements", Marine Structures, Vol. 1, N^o 1, 1988, pp. 71-80.

⁹²**Y. Ueda and T. Yao**, "The Influence of Complex Initial Deflection Modes on the Behaviour and Ultimate Strength of Rectangular Plates in Compression", J. Constructional Steel Research, N^o 5, 1985, pp.265-302.

⁹³**T.H. Soreide and J. Czujko**, "Load-carrying Capacity of Plates Under Combined Lateral Load and Axial/Biaxial Compression, Proc.2nd Int. Symp. on Practical Design in Shipbuilding (PRADS 83), Tokyo, 1983.

⁹⁴**S. Valsgard**, "Ultimate Capacity of Plates in Transverse Compression", Rep. 79-104, Det norske Veritas, 1979.

⁹⁵**ABS-Rules for Building and Classing Steel Vessels**, American Bureau of Shipping, USA, 1990.

⁹⁶**A.F. Dier and P.J. Dowling**, "Plates Under Combined Lateral Loading and Biaxial In-Plane Compression", Final Report for the British Ship Research Association, Imperial College, Dept. of Civil Engng., London, CESLIC Report SP8, Set. 1980.

⁹⁷**R.W.P. Stonor, C.D. Bradfield, K.E. Moxham and J.B. Dwight**, "Tests on Plates Under Biaxial Compression", Report CUED/D-Structure/TR98, Cambridge University, Engineering Department, 1983.

⁹⁸**BS 5400: Steel, Concrete and Composite Bridges**. British Standards Institution: Part 3, "Code of Practice for Design of Steel Bridge", BSI, London, 1982.

⁹⁹**Det norske Veritas (DnV-SS)**, "Rules for Classification of Steel Ships", Norway, 1988.

¹⁰⁰**D. Faulkner**, "Compression Strength of Welded Grillages", Ship Structural Design Concepts, J.M. Evans (Ed), Cornell Maritime Press, 1975, pp. 633-712.

¹⁰¹**API Bulletin 2U** - "Bulletin on Stability Design of Cylindrical Shells" (for use with RP2T), American Petroleum Institute, April 1987.

¹⁰²**Det norske Veritas (DnV-CN)**, "Buckling Strength Analysis", Classification Notes N°30.1, Norway, July 1982. (Issued for Mobile Offshore Units, June 1984)

¹⁰³**European Convention on Construction Steelwork**, European Recommendations for Steel Construction, Section 4.6, Buckling of Shells. Publication 29, Second Edition, 1983.

¹⁰⁴**C. Guedes Soares and T.H. Soreide**, "Behaviour and Design of Stiffened Plates under Predominantly Compressive Loads", International Shipbuilding Progress, Vol.30, N^o341, January 1983, pp. 13-27.

¹⁰⁵**C.S. Smith, P.C. Davidson, J.C. Chapman and P.J. Dowling**, "Strength and Stiffness of Ship's Plating under In-plane Compression and Tension", Trans RINA, Vol.130, 1988, pp.277-296.

¹⁰⁶**J. Kuzniar**, "Charakterystyki geometryczne paneli występujących w rzeczywistych konstrukcjach okretowych", Politechnika Szczecińska Report N^o 61-S, 1986.(in Polish)

¹⁰⁷**F. Ziloto et al.**, "Comparison of Different Finite Element Analysis of the Transverse Frame of a 350 000 TDW Tanker", Marine Structures, Vol. 4, 1991, pp. 231-255.

¹⁰⁸**C. Guedes Soares and M. Kmiecik**, "Simulation of the Ultimate Compressive Strength of Unstiffened Rectangular Plates", Marine Structures, Vol. 6, 1993, pp. 553-569.

¹⁰⁹**D. Faulkner**, "Discussion of the Ultimate Longitudinal Strength", Trans. Royal Institution of Naval Architects, Vol. 107, 1965.

¹¹⁰**C. Guedes Soares and D. Faulkner**, "Probabilistic Modelling of the Effect of Initial Imperfections on the Compressive Strength of Rectangular Plates", Proc. Third International Symposium on Practical Design of Ships and Mobile Units (PRADS), Vol. 2, Trondheim, June 1987, pp. 783-795.

¹¹¹**A.C. Antoniou**, "On the Maximum Deflection of Plating in Newly Built Ships", J. Ship Research, Vol. 24, 1980, pp. 31-39.

¹¹²**F. Blanc**, "Discussion to Ultimate Longitudinal Strength", Trans. RINA, Vol. 107, 1965, pp. 426-430.

¹¹³**F. Bleich**, “Buckling Strength of Metal Structures”,Mc Graw Hill Book Co., New York, 1952.

¹¹⁴**C.Guedes Soares and J.M. Gordo**, “Compressive Strength of Rectangular Plates Under Transverse Loading”, accepted for publication in the Journal of Constructional Steel Research, 1995.

¹¹⁵**C.Guedes Soares and J.M. Gordo**, “Compressive Strength of Rectangular Plates Under Biaxial Load and Lateral Pressure”, accepted for publication in the Thin Walled Structures Journal, 1995.

¹¹⁶**H. Becker et al.**, “Compressive Strength of Ship Hull Girders. Part 1 - Unstiffened Plates”,Report SSC-217, Ship Structures Committee,Washington D.C., 1970.

¹¹⁷**H. Becker**, “Instability Strength of Poliaxially-loaded Plates and Relation to Design”, Steel Plated Structures, P.J. Dowling et al.(Eds), Crosby, Lockwood and Staples, London,1977, pp. 559-580.

¹¹⁸**C.D. Bradfield and R.P. Goff**, “Compressive Tests on Steel Plates of Low Aspect Ratio”,Report CUED/C - Struct/TR48, Cambridge University, Engineering Department, 1975.

¹¹⁹**P.J. Dowling, J.E. Harding and J.E. Slatford**, “Plates in Biaxial Compression - Final Report”, CESLIC Rep.SP4, Department of Civil Engineering, Imperial College of Science and Technology, 1979.

¹²⁰**C. Smith et al.**, "Nonlinear Structural Response", Proc. of the 7th Int.Ship Structures Congress, Vol. 1, 1979, pp.II.2-1, II.2-87.

¹²¹**V Tvergaard and A. Needleman**, "Buckling of Eccentrically Stiffened Elastic-plastic Panels on two Simple Supports or Multiply Supported", *Int. Journal Solid Structures*, Vol.11, 1975, pp.647.

¹²²**T.H. Soreide, T. Moan and N.T. Nordsve**, "On the Behaviour and Design of Stiffened Plates in Ultimate Limit State", *Journal of Ship Research*, Vol. 22, N^o 4, 1978, pp. 238-244.

¹²³**W.C. Fok, A.C. Walker and J. Rhodes**, "Buckling of Locally imperfect stiffeners in plates", *Journal Engineering Mechanics Div., American Society of Civil Engineers*, (ASCE), Vol. 103, 1977, pp. 895-911.

¹²⁴**C.P. Ellinas and J.G.A. Croll**, "The basis of a design approach for stiffened plates", *Stability Problems in Engineering Structures and Components*, Applied Science Pub., London, 1979, pp. 401-422.

¹²⁵**A. Ostapenko**, "Ultimate strength design of wide stiffened plates loaded axially and normally", *Structural Analysis non-linear Behaviour and Techniques*, Supplementary Report N^o 164UC, Transport and Road Research Laboratory, England, 1974, pp. 175-180.

¹²⁶**J.B. Dwight and G.H. Little**, "Stiffened Steel Compression Flanges - A Simpler Approach", *The Structural Engineer*, Vol. 54A, 1976, pp. 501-509.

¹²⁷**M.R. Horne and R. Narayanan**, "Design of Axially Loaded Stiffened Plates", *Journal Structural Div., ASCE*, Vol. 103, 1977, pp. 2243-2257.

¹²⁸**S. Chatterjee and P.J. Dowling**, "The Design of Box Girder Compression Plates Under Combined In-plane and Lateral Loading", *Steel Plated Structures*, Crosby Lockwood Staples, London, 1977, pp. 743-763.

¹²⁹**N.W. Murray**, "Analysis and Design of Stiffened Plates for Collapse Load", *The Structural Engineer*, Vol. 53, 1975, pp. 153-158.

¹³⁰**D. Faulkner**, "Compression Tests on Welded eccentrically stiffened plate panels", Steel Plated Structures, P.J. Dowling et al. (Eds.), Crosby Lockwood Staples, London, 1977, pp.130-139.

¹³¹**M.R. Horne and R. Narayanan**, "Ultimate Capacity of Stiffened Plates Used in Girders", Proc. Inst. Civil Engrs., Vol. 61, 1976, pp. 253-280.

¹³²**M.R. Horne, P. Montague and R. Narayanan**, "Influence on Strength of Compression Panels of Stiffener Section, Spacing and Welded Connection", Proc. Inst. Civil Engrs., Vol. 63, Part 2, 1977, pp. 1-20.

¹³³**J.I. Mathewson and A.C. Vinner**, "The Strength and Stiffness of Plating Stiffened by Flat Bars - Part 1: Axial Compressive Loading Tests", ESRA, Rep.N392, 1962.

¹³⁴**C.S. Smith**, "Compressive Strength of Welded Steel Ship Grillages", Trans. RINA, Vol. 117, 1975, pp. 325-359.

¹³⁵**F. Moolani and P.J. Dowling**, "Ultimate Load Behaviour of Stiffened Plates in Compression", Steel Plated Structures, Crosby Lockwood Staples, London, 1977, pp. 51-88.

¹³⁶**C. Guedes Soares and T. Moan**, "Statistical Analysis of Still-Water Load Effects in Ship Structures", Transactions of the Society of Naval Architects and Marine Engineers, New York, Vol. 96, 1988, pp. 129-156.

¹³⁷**C. Guedes Soares and L.D. Ivanov**, "Time Dependent Reliability of the Primary Ship Structure", Reliability Engineering and System Safety, Vol. 26, 1989, pp. 59-71.

¹³⁸**C. Guedes Soares**, "Stochastic Models of Load Effects for the Primary Ship Structure", Structural Safety, Vol. 8, 1990, pp. 353-368.

¹³⁹**D. Faulkner**, "Criteria and Guidance for Good Strength Models", Department of Naval Architecture and Ocean Engineering, Report NAOE-91-15, University of Glasgow, July 1991.

¹⁴⁰**D.M. Warwick and D. Faulkner**, "Economic Structures from Improved Design Code Strength Modelling", 4th Intl. Colloquium on Stability of Metal Structures, Code Differences Around the World, SSRC, New York, April 1989, 13 pp..

¹⁴¹**P.K. Das, D. Faulkner and A.G. Silva**, "Limit State Formulations and Modelling for Reliability-based Analysis of Orthogonally Stiffened Cylindrical Shell Structural Components", Dept. of Naval Architecture and Ocean Engineering Report NAOE-91-26, University of Glasgow, August 1991.

¹⁴²**D.M. Warwick and D. Faulkner**, "Strength of Tubular Members in Offshore Structures", Dept. of Naval Architecture and Ocean Engineering Report NAOE-88-36, University of Glasgow, June 1988.

¹⁴³**ASME - Boiler and Pressure Vessel Code-Nuclear Components-Section III, Code Case N-284**, American Society Mechanical Engineers, New York, 1980.

¹⁴⁴**Buckling of Offshore Structures: Stringer-Stiffened and Orthogonally-Stiffened Cylinders**, Background report N^oIII, OT/0/8313, Department of Energy [UK.], London 1983.

¹⁴⁵**Buckling of Offshore Structures: Data Volume**, OT/0/8321, Department of Energy-UK, London 1983.

¹⁴⁶**P.A. Frieze**, "Lessons Learnt from Reliability Analysis Studies of Offshore Platforms", Wimpey Offshore Engineers and Constructors Report, 1986.

¹⁴⁷**AISI-Cold-Formed Steel Design**, American Iron and Steel Institute Edition, 1983.

¹⁴⁸**S.P. Timoshenko and J.M. Gere**, "Theory of Elastic Stability", 2nd Edition, Mc Graw Hill, New York, 1961.

¹⁴⁹**W.T. Koiter**, "Buckling and post-buckling of a cylindrical panel under compression". Trans. Nat. Aero. Res. Inst. Amsterdam, Vol. 20, N^o 71, 1956.

¹⁵⁰**B.G. Johnston ed.**, "Guide to the Stability Design Criteria for Metal Structures", 3rd Edition, Wiley, 1976.

¹⁵¹**D. Faulkner**, "Effects of Residual Stresses on the Ductile Strength of Plane Welded Grillages and of Ring stiffened Cylinders", Jnl. Strain Analysis, Vol. 12, April 1977, pp. 130-139.

¹⁵²**J.G. Oliveira**, "Design code formulations for ring/stringer stiffened cylinders". Report N^o M-29-83. Conoco Inc., Houston, 1983.

¹⁵³**C.D. Miller, R.B. Grove and I.F. Vojta**, "Design of Stiffened Cylinders for Offshore Structures", Welded Offshore Structures Conference, American Welding Society, New Orleans, Louisiana, December 1983.

¹⁵⁴**C.D. Miller and R.B. Grove**, "Current Research Related to Buckling of Shells for Offshore Structures", Paper OTC 4474, Offshore Technology Conference, May 1983, pp. 277-283.

¹⁵⁵**M.J. Stephens, G. Kulak and C.J. Montgomery**, "Local Buckling of Thin-Walled Tubular Steel Members", Proceedings of Third International Colloquium on Stability of Metal Structures, Toronto, Canada, SSRC, May 1983, pp. 489-508.

¹⁵⁶**D.R. Sherman**, "Flexural Tests of Fabricated Pipe Beams", Proceedings of Third International Colloquium on Stability of Metal Structures, Toronto, Canada, SSRC, May 1983.

¹⁵⁷**J. Odland**, "Buckling of unstiffened and stiffened circular cylindrical shell structures", Norwegian Maritime Research, Vol. 6, № 3, 1978.

¹⁵⁸**D. Faulkner**, "Inelastic Interactive (Shell) Buckling". ABS-Conoco RCC Note, 13 September 1983.

¹⁵⁹**R. Milligan et al.**, "General Instability of Orthotropically Stiffened Cylinders; Part I - Axial Compression, Torsion and Hydrostatic Pressure Loading", Air Force Flight Dynamics Labs, AFF DL-TR-65-191, Part I, 1965.

¹⁶⁰**L. Katz**, "Compression Tests on Integrally Stiffened Cylinders", NASA TMX-55315, Aug 1965.

¹⁶¹**T. Weller, J. Singer and S. Nachmani**, "Recent Experimental Studies on the Buckling of Stringer-stiffened Cylindrical Shells", TAE Report 100, Technion-Israel Institute of Technology, Department of Aeronautical Engineering, Haifa, Israel, 1970.

¹⁶²**T. Weller and J. Singer**, "Experimental Studies on the Buckling of 7075-T6 Aluminium Alloy Integrally Stringer-stiffened Shells", TAE Report 135, Technion Research and Development Foundation, Haifa, Israel, 1971.

¹⁶³**A. Rosen and J. Singer**, "Further Experimental Studies on the Buckling of Integrally Stiffened Cylindrical Shells", TAE Report 207, Technion-Israel Institute of Technology, Department of Aeronautical Engineering, Haifa, Israel, 1974.

¹⁶⁴**J. Singer and H. Abramovich**, "The Influence of Practical Boundary Conditions on the Vibrations and Buckling of Stiffened Cylindrical Shells", TAE Report 288, March 1978.

¹⁶⁵**H. Abramovich and J. Singer**, "Correlation Between Vibration and Buckling of Stiffened Cylindrical Shells under External Pressure and Combined Loading", Israel Journal of Technology, №16, 1978, pp. 34-44.

¹⁶⁶**J. Singer and H. Abramovich**, "Vibration Techniques for Definition of Practical Boundary Condition in Stiffened Shells", AIAA Journal, №17, pp. 762-769, 1979.

¹⁶⁷**H. Abramovich, J. Singer and A. Grunwald**, "Non-destructive Determination of Interaction Curves for Buckling of Stiffened Shells", TAE Report 341, Technion-Israel Institute of Technology, Department of Aeronautical Engineering, Haifa, Israel, December 1981.

¹⁶⁸**T. Weller, J. Singer and D. Koss**, "Further Vibration Correlation Studies on Stiffened Shells with Practical Boundary Conditions", TAE Report 499, Technion-Israel Institute of Technology, Department of Aeronautical Engineering, Haifa, Israel, April 1987.

¹⁶⁹**T. Weller, H. Abramovich and J. Singer**, "Correlation Between Vibrations and Buckling of Cylindrical Shells Stiffened by SPOT-Welded and Riveted Stringers", TAE Report 537, Technion-Israel Institute of Technology, Department of Aeronautical Engineering, Haifa, Israel, January 1988.

¹⁷⁰**S. Sridharan and A.C. Walker**, "Experimental Investigation of the Buckling Behaviour of Stiffened Cylindrical Shells", Dept. of Energy U.K., Report OT-R7835, London, 1980.

¹⁷¹**A.C. Walker and P. Davies**, "The Collapse of Stiffened Cylinders", Int. Conference on Steel Plated Structures", Paper 33, Ed. P.J. Dowling et al.-Crosby Lockwood Staples, 1977, pp.791-808.

¹⁷²**P.J. Dowling and J.E. Harding**, "Experimental Behaviour of Ring and Stringer Stiffened Shells", Buckling of Shells in Offshore Structures, Ed. J.E. Harding et al.-Granada, London, 1982, pp.73-107.

¹⁷³**S. McCall and A.C. Walker**, "Buckling Tests on Stringer-Stiffened Cylinders Models Subject to Load combinations", Det norske Veritas, Rep. 82-0299, 1982.

¹⁷⁴**N. Algelidis**, "Collapse of Stringer Stiffened Cylinders", Phd Thesis, University of London, 1984.

¹⁷⁵**D.R. Green and H.M. Nelson**, "Compression Tests on Large Scale, Stringer Stiffened Tubes", Buckling of Shells in Offshore Structures, Ed. J.E. Harding et al.-Granada, London, 1982, pp.491-548.

¹⁷⁶**Y. Chen, R.A. Zimmer, J.G. de Oliveira and H.Y. Jan**, "Buckling and Ultimate Strength of Stiffened Cylinders: Model Experiments and Strength Formulations", Proc. Offshore Technology Conference OTC, Vol.1, May 1985, pp. 113-124.

¹⁷⁷**S. Valsgard and G. Foss**, "Buckling Research in Det norske Veritas", Buckling of Shells in Offshore Structures, Ed. J.E. Harding et al.-Granada, London, 1982, pp.491-548.

¹⁷⁸**R.K. Kinra**, "Hydrostatic and Axial Collapse Tests Of Stiffened Cylinders", OTC, 1976, Paper N^o 2685.

¹⁷⁹**C. Guedes Soares and T. Moan**, "On the Uncertainties Related to the Extreme Hydrodynamic Loading of a Cylindrical Pile", Reliability Theory and Its Application in Structural and Soil Mechanics", Ed. Thoft-Christensen, Martinus Nijhoff Publ., The Hague, 1983, pp. 351-364.

¹⁸⁰**J.W. Hutchinson and W.T. Koiter**, "Post-buckling Theory", Applied Mechanics Reviews, Vol. 23, 1971, pp 1353-1362.

¹⁸¹**Engineering Science Data Unit**, London, Structures Data Sheet, Issue 1, ESDU 83034, "Elastic Load Buckling Stresses of Thin-Walled Unstiffened Circular Cylinders Under Combined Axial Compression and Internal Pressure", December 1983.

¹⁸²**J. Odland**, "On the strength of Welded Ring-stiffened Cylindrical Shells Primarily Subjected to Axial Compression", NIT Report, Trondheim, 1981.

¹⁸³**D. Faulkner**, "Effects of Residual Stresses on the Ductile Strength of Plane Welded Grillages and Ring Stiffened Cylinders", Jnl. Strain Analysis, Vol 12, n°2, April 1977, pp 130-139.

¹⁸⁴**C. Guedes Soares**, "Design Equation for Ship Plate Elements Under Compression", J. Constructional Steel Research, Vol.22, 1992, pp. 99-114.

¹⁸⁵**N.C. Lind**, "Reliability Based Structural Codes Practical Calibration", in Safety of Structures under Dynamic Loading, D. Kavlie et al. (Eds.), Tapir Pub., Trondheim, Norway, 1978, pp. 149-160.

¹⁸⁶**C. Guedes Soares**, "Metodos Probabilisticos para la Quantification de la Seguridad en los Reglamentos de Estructuras Navales", Ingenieria Naval, Vol. , N° 645, 1989, pp. 109-118.

¹⁸⁷**Rule Case Committee paper**: "Tripping Formulations and Design", RCC(c) 09/DF, American Bureau of Shipping, 12 July 1982.

¹⁸⁸**Det norske Veritas (DnV-OS)**, "Rules for the Design, Construction and Inspection of Offshore Structures - Appendix C: Steel Structures", Hovik, Norway 1977.

¹⁸⁹**Rule Case Committee paper**: "Stringer Stiffened Cylinders - Provisional Strength Formulations", RCC(c) 12/DF, American Bureau of Shipping, 12 August 1982.

¹⁹⁰**Strength of Metal Structures**, Ed. for the Structural Stability Research Council, FEL, Leigh, 1991.

¹⁹¹**D. Faulkner**, “Toward a Better Understanding of Compression Induced Stiffener Tripping”, Intl. Conf. Steel and Aluminium Structures, Vol.3, Cardiff, Elsevier Applied Science Publishers, July 1987, pp.159-175.

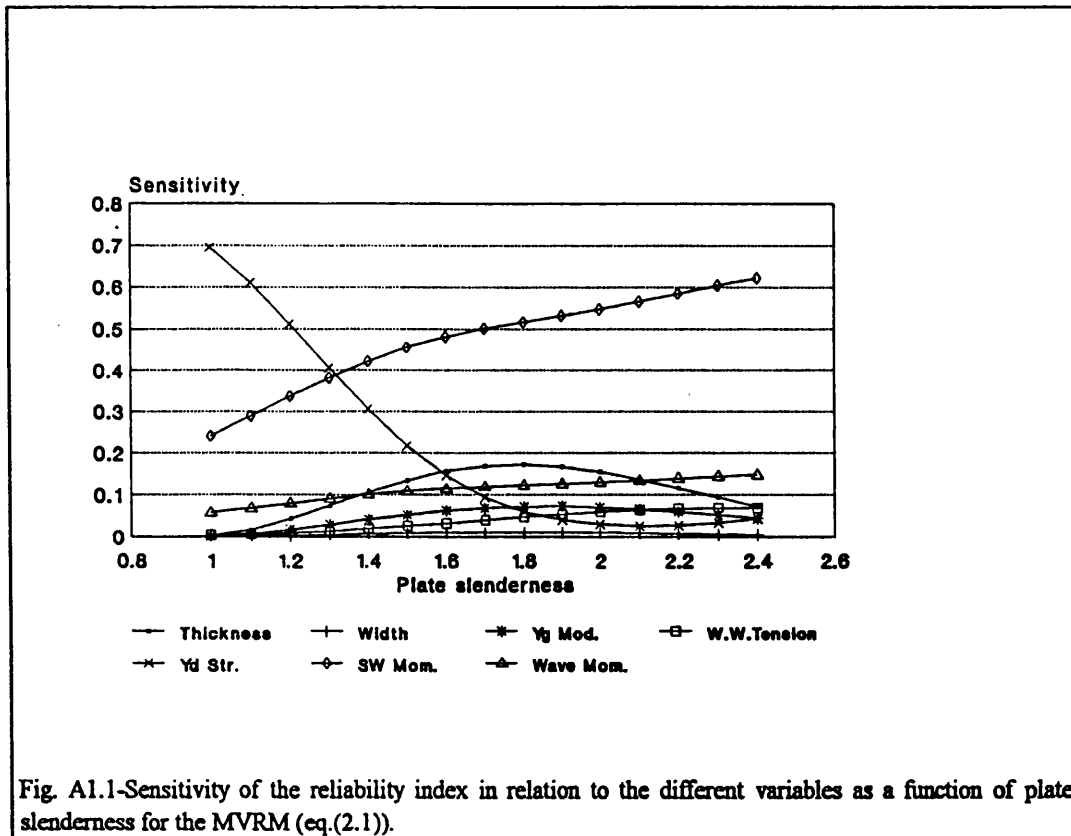
¹⁹²**D. Faulkner**, “Application of Reliability Theory in Submarine Design”, in Advances in Marine Structures - 2, Elsevier Applied Science Publishers, 1991, pp.566-595.

¹⁹³**D. Faulkner and P. K. Das**, “Application of Reliability Theory to Structural Design and Assessment of Submarines and Other Externally Pressurised Cylindrical Structures”, Integrity of Offshore Structures - 4, Elsevier Applied Science Publishers, 1990, pp.199-230.

APPENDIX 1 - PLATES RELIABILITY ANALYSIS - GRAPHICAL OUTPUT.

1 - Unstiffened plates.

The results of the reliability analyses for the various load cases were plotted in graphs showing, for the different formulations, the variation of the safety index (β_f) with the unstiffened plate slenderness. The relative importance of the variables is presented in sensitivity plots.



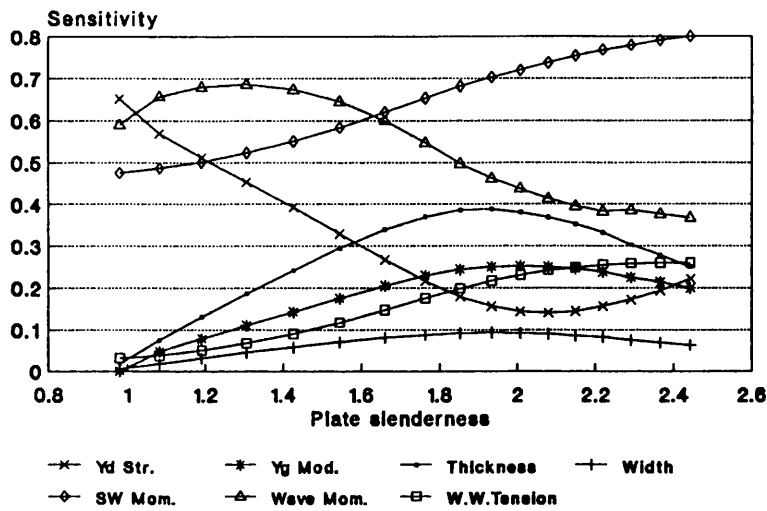


Fig. A1.2-Sensitivity of the reliability index in relation to the different variables as a function of plate slenderness for the FORM (eq.(2.1)).

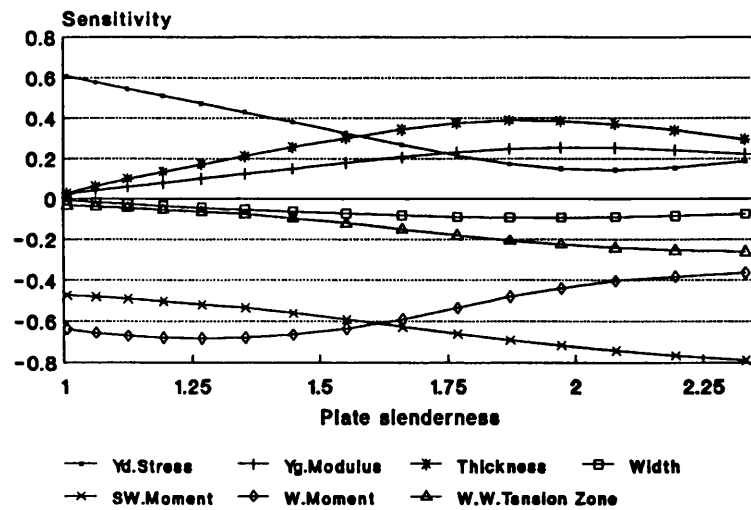


Fig. A1.3-Sensitivity of (β_r) in relation to different variables as a function of plate slenderness (β) for the method of Faulkner without modelling uncertainty (eqs. (2.1)-(2.7)).

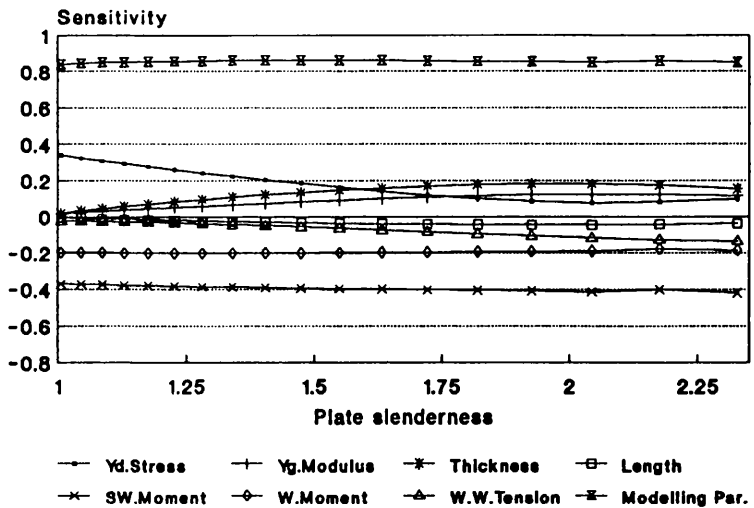


Fig. A1.4-Sensitivity of (β_r) in relation to different variables as a function of plate slenderness (β) for the method of Faulkner with uncertainty double than real (COV=22%)(eqs. (2.1)-(2.7)).

1.1. - Longitudinal compression.

The variation of the safety index (β_r) with the plate slenderness for simply supported plates with initial distortions and residual stresses is shown in figure (2.7) for the different formulations. The respective sensitivity plots are shown in figures ((2.8)-(2.9) and (A1.5)-(A1.8)).

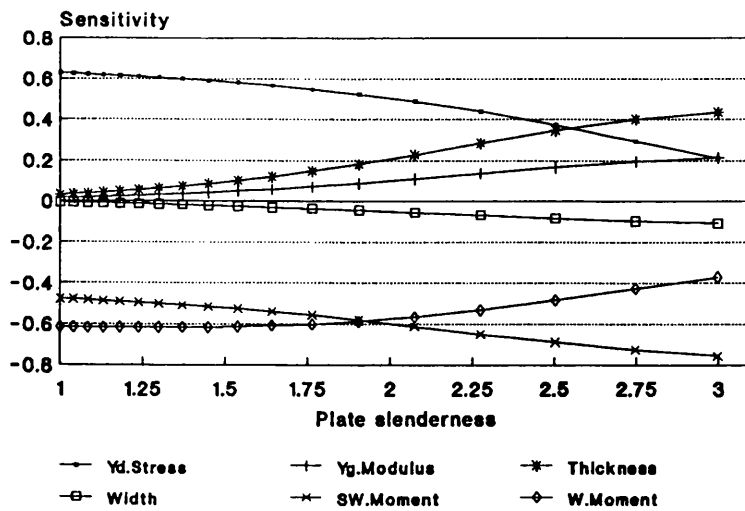


Fig. A1.5-Sensitivity of (β_r) in relation to different variables as a function of plate slenderness (β) for the method of Ivanov and Rousev (eq.(2.9)).

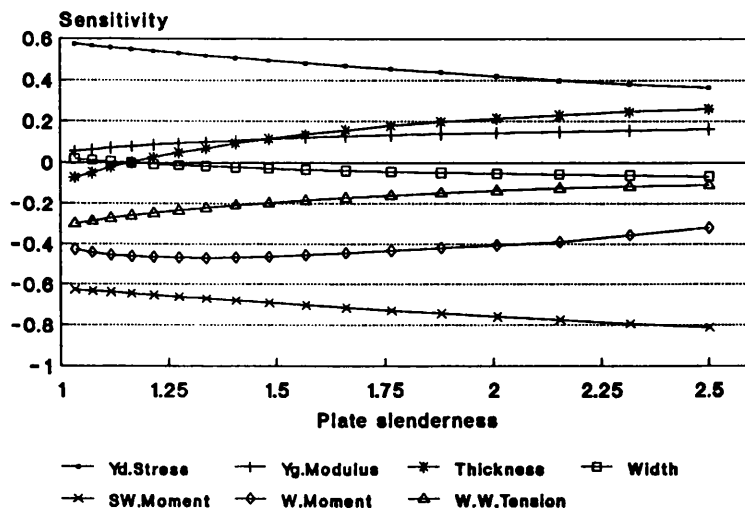


Fig. A1.6-Sensitivity of (β_r) in relation to different variables as a function of plate slenderness (β) for the method of Carlsen (eq. (2.10)).

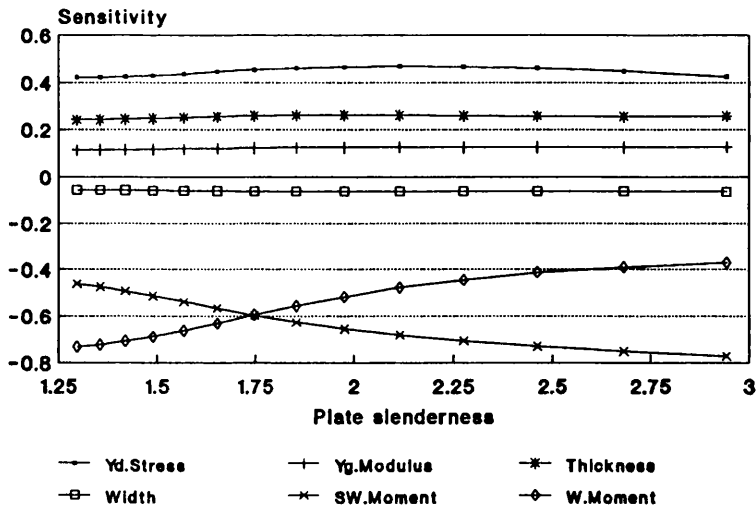


Fig. A1.7-Sensitivity of (β_I) in relation to different variables as a function of plate slenderness (β) for the method of Ueda and Yao (eq.(2.14)).

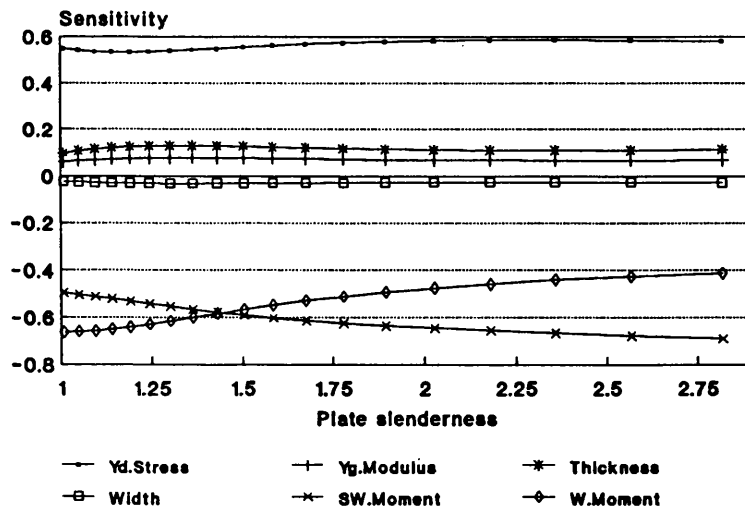
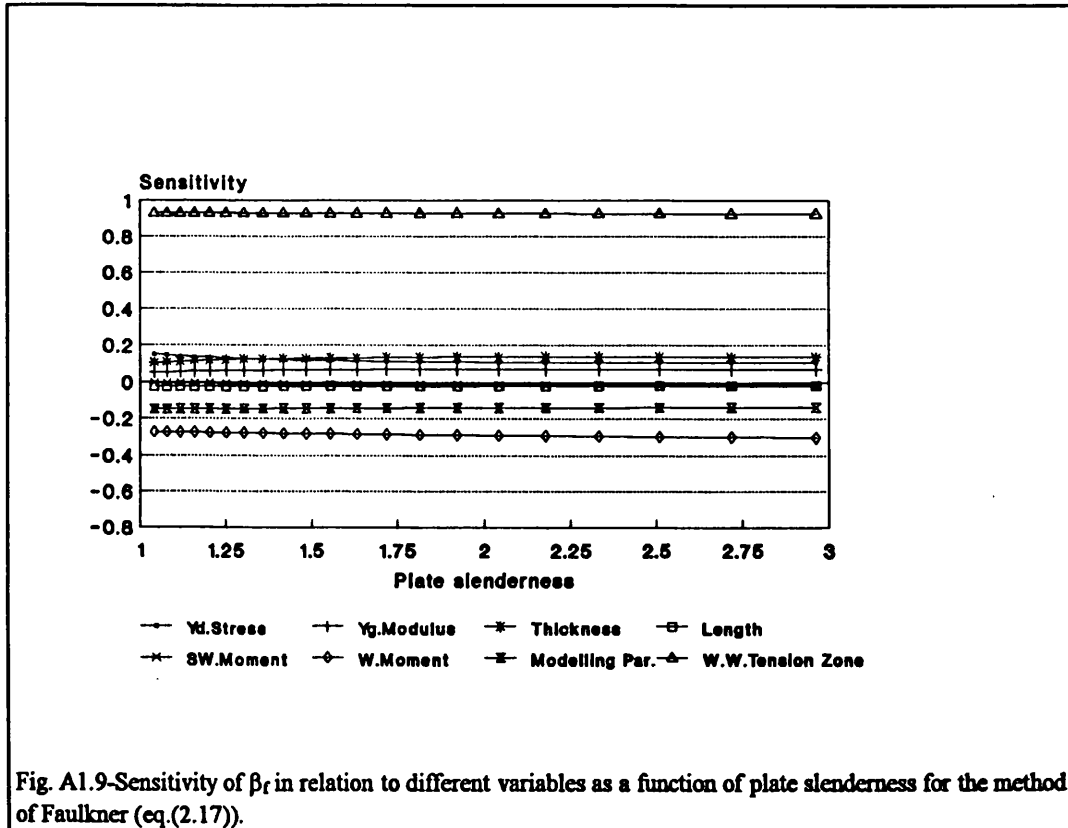
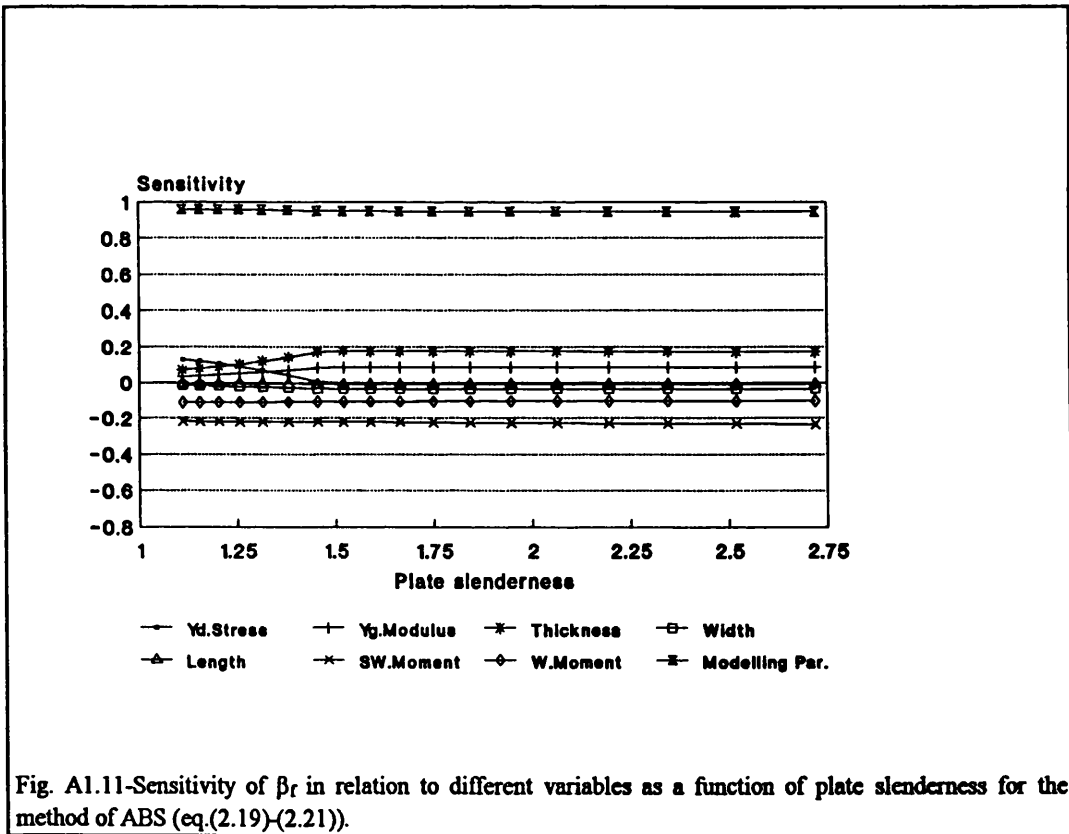
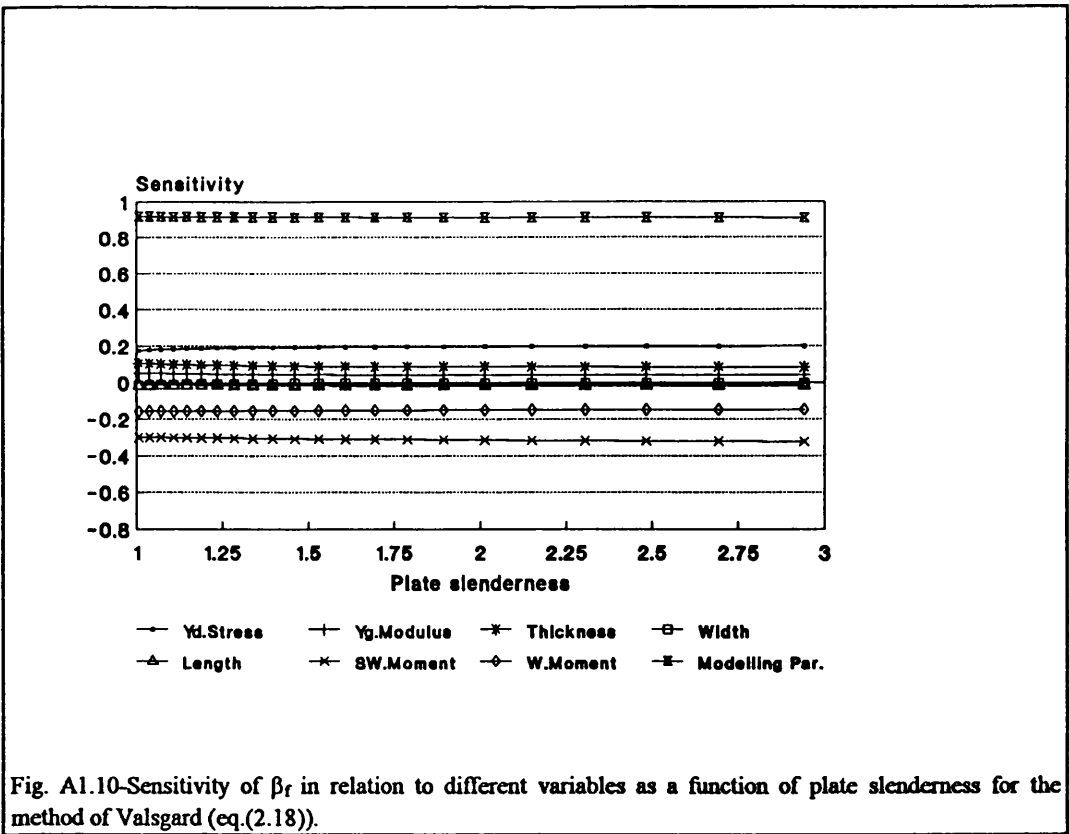


Fig. A1.8-Sensitivity of (β_I) in relation to different variables as a function of plate slenderness (β) for the method of Soreide et al. (eqs. (2.15)-(2.16)).

1.2. - Transverse compression.

The variation of the safety index (β_r) with the plate slenderness for simply supported plates is shown in figure (2.10) and (A1.12) for the different formulations. The sensitivity plots for plate slenderness are shown in figures ((A1.9)-(A1.11)).





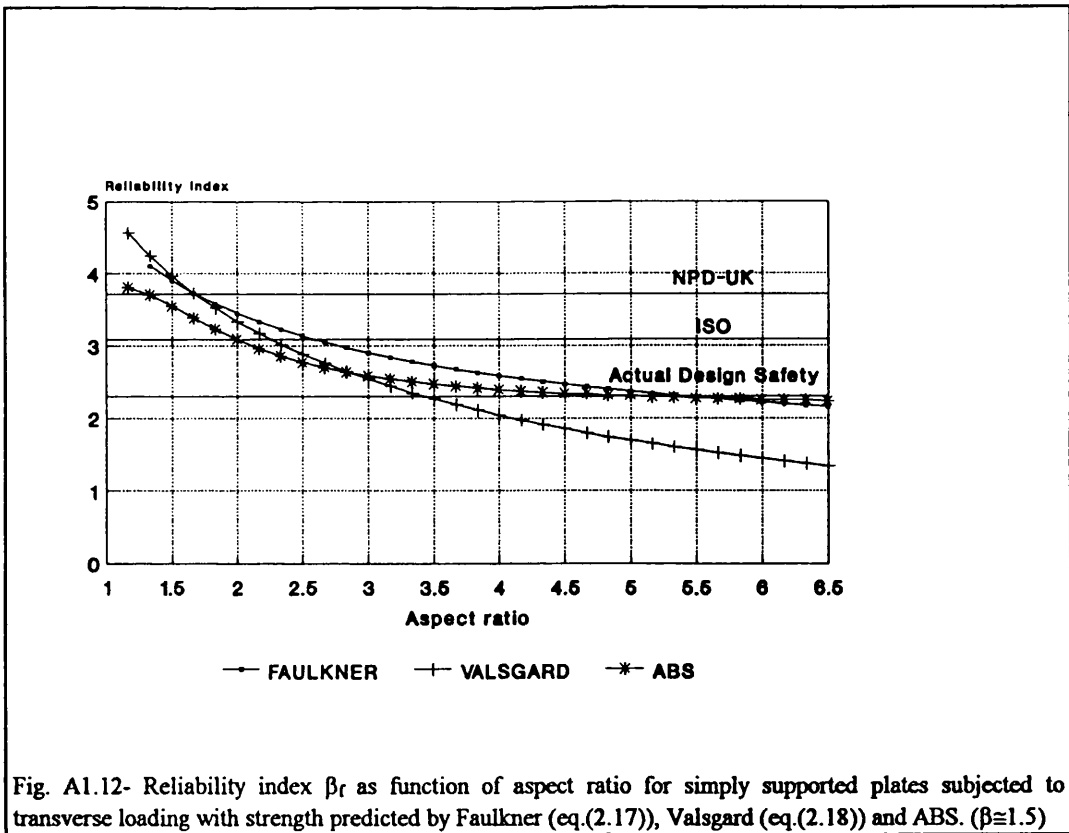


Fig. A1.12- Reliability index β_r as function of aspect ratio for simply supported plates subjected to transverse loading with strength predicted by Faulkner (eq.(2.17)), Valsgard (eq.(2.18)) and ABS. ($\beta \cong 1.5$)

1.3. - Biaxial compression.

The variation of the safety index (β_r) with the plate slenderness for simply supported plates with initial distortions is shown in figure (2.11) for the different formulations. The sensitivity plot for Faulkner formulation is shown in figure (A1.14). The variation with the load ratio is shown in figure (A1.13).

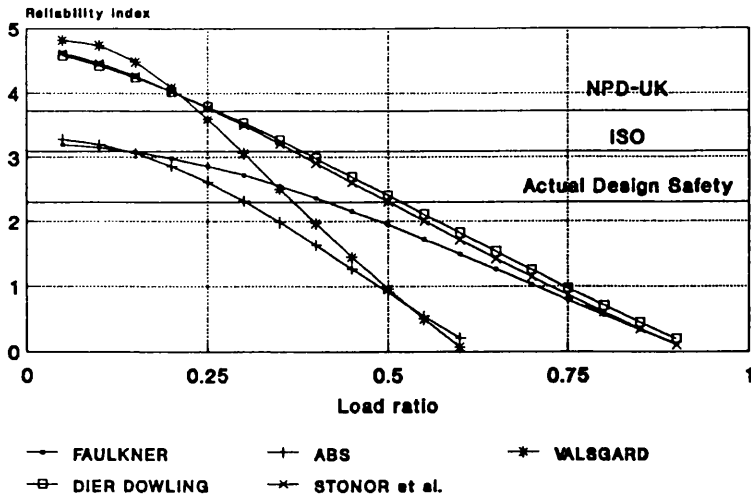


Fig. A1.13-Reliability index β as function of the ratio of the transverse to longitudinal load for simple supported plate with initial distortions with strength predicted by different methods.

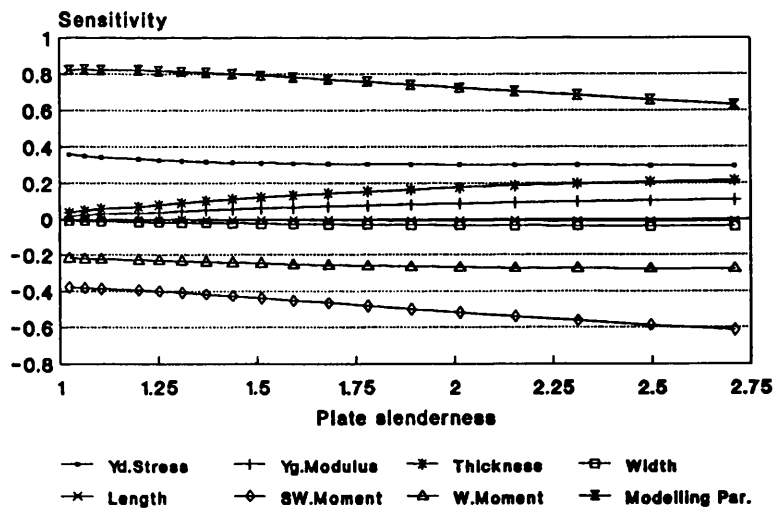


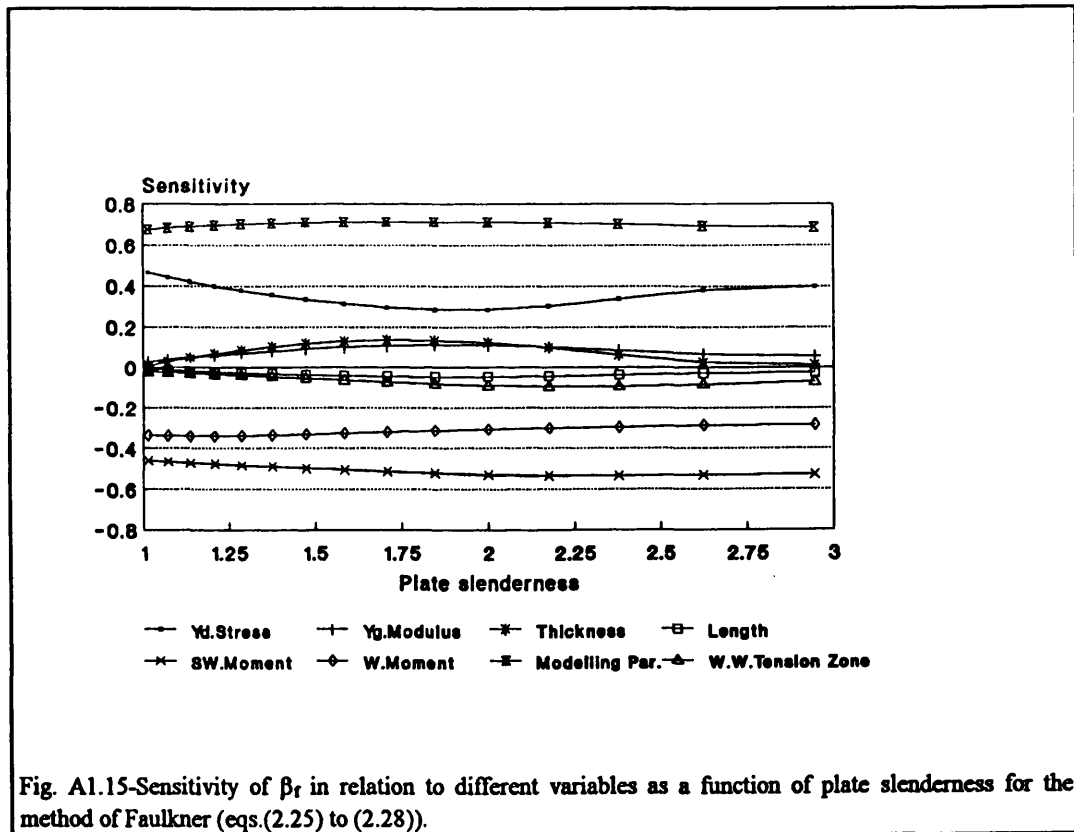
Fig. A1.14-Sensitivity of β_r in relation to different variables as a function of plate slenderness for the method of Faulkner (eqs.(2.1), (2.17) and (2.22)).

2 - Stiffened plates.

The results of the reliability analyses for the longitudinal compression cases were plotted in graphs showing, for the different formulations, the variation of the safety index (β_r) with the plate slenderness. The relative importance of the variables is presented in sensitivity plots.

2.1. - Longitudinal compression.

The variation of the safety index (β_r) with the plate slenderness is shown in figure (2.12) for the different formulations. The respective sensitivity plots are shown in figures ((A1.15)-(A1.17)).



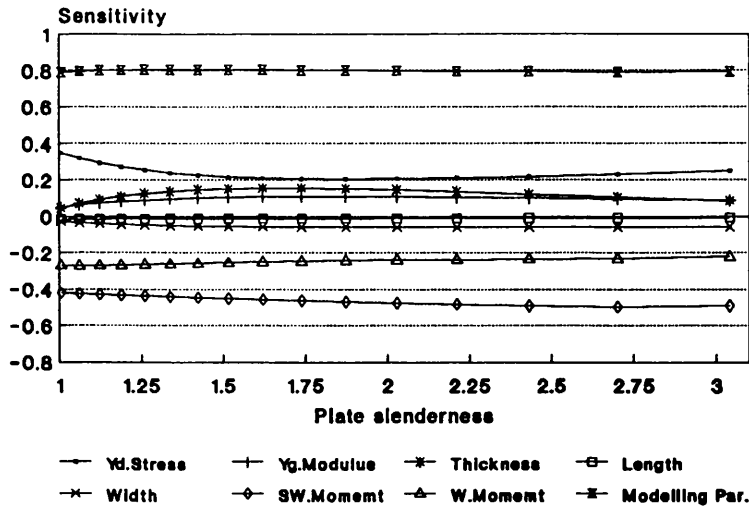


Fig. A1.16-Sensitivity of β_r in relation to different variables as a function of the plate slenderness for the method of Carlsen-plate induced interframe buckling (eq.(2.30) and (2.31a)).

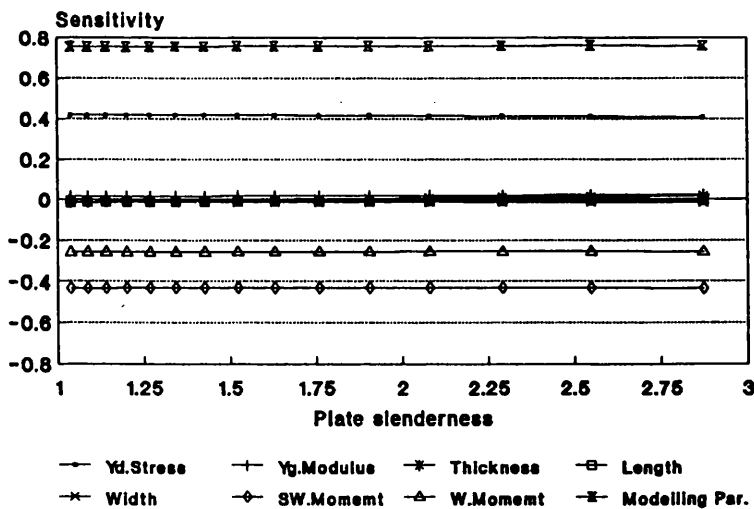


Fig. A1.17-Sensitivity of β_r in relation to different variables as a function of the plate slenderness for the method of Carlsen-stiffener induced interframe buckling (eq.(2.30) and (2.31b)).

APPENDIX 2 - CYLINDERS UNCERTAINTY MODELLING - TABLES

1 - Aerospace experimental data.

The collected Aerospace experimental data can be subdivided into two major groups. The first one has test specimens made of high strength steel alloys and the second one contains specimens made of aluminium alloy. These tests were mainly conducted in the elastic range. In these test specimens a large number of stringers were used, which implies a close space between them. They were machined finished, which means minimal distortions and residual stresses.

From the aerospace data 193 axial compression test specimens have been used in the study; 84 steel and 109 aluminium (Tables A2.1-A2.2). Further test results were collected but not used; 27 axial compression test specimens, 9 radial pressure and 20 combined axial and radial pressure. The details of these test specimens are shown in Table A2.3.

Table A2.4 shows the X_m and the associated buckling modes ($m*n$) for some of the 84 aerospace steel specimens using orthotropic theory. These specimens were chosen in which the buckling modes were obvious from the test results.

2 - Offshore finite element data.

The experimental work at Imperial College lead to the development of a non-linear finite element analysis tool suitable for stiffened shell structures. The resulting FE package was used to systematically reproduce numerical test behaviour. This test data is grouped into two classes (elastic and elastoplastic buckling) and are presented in Tables A2.5-A2.6.

Model	Mat.	Tk	Ns	Rad	L	dw	tw	E	SigY	Sigu
AB1	alu.	0.257	85	120.	110.4	1.779	0.9	73.6	594.0	139.32
AB2	alu.	0.253	85	120.1	110.5	1.757	0.9	73.6	594.0	147.42
AB3	alu.	0.253	85	120.1	153.8	1.747	0.9	73.6	594.0	102.60
AB4	alu.	0.253	85	120.1	153.8	1.742	0.9	73.6	594.0	109.08
AB5	alu.	0.252	85	120.2	129.8	1.700	0.8	73.6	594.0	114.48
AB6	alu.	0.254	85	120.1	129.7	1.484	0.9	73.6	594.0	129.06
RO-3	alu.	0.253	84	120.1	237.9	1.242	0.97	73.6	594.0	90.18
RO-4	alu.	0.241	84	120.0	236.4	0.572	1.0	73.6	594.0	85.32
RO-5	alu.	0.254	84	120.1	237.8	1.260	1.0	73.6	594.0	96.66
RO-9	alu.	0.236	84	120.1	150.1	0.484	0.9	73.6	594.0	74.52
RO-15	alu.	0.242	84	120.0	150.0	0.503	0.9	73.6	594.0	87.48
RO-16	alu.	0.239	84	120.2	150.2	1.053	0.95	73.6	594.0	115.02
RO-17	alu.	0.247	84	120.0	180.0	0.497	0.9	73.6	594.0	85.32
RO-18	alu.	0.243	84	120.0	180.0	0.980	0.9	73.6	594.0	116.1
RO-19	alu.	0.242	84	120.0	150.0	1.002	0.9	73.6	594.0	113.94
RO-20	alu.	0.240	84	120.0	150.0	0.504	0.9	73.6	594.0	85.86
RO-25	alu.	0.253	84	120.1	129.7	1.504	0.9	73.6	594.0	118.8
RO-26	alu.	0.251	84	120.2	129.8	1.487	0.9	73.6	594.0	64.26
RO-27	alu.	0.254	84	120.1	129.7	1.479	0.9	73.6	594.0	80.46
RO-28	alu.	0.254	84	120.1	129.7	0.979	0.9	73.6	594.0	108.54
RO-29	alu.	0.255	84	120.1	129.7	0.973	0.9	73.6	594.0	63.72
RO-30	alu.	0.259	84	119.9	129.5	0.98	0.9	73.6	594.0	76.14
RO-31	alu.	0.249	84	120.	214.8	1.655	0.75	73.6	594.0	136.08
RO-32	alu.	0.257	84	120.0	120.0	1.983	0.9	73.6	594.0	133.92
RO-33	alu.	0.251	84	120.2	170.7	1.745	0.9	73.6	594.0	130.68
RO-34	alu.	0.245	84	120.0	170.4	1.748	0.9	73.6	594.0	130.14
RO-41	alu.	0.244	84	120.0	120.0	1.749	0.9	73.6	594.0	144.18
RO-42	alu.	0.247	84	120.	120.0	1.739	0.9	73.6	594.0	149.58
RO-43	alu.	0.234	84	120.0	150.0	0.53	0.9	73.6	594.0	79.92
RO-44	alu.	0.231	84	120.1	150.1	1.03	0.9	73.6	594.0	116.64
RO-45	alu.	0.237	84	120.1	150.1	0.528	0.9	73.6	594.0	90.18
RO-46	alu.	0.234	84	120.	150.0	1.029	0.9	73.6	594.0	106.92
AS-2	alu.	0.197	80	101.8	140.5	0.48	1.667	70.0	264.0	77.52
AS-3	alu.	0.281	80	101.7	140.3	0.444	1.678	70.0	264.0	95.04
AS-4	alu.	0.259	80	101.5	140.1	0.295	1.651	70.0	264.0	84.00
AS-1S	alu.	0.229	84	120.6	60.34	0.756	1.06	73.6	594.0	82.08
AS-1L	alu.	0.241	84	120.5	181.9	0.75	1.06	73.6	594.0	89.64
AS-2L	alu.	0.24	84	120.7	230.5	0.747	1.06	73.6	594.0	79.92
AS-3L	alu.	0.256	84	120.5	346.0	0.764	1.06	73.6	594.0	90.18
AS-4S	alu.	0.258	83	120.4	60.24	1.239	1.06	73.6	594.0	167.4
AS-4L	alu.	0.254	83	120.6	177.3	1.249	1.06	73.6	594.0	104.76
AS-5L	alu.	0.246	83	120.5	248.3	1.26	1.06	73.6	594.0	105.84
AS-6L	alu.	0.265	83	120.5	314.7	1.269	1.06	73.6	594.0	92.34
AS-7S	alu.	0.261	68	120.5	60.3	0.698	1.19	73.6	594.0	80.46
AS-7L	alu.	0.256	68	120.5	182.0	0.729	1.189	73.6	594.0	101.52
AS-8L	alu.	0.248	68	120.5	247.0	0.741	1.189	73.6	594.0	100.44
AS-9L	alu.	0.261	68	120.5	344.8	0.748	1.19	73.6	594.0	85.86

Table A2.1 - Aluminium test specimens of aerospace test programmes.

Model	Mat.	Tk	Ns	Rad	L	dw	tw	E	SigY	Sigu
5A-1	alu.	0.953	68	661.3	1408.0	5.397	2.698	72.4	275.0	39.75
5A-2	alu.	0.953	68	661.3	1408.0	5.397	2.698	72.4	275.0	37.5
5B-1	alu.	0.953	95	659.4	1404.0	5.397	2.698	72.4	275.0	36.00
5B-2	alu.	0.953	95	659.4	1404.0	5.397	2.698	72.4	275.0	34.75
10L	alu.	0.25	68	120.5	347.0	1.279	1.22	73.6	594.0	97.74
11S	alu.	0.262	68	120.5	61.5	1.229	1.219	73.6	594.0	154.98
11L	alu.	0.256	68	120.5	182.0	1.25	1.22	73.6	594.0	110.16
12L	alu.	0.248	68	120.5	243.4	1.25	1.219	73.6	594.0	109.62
13M	alu.	0.24	68	120.7	123.1	1.269	1.219	73.6	594.0	119.88
14M	alu.	0.244	68	120.5	114.5	1.25	1.21	73.6	594.0	111.78
15S	alu.	0.244	56	120.5	61.5	0.758	1.589	73.6	594.0	92.34
15L	alu.	0.238	56	120.6	179.7	0.774	1.59	73.6	594.0	98.28
16MA	alu.	0.228	56	120.6	90.45	1.239	1.609	73.6	594.0	99.9
16MB	alu.	0.239	56	120.6	91.7	1.229	1.619	73.6	594.0	103.68
17MA	alu.	0.236	83	120.5	90.44	1.27	1.08	73.6	594.0	82.08
17MB	alu.	0.237	83	120.6	89.26	1.279	1.08	73.6	594.0	73.44
18MA	alu.	0.235	83	120.5	121.7	1.53	1.09	73.6	594.0	115.02
18MB	alu.	0.239	83	120.6	121.9	1.53	1.09	73.6	594.0	103.68
19MA	alu.	0.257	68	120.5	121.7	1.47	1.219	73.6	594.0	73.98
19MB	alu.	0.24	68	120.7	121.9	1.49	1.22	73.6	594.0	109.62
20MA	alu.	0.223	56	120.6	120.6	1.52	1.629	73.6	594.0	125.82
21S	alu.	0.236	56	120.5	61.5	1.27	1.62	73.6	594.0	95.12
21L	alu.	0.24	56	120.7	179.8	1.26	1.62	73.6	594.0	157.14
22L	alu.	0.231	56	120.5	244.7	1.279	1.62	73.6	594.0	103.68
23L	alu.	0.236	56	120.5	247.2	0.742	1.59	73.6	594.0	61.02
21L	alu.	0.24	56	120.7	179.8	1.26	1.62	73.6	594.0	103.68
24S	alu.	0.218	56	120.5	57.86	0.774	1.59	73.6	594.0	79.92
24L	alu.	0.227	56	120.5	300.1	0.764	1.589	73.6	594.0	55.08
25S	alu.	0.218	56	120.5	71.1	1.279	1.619	73.6	594.0	120.42
25L	alu.	0.215	56	120.6	301.5	1.279	1.62	73.6	594.0	78.3
26M1	alu.	0.23	84	120.5	71.1	1.265	1.072	73.6	594.0	92.34
26M2	alu.	0.24	84	120.7	85.7	1.242	1.073	73.6	594.0	96.66
26M3	alu.	0.235	84	120.5	84.4	1.25	1.073	73.6	594.0	77.76
27M1	alu.	0.195	56	120.5	78.3	1.31	1.53	73.6	594.0	136.08
27M2	alu.	0.204	56	120.5	78.4	1.293	1.531	73.6	594.0	122.04
27M3	alu.	0.202	56	120.5	78.4	1.301	1.53	73.6	594.0	145.26
34	alu.	0.254	84	119.8	129.4	1.254	0.967	73.6	594.0	93.42
35	alu.	0.25	84	120.0	129.6	1.269	0.97	73.6	594.0	95.58
DUD-2	alu.	0.253	84	120.1	200.0	1.779	0.8	73.6	594.0	120.96
DUD-3	alu.	0.23	84	120.1	150.0	1.01	0.85	73.6	594.0	75.6
DUD-4	alu.	0.229	84	120.1	200.0	1.771	0.83	73.6	594.0	81.0
DUD-6	alu.	0.243	84	120.1	200.0	1.751	0.83	73.6	594.0	75.06
DUD-7	alu.	0.246	84	120.1	200.0	1.756	0.83	73.6	594.0	91.8
KR-1	alu.	0.254	84	120.1	200.0	1.493	0.89	73.6	594.0	115.56
KR-5	alu.	0.26	84	120.1	200.0	1.47	0.89	73.6	594.0	95.12
KR-6	alu.	0.261	84	120.1	200.0	1.468	0.89	73.6	594.0	88.02
MGL-13	alu.	0.267	200	96.65	50.28	0.172	1.525	70.0	264.0	94.40
MGL-14	alu.	0.264	200	96.62	50.24	0.187	1.523	70.0	264.0	101.28
MGL-15	alu.	0.305	200	96.38	51.08	0.106	1.525	70.0	264.0	112.56
MGL-16	alu.	0.338	200	96.66	52.20	0.094	1.524	70.0	264.0	122.40
MGL-22	alu.	0.147	200	96.57	101.40	0.234	1.519	70.0	264.0	65.76
MGL-23	alu.	0.14	200	96.46	76.2	0.259	1.527	70.0	264.0	62.16
MGL-24	alu.	0.254	200	96.52	101.3	0.198	1.524	70.0	264.0	102.0
MGL-25	alu.	0.254	200	96.52	76.25	0.083	1.524	70.0	264.0	95.76
MGL-26	alu.	0.277	200	96.39	50.12	0.193	1.524	70.0	264.0	114.0
MGL-27	alu.	0.300	200	96.60	77.28	0.205	1.525	70.0	264.0	102.72
MGL-28	alu.	0.160	200	96.48	51.13	0.240	1.523	70.0	264.0	73.44
MGL-31	alu.	0.328	200	96.43	101.2	0.094	1.525	70.0	264.0	107.76
MGL-36	alu.	0.343	200	96.38	76.14	0.096	1.524	70.0	264.0	116.16
MGL-38	alu.	0.307	200	96.39	76.15	0.121	1.522	70.0	264.0	110.4
MGL-41	alu.	0.307	200	96.39	85.79	0.200	1.522	70.0	264.0	127.92
MGL-43	alu.	0.157	200	96.55	88.83	0.278	1.519	70.0	264.0	90.24

Table A2.1 - Aluminium test specimens of aerospace test programmes (cont.).

Model	Mat.	Tk	Ns	Rad	L	dw	tw	E	SigY	Sigu
SZ-2	st.	0.238	132	127.5	136.4	0.363	1.06	196.0	462.0	170.52
SZ-2S	st.	0.264	132	127.7	42.16	0.243	1.059	196.0	462.0	168.42
SZ-3S	st.	0.304	132	127.6	42.13	0.303	1.06	196.0	462.0	156.66
SZ-3	st.	0.305	132	127.7	136.7	0.303	1.059	196.0	462.0	182.28
4-L	st.	0.247	132	127.6	90.66	0.267	1.059	196.0	462.0	158.76
4-M	st.	0.238	132	127.5	59.95	0.269	1.06	196.0	462.0	162.54
4-S	st.	0.227	132	127.5	30.6	0.274	1.06	196.0	462.0	139.02
5-L	st.	0.229	132	127.5	90.56	0.241	1.06	196.0	462.0	150.78
5-M	st.	0.236	132	126.4	59.45	0.236	1.05	196.0	462.0	127.26
5-S	st.	0.242	132	127.5	30.6	0.254	1.06	196.0	462.0	148.68
6-L	st.	0.3	132	127.8	145.6	0.296	1.06	196.0	462.0	148.68
6-S	st.	0.307	132	127.7	39.6	0.32	1.06	196.0	462.0	164.64
7-L	st.	0.286	132	127.8	145.7	0.323	1.06	196.0	462.0	178.08
7-S	st.	0.288	132	127.5	39.55	0.348	1.06	196.0	462.0	141.12
8-S	st.	0.268	132	127.8	25.56	0.586	1.06	196.0	462.0	231.
9-L	st.	0.271	132	127.6	90.6	0.585	1.06	196.0	462.0	201.6
9-M1	st.	0.27	132	127.7	60.	0.587	1.06	196.0	462.0	186.06
9-M2	st.	0.227	132	127.5	60.	0.274	1.06	196.0	462.0	117.6
10-M1	st.	0.251	132	127.7	60.0	0.361	1.06	196.0	462.0	162.54
10-M2	st.	0.243	132	127.8	60.1	0.369	1.06	196.0	462.0	150.78
10-S1	st.	0.236	132	127.6	25.53	0.375	1.06	196.0	462.0	166.32
10-S2	st.	0.238	132	127.5	25.5	0.374	1.06	196.0	462.0	152.88
11-L	st.	0.272	132	127.8	86.9	0.581	1.06	196.0	462.0	213.36
11-M	st.	0.26	132	127.6	62.55	0.587	1.06	196.0	462.0	174.3
11-S	st.	0.247	132	127.6	33.2	0.391	1.06	196.0	462.0	250.74
12-M1	st.	0.292	160	175.4	68.44	0.416	1.919	196.0	605.0	144.65
12-M2	st.	0.292	160	175.4	68.44	0.408	1.919	196.0	605.0	172.15
12-S	st.	0.29	160	175.7	40.4	0.414	1.92	196.0	605.0	189.75
13-L	st.	0.291	160	175.4	177.2	0.405	1.92	196.0	605.0	164.45
14-L	st.	0.291	160	175.4	180.7	0.401	1.92	196.0	605.0	176.
15-L	st.	0.291	160	175.4	140.3	0.418	1.92	196.0	605.0	168.3
15-S	st.	0.288	160	175.3	40.3	0.422	1.92	196.0	605.0	197.45
16-L	st.	0.27	120	175.5	140.4	0.451	4.22	196.0	605.0	168.3
16-S	st.	0.267	120	175.4	40.3	0.46	4.221	196.0	605.0	201.85
17-L	st.	0.283	120	175.4	140.3	0.417	4.219	196.0	605.0	178.2
17-S	st.	0.282	120	175.4	40.3	0.43	4.218	196.0	605.0	193.6
18-M1	st.	0.266	92	175.5	87.8	0.732	2.039	196.0	605.0	183.7
18-M2	st.	0.269	92	175.3	87.7	0.728	2.04	196.0	605.0	205.7
19-M1	st.	0.278	92	175.4	70.16	0.762	2.039	196.0	605.0	205.7
19-M2	st.	0.278	92	175.4	70.16	0.777	2.039	196.0	605.0	209.55
19-S	st.	0.271	92	175.6	40.4	0.785	2.04	196.0	605.0	250.8
20-M1	st.	0.251	92	175.4	70.2	0.669	2.03	196.0	605.0	195.8
20-M2	st.	0.241	92	175.4	70.2	0.686	2.029	196.0	605.0	191.95
20-S	st.	0.242	92	175.4	36.84	0.696	2.029	196.0	605.0	246.95
21-L1	st.	0.231	92	175.5	87.8	0.678	2.03	196.0	605.0	140.8
21-L2	st.	0.237	92	175.6	87.8	0.659	2.029	196.0	605.0	158.4

Table A2.2 - Steel test specimens of aerospace test programmes.

Model	Mat.	Tk	Ns	Rad	L	dw	tw	E	SigY	Sigu
22-M1	st.	0.286	92	175.6	70.24	0.314	2.03	196.0	605.0	143.
22-M2	st.	0.275	92	175.4	70.2	0.328	2.03	196.0	605.0	134.75
22-S	st.	0.262	92	175.2	36.8	0.337	2.02	196.0	605.0	152.35
23-L1	st.	0.303	92	175.7	89.6	0.308	2.03	196.0	605.0	156.75
23-L2	st.	0.300	92	175.5	89.5	0.314	2.03	196.0	605.0	144.65
24-L	st.	0.266	92	175.5	170.2	0.357	2.03	196.0	605.0	129.25
25-M1	st.	0.266	100	175.5	75.5	0.356	1.06	196.0	605.0	119.35
25-M2	st.	0.26	100	175.5	75.46	0.359	1.06	196.0	605.0	121.
26-M1	st.	0.273	100	175.5	61.4	0.333	1.06	196.0	605.0	129.25
26-M2	st.	0.275	100	175.4	61.4	0.323	1.06	196.0	605.0	119.35
26-S	st.	0.265	100	175.4	42.1	0.35	1.06	196.0	605.0	140.8
27-M1	st.	0.241	100	175.4	66.67	0.784	1.07	196.0	605.0	185.9
27-M2	st.	0.252	100	175.3	66.64	0.763	1.069	196.0	605.0	154.55
27-S	st.	0.235	100	175.5	38.6	0.802	1.069	196.0	605.0	209.55
28-M1	st.	0.273	100	175.5	84.25	0.734	1.08	196.0	605.0	160.6
28-M2	st.	0.261	100	175.3	85.9	0.753	1.08	196.0	605.0	160.6
29-L	st.	0.286	100	175.6	154.5	0.33	1.06	196.0	605.0	134.75
30-L	st.	0.252	92	175.3	154.3	0.745	2.03	196.0	605.0	182.05
31-L	st.	0.177	100	175.5	131.6	0.812	1.07	196.0	605.0	99.55
32-L	st.	0.302	92	175.7	156.4	0.583	2.04	196.0	605.0	185.9
33-M	st.	0.25	88	175.5	105.3	0.766	2.58	196.0	605.0	168.3
34-L	st.	0.273	88	175.5	117.6	0.732	2.59	196.0	605.0	199.65
34-S	st.	0.278	88	175.4	35.1	0.722	2.59	196.0	605.0	282.15
35-M1	st.	0.257	88	175.5	75.5	0.743	2.58	196.0	605.0	188.1
35-M2	st.	0.252	88	175.3	77.2	0.75	2.58	196.0	605.0	176.
36-L	st.	0.271	84	175.6	103.6	0.489	3.18	196.0	605.0	127.05
36-S	st.	0.25	84	175.5	35.1	0.491	3.17	196.0	605.0	233.2
36-S1	st.	0.266	84	175.5	35.1	0.486	3.18	196.0	605.0	219.45
37-L	st.	0.244	84	175.4	115.7	0.5	3.17	196.0	605.0	143.
38-L	st.	0.258	68	127.1	148.8	0.731	1.81	196.0	462.0	229.32
38-S	st.	0.277	68	127.1	30.5	0.715	1.819	196.0	462.0	297.78
39-L	st.	0.257	68	127.2	153.9	0.477	1.8	196.0	462.0	186.06
39-S	st.	0.279	68	127.2	30.5	0.464	1.8	196.0	462.0	233.1
40-L	st.	0.265	68	127.2	142.4	0.5	1.8	196.0	462.0	213.36
40-S	st.	0.292	68	127.	41.9	0.479	1.81	196.0	462.0	213.36
41-L	st.	0.274	68	127.1	144.9	0.713	1.81	196.0	462.0	242.76
41-S	st.	0.307	68	127.0	40.7	0.693	1.83	196.0	462.0	246.96
LZ-1	st.	0.362	160	175.5	200.1	0.945	1.88	196.0	605.0	287.65

Table A2.2 - Steel test specimens of aerospace test programmes (cont.).

Model	Mat.	Tk	Na	Rad	L	dw	tw	E	SigY	Sigu	
DUD-8	alu.	0.249	84	120.1	200.0	1.754	0.85	73.6	594.0	102.2	
DUD-9	alu.	0.252	84	120.1	200.0	1.690	0.85	73.6	594.0	88.13	
DUD-10	alu.	0.252	84	120.1	200.0	1.775	0.85	73.6	594.0	101.84	
SN-1	alu.	0.257	84	120.1	100.0	1.998	0.8	73.6	594.0	155.27	
SN-2	alu.	0.250	84	120.1	100.0	1.995	0.8	73.6	594.0	82.0	
SN-3	alu.	0.255	84	120.1	100.0	1.997	0.8	73.6	594.0	112.51	
SN-4	alu.	0.272	84	120.1	100.0	1.593	0.9	73.6	594.0	141.43	
SN-5	alu.	0.268	84	120.1	100.0	1.595	0.9	73.6	594.0	110.41	
SN-6	alu.	0.272	84	120.1	100.0	1.588	0.9	73.6	594.0	93.09	
SN-7	alu.	0.271	84	120.1	100.0	1.585	0.9	73.6	594.0	81.28	
DK-1	alu.	0.261	84	120.1	152.0	1.693	0.85	73.6	594.0	121.79	
DK-2	alu.	0.251	84	120.1	152.0	1.722	0.85	73.6	594.0	79.89	
DK-3	alu.	0.234	84	120.1	137.0	1.745	0.85	73.6	594.0	88.23	
DK-4	alu.	0.232	84	120.1	148.0	1.733	0.85	73.6	594.0	68.55	
DK-5	alu.	0.255	84	120.1	152.0	1.704	0.85	73.6	594.0	124.18	
DK-6	alu.	0.250	84	120.1	167.0	1.679	0.85	73.6	594.0	64.16	
DK-7	alu.	0.255	84	120.1	167.0	1.680	0.85	73.6	594.0	68.71	
AAC-1	alu.	0.49	79	250.0	325.0	5.5	0.84	73.6	594.0	105.6	
AAC-2	alu.	0.49	79	250.0	325.0	5.5	0.84	73.6	594.0	109.81	
AAC-3	alu.	0.49	79	250.0	305.0	5.5	0.84	73.6	594.0	140.3	
AAC-4	alu.	0.49	79	250.0	305.0	6.0	0.49	73.6	594.0	117.37	
AAC-5	alu.	0.49	79	250.0	305.0	6.0	0.49	73.6	594.0	118.84	
AAC-6	alu.	0.49	79	250.0	305.0	5.5	0.84	73.6	594.0	130.0	
AAC-7	alu.	0.49	79	250.0	305.0	6.0	0.49	73.6	594.0	127.15	
AACX-1	alu.	0.49	79	250.0	305.0	5.5	0.84	73.6	594.0	95.4	
AACX-2	alu.	0.49	79	250.0	305.0	5.5	0.84	73.6	594.0	115.61	
ST-3	stl.	0.24	100	129.1	150.0	0.499	1.0	196.0	482.0	120.21	
Model	Mat.	Tk	Na	Rad	L	dw	tw	E	SigY	Pu	
KR-2	alu.	0.254	84	120.1	200.0	1.491	0.89	73.6	594.0	0.017	
KR-5rp	alu.	0.284	84	120.1	200.0	1.47	0.89	73.6	594.0	0.016	
KR-8rp	alu.	0.261	84	120.1	200.0	1.468	0.89	73.6	594.0	0.016	
DUD-5rp	alu.	0.245	84	120.1	200.0	1.751	0.83	73.6	594.0	0.011	
DUD-7rp	alu.	0.246	84	120.1	200.0	1.756	0.83	73.6	594.0	0.010	
DUD-8rp	alu.	0.249	84	120.1	200.0	1.754	0.85	73.6	594.0	0.014	
DUD-7rp	alu.	0.252	84	120.1	200.0	1.755	0.85	73.6	594.0	0.013	
ST-1rp	stl.	0.231	100	129.1	150.0	0.508	1.0	196.0	482.0	0.024	
ST-4rp	stl.	0.239	100	129.1	150.0	0.499	1.0	196.0	482.0	0.031	
Model	Mat.	Tk	Na	Rad	L	dw	tw	E	SigY	Sigu	Pu
KR-3	alu.	0.247	84	120.1	200.0	1.497	0.89	73.6	594.0	23.0	0.012
KR-4	alu.	0.242	84	120.1	200.0	1.505	0.89	73.6	594.0	49.81	0.009
KR-5cl	alu.	0.284	84	120.1	200.0	1.47	0.89	73.6	594.0	48.02	0.008
KR-8rp	alu.	0.261	84	120.1	200.0	1.468	0.89	73.6	594.0	70.3	0.005
DUD-61cl	alu.	0.243	84	120.1	200.0	1.751	0.83	73.6	594.0	12.83	0.009
DUD-62cl	alu.	0.243	84	120.1	200.0	1.751	0.83	73.6	594.0	19.25	0.081
DUD-63cl	alu.	0.243	84	120.1	200.0	1.751	0.83	73.6	594.0	32.08	0.070
DUD-64cl	alu.	0.243	84	120.1	200.0	1.751	0.83	73.6	594.0	40.1	0.058
DUD-65cl	alu.	0.243	84	120.1	200.0	1.751	0.83	73.6	594.0	48.13	0.046
DUD-71cl	alu.	0.246	84	120.1	200.0	1.756	0.83	73.6	594.0	19.09	0.099
DUD-72cl	alu.	0.246	84	120.1	200.0	1.756	0.83	73.6	594.0	31.81	0.088
DUD-73cl	alu.	0.246	84	120.1	200.0	1.756	0.83	73.6	594.0	38.17	0.083
DUD-74cl	alu.	0.246	84	120.1	200.0	1.756	0.83	73.6	594.0	50.9	0.082
DUD-81cl	alu.	0.249	84	120.1	200.0	1.754	0.85	73.6	594.0	12.77	0.012
DUD-82cl	alu.	0.249	84	120.1	200.0	1.754	0.85	73.6	594.0	25.55	0.011
DUD-101cl	alu.	0.252	84	120.1	200.0	1.755	0.85	73.6	594.0	35.19	0.004
DUD-102cl	alu.	0.252	84	120.1	200.0	1.755	0.85	73.6	594.0	35.82	0.004
ST-1cl	stl.	0.231	100	129.1	150.0	0.508	1.0	196.0	482.0	61.72	0.025
ST-2cl	stl.	0.249	100	129.1	150.0	0.510	1.0	196.0	482.0	58.29	0.025
ST-4rp	stl.	0.239	100	129.1	150.0	0.499	1.0	196.0	482.0	40.2	0.024

Table A2.3 - Recent test specimens of aerospace test programmes.

Model	X_m	m^*n (theory)	m^*n (test)
SZ-2	1.05	1*11	1*11
SZ-3	.95	1*10	1*11
4-M	.89	1*15	1*13
4-S	.67	2*7	1*12
5-L	.93	1*13	1*12
6-S	.70	1*16	1*13
7-L	.99	1*10	1*11
7-S	.60	1*16	1*16
8-S	.87	1*13	1*9
9-L	.96	1*12	1*10
10-M1	.81	1*15	1*14
10-M2	.75	1*15	1*13
10-S1	.67	2*2	1*13
10-S2	.62	2*2	1*13
11-L	1.00	1*12	1*12
11-M	.74	1*14	1*12
11-S	1.04	1*16	1*13
12-M1	.68	2*4	1*16
12-M2	.82	2*4	1*15
12-S	.93	2*2	1*15
14-L	.96	1*11	1*11
16-L	.79	2*6	1*11
17-L	.85	2*7	1*11
18-M1	.66	1*13	1*15
19-M2	.66	1*13	1*12
20-M1	.63	1*13	1*15
20-M2	.59	1*13	1*14
21-L1	.48	1*13	1*16
21-L2	.56	1*13	1*16
22-M2	.78	2*4	1*18
22-S	.87	2*2	1*18
25-M2	.90	1*17	1*16
26-M1	.92	1*18	1*17
26-M2	.85	1*18	1*16
26-S	.94	1*20	1*20
27-M1	1.06	1*17	1*14
27-M2	.89	1*17	1*14
27-S	.92	1*18	1*14
28-M1	.99	1*16	1*16
28-M2	1.00	1*16	1*14
30-L	.87	1*11	1*10
31-L	.83	1*14	1*13
33-M	.49	2*4	1*11
34-L	.60	1*11	1*11
35-M1	.55	2*3	1*11
35-M2	.52	2*3	1*11
36-S	.81	2*2	1*12
36-L	.47	2*5	1*11
37-L	.51	2*6	1*10
38-L	.93	1*9	1*10
39-S	.86	2*2	1*14
40-S	.79	1*13	1*13
40-L	.94	1*10	1*11
41-S	.87	1*12	1*11

Table A2.4 - X_m and the associated buckling modes using orthotropic theory.

Model	Tk	Ns	Rad	L	dw	tw	E	SigY	Sigu
CE 1	1.0	20	300.0	200.0	.895	.089	210.0	250.0	148.4
CE 2	1.0	20	400.0	200.0	.895	.089	210.0	250.0	106.0
CE 3	1.0	20	500.0	200.0	.895	.089	210.0	250.0	83.6
CE 4	1.0	40	600.0	300.0	1.03	.103	210.0	250.0	132.4
CE 5	1.0	20	400.0	100.0	1.732	.173	210.0	250.0	139.7
CE 6	1.0	20	400.0	200.0	1.732	.173	210.0	250.0	117.8
CE 7	1.0	20	400.0	400.0	1.732	.173	210.0	250.0	122.4
CE 8	1.0	20	600.0	150.0	1.732	.173	210.0	250.0	96.6
CE 9	1.0	20	600.0	300.0	1.732	.173	210.0	250.0	92.5
CE 10	1.0	40	600.0	300.0	1.732	.173	210.0	250.0	142.0
CE 11	1.0	20	600.0	600.0	1.732	.173	210.0	250.0	74.8
CE 12	1.0	20	600.0	300.0	2.236	.224	210.0	250.0	87.9
CE 13	1.0	40	600.0	300.0	2.236	.224	210.0	250.0	145.3
CE 14	1.0	20	600.0	400.0	2.236	.224	210.0	250.0	87.6
AE 15	1.0	20	400.0	200.0	0.895	.089	210.0	350.0	103.8
AE 16	1.0	40	600.0	300.0	1.03	.103	210.0	350.0	134.0
CE 17	1.0	20	300.0	400.0	1.732	.173	210.0	350.0	248.2
CE 18	1.0	20	400.0	500.0	1.732	.173	210.0	350.0	145.0
CE 19	1.0	20	600.0	100.0	1.732	.173	210.0	350.0	131.9
AE 20	1.0	20	600.0	150.0	1.732	.173	210.0	350.0	104.3
AE 21	1.0	20	600.0	600.0	1.732	.173	210.0	350.0	74.8
AE 22	1.0	20	400.0	200.0	2.236	.224	210.0	350.0	115.8
CE 23	1.0	20	400.0	400.0	2.236	.224	210.0	350.0	125.1
AE 24	1.0	20	600.0	300.0	2.236	.224	210.0	350.0	88.3
AE 25	1.0	20	400.0	200.0	1.732	.173	210.0	350.0	226.6
AE 26	1.0	20	400.0	200.0	1.732	.173	210.0	350.0	117.8
AE 27	1.0	20	400.0	200.0	1.732	.173	210.0	350.0	117.8
AE 28	1.0	20	400.0	400.0	1.732	.173	210.0	350.0	177.8
AE 29	1.0	20	400.0	400.0	1.732	.173	210.0	350.0	122.4
AE 30	1.0	20	400.0	400.0	1.732	.173	210.0	350.0	122.4
CE 31	1.0	20	500.0	250.0	1.732	.173	210.0	350.0	191.2
CE 32	1.0	20	500.0	250.0	1.732	.173	210.0	350.0	101.6
CE 33	1.0	20	500.0	250.0	1.732	.173	210.0	350.0	101.6
CE 34	1.0	20	500.0	500.0	1.732	.173	210.0	350.0	144.4
CE 35	1.0	20	500.0	500.0	1.732	.173	210.0	350.0	91.5
CE 36	1.0	20	500.0	500.0	1.732	.173	210.0	350.0	91.5
CE 37	1.0	30	600.0	150.0	1.732	.173	210.0	350.0	121.8
CE 38	1.0	30	600.0	150.0	1.732	.173	210.0	350.0	110.7
CE 39	1.0	30	600.0	150.0	1.732	.173	210.0	350.0	110.7
AE 40	1.0	20	600.0	300.0	1.732	.173	210.0	350.0	173.2
AE 41	1.0	20	600.0	300.0	1.732	.173	210.0	350.0	92.0
AE 42	1.0	20	600.0	300.0	1.732	.173	210.0	350.0	92.0
AE 43	1.0	40	600.0	300.0	1.732	.173	210.0	350.0	169.8
AE 44	1.0	40	600.0	300.0	1.732	.173	210.0	350.0	139.0
AE 45	1.0	40	600.0	300.0	1.732	.173	210.0	350.0	138.0

Table A2.5 - Finite element test specimens - Elastic failure.

Model	Tk	Ns	Rad	L	dw	tw	E	SigY	Sigu
CEP1	1.0	20	200.0	50.0	1.261	.126	210.0	250.0	225.8
CEP2	1.0	20	200.0	100.0	1.261	.126	210.0	250.0	201.0
CEP3	1.0	30	400.0	200.0	.895	.089	210.0	250.0	169.1
CEP4	1.0	40	400.0	200.0	1.261	.126	210.0	250.0	210.0
CEP5	1.0	60	600.0	150.0	1.261	.126	210.0	250.0	183.8
CEP6	1.0	20	200.0	50.0	1.732	.173	210.0	250.0	216.7
CEP7	1.0	40	200.0	50.0	1.732	.173	210.0	250.0	238.9
CEP8	1.0	20	200.0	100.0	1.732	.173	210.0	250.0	187.2
CEP9	1.0	40	200.0	100.0	1.732	.173	210.0	250.0	244.1
CEP10	1.0	20	200.0	200.0	1.732	.173	210.0	250.0	246.6
CEP11	1.0	40	400.0	100.0	1.732	.173	210.0	250.0	183.0
CEP12	1.0	60	400.0	100.0	1.732	.173	210.0	250.0	237.2
CEP13	1.0	40	400.0	200.0	1.732	.173	210.0	250.0	214.9
CEP14	1.0	40	600.0	150.0	1.736	.173	210.0	250.0	120.0
CEP15	1.0	60	600.0	150.0	1.736	.173	210.0	250.0	184.7
CEP16	1.0	60	200.0	50.0	2.236	.224	210.0	250.0	243.9
CEP17	1.0	20	200.0	100.0	2.236	.224	210.0	250.0	193.6
CEP18	1.0	60	400.0	100.0	2.236	.224	210.0	250.0	238.7
CEP19	1.0	40	400.0	200.0	2.236	.224	210.0	250.0	217.1
CEP20	1.0	60	600.0	150.0	2.236	.224	210.0	250.0	181.8
AEP21	1.0	20	200.0	50.0	1.261	.126	210.0	350.0	285.4
AEP22	1.0	20	200.0	100.0	1.261	.126	210.0	350.0	226.5
AEP23	1.0	20	400.0	100.0	.895	.089	210.0	350.0	139.0
AEP24	1.0	40	400.0	200.0	1.261	.126	210.0	350.0	237.4
AEP25	1.0	60	600.0	150.0	1.261	.126	210.0	350.0	221.0
AEP26	1.0	20	200.0	50.0	1.732	.173	210.0	350.0	277.7
AEP27	1.0	40	200.0	50.0	1.732	.173	210.0	350.0	329.4
AEP28	1.0	60	200.0	50.0	1.732	.173	210.0	350.0	307.8
AEP29	1.0	20	200.0	200.0	1.732	.173	210.0	350.0	322.8
CEP30	1.0	20	500.0	150.0	1.732	.173	210.0	350.0	109.5
AEP31	1.0	40	600.0	150.0	1.732	.173	210.0	350.0	149.7
AEP32	1.0	60	600.0	150.0	1.732	.173	210.0	350.0	221.8
AEP33	1.0	60	200.0	50.0	2.236	.224	210.0	350.0	337.1
AEP34	1.0	20	200.0	100.0	2.236	.224	210.0	350.0	230.6
AEP35	1.0	40	200.0	100.0	2.236	.224	210.0	350.0	350.9
AEP36	1.0	60	400.0	100.0	2.236	.224	210.0	350.0	311.6
AEP37	1.0	40	400.0	200.0	2.236	.224	210.0	350.0	262.2
AEP38	1.0	60	600.0	150.0	2.236	.224	210.0	350.0	215.5
AEP39	1.0	40	600.0	300.0	2.236	.224	210.0	350.0	145.3
AEP40	1.0	20	200.0	100.0	1.732	.173	210.0	350.0	304.3
AEP41	1.0	20	200.0	100.0	1.732	.173	210.0	350.0	229.4
AEP42	1.0	20	200.0	100.0	1.732	.173	210.0	350.0	229.4
AEP43	1.0	40	200.0	100.0	1.732	.173	210.0	350.0	338.4
AEP44	1.0	40	200.0	100.0	1.732	.173	210.0	350.0	339.0
AEP45	1.0	40	200.0	100.0	1.732	.173	210.0	350.0	338.8
AEP46	1.0	20	400.0	100.0	1.732	.173	210.0	350.0	213.6
AEP47	1.0	20	400.0	100.0	1.732	.173	210.0	350.0	150.6
AEP48	1.0	20	400.0	100.0	1.732	.173	210.0	350.0	111.9
AEP49	1.0	40	400.0	100.0	1.732	.173	210.0	350.0	261.8
AEP50	1.0	40	400.0	100.0	1.732	.173	210.0	350.0	213.0
AEP51	1.0	40	400.0	100.0	1.732	.173	210.0	350.0	192.5
AEP52	1.0	60	400.0	100.0	1.732	.173	210.0	350.0	331.2
AEP53	1.0	60	400.0	100.0	1.732	.173	210.0	350.0	313.5
AEP54	1.0	60	400.0	100.0	1.732	.173	210.0	350.0	296.5
AEP55	1.0	40	400.0	200.0	1.732	.173	210.0	350.0	288.3
AEP56	1.0	40	400.0	200.0	1.732	.173	210.0	350.0	243.7
AEP57	1.0	40	400.0	200.0	1.732	.173	210.0	350.0	222.3

Table A2.6 - Finite element test specimens - Elastoplastic failure.

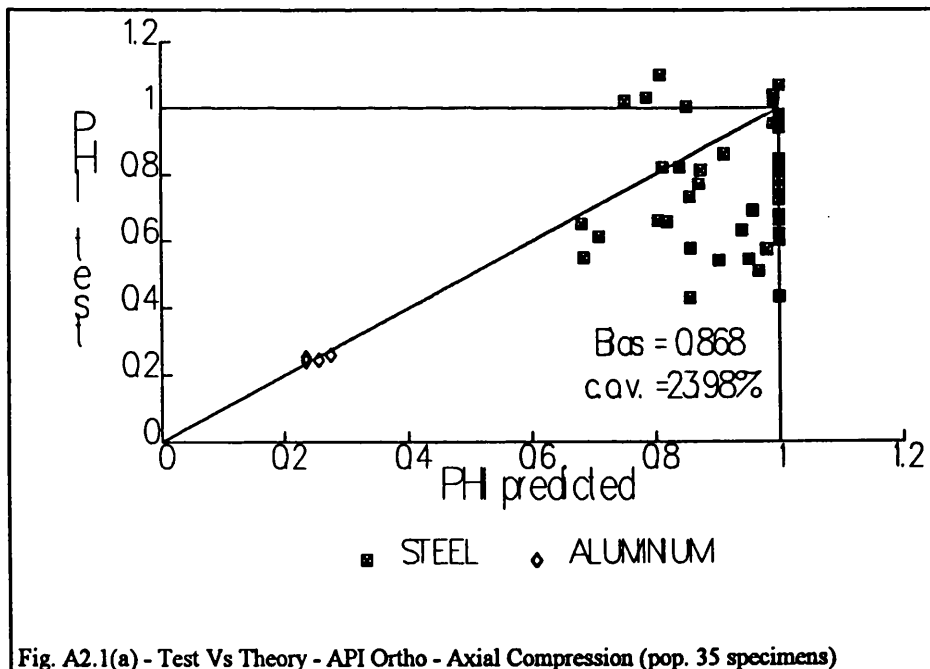
APPENDIX 3 - CYLINDERS UNCERTAINTY MODELLING - GRAPHICAL OUTPUT.

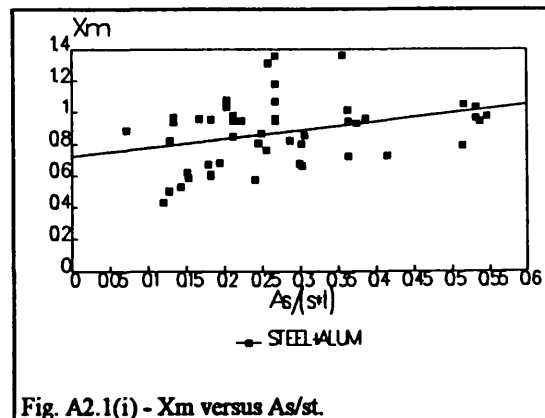
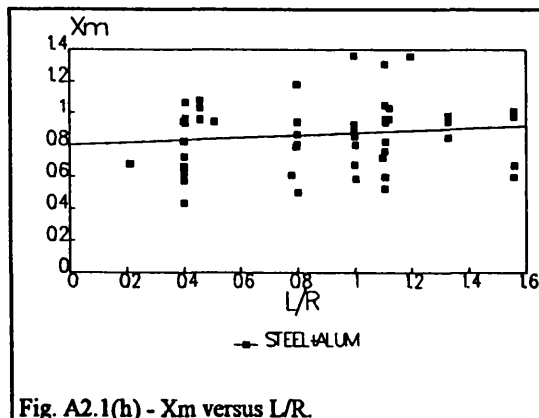
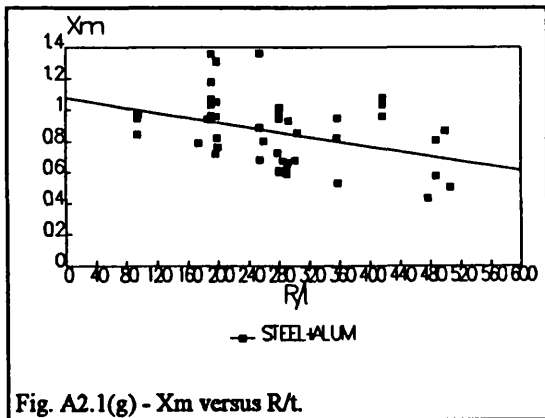
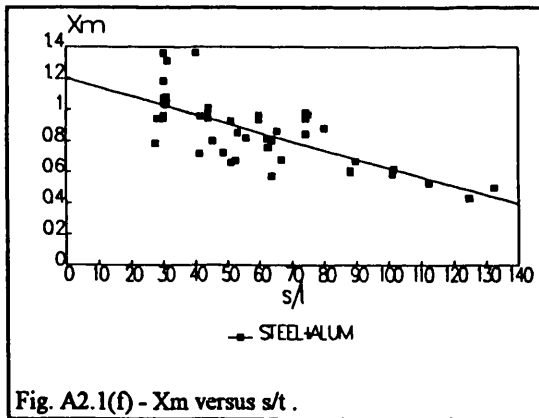
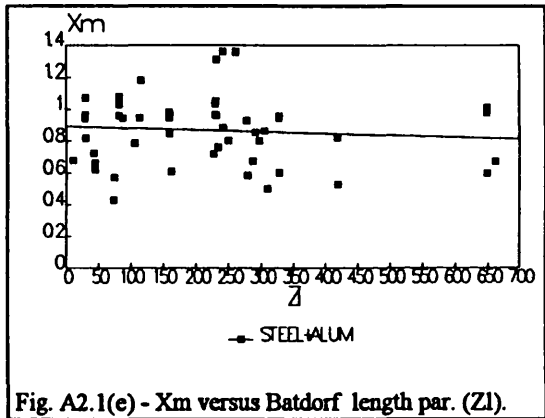
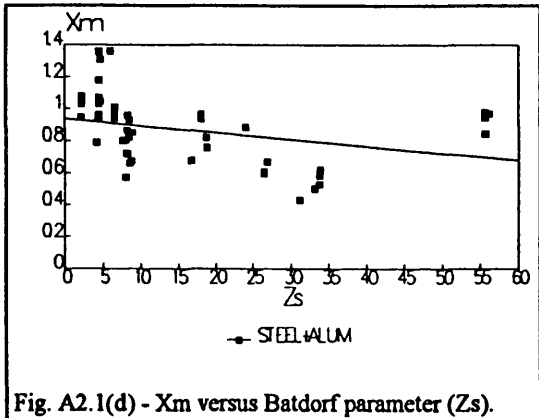
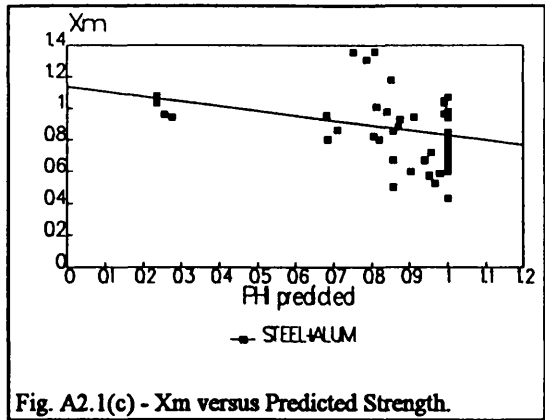
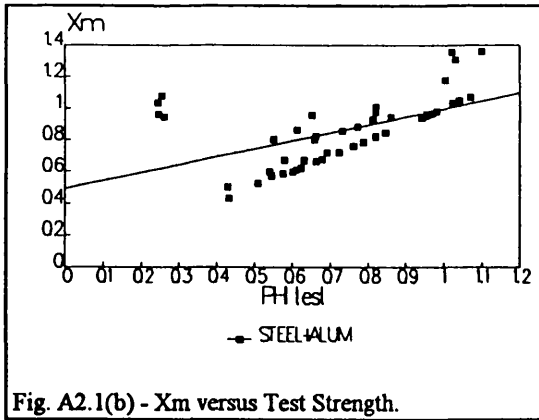
1 - Axial compression

The results of the statistical analyses for the API Bul 2U, the RCC recommendations, the DnV Classification notes and the ECCS rules are plotted in graphs showing the variation of the modelling parameter X_m with the test and predicted strengths and with different geometric parameters of cylinders . The full sets of population were used - Offshore Steel & Aluminium (population = 52 test specimens) and Aerospace Steel & Aluminium (population = 193 test specimens).

1.1.1. API Bul 2U (Orthotropic formulation)(Offshore Steel & Aluminium Test specimens)

The variation of X_m with predicted strength, test strength and with other parameters for the API orthotropic formulation using all offshore population is shown in the following figures A2.1(a) - A2.2(i).



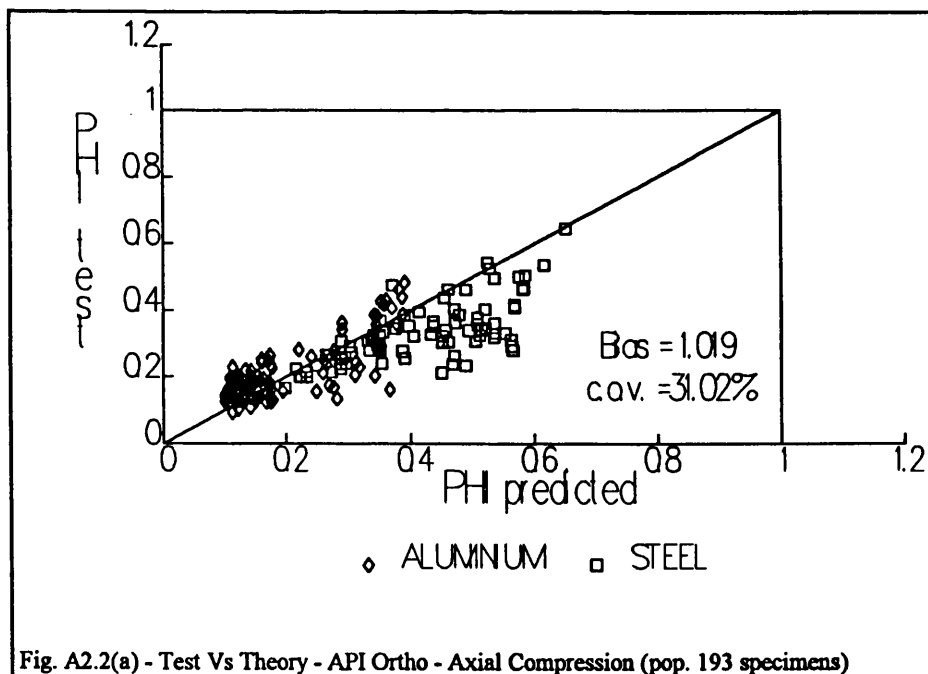


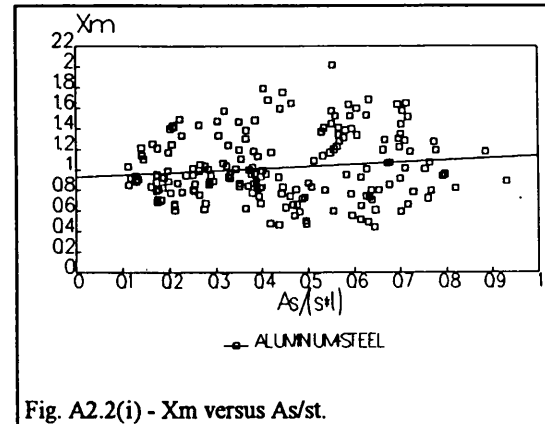
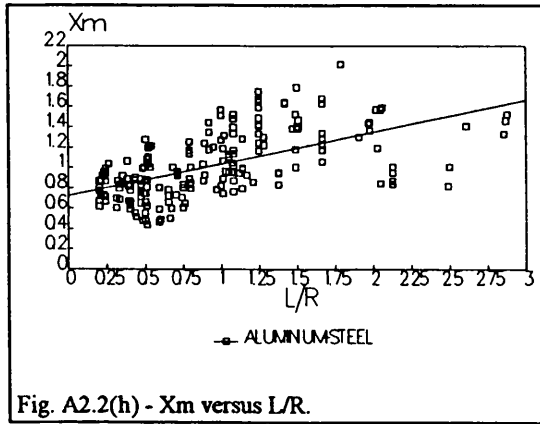
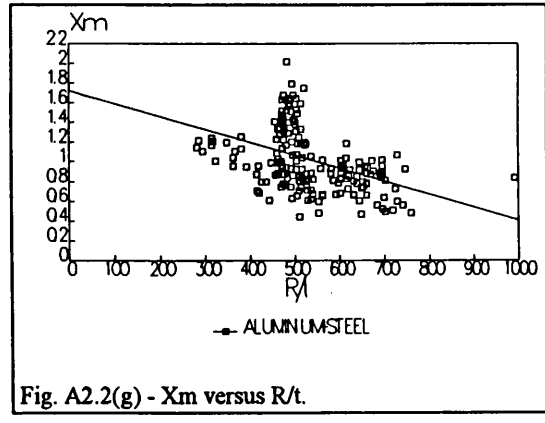
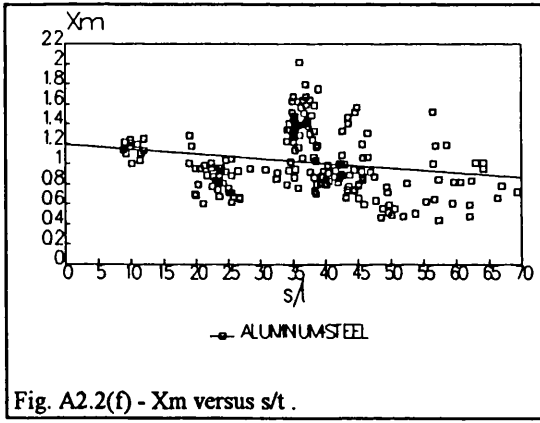
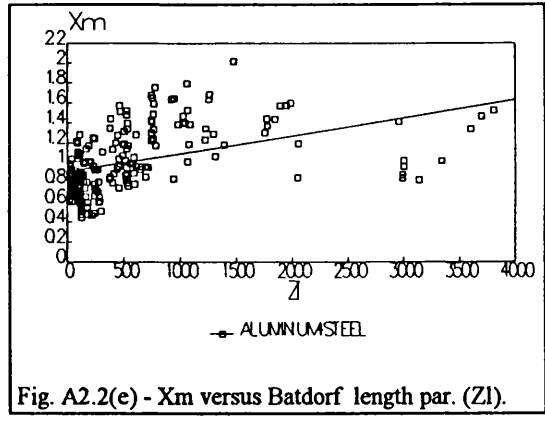
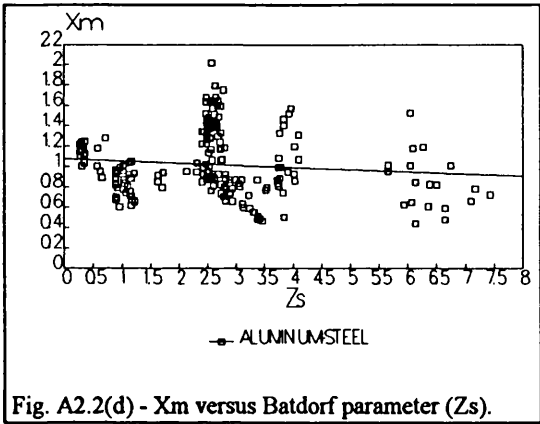
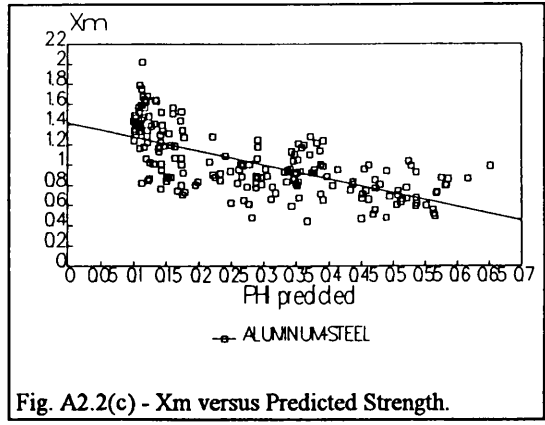
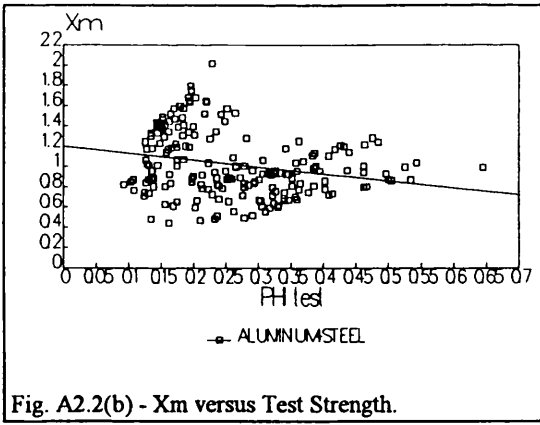
The test/theory plot (fig. A2.1(a)) shows a poor correlation between predictions and test results except for the aluminium specimens where the fit is perfect. A moderate scatter for X_m [0.5-1.36] to all cylinders is shown in figure (A2.1(b)).

It is important to mention the relatively large number of specimens lying in $\phi_{pred}=1$. This is due to the limits imposed by the plasticity reduction factor eq.(3.3) to the test specimens with $\sigma_{icr}/\sigma_y \geq 6.25$. The formulation also exhibits a great dependency of the slenderness with a strong tendency to overpredict the strength of medium and stocky cylinders (fig. A2.1(c)). Some dependence of X_m exists with Z_s (fig. A2.1(d)), s/t (fig. A2.1(f)), R/t (fig. A2.1(g)) and $As/(s*t)$ (fig. A2.1(i)). This formulation is not suited for the offshore steel data set (large COV and high skewness) and can be considered a dangerous lower bound formulation (bias lower than one and more than 80% of the specimens fails under the predictions).

1.1.2. API Bul 2U (Orthotropic formulation)(Aerospace Steel & Aluminium Test specimens)

The variation of X_m with predicted strength, test strength and with other parameters for the API orthotropic formulation using all aerospace population is shown in the following figures A2.2(a) - A2.2(i).





The test/theory plot (fig. A2.2(a)) shows a fair agreement between predictions the test results and exhibit a moderate scatter for X_m [0.4-2.0] to slender and very slender cylinders (fig. A2.2(b)). The formulation also shows a moderate dependency with the slenderness. For the more slender cylinders the results ranges from conservative to dangerous with the formulation clearly overpredicting the strength for the aluminium and underpredicting for the steel over a wide range of slenderness(fig. A2.2(c)). Great dependence of X_m with the geometrical parameters, particularly for Z_s (fig. A2.2(d)), s/t ratio (fig. A2.2(f)) and L/R ratio (fig. A2.2(h)). As conclusion this formulation is poorly suited for the Aerospace data set (large COV and high skewness).

1.2.1. API Bul 2U (Discrete formulation)(Offshore Steel & Aluminium Test specimens)

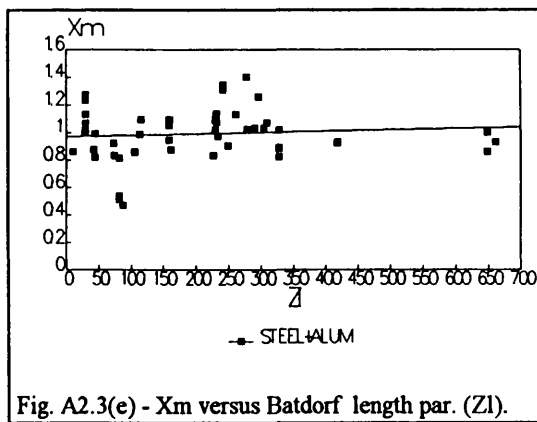
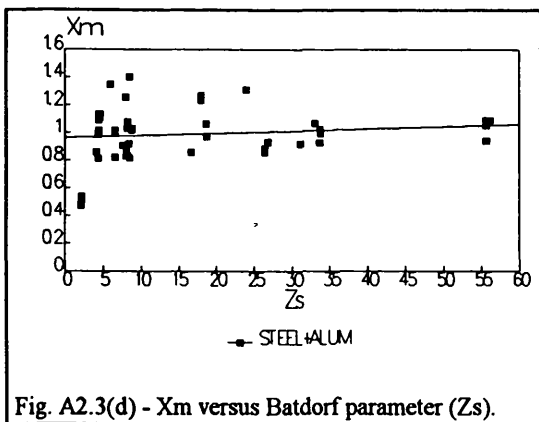
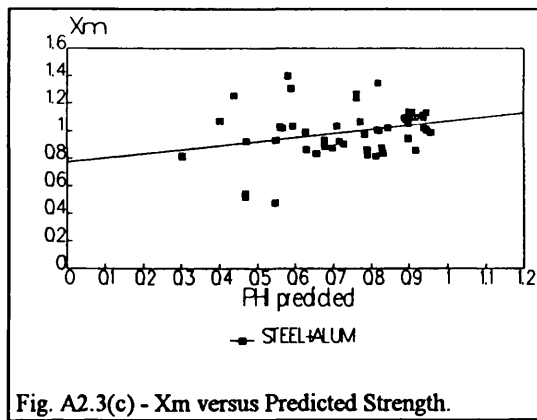
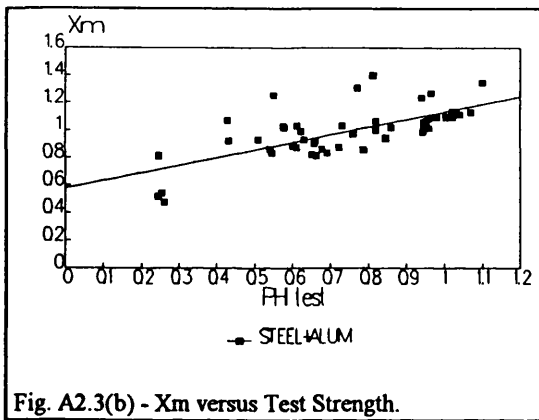
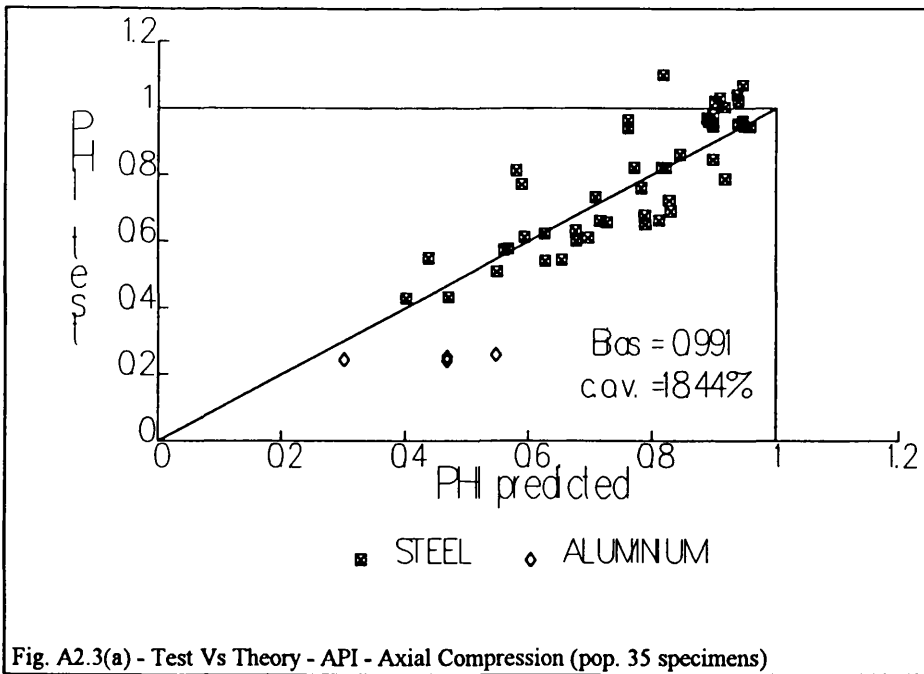
The variation of X_m with predicted strength, test strength and with other parameters for the API formulation using all offshore population is shown in the following figures A2.3(a) - A2.3(i).

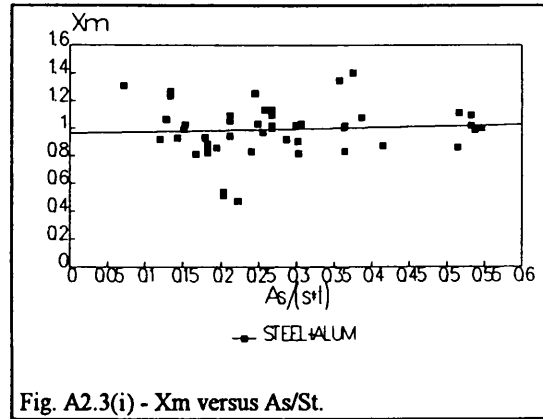
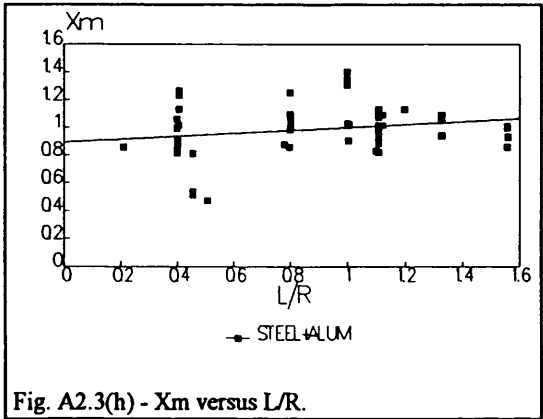
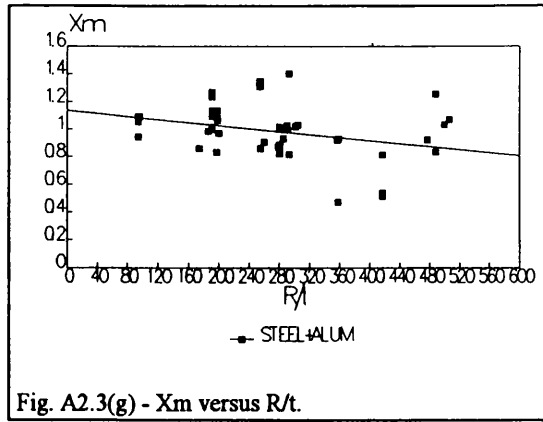
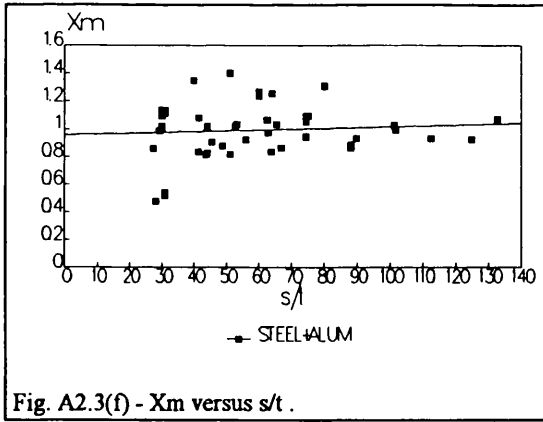
The test/theory plot (fig. A2.3(a)) shows a good correlation between predictions and test with the results lying in the oblique line or near, except for the aluminium specimens with its strength over predicted by the formulation. The figure (A2.3(b)) shows a moderate scatter for X_m [0.82-1.4] to all test specimens. The formulation also shows tendency to under predicted the strength ($X_m > 1.$) for the stocky cylinders (fig. A2.3(c)) but doesn't show significant dependency with the geometrical parameters (fig. A2.13(d)) - (fig. A2.13(i)). This formulation is suited for offshore structural design (moderate COV and no skewness) and can be considered a reasonable mean value formulation (bias little above unity).

1.2.2. API Bul 2U (Discrete formulation)(Aerospace Steel & Aluminium Test specimens)

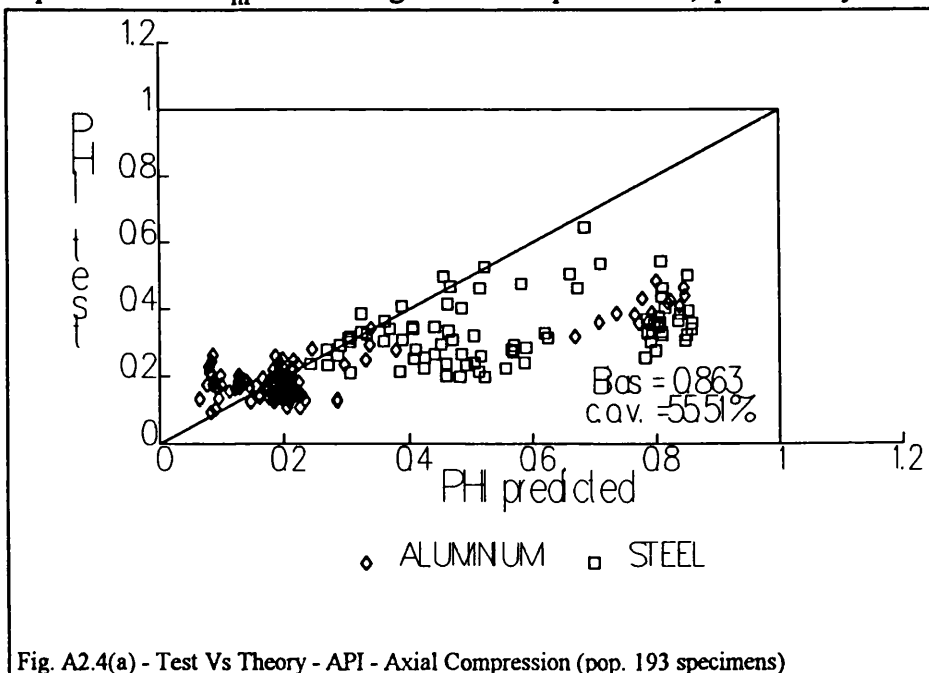
The variation of X_m with predicted strength, test strength and with other parameters for the API formulation using all aerospace population is shown in the following figures A2.4(a) - A2.4(i).

The test/theory plot (fig. A2.4(a)) shows a poor agreement between predictions clearly over predicting the test specimen strength, especially for the steel specimens and for the stronger aluminium ones. The test results exhibits a high scatter for X_m [0.3, 3.0] to slender and very

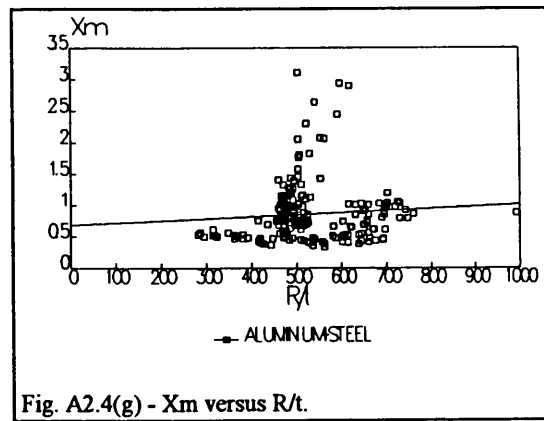
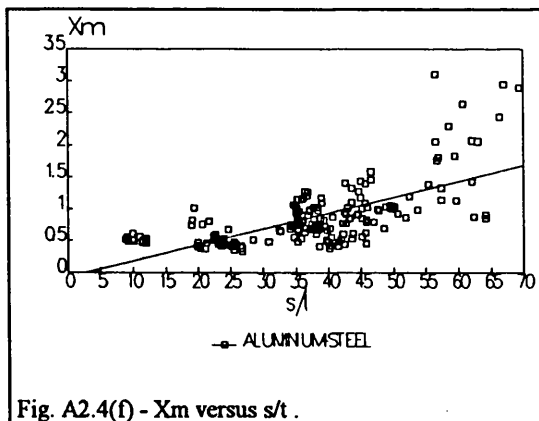
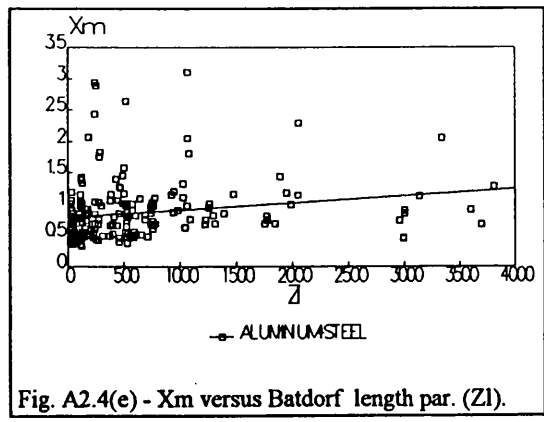
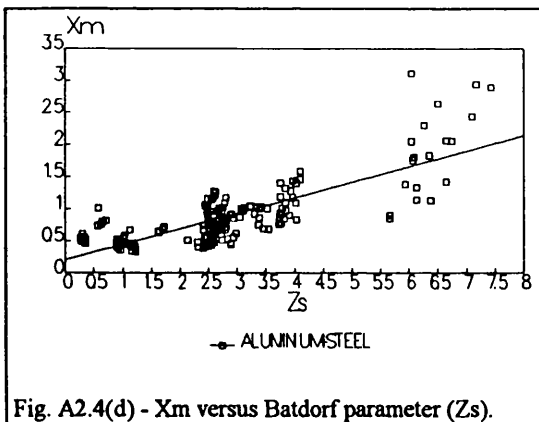
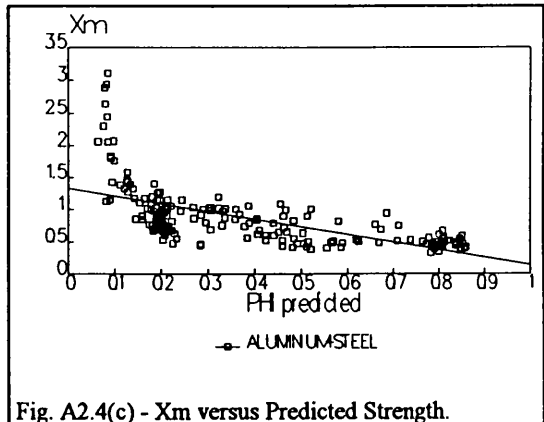
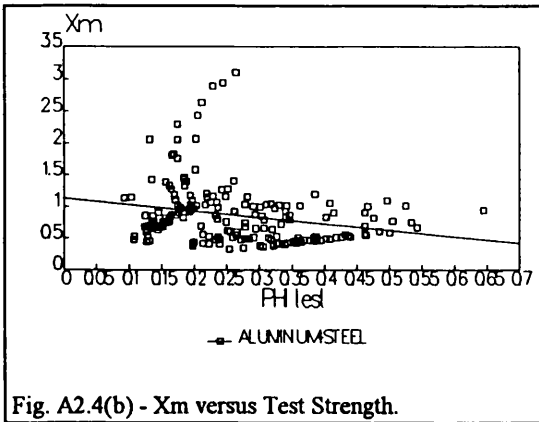


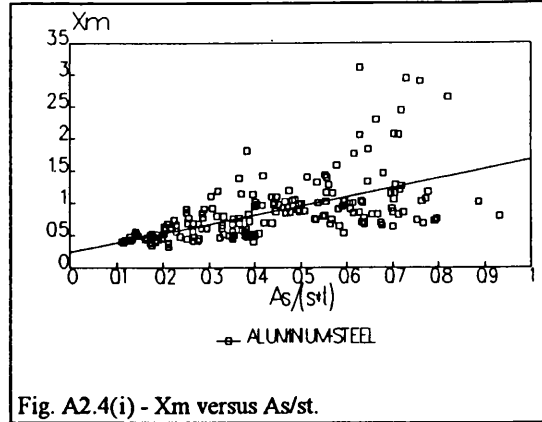
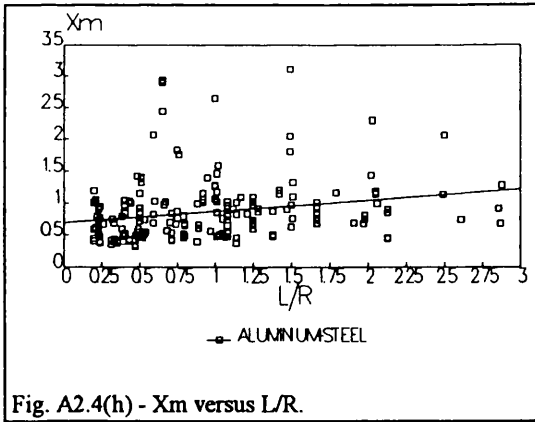


slender cylinders (fig. A2.4(b)). The formulation also shows a high dependency with the slenderness (more for the aluminium than for steel), for the more slender cylinders the results ranges from conservative to dangerous and the formulation shows a strong tendency to over predict the strength over a wide range of slenderness(fig. A2.4(c)). Great dependence of X_m with the geometrical parameters, particularly for Zs (fig.



A2.4(d)), s/t ratio (fig. A2.4(f)) and $As/(s*t)$ ratio (fig. A2.4(i)) Thus there are in this formulation a strong tendency for unsafe design of cylinders with narrow panels, stocky shells between stiffeners and small stiffeners. As conclusion this formulation is not suited for the Aerospace data set (large COV and high skewness).

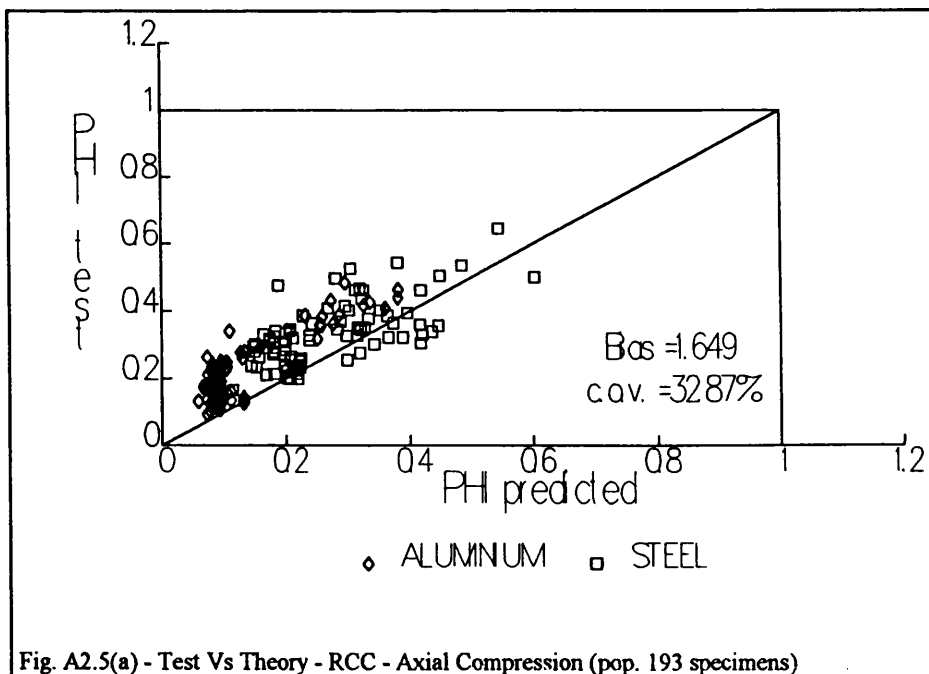




1.3. RCC formulation (Aerospace Steel & Aluminium Test specimens)

The variation of X_m with predicted strength, test strength and with other parameters for the RCC formulation using all aerospace population is shown in the following figures A2.5(a) - A2.5(i).

The test/theory plot (fig. A2.5(a)) shows no correlation between predictions and test results with a high scatter for X_m [0.5-3.5] to slender and very slender cylinders as can be seen in figure (A2.5(b)). The formulation also exhibits a high dependency with the slenderness (more than API discrete formulation), for the more slender cylinders the results ranges from conservative to normal (fig. A2.5(c)). The dependence of X_m with the geometrical parameters is generalised (fig. A2.5(d)) - (fig. A2.5(i)) except for the R/t ratio (fig. A2.5(g)). This formulation is not suited for the Aerospace data set (large COV and skewness).



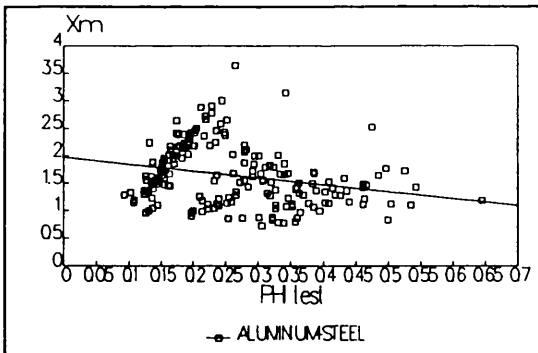


Fig. A2.5(b) - X_m versus Test Strength.

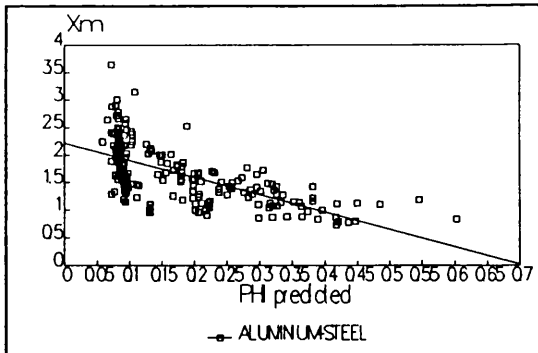


Fig. A2.5(c) - X_m versus Predicted Strength.

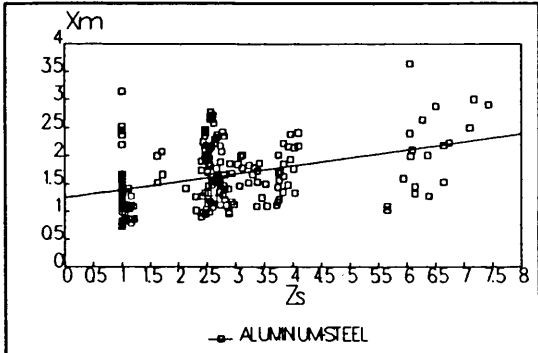


Fig. A2.5(d) - X_m versus Batdorf parameter (Z_s).

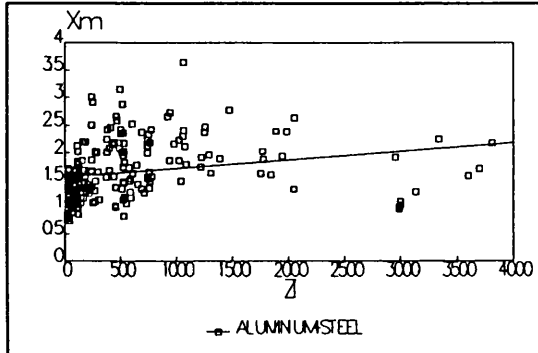


Fig. A2.5(e) - X_m versus Batdorf length par. (Z_l).

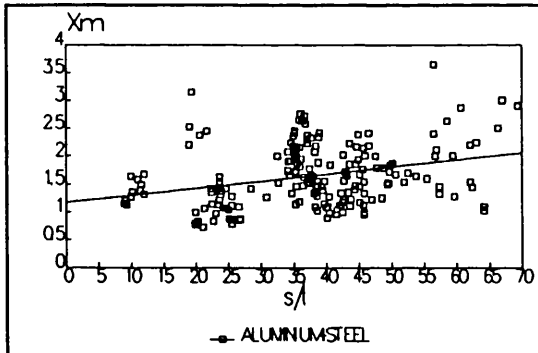


Fig. A2.5(f) - X_m versus s/t .

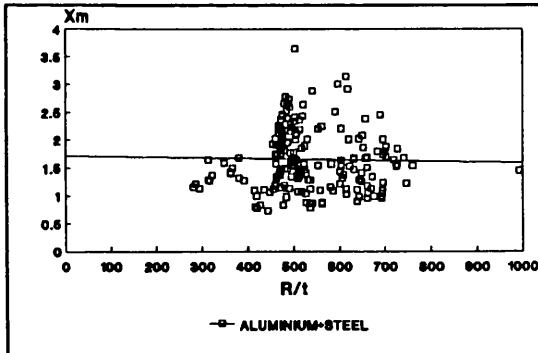


Fig. A2.5(g) - X_m versus R/t .

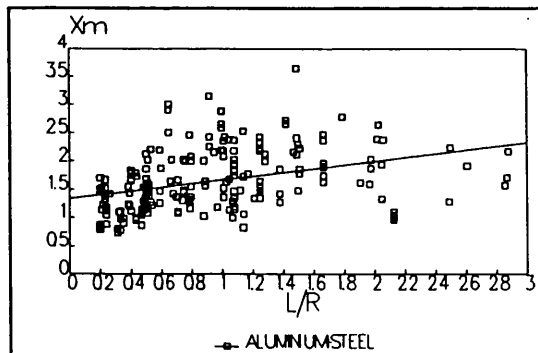


Fig. A2.5(h) - X_m versus L/R .

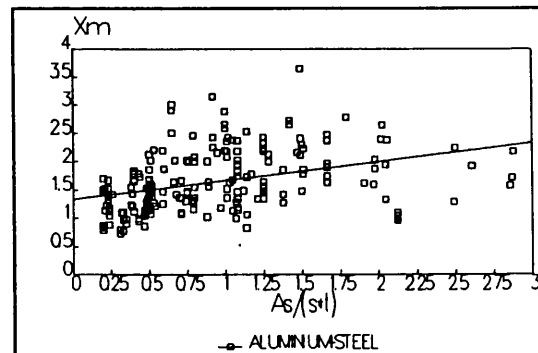
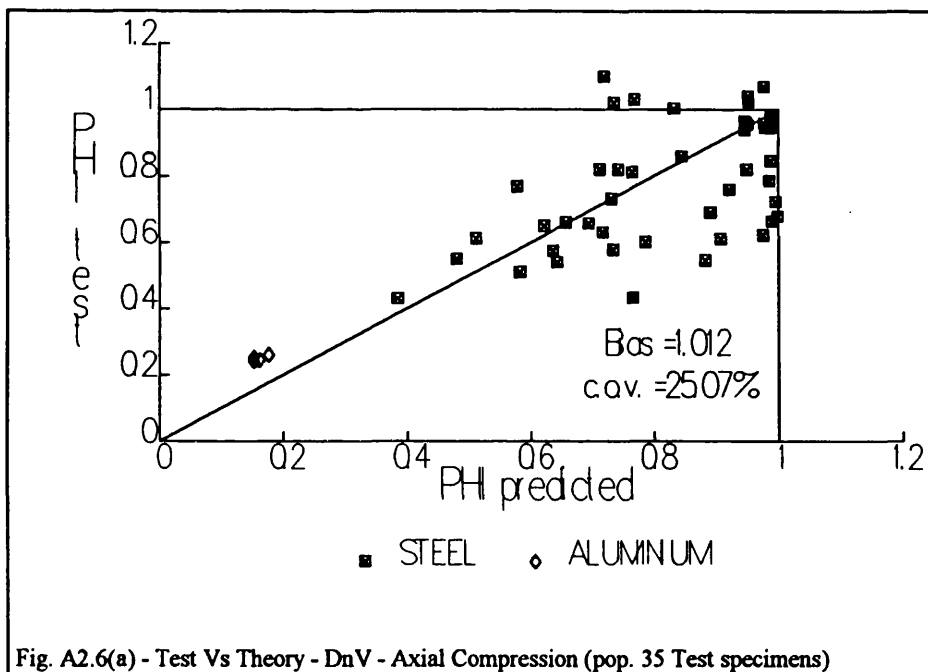


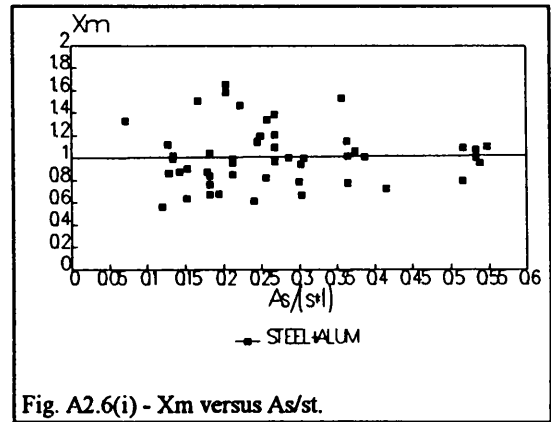
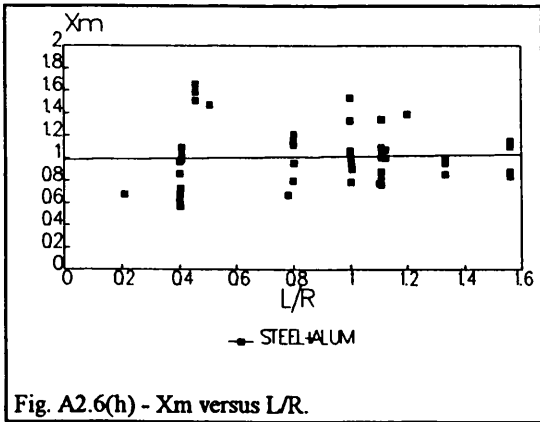
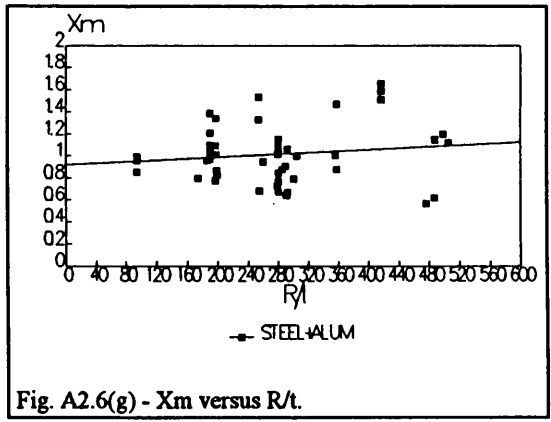
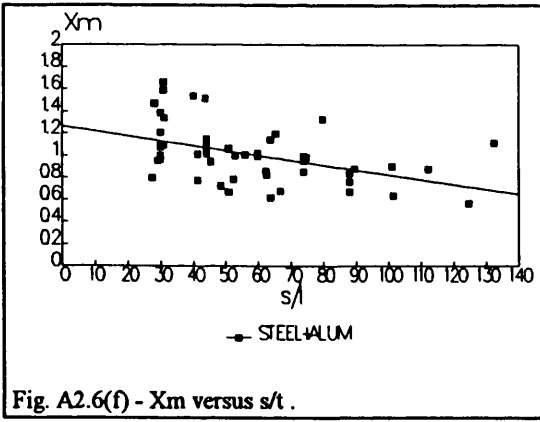
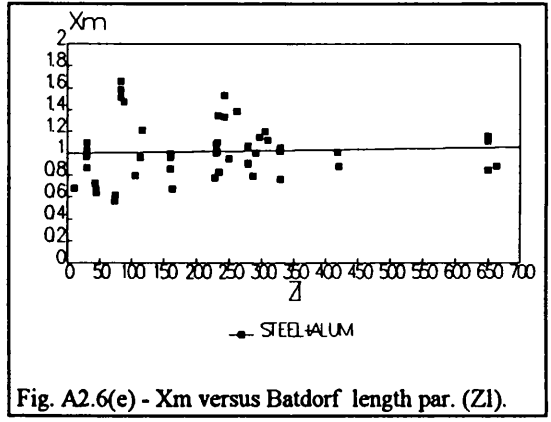
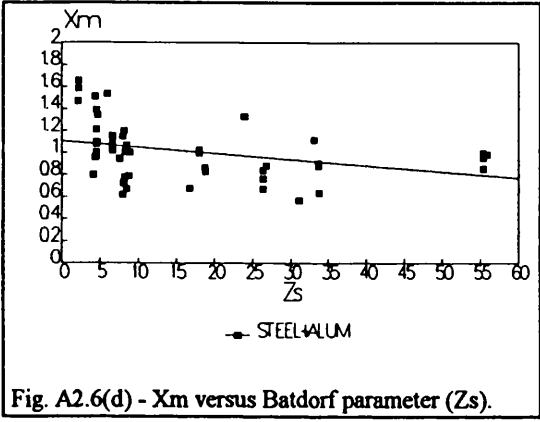
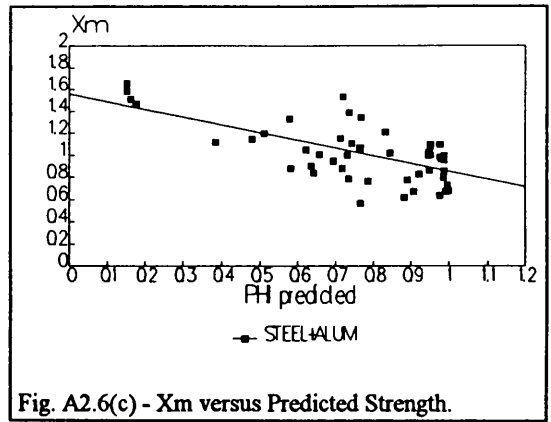
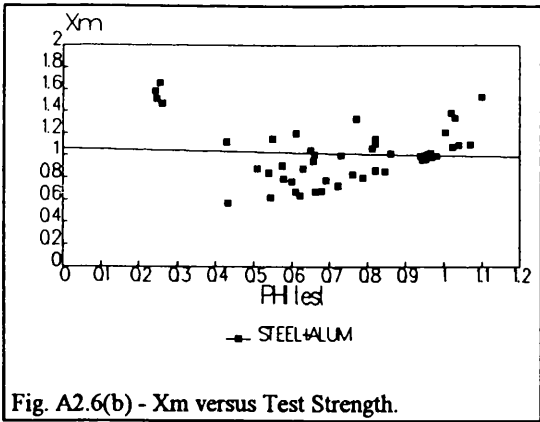
Fig. A2.5(i) - X_m versus A_s/st .

1.4.1. DnV formulation (Offshore Steel & Aluminium Test specimens)

The variation of X_m with predicted strength, test strength and with other parameters for the DnV formulation using all offshore population is shown in the following figures A2.6(a) - A2.6(i).

The test/theory plot (fig. A2.6(a)) shows poor correlation between predictions and test results with moderate scatter for X_m [0.56-1.66] to medium cylinders as can be seen in figure (A2.6(b)). The formulation also exhibits a high dependency of the slenderness being very conservative for the aluminium cylinders and clearly over predicting the strength of the stocky cylinders (fig. A2.6(c)). No major dependence of X_m with the geometrical parameters is visible except for the s/t ratio (fig. A2.6(f)) which denotes some dependency with the slenderness of the shell between stiffeners. This mean value formulation is fairly suited for the Offshore data set (bias near one, large COV and no skewness) with limitations for stocky cylinders.





1.4.2. DnV formulation (Aerospace Steel & Aluminium Test specimens)

The variation of X_m with predicted strength, test strength and with other parameters for the DnV formulation using all aerospace population is shown in the following figures A2.7(a) - A2.7(i).

The test/theory plot (fig. A2.7(a)) shows no correlation between predictions and test results with a high scatter for X_m [1.0-3.5] to slender and very slender cylinders as can be seen in figure (A2.7(b)). The formulation also exhibits a high dependency with the slenderness and for the more slender cylinders the results ranges from conservative to normal (fig. A2.7(c)). The dependence of X_m with the geometrical parameters is moderate for Z_s (fig. A2.7(d)), s/t ratio (fig. A2.7(f)) and $As/(s*t)$ ratio (fig. A2.7(i)) This formulation is fairly suited for the Aerospace data set (large COV and moderate skewness) and can be considered as a conservative low bound formulation (bias above one).

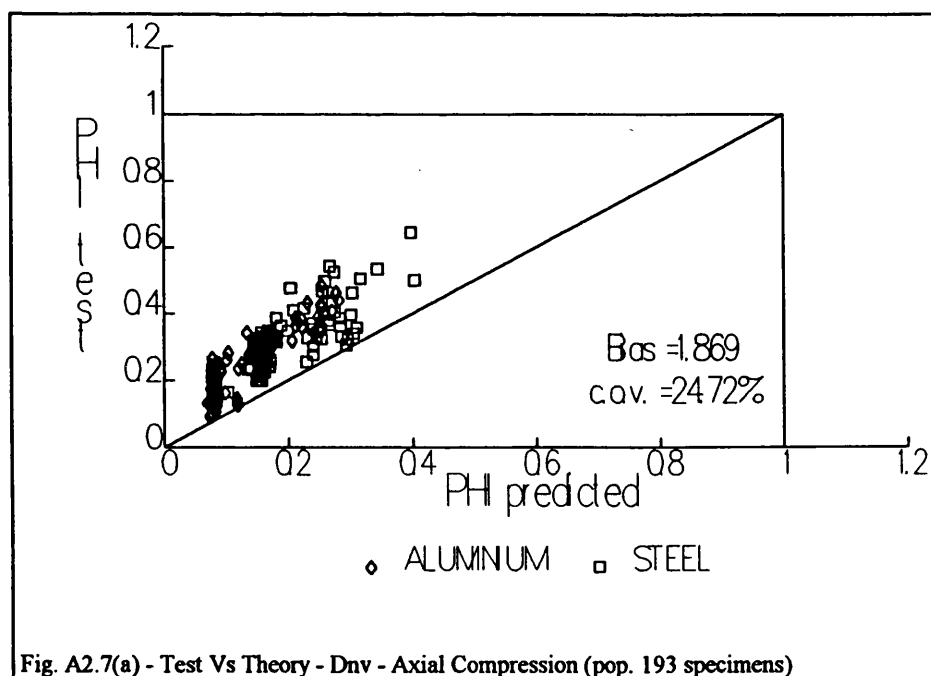


Fig. A2.7(a) - Test Vs Theory - Dnv - Axial Compression (pop. 193 specimens)

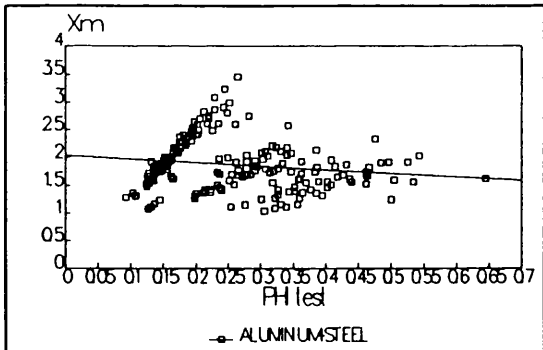


Fig. A2.7(b) - X_m versus Test Strength.

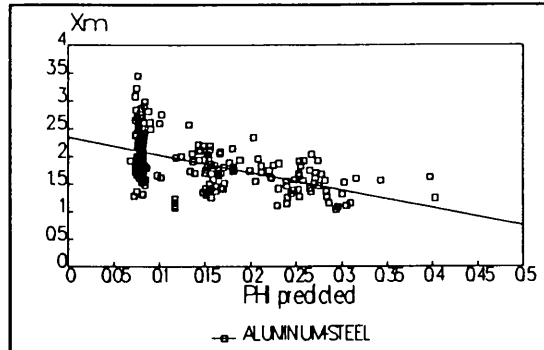


Fig. A2.7(c) - X_m versus Predicted Strength.

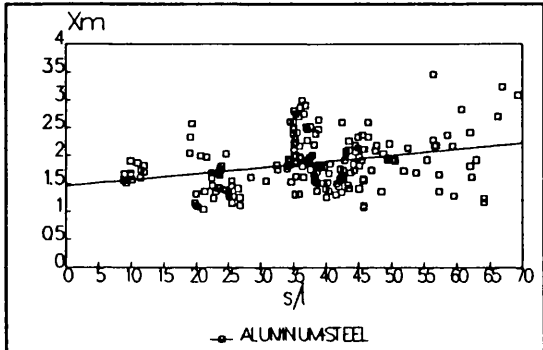


Fig. A2.7(d) - X_m versus Batdorf parameter (Z_s).

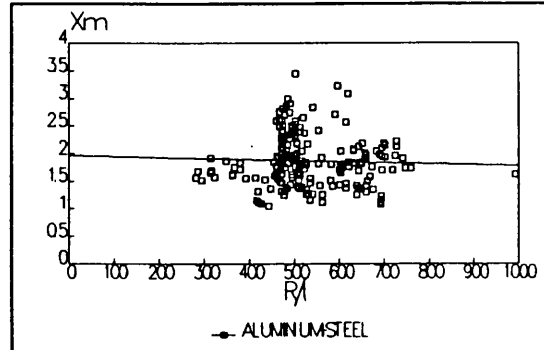


Fig. A2.7(e) - X_m versus Batdorf length par. (Z_l).

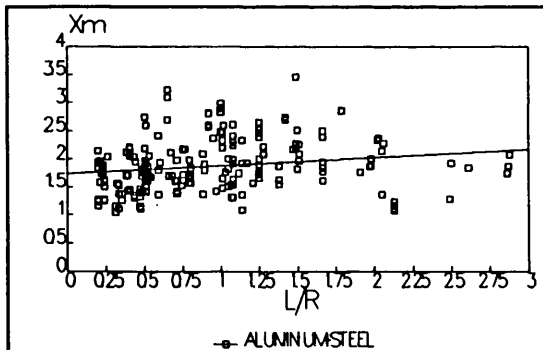


Fig. A2.7(f) - X_m versus s/t .

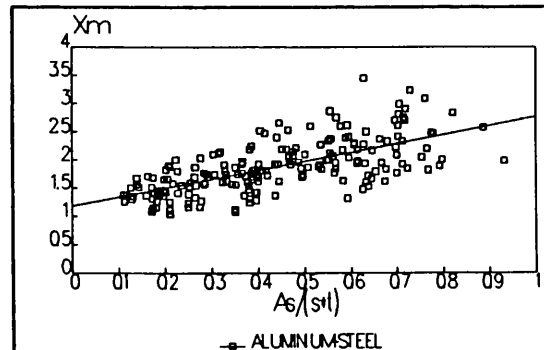


Fig. A2.7(g) - X_m versus R/t .

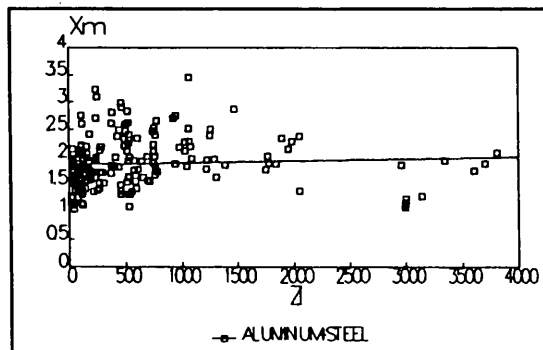


Fig. A2.7(h) - X_m versus L/R .

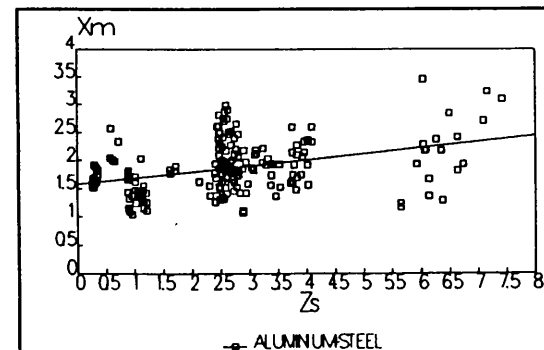
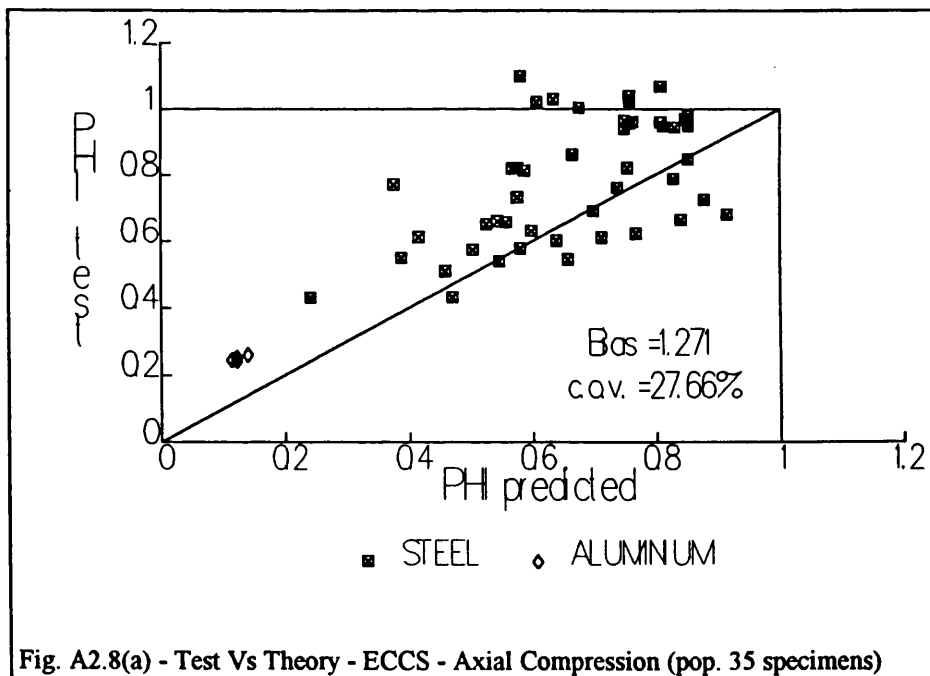


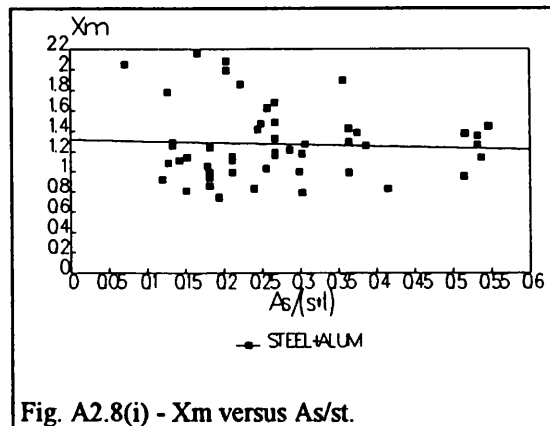
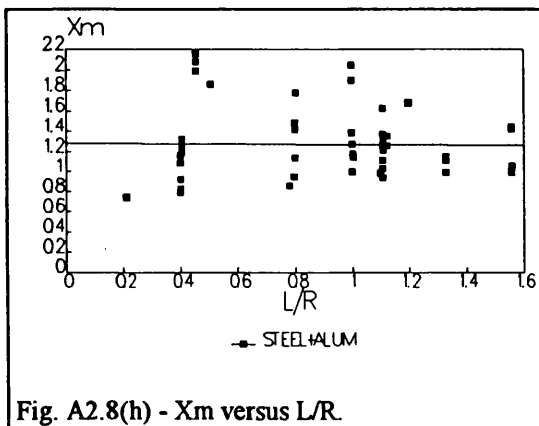
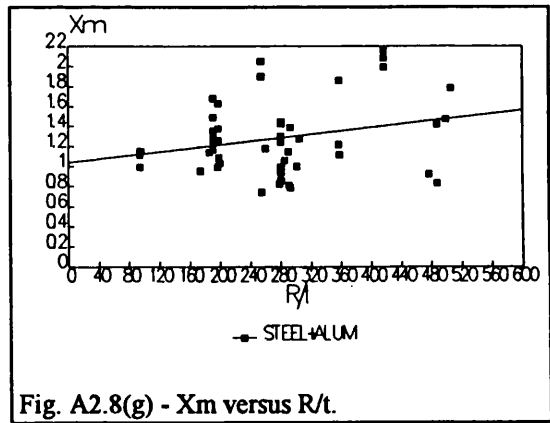
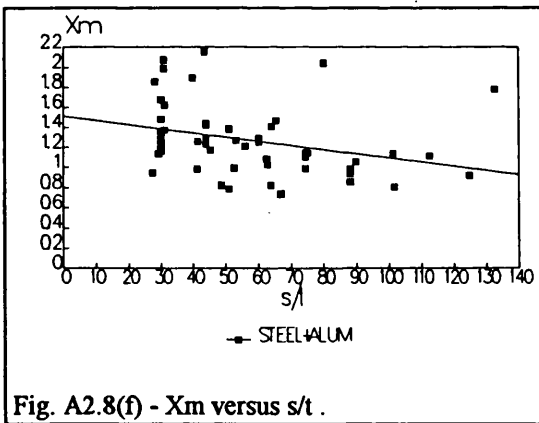
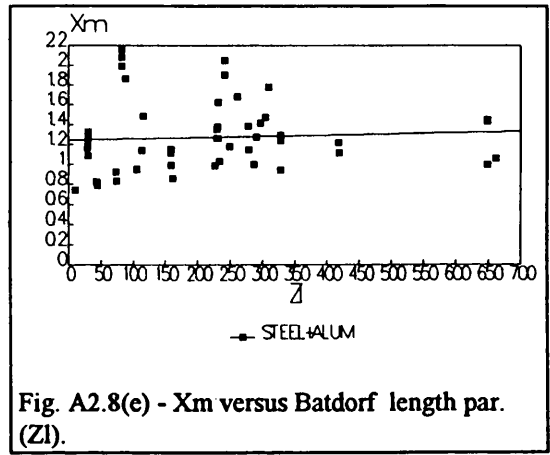
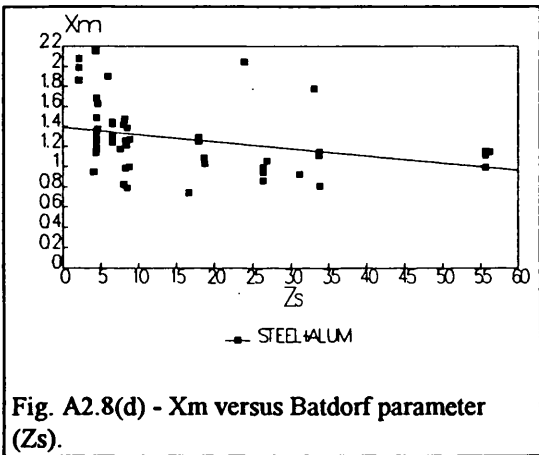
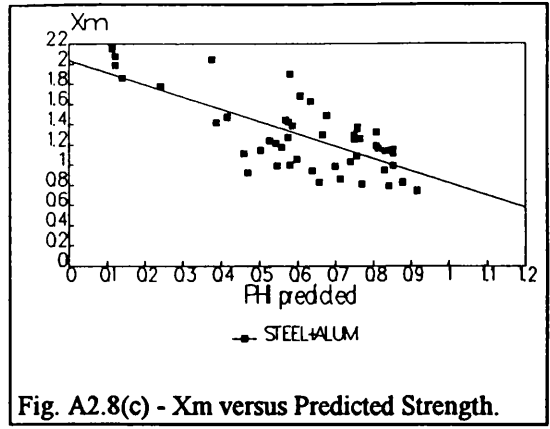
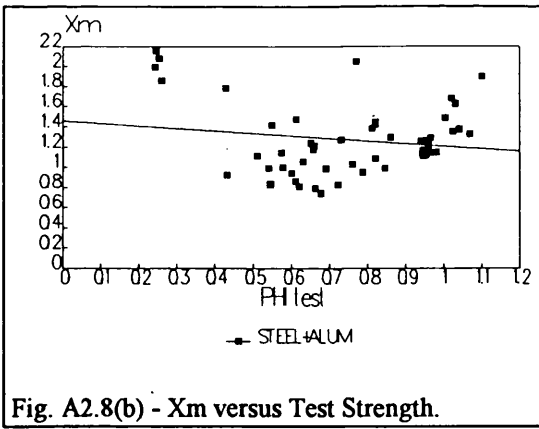
Fig. A2.7(i) - X_m versus As/st .

1.5.1. ECCS formulation (Offshore Steel & Aluminium Test specimens)

The variation of X_m with predicted strength, test strength and with other parameters for ECCS formulation using all offshore population is shown in the following figures A2.8(a) - A2.8(i).

The test/theory plot (fig. A2.8(a)) shows poor correlation between predictions and test results with high scatter for X_m [0.7-2.2] to slender and medium cylinders as can be seen in figure (A2.8(b)). The formulation also exhibits a high dependency of the slenderness being very conservative for the aluminium cylinders and over predicting the strength of the stocky cylinders (fig. A2.8(c)). The dependence of X_m with the geometrical parameters is moderate for Z_s (fig. A2.8(d)) and s/t (fig. A2.8(f)) and R/t ratio (fig. A2.8(g)). This formulation poorly suited for the Offshore data set (large COV and moderate skewness) and can be also considered as a poor low bound formulation (bias above one and 25% of the specimens fails under the predictions).

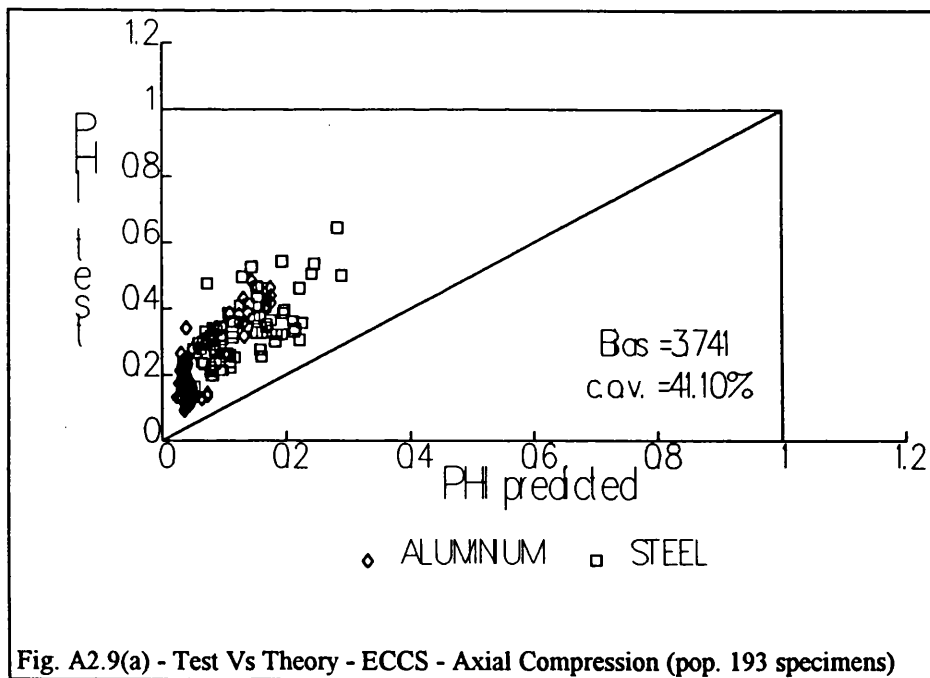


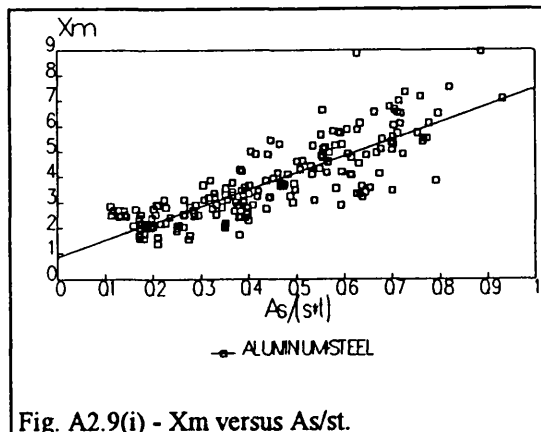
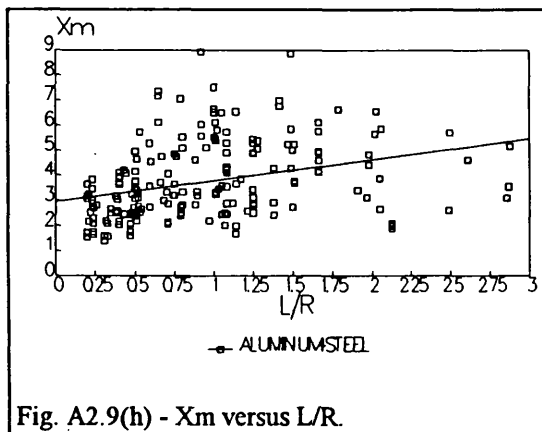
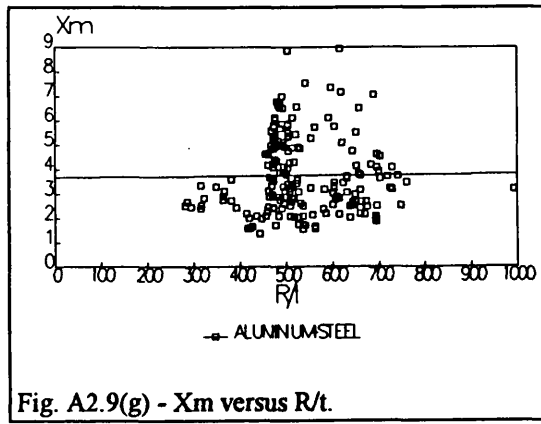
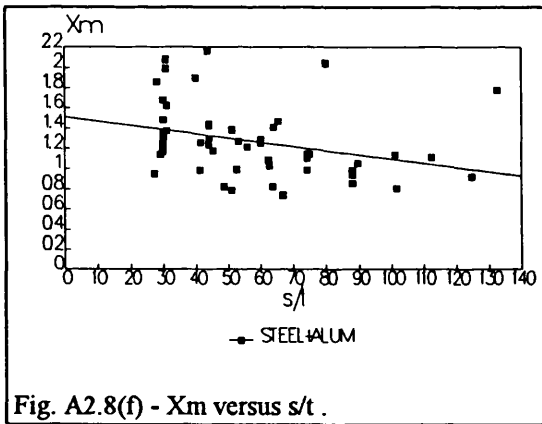
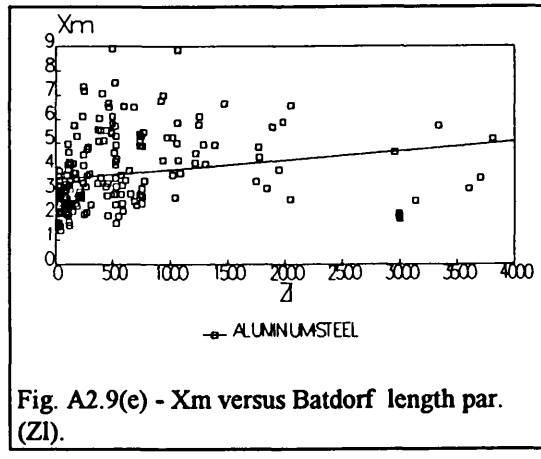
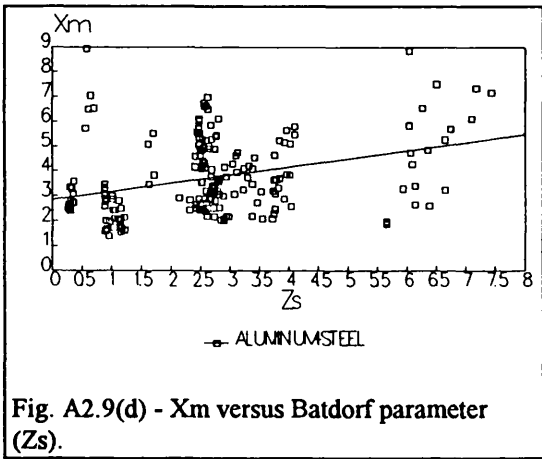
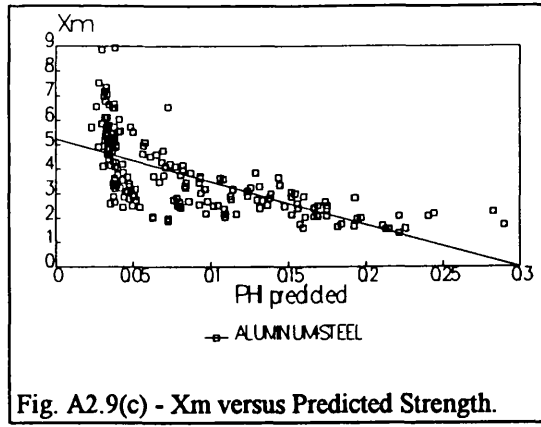
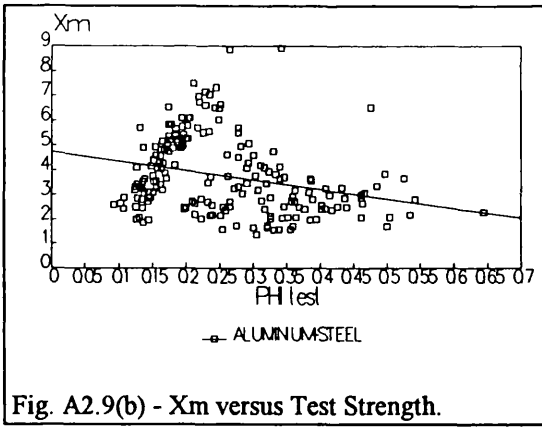


1.5.2. ECCS formulation (Aerospace Steel & Aluminium Test specimens)

The variation of X_m with predicted strength, test strength and with other parameters for the ECCS formulation using all aerospace population is shown in the following figures A2.9(a) - A2.9(i).

The test/theory plot (fig. A2.9(a)) shows no correlation between predictions and test results with a very high scatter for X_m [1.0-9.0] to slender and very slender cylinders as can be seen in figure (A2.9(b)). The formulation also exhibits a enormous dependency of the slenderness being extremely conservative for the more slender cylinders (fig. A2.9(c)). The dependence of X_m with the geometrical parameters is generalised (fig. A2.9(d)) - (fig. A2.9(i)) with exception of R/t ratio (fig. A2.9(g)). This formulation is not suited for the Aerospace data set (very large COV and high skewness) and can be considered as a very conservative low bound formulation (bias high above one).





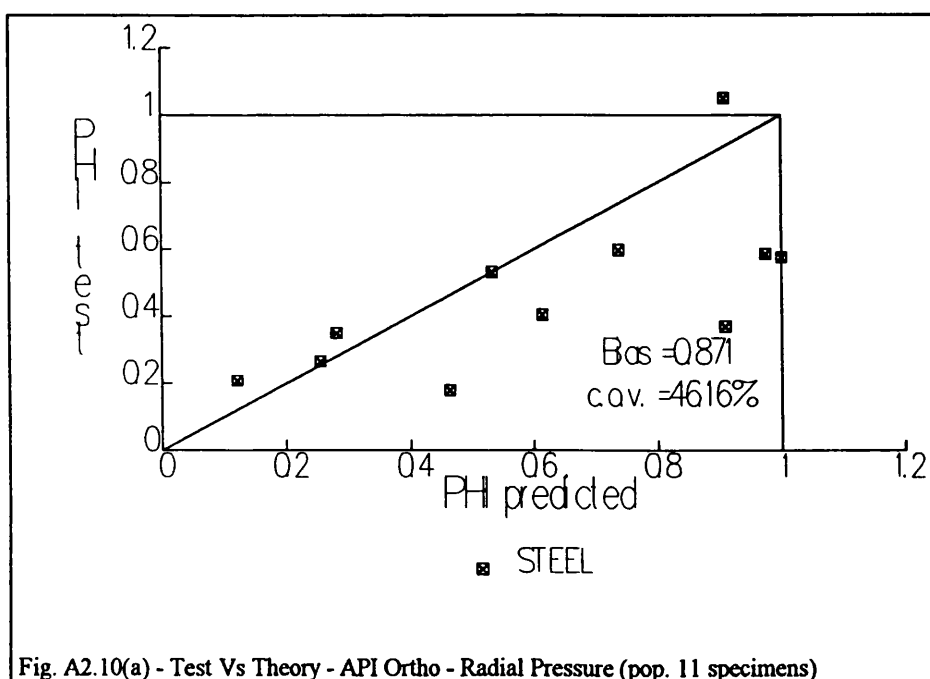
2 - Radial pressure formulations

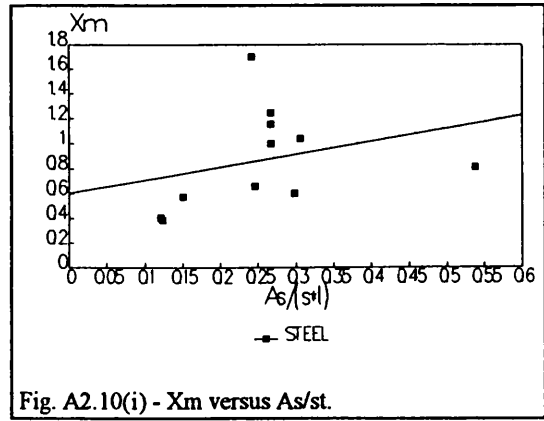
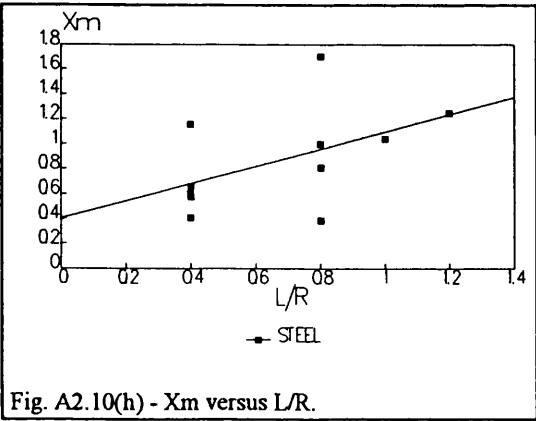
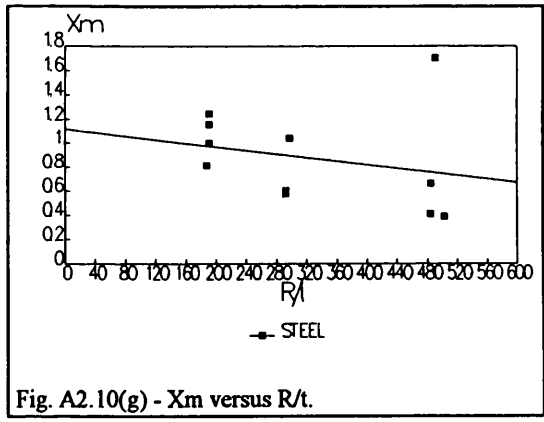
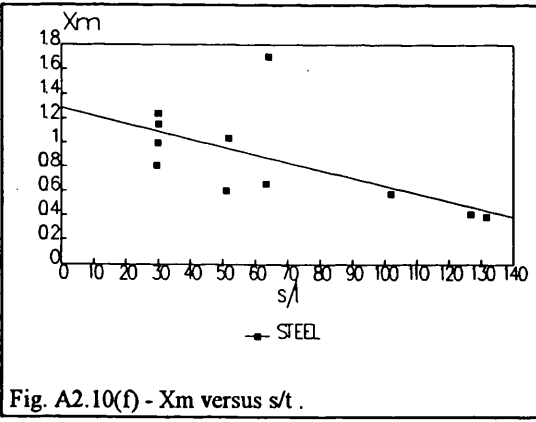
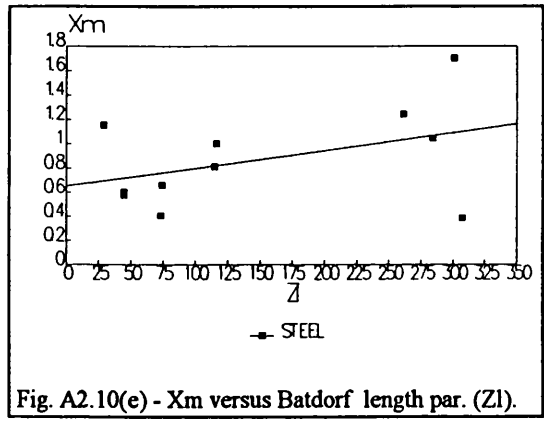
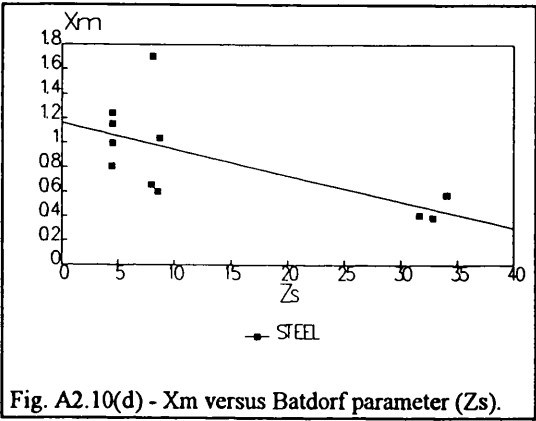
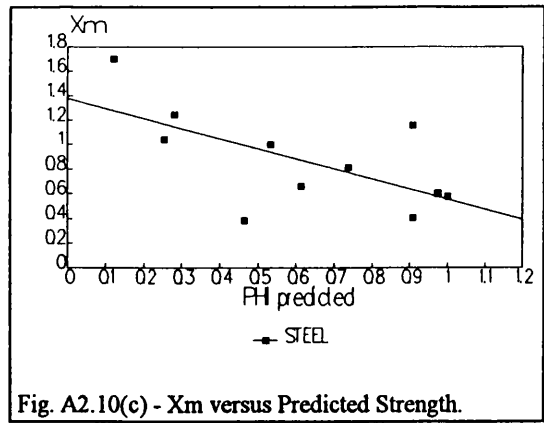
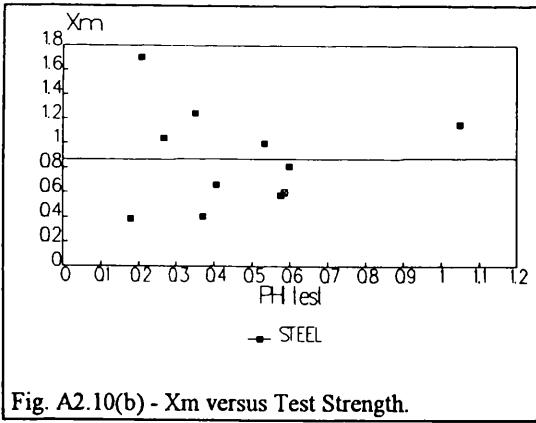
The results of the statistical analyses for the API Bul 2U, the RCC recommendations and the DnV Classification notes are plotted in graphs showing the variation of the modelling parameter X_m with the test and predicted strengths and with different geometric parameters of the cylinders. The Offshore Steel test specimens were used (population = 11 specimens).

2.1. API Bul 2U Orthotropic formulation (Offshore Steel Test specimens)

The variation of X_m with predicted strength, test strength and with other parameters for the API Orthotropic formulation using all aerospace population is shown in the following figures A2.10(a) - A2.10(i).

The test/theory plot (fig. A2.10(a)) shows a very poor correlation between predictions and test results with a high scatter for X_m [0.4-1.7] to very slender cylinders as can be seen in figure (A2.10(b)). The formulation also exhibits a great dependency of the slenderness with a strong tendency to over predicted the strength of medium and stocky cylinders (fig. A2.10(c)). The dependence of X_m with the geometrical parameters is generalised (fig. A2.10(d)) - (fig. A2.10(i)) with exception of R/t ratio (fig. A2.10(g)). This formulation is not suited for the offshore data set (very large COV and high skewness) and can be considered as a dangerous formulation (bias lower than one and more than 60% of the test specimens fails under the predictions).





2.2. API Bul 2U formulation (Offshore Steel Test specimens)

The variation of X_m with predicted strength, test strength and with other parameters for API Bul 2U formulation using all aerospace population is shown in the following figures A2.11(a) - A2.11(i).

The test/theory plot (fig. A2.11(a)) shows a good correlation between predictions and test results with a moderate scatter for X_m [1.0-1.55] for the very slender cylinders (fig. A2.11(b)). The formulation underpredicted the strength ($X_m > 1.$) for all test specimens (fig. A2.11(a)) and doesn't show significant dependency with slenderness or the geometrical parameters (fig. A2.13(b)) - (fig. A2.13(i)). This formulation is fair for the offshore data set (moderate COV and no skewness) and can be considered a good low bound formulation (bias little over unity and 100% fails above prediction).

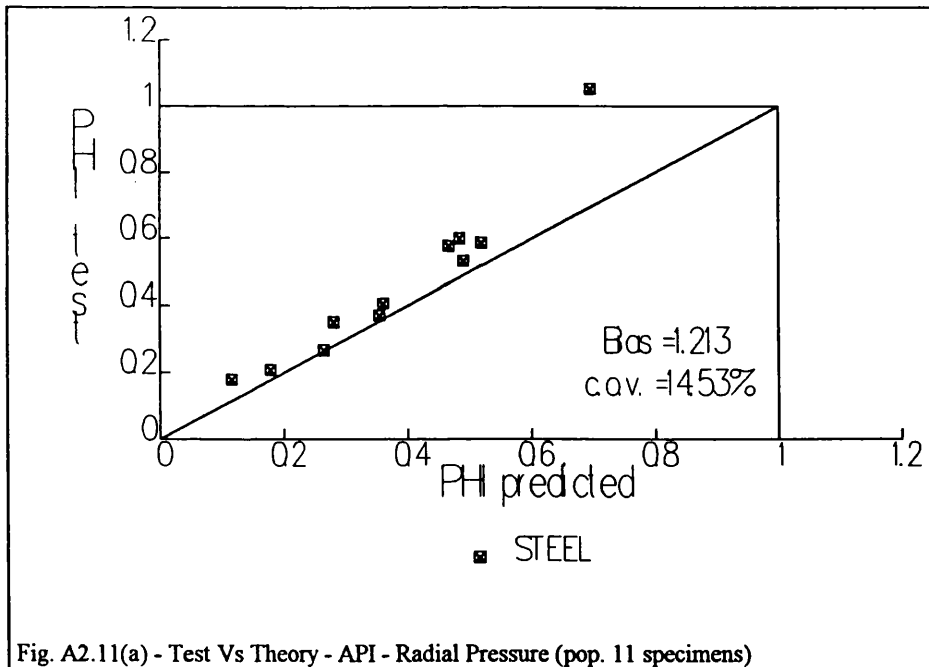
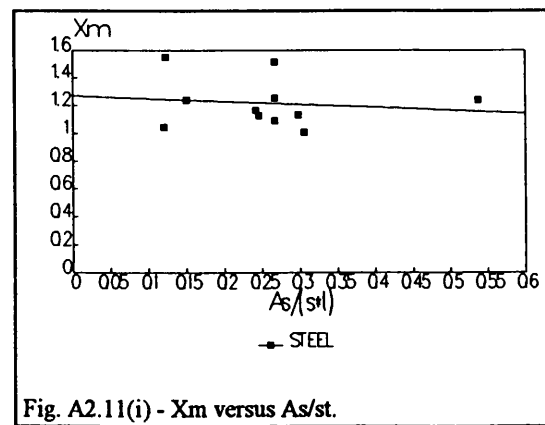
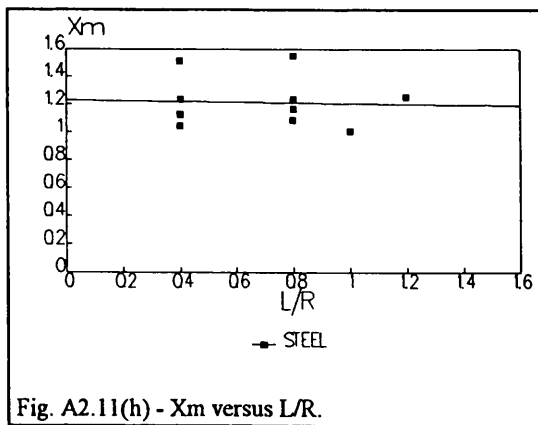
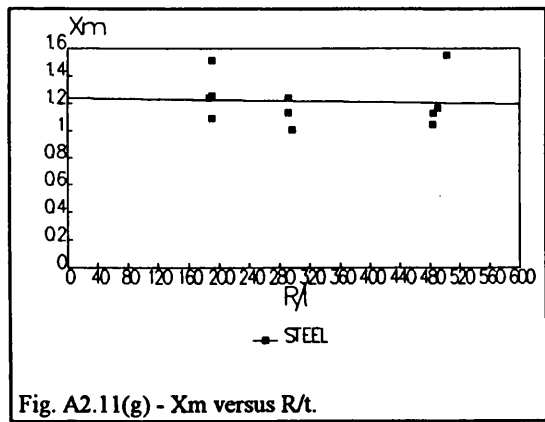
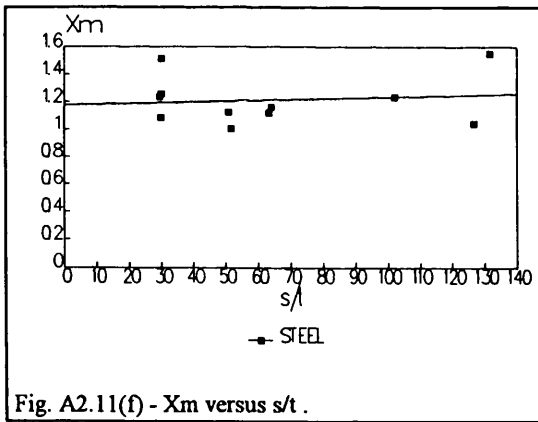
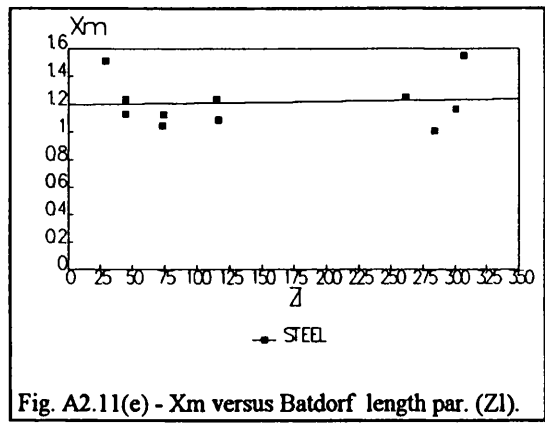
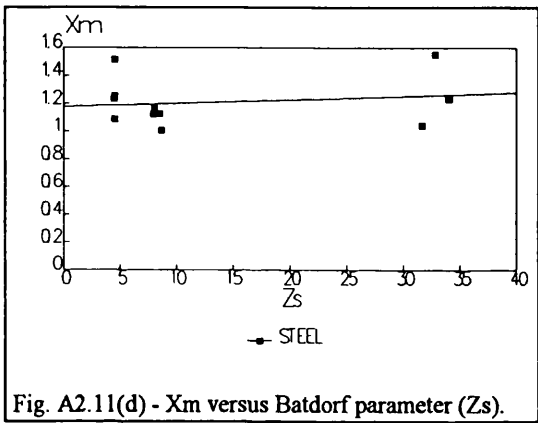
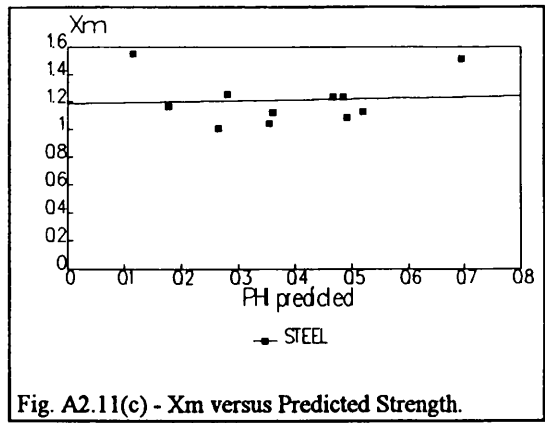
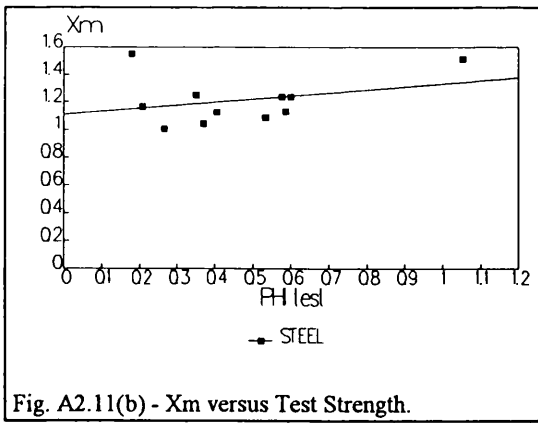


Fig. A2.11(a) - Test Vs Theory - API - Radial Pressure (pop. 11 specimens)



2.3. DnV formulation (Offshore Steel Test specimens)

The variation of X_m with predicted strength, test strength and with other parameters for the DnV formulation using all population is shown in the following figures A2.12(a) - A2.12(i).

The test/theory plot (fig. A2.12(a)) shows a poor correlation between predictions and test results with a high scatter for X_m [1.2-2.5] to slender and very slender cylinders as can be seen in figure (A2.12(b)). The formulation also exhibits a great dependency of the slenderness with a strong tendency to over predicted the strength of medium and stocky cylinders (fig. A2.12(c)). The dependence of X_m with the geometrical parameters is generalised (fig. A2.10(d)) - (fig. A2.10(i)). This formulation is not suited for the offshore data set (very large COV and high skewness) and can be considered as a poor low bound formulation (bias high above one and more than 25% of the specimens fails under the predictions).

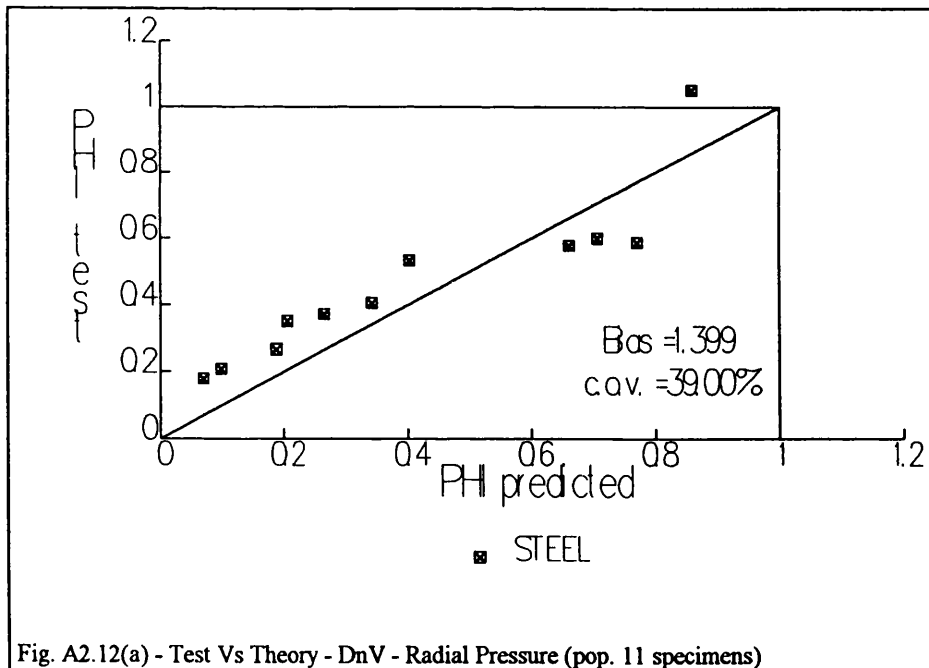
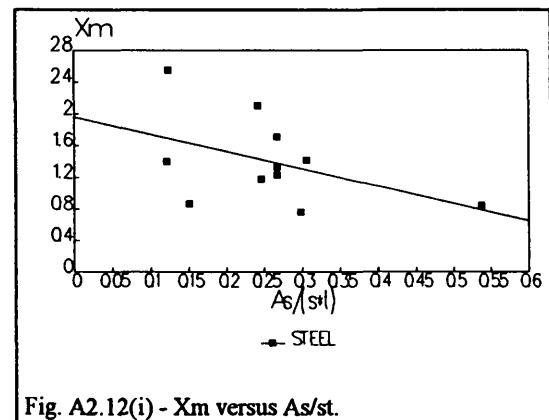
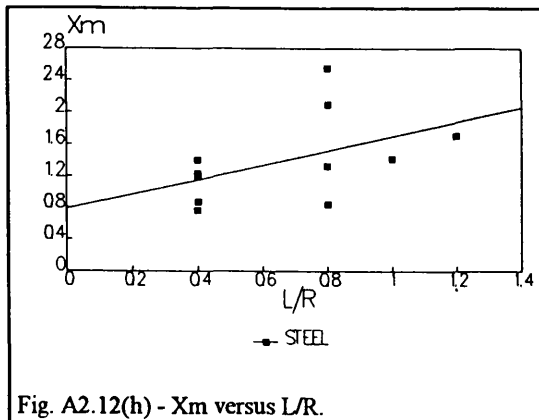
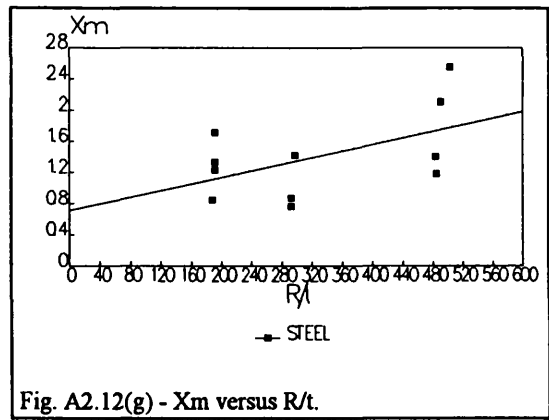
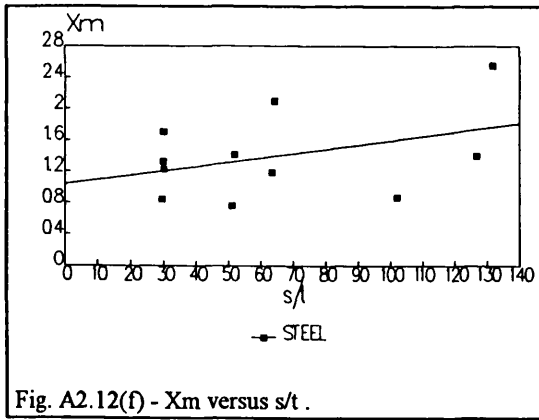
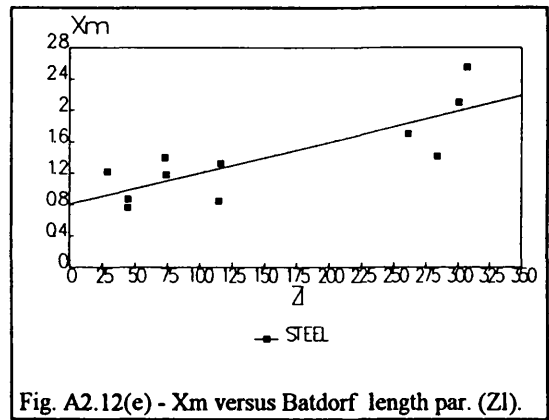
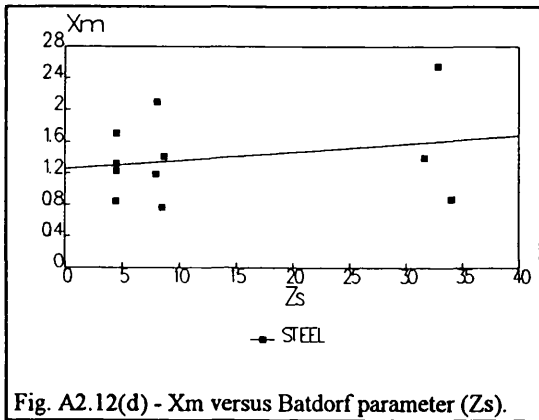
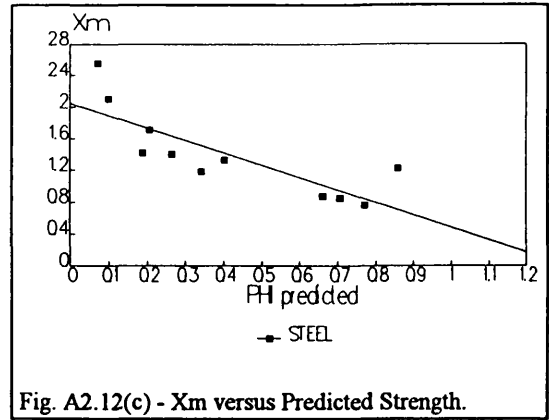
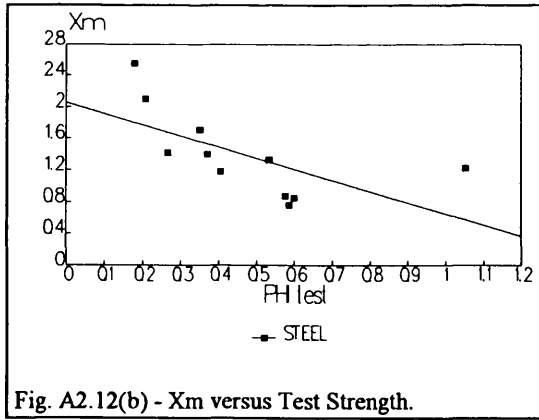


Fig. A2.12(a) - Test Vs Theory - DnV - Radial Pressure (pop. 11 specimens)



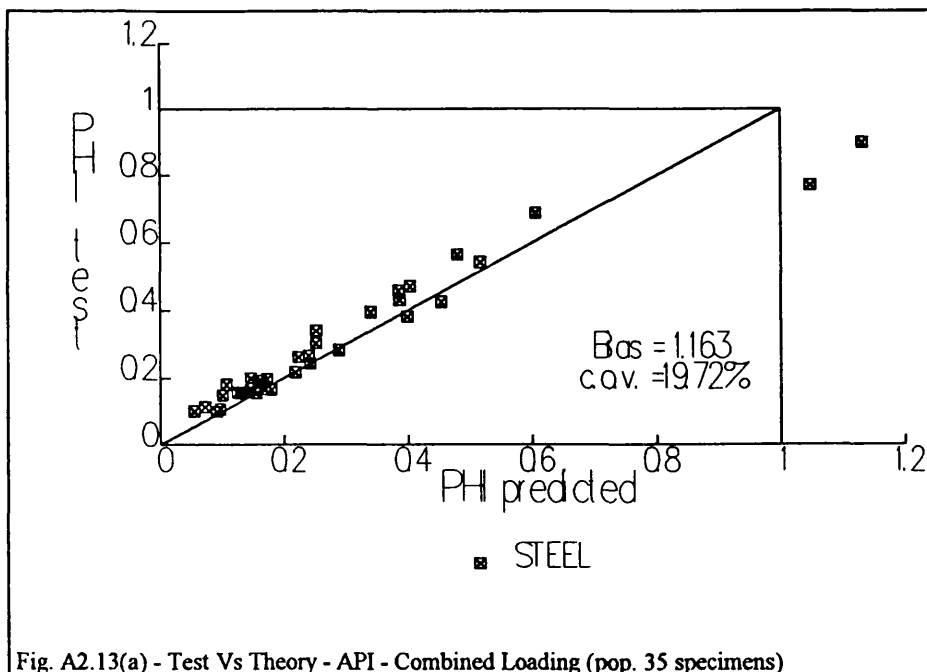
3 - Combined loading formulations

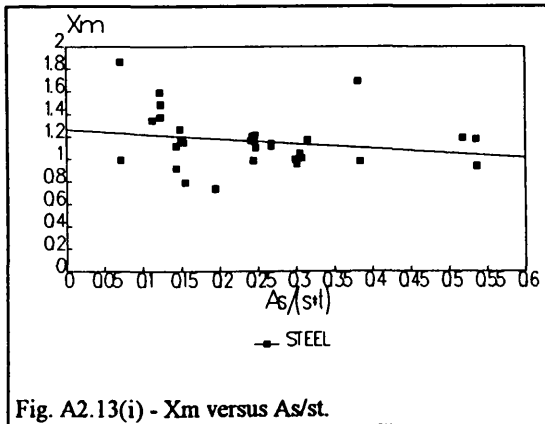
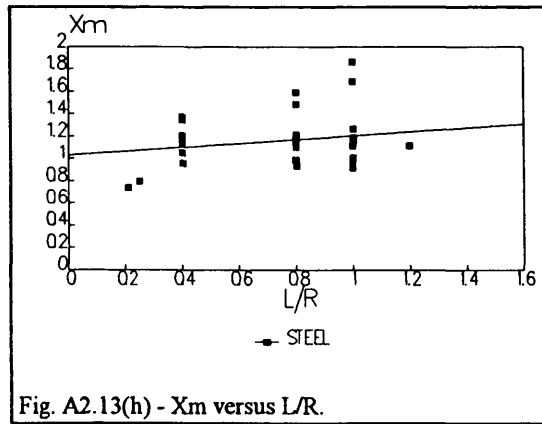
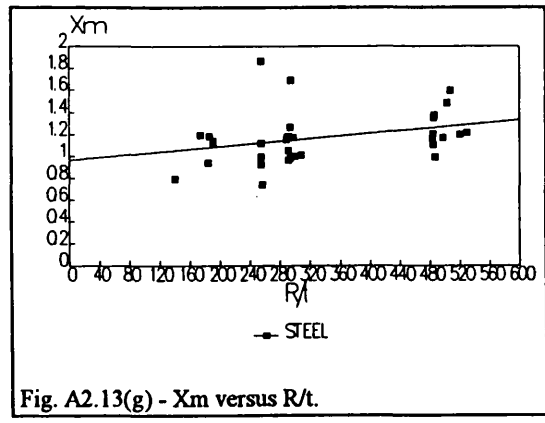
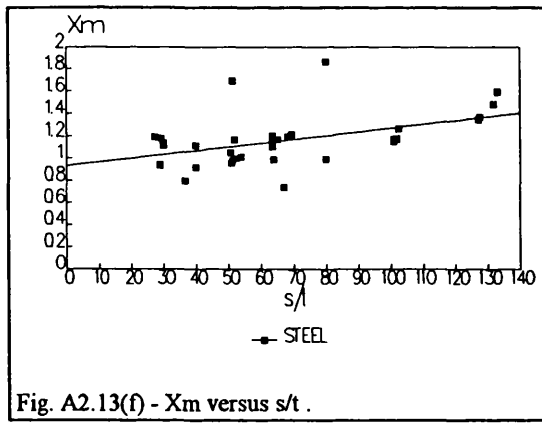
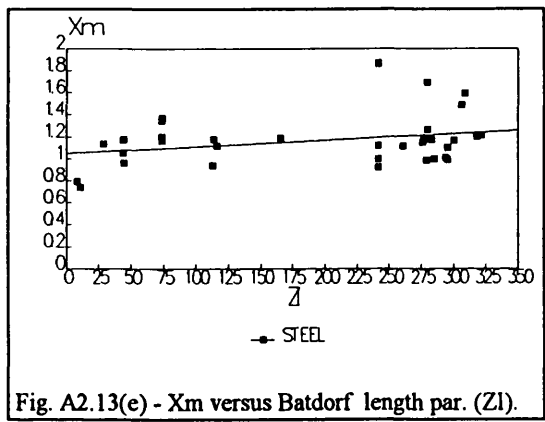
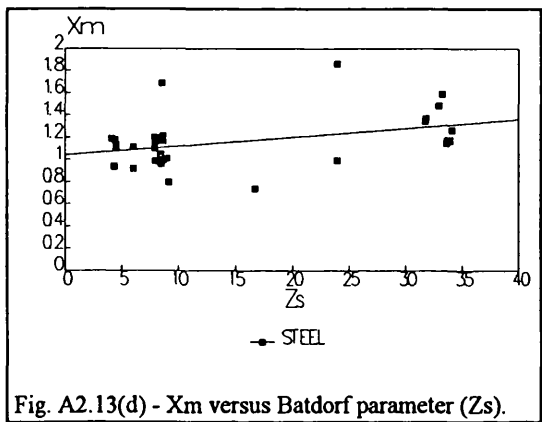
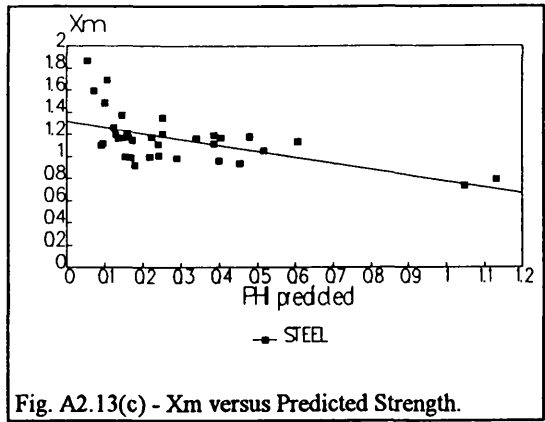
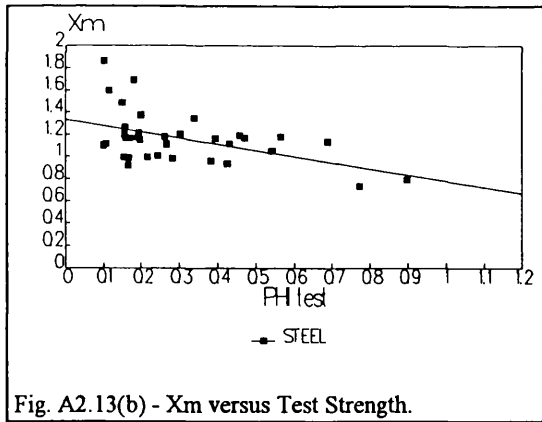
The results of the statistical analyses for the API Bul 2U, the RCC recommendations and the DnV Classification notes were plotted in graphs showing the variation of the modelling parameter X_m with the test and predicted strengths and with different geometric parameters of the cylinders. The Offshore Steel test specimens were used (population = 35 specimens).

3.1. API formulation (Offshore Steel Test specimens)

The variation of X_m with predicted strength, test strength and with other parameters for the API formulation using all offshore population is presented in the following figures A2.13(a) - A2.13(i).

The test/theory plot (fig. A2.13(a)) shows a fair correlation between predictions and test results with a moderate scatter for X_m to all slenderness with the exception of the very slender cylinders in which the maximum scatter occurs (fig. A2.13(b)). The formulation also shows some tendency to overpredicted the strength of stocky cylinders (fig. A2.13(c)) and doesn't show significant dependency of the geometrical parameters (fig. A2.13(d)) - (fig. A2.13(i)). This formulation is fair (moderate COV and no skewness) and can be considered as mean value formulation (bias near unity)for the offshore data set.

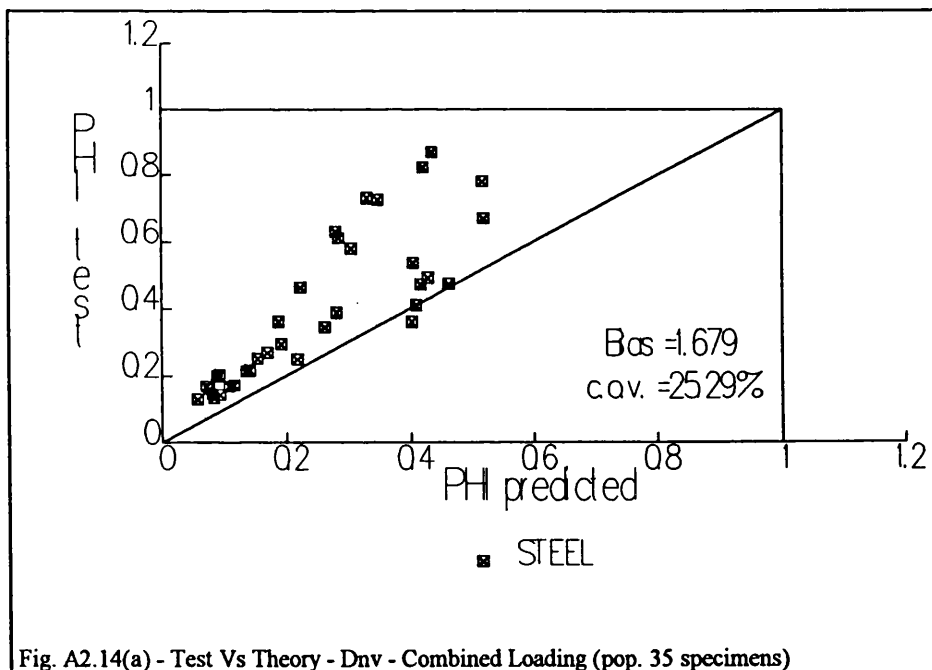


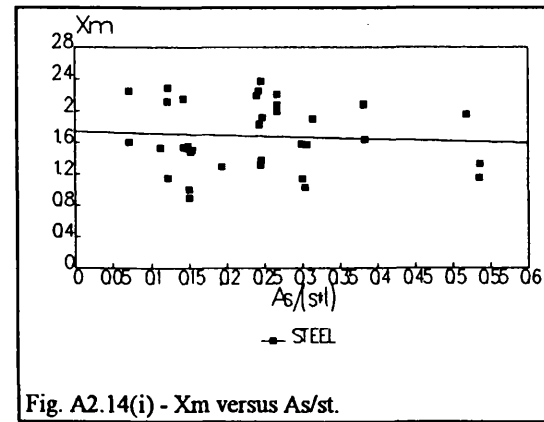
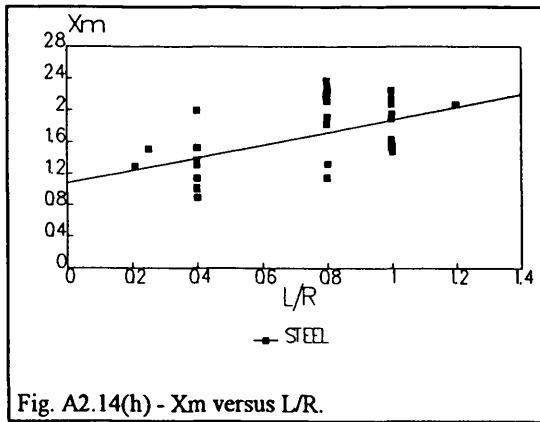
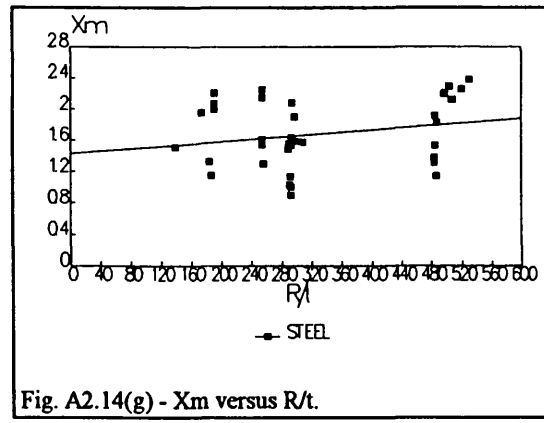
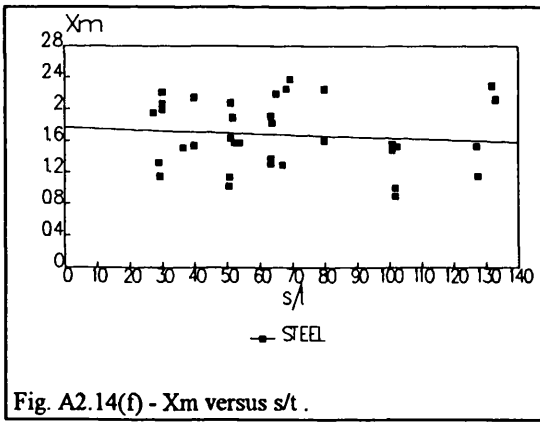
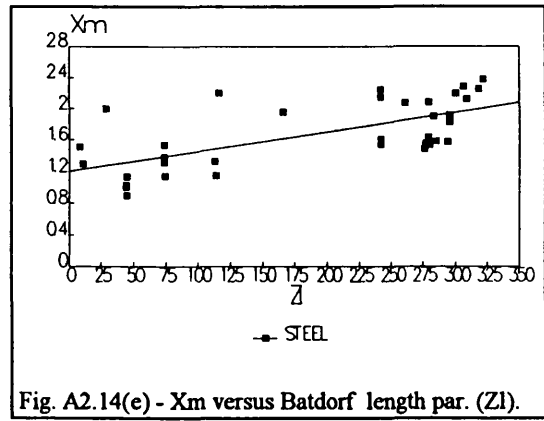
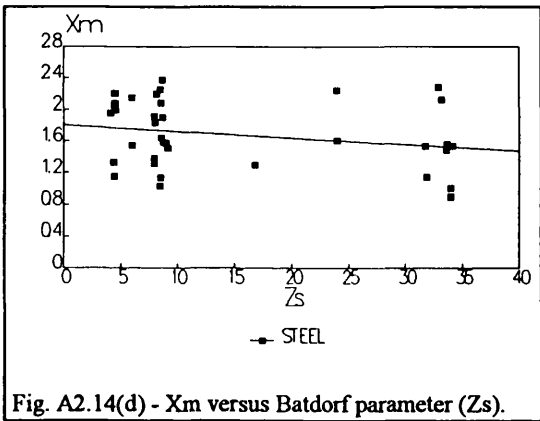
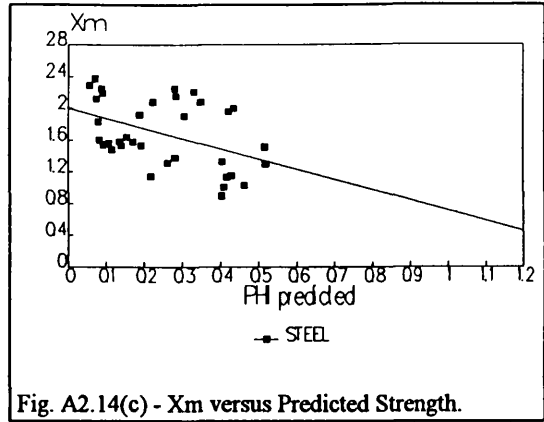
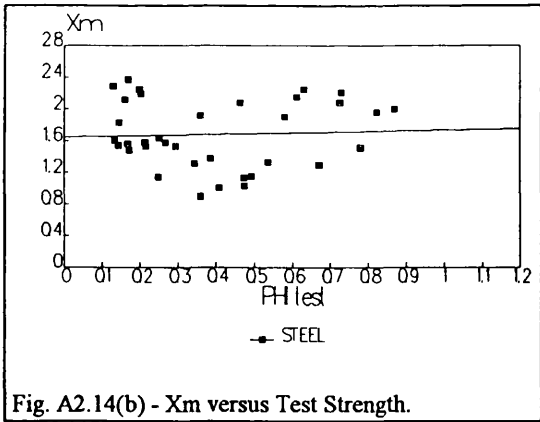


3.2. DnV formulation (Offshore Steel Test specimens)

The variation of X_m with predicted strength, test strength and with other parameters for DnV formulation using all offshore population is presented in the following figures A2.14(a) - A2.14(i).

The test/theory plot (fig. A2.14(a)) shows a poor correlation between predictions and test results. A moderate scatter for X_m to all slenderness can be seen (fig. A2.14(b)). The formulation also exhibit a great dependency of the slenderness with a strong tendency to overpredicted the strength of stocky cylinders (fig. A2.14(c)). The dependence of X_m with the geometrical parameters exists, particularly for Z1 (fig. A2.14(e)) and L/R (fig. A2.14(h)). This formulation is poor (large COV and high skewness) but can be considered as a lower bound formulation (high bias and less than 6% fails under the predictions) for the offshore data set.





APPENDIX 4 - CYLINDERS RELIABILITY ANALYSIS - GRAPHICAL OUTPUT.

1 - Axial compression

